INSIGHTS INTO THE STRATIGRAPHIC EVOLUTION OF THE EARLY PENNSYLVANIAN POCAHONTAS BASIN, VIRGINIA

Ryan Paul Grimm

Dissertation submitted to the faculty of the Virginia Polytechnic Institute and State University in partial fulfillment of the requirements for the degree of

Doctor of Philosophy
In
Geosciences

Kenneth Eriksson
J. Fred Read
Michal Kowalewski
William Henika
Stephen Greb

December 8th, 2010
Blacksburg, VA

Keywords: Appalachian Basin, Pennsylvanian, Facies Analysis, Sequence Stratigraphy, Seal Evaluation, Alleghanian Orogeny

INSIGHTS INTO THE STRATIGRAPHIC EVOLUTION OF THE EARLY PENNSYLVANIAN POCAHONTAS BASIN, VIRGINIA

Ryan Paul Grimm

ABSTRACT

Early Pennsylvanian, coal-bearing, siliciclastic strata of the Breathitt Group within the Pocahontas Basin, southwestern Virginia, define a southeasterly thickening clastic wedge deposited in continental to marginal marine environments influenced by recurring, high-magnitude relative sea-level fluctuations and low-frequency changes in tectonic loading. A robust dataset of >1200 well logs, cores and numerous outcrops allowed a unique review of the Central Appalachian lithologic record during both the Late Paleozoic Ice Age and onset of the Alleghanian Orogeny.

The tropical depositional landscape produced stacked deposits of braided-fluvial channels, broad alluvial plains, tidally-influenced estuaries and small deltas. Trends in facies associations allowed development of a high-resolution sequence stratigraphic architecture based on regional flooding surfaces and bounding discontinuities. Analysis of vertical stacking patterns of lithofacies on regional cross-sections identified 15 widespread, unconformity-bounded depositional sequences with an average duration of ~80 kyr based on available geochronology.

Glacioeustatic control on stratigraphic architecture is supported by corresponding sequence duration within the short-eccentricity periodicity of the Milankovitch band, as well as the magnitude and extent of rapid facies shifts, suggesting that far-a-field variations in overall Gondwanan ice-sheet size and volume impacted base-level changes in the tropical basin. The progressive increase in magnitude of transgressions, as indicated by brackish-marine ichnofacies and other faunal indicators within regional high-frequency transgressive system tracts, indicate extrabasinal trends in ice-volume and eustasy.

High-frequency eustatic sequences are nested within four asymmetric composite-sequences, attributed to low-frequency variations in tectonic accommodation. Evidence for tectonic forcing on foreland-basin accommodation is based on abrupt facies shifts, angular stratal terminations and wedge-shaped composite-sequence geometries. Spatial and temporal trends in facies associations within composite-sequences reveal episodic variation in tectonic loading overprinted by recurring high-frequency eustatic events.

Petrology and detrital-zircon geochronology indicates that sediment was derived from low-grade metamorphic Grenvillian-Avalonian terranes and recycling of older Paleozoic sedimentary rocks uplifted as part of the Alleghanian orogen towards the southeast and, in part, from the Archean Superior Province to the north.

Applications of the observed facies distribution and petrophysics of these coal-bearing sedimentary rocks indicate numerous confining intervals within regional mudstones overlying coalbeds, suggesting the potential for beneficial geological storage of CO_2 through enhanced-coal-bed-methane recovery.

To

My wonderful Parents

Wendell and Diane Grimm

&

My loving Wife

Katie O’Donnell

ACKNOWLEDGEMENTS

My interest in the Earth sciences was nurtured early on in my life. Growing up as part of a family with a significant agricultural heritage instilled an early fascination with seasonal changes in the weather and landscape. Following each spring plowing, I found my preschool-age self compelled to collect the new and interesting rocks brought by the harrow to the surface. We spent large majorities of our summer evenings with the family, picnicking on the shores of Lake Ontario, on beaches adjacent to our family's original New World settlement. Herein with my sister and cousins, we would collect buckets of our favorite stones, some rich with fossils, others valued for their semi-precious gem appearance. All had been made sparkling and smooth by the surf. It was here that we would sit with our grandfather, who would discuss how he had witnessed the landscape actively change over his lifetime. It was here that I had built an early realization of the concept of earth processes and deep time, on a landscape I would eventually study and grow to appreciate years later as a research topic for my undergraduate thesis.

At SUNY Brockport, after several semesters of classic undergraduate indecision, I found myself in a small Earth Sciences department where faculty encouraged undergraduates to become involved in their active research. It was there that I had the privilege to attend the lectures and discussions of Dr. Whitney Autin and Dr. Judy Massare, where the fundamentals of our interdisciplinary science were capably instilled into our young minds. Under their advisement, I was given the opportunity to add and expand their research of Pleistocene depositional and surficial processes of Western New York for my senior thesis on esker delta processes, on the same landmarks I had sat and chatted with my grandfather many years ago.

From there, I pressed on and prepared for graduate school. Travelling to Blacksburg for graduate school at Virginia Tech, I immediately found myself at home in the beautiful Valley and Ridge with a stellar group of faculty and graduate students from all over the world. Here I made life-long friendships with many of my lab colleagues, including Sam Denning, William Rouse, Tina Blue, Kat McFadden, Erik Haug, Phil Prince, Ben Roth, Clayton Loehn, Khalaf Al-Temimi, Nino Ripepi, Brad Kelley and JoBeth Carbaugh. These friends all played active roles in field and lab data acquisition, concept discussion and encouragement.

Special thanks are needed for my graduate advisor, Dr. Ken Eriksson. Throughout each of these projects, he has been a dedicated mentor, keen instructor, good-humored colleague, discerning wine enthusiast, and always a strong advocate for my professional development as a critical thinker and scientist. I look forward to partnering again with Ken on future research projects, exploring key issues in our understanding of the sedimentary record.

Finally, I need to recognize my wonderfully patient & beautiful wife, Katie O'Donnell and my kind and loving family, Wendell, Diane and Alissa Grimm. Their unwavering support and investments of time and treasure into my many years of education have been crucial to my success. It has been a long road, but it has certainly been worth it. I hope to one day give back as much as you all have given me.

TABLE OF CONTENTS

LIST OF FIGURES

CHAPTER 2

CHAPTER 3

LIST OF TABLES

Chapter 1 – INTRODUCTION

Preface: This chapter introduces the aims of several lines of research and outlines the contents of each chapter of the dissertation.

1.1 DISSERTATION AIMS

The chief objective of this dissertation is to investigate the siliciclastic stratigraphic response to icehouse-type, high-magnitude sea level fluctuations in a tectonically active foreland basin. Early Pennsylvanian strata of the Breathitt Group in the Pocahontas Basin of southwestern Virginia provide an opportunity for a unique review of spatial and temporal changes in depositional environments and accommodation during the concurrent Late Paleozoic Ice Age and the Alleghanian Orogeny. New surface exposures and a rich subsurface dataset of cores and wire line logs allow for a fresh assessment of this poorly understood interval. The primary motivation for this research is based upon the following scientific questions:

Question 1: What depositional environments can be recognized by facies analysis in the Pocahontas Basin? Question 2: How are these facies organized into a sequence stratigraphic basin architecture?

Rationale: The repetitive facies associations in these coal-bearing deposits of the Appalachian Basin were first termed cyclothems by **Wanless and Shepard (1936)** and have been inferred by many workers to be controlled by glacio-eustatic driven changes to global base level as continental ice volumes on Gondwana waxed and waned **(e.g. ., Busch and Rollins, 1984, Heckel, 1986; Isbell et al, 2003; Rygel et al., 2008; Greb et. al., 2008).** Interpreting these cycles with modern sequence stratigraphic concepts **(Posamentier and Vail 1988; Miall 1991; Posamentier and Allen 1999; Catuneanu, 2002)** together with a hydrodynamic deposystems process approach **(e.g. Dalrymple et. al., 1992; Schumm, 1993; Wright and Marriott, 1993; Shanley and McCabe, 1994)** allows for a comprehensive method to defining architectural elements and construction of a stratal hierarchy.

This study builds on previous stratigraphic interpretations of the Breathitt Group in Kentucky by **Aitken and Flint (1996) and Greb et al., (2004). Aitken and Flint (1996),** using

the methods of **Van Wagoner et al., (1988)**, constructed a sequence stratigraphic model of Middle Pennsylvanian strata in the Kentucky part of the Central Appalachian Basin. **Greb et al., (2004),** using sections from **Chesnut (1992; 1994)** and some additional data developed a sequence stratigraphic model for the same strata and extended into the Lower Pennsylvanian of Virginia along a single section line. Herein, we expand upon these studies spatially in the deeper part of the Pocahontas depocenter using multiple cross sections and core data to review detailed facies distribution patterns expanding facies descriptions and extending sequence stratigraphic interpretations into the Pocahontas depocenter of southwestern Virginia.

Question 3: What are the primary controls on facies distribution and sequence development? Question 4: How can they be differentiated to develop an accurate account of basin history?

Rationale: Alluvial facies distributions and resultant stratal patterns in alluvial/shallow marine foreland basins have been demonstrated to be controlled by a combination of tectonic phases and glacioeustatic sea level fluctuations (**Miall, 1981; Posamentier and Allen, 1993; Wright and Marriott, 1993; Shanley and McCabe, 1994; Mackey and Bridge, 1995).** Fundamental criteria for the recognition of tectonic controls in foreland basins include rapid changes in the relative distribution of longitudinal and transverse alluvial facies belts (**Burbank, 1992; Paola et al., 1992),** enhanced transgressions (**Tankard, 1986; Blair and Bilodeau, 1988),** intraformational unconformities and abrupt changes in siliciclastic provenance (**Miall and Arush, 2001**). In the Early Pennsylvanian Pocahontas Basin, the relative distribution of lowstand fluvial facies and long-term stacking patterns within the context of an ancient, marginal-marine foreland basin may provide independent stratigraphic evidence to disentangle a recurring, residual tectonic signature from high- frequency, periodic glacioeustatic events.

Question 5: How might our understanding of the facies distribution and petrophysics of these coal-bearing sedimentary rocks be applied to beneficial geological storage of CO_2?

Rationale: A potential method for reducing the amount of anthropogenic carbon dioxide (CO_2) released to the atmosphere is carbon capture and storage **(e.g., Pacala and Socolow, 2004)**. Carbon storage research in geological reservoirs has expanded in importance for industrial, academic, and government carbon management studies **(Reichle et al., 1999; Benson and Cole, 2008; USDOE - NETL, 2008a).** In the Appalachian region of the United States, research into potential geological storage reservoirs is especially important because much of this region relies on coal-fired electricity generation and has high per capita CO_2 emissions **(USDOE NatCarb Atlas, 2008).** The central Appalachian basin has several types of potential geologic storage options, including the use of deep, unmineable coal seams. This technique may allow for simultaneous carbon storage with the added economic benefit of CO_2 enhanced recovery of coal bed methane (ECBM).

Recent investigations by the U.S. Department of Energy's Southeast Regional Carbon Sequestration Partnership (SECARB) suggest that these coal-bearing sedimentary rocks have potential for use of CO2 with ECBM production **(USDOE-NETL, 2008a)**. SECARB estimates 1.3 billion tons of technically feasible CO_2 storage capacity in coal beds of the Pocahontas Basin, with enhanced recovery potentially increasing CBM reserves by an additional 2.5 TCF **(Ripepi, 2009)**. With the potential for using carbon dioxide to enhance coal bed methane recovery in this coal and gas rich interval **(Ripepi, 2009),** an improved stratigraphic and petrophysical understanding these coal-bearing sedimentary rocks is vital for better resource prediction and to optimize field development strategies for operators in southwestern Virginia. More research is considered critical to developing a regional leakage risk screening model suitable for ECBM site and target selection in central Appalachia.

1.2 DISSERTATION LAYOUT

This dissertation includes three separate manuscripts that have been submitted to or are in the process of submittal to international geological journals (Chapters 2, 3 and 4). The main objectives of each chapter are briefly reviewed below:

Chapter 2 (Manuscript submission pending to *Sedimentology*) introduces the primary dataset for the larger study: facies analysis from outcrops, cores, subsurface wireline log data and cross sections across the Pocahontas Basin depocenter. This manuscript constructs a sequence stratigraphic framework for evaluating controls on basin architecture.

Chapter 3 (Manuscript submission pending to *Basin Research*) builds upon the constructed sequence stratigraphic framework by integrating available petrographic, detrital zircon provenance and isopach data of major sandstones interpreted as ancient fluvial deposits. The distribution of contrasting fluvial networks can provide a measure to differentiate low-frequency variations in tectonic controls on accommodation from high-frequency glacioeustatically driven depositional sequences.

Chapter 4 (Manuscript submitted and in revision for the *International Journal of Coal Geology*) focuses on evaluation of the CO_2 confining properties and distribution of several key lithostratigraphic units hosting target CO_2-Enhanced Coal-Bed-Methane (ECBM) reservoirs in the Pocahontas Basin.

1.3 AUTHOR CONTRIBUTIONS

Chapter 2: Grimm, R. P., Eriksson, K.A., Rouse, W., Bodek, R., Denning, S.F.

Sequence Stratigraphy of Foreland Basin Siliclastic Deposits: Insight from the Early Pennsylvanian Pocahontas Basin, USA

Author contributions:

Grimm, R.P.: Principal investigator and author. All primary data collection, processing and interpretation.

Eriksson, K.A., Discussion and detailed manuscript review

Rouse, W., Field assistance, discussion and manuscript review

Bodek, R., Discussion and manuscript review

Denning, S., Field assistance, discussion and manuscript review

CHAPTER 3: Grimm, R.P., Eriksson, K.A., Carbaugh, J.

Orogenic Controls on the Spatial and Temporal Distribution of Longitudinal and Transverse Alluvial Facies in an Early Pennsylvanian Foreland Basin, Virginia

Author contributions:

Grimm, R.P.: Principal investigator and author. All primary data collection, processing and interpretation.

Eriksson, K.A., Discussion and detailed manuscript review

Carbaugh, J., Petrologic lab assistance, discussion and manuscript review

CHAPTER 4. Grimm, R.P., Eriksson, K.A., Ripepi, N., Eble, C., Greb, S.F

Seal Evaluation of Early Pennsylvanian coal-bearing strata, Virginia: The Potential for Safe Carbon Dioxide Storage with Enhanced Coal Bed Methane Recovery

Author contributions:

Grimm, R.P.: Principal investigator and author. All primary data collection, processing and interpretation.

Eriksson, K.A., Discussion and detailed manuscript review

Ripepi, Field assistance, discussion and detailed manuscript review

Eble, C., Lab assistance, discussion and manuscript review

Greb, S.F., Discussion and detailed manuscript review

CHAPTER 2
Sequence Stratigraphy of Foreland Basin Siliclastic Deposits:
Insight from the Early Pennsylvanian Pocahontas Basin, USA

RYAN P. GRIMM [1], KENNETH A. ERIKSSON [1], WILLIAM ROUSE [2], ROBERT BODEK [3], SAMUEL F. DENNING [4]

1. *Department of Geosciences, Virginia Tech, Blacksburg, Virginia 24061, USA*
2. *United States Geological Survey, Reston, Virginia USA*
3. *BP, Houston, Texas, USA*
4. *Huntington, West Virginia, USA*

ABSTRACT

Early Pennsylvanian, coal-bearing, siliciclastic strata of the Breathitt Group within the Pocahontas Basin, southwestern Virginia, define a southeasterly thickening clastic wedge deposited in continental to marginal marine environments influenced by recurring, high-magnitude relative sea level fluctuations and low frequency changes in tectonic loading. The dataset of more than 1200 well logs, five continuous cores and numerous outcrops allowed a unique review of the Central Appalachian lithologic record during both the Late Paleozoic Ice Age and onset of the Alleghanian Orogeny.

The tropical depositional landscape produced stacked deposits of braided fluvial channels, broad alluvial plains, tidally influenced estuaries and small deltas. Trends in facies associations allowed development of a high-resolution sequence stratigraphic architecture based on regional flooding surfaces and bounding discontinuities. Analysis of vertical stacking patterns of lithofacies on regional cross sections identified 15 widespread, unconformity-bounded depositional sequences with an average duration of approximately 80 kyr based on available geochronology.

The observed stratigraphic architecture can be explained by the interplay of glacioeustatic and tectonic mechanisms. Strong glacioeustatic control on stratigraphic architecture is strongly supported by corresponding sequence duration within the short eccentricity periodicity of the Milankovitch band, as well as themagnitude and extent of rapid facies shifts, suggesting that far-a-field variations in overall Gondwanan ice-sheet size and volume impacted base-level changes in the tropical basin. The progressive increase in magnitude and extent of transgressions, as indicated by increasing brackish-marine ichnofacies and other faunal indicators within regional

high frequency transgressive system tracts, are interpreted to indicate extrabasinal trends in ice volume and eustasy.

High-frequency eustatic sequences are nested within four asymmetric composite sequences, attributed to low frequency variations in tectonic accommodation. Evidence for tectonic forcing on foreland basin accommodation is based on abrupt facies shifts, angular stratal terminations and wedge-shaped composite sequence geometries. Spatial and temporal trends in facies associations within composite sequences reveal episodic variation in tectonic loading overprinted by recurring high-frequency eustatic events.

1. Introduction

Early Pennsylvanian strata of the Breathitt Group in the Central Appalachian Basin of southwestern Virginia provide an opportunity to investigate the siliciclastic stratigraphic response to icehouse-type, high-magnitude sea level fluctuations in a foreland basin. The repetitive facies associations in these coal-bearing deposits of the Appalachian Basin were first termed cyclothems by **Wanless and Shepard (1936)** and have been inferred by many workers to be controlled by glacio-eustatic driven changes to global base level as continental ice volumes on Gondwana waxed and waned **(e.g. ., Busch and Rollins, 1984, Heckel, 1986; Isbell et al, 2003; Rygel et al., 2008; Greb et. al., 2008).** Interpreting these cycles with modern sequence stratigraphic concepts **(Posamentier and Vail 1988; Miall 1991; Posamentier and Allen 1999; Catuneanu, 2002)** together with a hydrodynamic deposystems process approach **(e.g. Dalrymple et. al., 1992; Schumm, 1993; Wright and Marriott, 1993; Shanley and McCabe, 1994)** allows for a comprehensive method to defining architectural elements and construction of a stratal hierarchy.

The Early Pennsylvanian Breathitt Group extends over 8,200 km^2 in the central Appalachian Basin across southwestern Virginia, eastern Kentucky and southern West Virginia **(Fig. 2.1).** This interval is preserved as a clastic wedge in the Pocahontas Basin **(Arkle, 1974)**. Portions of the Early Pennsylvanian Breathitt Group are well exposed in outcrops along the flanks of the Pocahontas Basin. The stratigraphic succession is also penetrated in the subsurface because it is an important producer of coal bed methane, thus providing a robust dataset of core and geophysical wireline logs **(Fig. 2.2)**.

The major goals of this research are: (1) to integrate outcrop, core, and closely spaced well-log data to define key sedimentary facies associations and key stratigraphic surfaces; (2) to

develop a comprehensive, regional high-resolution depositional sequence model using stacking pattern analyses; and (3) to evaluate intrabasinal and extrabasinal controls on the stratigraphic architecture and stratal hierarchy in an ancient foreland basin. This study builds on previous stratigraphic interpretations of the Breathitt Group in Kentucky by **Aitken and Flint (1996) and Greb et al., (2004). Aitken and Flint (1996),** using the methods of **Van Wagoner et al., (1988)**, constructed a sequence stratigraphic model of Middle Pennsylvanian strata in the Kentucky part of the Central Appalachian Basin. **Greb et al., (2004),** using sections from **Chesnut (1992; 1994)** and some additional data developed a sequence stratigraphic model for the same strata and extended into the Lower Pennsylvanian of Virginia along a single section line. Herein, we expand upon these studies spatially in the deeper part of the Pocahontas depocenter using multiple cross sections and core data to review detailed facies distribution patterns expanding facies descriptions and extending sequence stratigraphic interpretations into the Pocahontas depocenter of southwestern Virginia. Moreover, with the potential for using carbon dioxide to enhance coal bed methane recovery in this coal and gas rich interval **(Ripepi, 2009),** an improved stratigraphic understanding these coal-bearing sedimentary rocks is vital for better resource prediction and to optimize field development strategies for operators in southwestern Virginia.

2. 1 General Geologic Setting

The Pocahontas Basin, a sub-basin of the Central Appalachian Basin, preserves the late Mississippian and earliest Pennsylvanian sedimentary record. This depocenter formed in response to foreland subsidence as successive thrust sheets loaded the Laurentian craton at the onset of collisional assembly with Gondwana during the Alleghanian Orogeny (e.g. **Quinlan**

and Beaumont, 1984; Tankard, 1986; Flemings and Jordan, 1990). In Virginia, the early Pennsylvanian, coal-bearing, siliciclastic strata of the Lower Pennsylvanian define a southeasterly thickening clastic prism that unconformably overlies late Mississippian rocks **(Chesnut, 1994; Beuthin, 1997)**. In the structurally deepest part of the depocenter, the Mississippian-Pennsylvanian unconformity persists, where basal Pennsylvanian sandstones fill broad incisions into the Arnsbergian age Bluestone formation or are separated by a thick paleosol complex (**Blake and Beuthin, 2008).**

Coal-bearing, immature siliciclastic strata of the Breathitt Group record deposition of transverse fluvio-estuarine facies of mudstones and sublithic sandstones, derived from southeastern low grade metamorphic and Grenvillian-Avalonian terranes uplifted during the Alleghanian orogen **(Davis and Ehrlich, 1974**; **Houseknecht, 1980; Eriksson et al., 2004; Reed et al., 2005).** These sediments formed channeled sandstone-mudstone bodies 1-10 km wide as much as to 30 m thick, which filled broad alluvial valleys transverse to the thrust front (**Korus, 2002).** This transverse system contrasts with quartzose sandstone bodies typically found in longitudinal belts across of eastern Kentucky (**Chesnut, 1992; Greb and Chesnut, 1996)**. These "Lee"-type sandstones are texturally and mineralogically mature quartzarenites that were deposited as strike-parallel elongate belts 17-100 km wide and as much as 200 m thick along the western periphery of the basin, between the lithic-rich Breathitt Group and the elevated Cincinnati Arch (**Rice, 1984; Chesnut, 1988)**. These mature quartzarenites were first interpreted as barrier bar deposits **(Hobday and Horne, 1977; Ferm and Horne, 1979**) but are now recognized as multi-cycle, braided, fluvial sandstones deposited within northeast to southwest-oriented axial drainages. Detailed sedimentology and architectural element analysis of the Bee Rock and Corbin member quartzarenites by **Wizevich (1992)** revealed strong evidence for a

braided-fluvial system. Closely-spaced erosion surfaces, fining-upward sequences, unidirectional paleocurrents for bedforms and macroforms, channel scour-and fill-structures, levee deposits, rhizoliths, the absence of marine body fossils, and extremely rare trace fossils in channel sandstones all support a braided fluvial origin over a tidal bar / barrier bar interpretation, although each belt locally exhibits vertical transitions to tidal-estuarine deposition (**Greb and Chesnut, 1996)**. This major river system, on the scale of the Amazon River, was head-watered in a northerly cratonic source area with some input from the Archean southern Canadian Shield (**Houseknecht, 1980; Rice, 1984; Rice and Schwietering, 1988; Archer and Greb, 1995; Greb and Chesnut, 1996; Eriksson et al., 2004).**

The regional drainage pattern was to the west and southwest, dispersing sediment down a paleoslope toward the Black Warrior Basin and Ouachita Foredeep (**Shlee, 1963; Graham et. al., 1975; Archer and Greb, 1995).** These early Pennsylvanian continental to marginal marine deposits filled the Pocahontas depocenter. It was positioned approximately 10 degrees south of the equator **(Scotese and McKerrow, 1990)** in an ever-wet tropical climate of chemically reduced substrates and base-depleted paleosols **(Cecil, 1990).** This environment periodically provided a setting conducive to widespread peat deposition, preserved as regional tabular, coalbeds that provide excellent marker beds for correlation.

The four coal-bearing lithostratigraphic units investigated include the Pocahontas, Bottom Creek, Alvy Creek and Grundy Formations of Chesnut (1992), which are juxtaposed against and are intercalated with the Warren Point **(Nelson, 1925)**, Sewanee **(Safford, 1893**) and Bee Rock (**Stevenson, 1881)** quartzarenite lenses of the Lee Formation **(Campbell, 1893).** These lithostratigraphic units are further subdivided by regionally thick, marine-influenced shale members; the Dark Ridge (**Englund, 1974; Rice et al., 1979)**, Hensley (**Englund and Delaney,**

1966) and Dave Branch (**Chesnut, 1994**) shales as summarized in the chart of lithostratigraphic relationships in **Figure. 2.3**.

Geochronologic data for the early Pennsylvanian of North America is limited, however biostratigraphic and radiometric dates within the Pocahontas Basin allow for an estimation of the total time represented by the study interval. Correlation of palynological data with European successions indicates that coalbeds within the basal portion of the Pocahontas Formation correlate with the Namurian C stage of Europe (**Eble, 1996; Fig. 2.3).** Additional chronostratigraphic data is provided by an age of **316.1 ± 0.8 Ma** for ash deposits in the Upper Banner coal (**Lyons et al., 1997; Fig. 2.3).** According to correlation charts assembled by **Gradstein et al., (2004) and Menning et al., (2006)** the base of the Namurian C is approximately 318.1 to 317.3 Ma. If the entire lower part of the Namurian C is preserved in the Pocahontas Basin, then the interval between the Banner Coal and the base of the study interval in southwestern Virginia represents approximately 2 to 1.2 m.y. of geologic time.

Most of the strata in the study are preserved in the Middlesboro Syncline of the Cumberland Overthrust Block. The Cumberland Overthrust Block is bound to the west by the Pine Mountain Thrust Fault (the western limit of Alleghanian deformation) and to the east by the Hunter Valley - St. Clair Fault Zone and older folded Paleozoic rocks (**Butts, 1927; Rich, 1933; Fig. 2.1**). Numerous smaller outcrops along the Hunter Valley Thrust allow examination of portions of the eastern proximal succession along minor river valleys and roadcuts**.** In addition to outcrop exposures, a dense subsurface database of geophysical well logs and exploratory cores from coal-bed methane and conventional gas development provides an exceptional opportunity for subsurface stratigraphic analysis (**Fig. 2.2)**. Data presented in this study are from

southwestern counties of Virginia, with additional data from southern West Virginia allowing the evaluation of the lateral continuity of key horizons.

3. Methods

Facies were described at **23** outcrop-measured sections in large roadcuts, abandoned mine workings and several natural ravines and in seven cores donated to Virginia Tech from coal exploration operations (**Fig. 2.2**). Facies were described based on color, lithology, bounding contacts, sedimentary structures, fossil/ichnofabric content and stratal geometries (**Table 2.1)**. Paleocurrent data were measured at several field locations containing accessible tabular and trough cross-beds and plotted as rose diagrams for each sandstone unit. Gamma ray scintillometer data were collected from outcrops as well as core descriptions to calibrate geophysical well logs and allow facies variability and key sequence surfaces to be traced into the subsurface. Measured section locations are provided as a Google Earth KMZ file in the appendix.

Data from **4,000** development wells were also used to compile **10** cross sections through the study interval (**Fig. 2.2**). Gamma ray and bulk density curves provided proxies for lithologies. Trends in texture and distinctive lithological contacts were interpreted from gamma ray log motifs and bulk density curves define coal horizons, which have dramatically lower densities than surrounding siliciclastic lithologies. Correlations were accomplished using pattern matching of distinctive stratigraphic surfaces and marker beds such as regional coals and thick shale submembers.

4. Facies Associations and Interpretations

Facies documented in **Table 2.1** are organized into five facies associations in **Table 2.2.** The facies associations represent fluvial-longitudinal, fluvial-transverse, estuarine, inner shelf and deltaic depositional settings. Each facies association is defined by a combination of physical and biogeochemical characteristics.

Fluvial Facies Association – Longitudinal

Description: This facies association is dominated by quartzarenite that forms 10-50 m thick, regional, multistory sandstone bodies of the Warren Point, Sewannee and Bee Rock formations **(Fig. 2.2).** Lithofacies range from massive quartz-pebble conglomerate (subfacies Gm) to fine-grained sandstone. These white to light gray sandstones tend to be coarser grained toward the base, with common channel lags of 1-5 cm diameter quartz pebbles, 0.2-1m long logs and oriented plant fragments observed at outcrops and in core (**Fig. 2.4A**). Lags and flute structures (**Fig. 2.4B**) define scoured basal contacts with underlying strata. Locally, conglomerate bodies are as much as **5** m thick. Crossbeds are dominantly planar (subfacies Sp, **Figs. 2.4C and 2.4D**), tangential (subfacies St, **Fig. 2.4E**) and trough (subfacies Str) and form long (25-100 m), traceable tabular to wedge-shaped bedsets, 0.5-1.5 m thick. Rarely, tabular crossbed sets are truncated by reactivation surfaces, which form the base for compound crossbedding (subfacies Sc, **Fig. 2.4F**). Paleocurrent data from well-exposed crossbedded units agree with the orientation of flute structures and log casts, and indicate unimodal paleocurrents to the west-southwest and south-southwest for the Warren Point and Bee Rock Sandstone members, respectively (**Fig. 2.4G and 4H**). Sandstone intervals are capped by rippled facies (subfacies Sr) overlain by heavily

rooted siltstones. In the subsurface, quartzarenites provide a very distinctive low, blocky gamma ray signature, with a well-defined, sharp base and with gamma ray values gently increasing at the top of sandstone bodies as a result of an increase in siltstone content (**Fig. 2.5**).

Interpretation: The conglomerate lags coupled with the size and variety of dune-scale cross strata, unimodal paleoflow indicators and floodplain type protosols (rooted siltstones) supports a braided- fluvial origin for this facies association, as previously interpreted by (**Rice, 1984; Rice and Schwietering, 1988; Wizevich, 1991; Archer and Greb, 1995; Greb and Chesnut, 1996)**. Large macroforms within the Bee Rock, Sewannee and Warren Point sandstones are commonly tabular to wedge-shaped, with rare convex-up macroforms which preserve dune crests, while others are concave-up, representing deep channel scour-and-fill deposits. Dominant macroforms are interpreted as downstream accreting elements and compound channel macroforms. Scours are interpreted as the result of erosion processes intrinsic to fluvial channel bends and confluences (**sensu Salter, 1993).** In braided systems, individual bars are commonly only partially preserved, as the architecture is modified by short-term subsequent scour and fill events **(Miall, 2006**). Macroforms provide an estimate of the maximum height of ancient bar forms (0.5-1.5 m) and minimum water depths (**Miall, 1996). Wizevich (1992)** estimated river depths of 20 m for similar quartzose sandstones of the Rockcastle Conglomerate of Kentucky, assuming that the macroform height is just less than half of bankfull depth. Width/thickness ratios of individual stories exceed 20:1, which further supports a sheet-braided fluvial origin (**Cotter, 1978**). Similar facies and stratal architectures have been interpreted as the depositional products of ancient braided fluvial systems **(Bristow, 1993; Lopez-Gomez and Archer, 1993; Miall and Jones, 2003),** analogous to the modern Brahmaputra River **(Bristow, 1987).**

Fluvial Facies Association – Transverse

Description: This facies association is dominated by coarse-to-fine-grained sandstone that forms 5-20 m-thick amalgamated sandstone bodies with a general fining-upward trend of stacked, erosionally bounded intervals. These sandstone bodies overlie sharp erosional surfaces that exhibit 2-10 m of localized relief (**Figs. 2.6A and 2.6B).** In outcrop and core, these sandstones are medium gray along fresh surfaces, with common basal siderite, shale fragment and plant debris conglomerate lags **(Fig. 2.6C**). Rare quartz pebbles exhibit a bluish tint suggestive of a Grenvillian provenance (**Herz and Force, 1984)**. Sandstones are rich with schistose metamorphic rock fragments, biotite, feldspar and polycrystalline quartz and are classified as sublitharenites (**sensu McBride, 1963; Dott, 1964**). Modal compositions average 77% quartz, 15% lithics, 8% feldspar, with metamorphic and sedimentary clasts dominate the lithic portion (**Reed, 2003; Reed et al., 2005).**

Trough cross beds (subfacies Str) predominate, **(Fig. 2.6D)** with minor planar crossbeds (subfacies Sp), horizontal parting laminations (subfacies Sh) and climbing ripples (subfacies Sr) at the top of sandstone bodies. Cosets range from 0.1-2 m thick. Paleocurrent modes are dominantly to the northwest (**Fig. 2.6E**), notably at right angles to the longitudinal facies association. Toward the top of several major sublitharenite sandstone bodies, lateral accretion sets are developed. These accretion surfaces extend laterally for 10's of meters (**Fig. 2.6F)** and are oblique to west-southwesterly paleoflow.

Sandstone bodies fine upward into complexly interbedded fine- to medium-grained sandstone and siltstone with common climbing ripples, ball-and-pillow structures, and rooted top surfaces below tabular coal horizons (**Fig. 2.6G).** Generally mudstone underlies coal seams at the

top of fining-upward intervals. Dark gray mudstone underlying coalbeds universally grades upward into thin, gleyed, rooted mudstones (subfacies Fu) with drab, blocky textures and common *Stigmaria* root structures and other plant fragments (**Fig. 2.6H).** Coalbeds (subfacies O) range from 0.1 m to 2 m in the study interval and are classified as low to high volatile bituminous rank with low sulfur contents **(Milici et al., 2000).**

In a similar manner to the longitudinal fluvial facies association, the transverse fluvial facies association exhibits a blocky gamma-ray signature that is capped by a sharp, bell-shaped increase in gamma ray values related to an increase in clay content. Sublitharenite is distinguished from quartzarenite by slightly higher gamma ray values (15-30 API units), which is caused by an overall increased lithic content as determined from core-log calibration **(Fig. 2.5).** Rarely, basal lags are indicated by increased gamma ray values at the base of major sublitharenite sandbodies. Coals register a very low spike on the bulk density wireline log curve (RHOB).

Interpretation: As with the fluvial longitudinal facies, the fluvial transverse facies association is interpreted as the deposit of braided fluvial channels and overbank and floodplain settings. A freshwater setting is supported by the paucity of bioturbation or marine body fossils and the abundance of terrestrial indicators such as regional and local coalbeds with associated rooting, pedogenetic modification of the exposed substrates, as well as plant-debris lags found within basal bedload lags. Siderite pebbles and angular shale fragments in basal conglomerates are poorly sorted with similar characteristics to underlying shales, suggestive of an intrabasinal origin.

The predominance of trough crossbeds indicates the migration of three-dimensional dunes, separated by scours filled with gravel lags produced by high-energy, fluvial currents. Planar to climbing-ripple structures at the top of sublitharenite sandstone bodies suggest waning-flood deposits. The local presence of planar crossbedding and the abundance of trough crossbedding indicate migration of unidirectional, subaqueous dunes as part of a bed-load dominated system, although of a smaller scale than those that existed in the longitudinal fluvial system, suggesting a smaller, possibly more perennial hydrodynamic regime **(sensu Schumm, 1981)**.

Rare lateral-accretion elements are interpreted as the product of meandering point-bar migration (**Allen, 1964; Miall, 1981**). This represents a change in fluvial style from a sand-dominated, low-sinuosity braided river system to a higher-sinuosity river system prior to channel abandonment (***sensu* Miall, 1996**). This facies association is considered equivalent to the "Major Stacked Fluvial Bodies Facies Association" described by **Aitken and Flint (1995)** in the middle Pennsylvanian system of eastern Kentucky. The transverse fluvial association is interpreted as the product of tributary rivers originating in the highlands to the southeast and sourcing sediments primarily from exhumed and recycled older sedimentary and metamorphic rocks from the emerging Alleghanian orogen.

Coalbeds and underlying rooted and mottled siliciclastics represent ancient histosol deposits (**Mack et al., 1993; Retallack, 2001**) The underlying sediments exhibit evidence of pedogenetic modification, such as blocky soil structure, small-scale slickenslides and drab redox mottling. The coal itself is interpreted as the product of *in situ* accumulation of organic matter as in the O horizon of soil horizon classification (**USDA, 1984),** which can form in a variety of peat-forming wetland settings (**Diessel, 1992; Hampson et al., 1999).** Appalachian coalbeds

have been interpreted as the accumulations of topogenous (planar, productivity and preservation from surface/ground water) and ombrogenous (raised, productivity from meteoric waters) peat mires **(Donaldson et al., 1985; Eble et al, 1991; Eble, 1996).** Peat development has been suggested to represent periods of prolonged humidity, whereas siliciclastic partings within coals may represent short-term depositional events **(Martino, 1996).** Low-sulfur concentrations in the coals of the Pocahontas Basin have been suggested to reflect a terrestrial depositional environment with very limited syndepositional or post-depositional sulfate contributions from overlying roof shales, as is common where coalbeds are overlain by open marine strata (**Casagrande, 1987; Staub, 2002**). In both the fluvial longitudinal and transverse facies associations, coals capping fining-upward successions are interpreted as having formed on drowned, abandoned floodplains. Silt partings in coals are interpreted as overbank deposits of crevasse splays from interdistributary channels.

Estuarine Facies Association

Description: Fluvial facies associations are gradationally overlain by a variety of **3-10 m** thick, tabular, fining- upward intervals of heterolithic facies of the estuarine facies association. Sandy heterolithic facies (subfacies Fis) dominate and consist of 1-4 m-thick intervals of wavy-flaser to bifurcated-wavy-flaser bedding (***sensu*** **Reineck and Wunderlich, 1968)** with intercalated thin beds of rippled, fine-grained sandstone (subfacies Sr). Ripple cross-laminated sets are separated by mm-thick, commonly bifurcating mudstone drapes (**Fig. 2.7A**) or by continuous mudstone partings up to 11 mm thick **(Fig. 2.7B)**. Heterolithic mudstone facies of the estuarine facies association are dominated by parallel-laminated siltstones (subfacies Fs) and lenticular bedding (subfacies Fif, **Fig. 2.7C**).

Laminae couplets of parallel-laminated sandstone-siltstone and thin layers of mudstone are common in this facies association and exhibit cyclic variations in laminae thicknesses (**Figs. 2.7D, 2.7E**). These variations in **Fig. 2.7E** display an apparent, gradual increase and decrease in thicknesses of sandstone-siltstone laminae, forming bundles (**Fig. 2.7F**). Bundles contain between 8 and 14 couplets. Rare rooting is present. Plant debris is abundant, with commonly preserved plant leaves (**Fig. 2.7G**) and rare upright, in-situ plant remains. At several field locations, *Calamites* are preserved in growth position within laminated siltstones. Bioturbation intensity is generally low, with dominant ichnogenera limited to horizontal burrows of *Planolites* and *Paleophycus* (**Fig. 2.7H)** and vertical *Lockeia*-type escape structures. The heterolithic nature of estuarine facies can have irregular wireline log characteristics, but generally exhibit upward-increasing gamma ray values, reflecting fining-upward grain size.

Interpretation: A variety of estuarine processes are represented within this facies association. Estuarine settings are typically brackish with seasonal fluvial inputs modified by tidal currents with a variety of periodicities. Transgressive Quaternary estuarine analogs for the estuarine facies association include the Bay of Mont-Saint-Michel (**Tessier et al., 1995**) and the James River estuary (**Nichols et al., 1995**).

Heterolithic flaser-bedded, wavy-bedded and lenticular bedded facies are indicative of periodic, short-lived bedload deposition alternating with suspension settling of fines during low-energy, slack-water stages and are suggestive of tidal influences (**Reineck and Wunderlich, 1968; Kvale et al, 1989**). Stronger evidence for tides is indicated by the thickening and thinning cycles of laminae couplets. Each couplet is interpreted as the result of suspension fall-out of silty sand during peak tidal currents and suspension fall-out of clay during the following slack-water period, reflecting semidiurnal tidal current deposition (**Kvale and Archer, 1989**). Thickening

and thinning bundles (**Fig. 2.7F**) are interpreted as neap-spring-neap cycles in which thicker couplets record spring tide deposition and thinner couplets record neap tide deposition. Most of the cycles are incomplete and this is attributed to limited sediment supply during the neap phase. Similar complete and incomplete neap-spring-neap cycles are widely reported from the Carboniferous record of the Central Appalachian Basin (**e.g., Martino and Sanderson, 1993; Greb and Chesnut, 1996; Martino, 1996; Miller and Eriksson, 1997; Adkins and Eriksson, 1998; Greb and Martino, 2005; Korus et al., 2008).** These rooted rhythmite deposits are interpreted as vegetated subtidal deposits, preserved in an upper estuarine setting where tidal signals were amplified, bioturbation was limited and aggradation rates were high **(Dalrymple, 1992; Tessier, 1993).**

The limited development of *Planolites* and *Paleophycus* feeding structures and subordinate occurrence of *Lockeia*, indicate a low-diversity benthic community stressed by fluctuating salinities (**Pemberton and Frey, 1982; Pemberton and Wightman 1992**). The presence of marginal-marine burrow traces as well as the *in-situ* burial of upright *Calamites* suggests a rising base level.

Inner Shelf Facies Association

Description: The estuarine facies association is gradationally overlain by 10-40 m thick, tabular intervals of fine-grained deposits of the inner shelf facies association. Dominant facies are black to dark gray, fissile, parallel-laminated, laterally persistent (100's km^2) shales (subfacies Fc) with high organic contents (TOC 2-15%) and common siderite stringer horizons or large siderite concretions (0.5-1m) (**Fig. 2.8A)**, that alternate with low to moderately bioturbated, laminated siltstone (subfacies Fs). Common ichnogenera include horizontal to oblique burrows of

Planolites, Helminthopsis, and distinctive horizons of *Neonerities Missouriensis* with *Phycosiphon* (**Figs. 2.8B, 2.8C, 2.8D).** *Neonerites-Missouriensis* burrows are on average 7 mm wide and typically more than 10 cm long with obvious backfill structures. Regular vertical burrows include *Phycodes* (**Fig. 2.8E)**, and *Cylindrichnus* (**Fig. 2.8F).** Localized occurrences of bivalve body fossils, including brachiopods **(Fig. 2.8G),** are present in the basal mudstone facies of this association in the Dave Branch Shale Member. Shelf facies are identified on wireline logs on the basis of uniformly high gamma ray values above upward increasing values of estuarine successions.

Interpretation: The inner shelf facies association is interpreted as deposits of a low-energy, restricted, marine-influenced, inner-shelf setting. Mud accumulation is common in central estuarine settings where flocculation promotes fallout of fine-grained material and high mud accumulation **(Kranck, 1981; Dyer, 1986).** Fissile black shale beds are widely recognized in the Appalachian Basin as deposits of deep marine, anoxic bottom water settings, where high fluvial input formed strong density gradients in basin centers and organic input from terrestrial sources promoted oxygen uptake (**Chesnut, 1981; Heckel, 1991; Pashin and Ettensohn, 1992; Bennington, 1996; Martino, 1996).**

The moderate abundance of deposit-feeding and rare suspension-feeding traces are typical of the *Cruziana* ichnofacies **(Frey and Pemberton, 1984).** *Neonerities missouriensis* are interpreted as shallow-marine deposit feeders (**Mangano et al., 2000).** Thin *Phycosiphon* bioturbated siltstones lamina sets are interpreted as the product of opportunistic deposit feeding behavior and colonization of storm-event sediments (**Wetzel and Bromley, 1994).** Concentrically lined burrows of suspension- and mining-feeding traces *Cylindrichnus* and

Phycodes indicate slow, continuous sedimentation rates **(Han and Pickerill, 1994; MacEachern and Pemberton, 1994).** The occurrence of marine invertebrate macrofossils within a low diversity *Cruziana* ichnofacies further supports a drowned, deepened embayment setting with occasional open-marine conditions that promoted intense bioturbation, and supported conditions favorable for occasional filter-feeding marine bivalves **(Buatois et al., 2005).**

Deltaic Facies Association

Description: The deltaic facies association gradationally overlies estuarine and inner-shelf associations, forming 10-50 m thick, coarsening-upward successions **(Fig. 2.9A)**. This association can be subdivided based on sedimentological characteristics into vertical successions of prodeltaic, delta front, distributary mouth bar, channel and interdistributary facies subassociations.

Prodeltaic facies are comprised of finely laminated mudstone (subfacies Fs) with rare thin (1-5 cm) interbeds of very fine-grained sandstone and siltstone (subfacies Fis). Silt-sand laminations thicken upward with an overall increase in grain size. Coarser-grained horizons are commonly cemented with siderite. Siltstone is sporadically burrowed with trace-fossil content limited to isolated examples of *Teichichnus* and *Planolites*. Several body fossils of *Carbonicola sp* . are present in cores within the regional Dave Branch shale member of the Grundy Formation **(Fig. 2.9B)**.

Prodeltaic facies coarsen upward into delta front facies, consisting of laminated siltstones (subfacies Fs) with intercalated sandstone beds (subfacies Sh). Non-rhythmic alternations of thin (0.5cm-1cm) interbedded siltstone and silty sandstone (subfacies Fis) contain wavy- to current ripple-laminated beds, rare slump features and common bioturbated intervals with vertical

fugichnia traces, *Skolithos* and *Rosselia* burrows. Very fine-grained sandstone beds (subfacies Sh) are commonly sharp-based, laminated to structureless, forming 1-30 cm thick tabular bodies that extend laterally for 100's of meters at outcrops, commonly containing abundant plant debris and ball-and-pillow dewatering structures and soft-sediment deformation **(Figs. 2.9C and 2.9D)**. Sandstone intervals are separated by 0.1-1 m thick silty mudstones (subfacies Fis, Fif, Fs) that contain high concentrations of preserved detrital plant debris **(Fig. 2.9E)** and bioturbated intervals containing common to abundant examples of *Teichichnus*, *Taenidium*, and more rarely, *Ophiomorpha* **(Figs. 2.9F and 2.9G)** and *Thalassinoides* **(Fig. 2.9H)**. Rare *lingulid* shells were found within the siltstones overlying the regional Dave Branch shale member of the Grundy Formation **(Fig. 2.9I)**.

Delta-front facies coarsen upward from interbedded silty-sandstone (subfacies Fis) to fine-grained sandstone beds (subfacies Sh, Sr), 5-140 cm thick, which are typically flaser and wavy-bedded to parallel laminated and normally graded beds of the distributary mouth bar facies. Mouth bar sandstone intervals are typically separated by 3-5 cm thick siltstone beds (subfacies Fif, Fis) with local lenses of plant debris. Locally, the tops of sandstone beds are intensely bioturbated, with burrow structures dominated by suites of *Fugichnia, Skolithos, Rosselia, Paleophycus,* and *Planolites* **(Fig. 2.9J)**.

Distributary channel facies are represented by 3-8 m thick, single-story, lenticular to tabular sandstone bodies. Channel facies typically fill 1-3 m deep incisions into underlying distributary mouth bar and delta front deposits with poorly sorted basal lags of coarse sandstone and plant debris overlain by massive to plane-parallel bedded fine-medium grained sandstones (subfacies Sh). Sandstone intervals fine upward and are commonly mantled by 1-5 m thick interdistributary deposits. These sheet-form packages are dominated by repetitive intervals of

laminated siltstone (subfacies Fs) interlayered with poorly sorted silty sandstone (subfacies Fis) and drab, mottled carbonaceous mudstones (subfacies Fu). Abundant root structures, drab mottles and thin, localized coalbeds (subfacies O) are common.

In the subsurface, the gamma ray log motif of the deltaic facies association form stacked intervals of gradationally decreasing gamma ray signatures as a result of progressive increases in sandstone content (**Fig. 2.5**), commonly capped by thin coalbeds marked by sharp decreases on the bulk density curve.

Interpretation: Thick deposits of laminated mudstones with rare body fossils and lacking root traces or signs of pedogenic alteration are interpreted as deposited in a subaqueous, low-energy environment, with an impoverished trace fossil assemblage indicative of harsh benthic conditions. Siderite is a common form of early diagenesis in fluvial-dominated deltaic systems (**Sellwood, 1971; Coleman and Prior, 1982; Bhattacharya and Walker, 1991**). Similar *Carbonicola*-type fossils have been observed in prodeltaic elements within Westphalian A sedimentary deposits of northern England (**Eagar, 1974**). Textural trends with overlying coarser deposits of delta-front elements support a prodeltaic interpretation with mudstone forming the base of classical progradational deltaic facies (**Barrell, 1912).**

Alternating deposits of sand and mud laminae with thick, sharp-based, interbedded sandstone sheets are interpreted as the product of seasonal variations in sediment-rich turbidity currents, fed from upland fluvial settings. Slump and dewatering/flowage structures provide additional evidence for episodic increases in sedimentation rates and resultant substrate failures due to rapid rates of sediment loading and compaction, and delta slope instability (**Coleman et al., 1998)**. Flaser- and wavy-bedding upwards in interval suggest shallow-water settings

influenced by a combination of tides and waves. The upward increase in proportion of laminated sandstone in the distributary mouth bar facies association support the general interpretation of continued progradation of delta systems over prodelta muds by aggradation of sediment settling out from a sediment plume immediately within and in front of a distributary channel mouth.

The observed coarsening-upward profiles have long been interpreted as the product of prograding deltas (e.g. **Ferm and Horne, 1979)**, now further substantiated by ichnological data. The dominance of a mixed *Cruziana-Skolithos* trace-fossil assemblage of deposit feeders suggests a low-oxygen, variable salinity, low energy environment, with considerable inputs of freshwater and organic material (**Gernant ,1972; Ranger and Pemberton, 1988; Strobl, 1988; Beynon and Pemberton, 1992; Buatois et al., 1997)**. Rare *Ophiomorpha* burrows further support a stressed environment and suggest a tropical–subtropical setting (**Goldring et al., 2004**), supported by regional paleogeographic interpretations **(Scotese and McKerrow, 1990)**.. The abundance of *Rosselia* and occasional *Thalassinoides* burrows within wavy-rippled beds supports a proximal delta- front setting with a shallow- marine influence during deposition. *Rosselia* dwelling burrows and *Lockeia* resting traces have been interpreted to form in marginal marine, brackish littoral environments with episodic sedimentation and fluctuations in salinity and flow energy (**Howard, 1975; Pemberton and Wightman, 1992; Martino, 1994; Buatois, et al, 1998; Pemberton et al., 2001; Nara, 2002**). Rare lingulid body fossils may suggest the organism responsible for preserved Lockeia feeding and resting behavior. *Thalassinoides* traces are interpreted as dwelling/feeding structures of endobenthic crustaceans which preferred silty-sand substrates in marginal marine, brackish-water salinity settings (**Pemberton et al., 1992; 2001**).

Distributary channel facies are interpreted as the product of channel infill, as these broad elements are weakly incised into underlying coarsening-upward deltaic deposits. Analogous distributary channel facies have been interpreted from the Middle Pennsylvanian of Kentucky (**Aitken and Flint, 1995; Ferm, 1970**) and the modern Mississippi delta (**Fisk et al., 1954; van Heerden and Roberts, 1988**). Interdistributary facies are recognized as the result of multiple surface processes on a delta plain, including moderate energy levee and overbank crevasse splays, and low energy interdistributary bay-fills succeeded by subaerial, root-penetrated peat mire deposits **(Elliot, 1974; Baganz et al., 1975**).

Overall, the deltaic facies association is the product of prograding, fluvial-dominated deltas, evidenced by the presence of thick basal mudstones, the gradual coarsening-upward trend of beds, channelization and subaerial exposure at the top of the succession, significant amounts of detrital organic matter, limited bioturbation and trace fossil diversity, uncommon wave modified sedimentary structures and common slump and dewatering features. Comparable fluvial-dominated deltaic deposits have been interpreted from the Westphalian of Europe (**De Raaf et al., 1965; Fielding, 1986**), Cretaceous (**Bhattacharya and Walker, 1991**) and modern deltaic settings (**Sidi et al., 2003; Olariu and Bhattacharya, 2006**).

5. Sequence Stratigraphy

Sequence stratigraphic techniques provide a method to integrate subsurface well log and outcrop datasets into a chronostratigraphic framework. Depositional sequences are defined as packages of genetically conformable, related facies enclosed by unconformities produced during falling sea level **(Mitchum, 1977; Van Wagoner et al., 1990).** Sequences can be identified in the study interval by recognizing major landward or seaward shifts in the vertical and lateral

distribution of facies, allowing for a geometric and temporal review of the sedimentary response to variations in accommodation through time **(Posamentier and Allen, 1999; Catuneanu, 2006).** Accommodation is defined as the amount of space available for sediment accumulation, which is controlled by variations in relative base-level, a product of both fluctuating eustatic levels and tectonic subsidence **(Sloss, 1962; Jervey, 1988).**

At several locations, the close proximity of roadcut and natural exposures to well control provides effective correlation from the surface to subsurface datasets. Example facies successions from core, outcrop and wireline data sets of portions of the core of the Bottom Creek Formation of the southern Nora Field and from the Alvy Creek Formation exposed in Grundy, Virginia are interpreted and shown in **Figures 2.10 and 2.11**. The Grundy section (**Fig. 2.11**) measures approximately 120 m in height and 1 km in length, and permits near-complete access for examination of stratal surfaces that are comparable to those observed on nearby well-log cross sections.

In both examples, the vertical progression of facies associations are interpreted as conformable sequences of stacked depositional settings, each formed during a specific episode of regional accommodation controlled by relative sea-level position. These specific episodes of regional accommodation further subdivide a depositional sequence into contemporaneous system tracts designated by relative sea-level position as, lowstand, transgressive and highstand system tracts **(Brown and Fisher, 1977; Van Wagoner et. al., 1990).**

Sequence boundaries are recognized as regional, erosional disconformities below basinward shifts in facies (**Van Wagoner et al., 1988)**. In outcrop and core, the sharp, erosional bases beneath fluvial facies associations deposits of cross-bedded sandstone and conglomerate are interpreted as sequence boundaries (**Fig. 2.6)**. These erosional surfaces commonly incise 5 –

10 m into underlying deltaic and inner shelf facies associations. In the subsurface, regional sequence boundaries were correlated from outcrops and cores across multiple wireline logs and are indicated by sharp gamma ray decreases to the left with blocky, low gamma ray signatures due to sharp based sandstones and a sudden coarsening of facies of braided fluvial gravel bar deposits overlying mudstones. Where possible, this gamma ray signature was confirmed using field-gamma-scintillometer measurements, shown in white at Grundy (**Fig. 2.11**).

Sequence boundaries are interpreted as the products of pronounced drops in base level, with common evidence for degradation and destruction of earlier sediment infill due to negative accommodation space. Regional scours at the bases of fluvial sandstones represent surfaces formed during late highstand and early lowstand, when falling baselevel contributed to incision of broad valleys and fluvial sediment bedloads bypassed the Pocahontas Basin.

Lowstand System Tracts

Sequence boundaries are overlain by laterally amalgamated braided channel fluvial association deposits, classified as multilateral, broad sheets (*sensu* **Gibling, 2006**). Braided fluvial systems are commonly associated with lowstands, as increased fluvial gradients following base level fall supported the development of multi-channel rivers (**Hampson et al., 1996**). In the updip setting of the Pocahontas Basin, earliest lowstand deposits are likely absent, with possible development of lowstand wedges along the distal shelf margin to the southwest in the Ouachita foredeep and unconformity development in the Pocahontas Basin during this time interval. The majority of aggradation in fluvial channels is considered to resume during the late lowstand into early transgressive system tracts **(Figs. 2.10 and 2.11)**.

Transgressive Systems Tracts

As accommodation continued to increase, fluvial deposystems effectively aggraded remaining accommodation in incised valleys and developed broad alluvial plains capped by regional peat mires. Mire development was promoted by rising base level that contributed to perched water table conditions and water logging of surface substrates, producing widespread peat-forming mire conditions. Early transgressive system tracts would allow for preservation of thick, laterally extensive coals because of prolonged periods of increasing accommodation space and concomitant reduction in hydrologic gradients, with decreased clastic sediment supply (**Cross, 1988; Flint et al., 1995; Bohacs and Suter, 1997**).

Continued transgression submerged alluvial systems and deposited fining- upward successions of sandy and muddy heterolithic facies, with evidence for tidal influences within estuarine settings **(Figs. 2.10 and 2.11)**. This landward step of environments is diagnostic of transgressive system tracts. Multiple transgressive successions are recognized in younger Pennsylvanian intervals of the Breathitt Group in the Central Appalachian Basin (**Greb and Chesnut, 1992; Greb and Martino, 2005**).

Maximum Flooding Surface

At the peak of transgression, a shallow-marine setting blanketed the shelf with condensed section muds. These shales commonly contain open marine traces and marginal marine body fossils characteristic of the shelf facies association. The base of these marine influenced shale facies equate with the maximum flooding surface (MFS) of **Van Wagoner et al. (1990) (Figs. 2.10 and 2.11)**. The MFS corresponds to the inflection point on the base level curve, where the rate of accommodation space creation is at a maximum and marks the peak of lateral

retrogradation. This high rate of accommodation creation reduces sedimentation rates to very low levels and is theoretically the period where the growing embayment in the foreland basin can achieve near normal marine salinities due to greater connections with the sea. This promoted intense bioturbation in response to reduced sedimentation rates and increased benthic salinities and oxygen levels during periods of rapid transgression. The base of marine shales combined with infaunal deposit feeding traces have been used to define maximum flooding surfaces in the Middle Pennsylvanian intervals of the Central Appalachian Basin (**Chesnut, 1992; Aitken and Flint, 1994,1995; Martino, 1996; Greb and Martino, 2005)**.

In the subsurface, the MFS is identified primarily from gamma-ray signatures, corroborated with core descriptions and outcrop observations. The MFS is associated with a high spike in gamma-ray values as a result of increased uranium concentrations within a condensed shale mineralogy. Maximum flooding surfaces are defined at the transition from fining-upward to coarsening-upward successions (**Figs. 2.10 and 2.11**).

Highstand Systems Tract

Above the MFS is the highstand system tract (HST), recognized by coarsening-upward, basinward shifts in facies. Stacking patterns within the HST reveal aggradation followed by progradation, interpreted in the Pocahontas Basin as the prograding deltaic facies association (**Figs. 2.10 and 2.11**). As the rate of accommodation growth slowed, sediment supply began to catch up and constructive deltaic systems began to prograde into the basin, infilling the embayment with diagnostic coarsening-upward successions during relative highstands of sea level. One or more coal beds also typically are present in the early highstand systems tract. These coal beds are laterally variable in extent and commonly mantle coarsening-upward

successions, interpreted as peats that formed in paralic settings. The highstand systems tract is terminated at the overlying sequence boundary, that developed during the subsequent drop in baselevel.

6. Stratal Architecture

Ten cross-sections were constructed in transects across the study area (**Fig. 2.2**); seven approximately parallel to the dip of the basin (transects A – G, **Fig. 2.2**) and three along transects parallel to basin strike (transects X – Z, **Fig. 2.2**). The cross-sections were arranged such that they intersected at common well data points. Two of these cross sections (E-E' and Y-Y') are included in this paper as **Figs. 2.12, 2.13,** with the remainder included in the journal archive.

Depositional facies stacking patterns and sequence stratigraphic surfaces of >**1200** closely spaced (2-5 km) well logs and 7 cores within the Pocahontas Basin can be used to subdivide the lower Breathitt Group into at least **15** regionally extensive unconformity-bounded depositional sequences. Due to the high vertical and lateral heterogeneity of the study interval, initial correlations were based on major marine shale zones and identifiable coal seams. The marine zones correspond with the bottom three regional marine zones proposed by **Chesnut (1994)**, the Dark Ridge, Hensley and Dave Branch Shale members. Each cross section is stratigraphically balanced on the Dave Branch Shale Member datum. This well-constrained datum is the first major flooding surface within the Grundy Formation and is closely associated with the Kennedy coal bed.

Individual high-frequency sequences stack into lower-frequency composite sequences (***sensu* Mitchum and Van Wagoner, 1991)**, separated by major discontinuities based on their aerial extent, depth of incision, truncation of older sequences and changes in clast composition.

Major discontinuities are located at the Mississippian-Pennsylvanian unconformity and at the base of the widespread, sheet-like, fluvial, longitudinal quartzarenite bodies of the uppermost tongues of the Warren Point, Sewanee and Bee Rock Sandstone Formations (**Figs. 2.12, 2.13**). These surfaces are demonstrated to regionally truncate underlying strata, including several eastward-dipping sequences, and to merge towards the western forebulge. **Korus et al. (2008)** identified comparable truncation of underlying sequences by equivalent upper Sewanee member exposures in southern West Virginia. The major discontinuities form the composite sequence boundaries of the Pocahontas, Bottom Creek and Alvy Creek composite sequences.

6.1 Pocahontas Composite Sequence (Sequences P1-P3)

The Pocahontas composite sequence is the oldest studied interval, representing a lens of earliest Pennsylvanian siliciclastics sharply overlying the Mississippian-Pennsylvanian unconformity. This mid-Carboniferous surface coincides with the cratonic sequence boundary defined by **Sloss (1963)**, and forms the base of the Atokan supersequence. The unconformity is recognized by a diagnostic facies shift from Mississippian red-colored mudstones and siltstones to amalgamated fluvial sandstones of the Pocahontas Formation. In all dip-oriented cross sections, the earliest Pennsylvanian strata of the Pocahontas Formation onlap the unconformity (**Fig. 2.12, 2.13)**. In strike orientation, a sharp offset in the Pride Shale and an abrupt increase in preferential preservation of Late Mississippian and Early Pennsylvanian strata is takes place across the Glamorgan Fault **(Fig. 2.13)** suggesting syndepositional normal fault motion**.**

The Pocahontas compound sequence consists of one to three high-frequency sequences, with increasingly older sequences preserved toward the southeastern limits of the study area. High- frequency sequences of the Pocahontas compound sequence average 40 m in thickness and

contain dominantly non-marine, transverse, fluvial sandstones and overlying associated estuarine facies associations. These sequences are severely top-truncated, with limited preservation of highstand deltaic facies. Ichnofabrics within this interval are notably absent. The preferential preservation of lowstand and trangressive system tract deposits results in an overall package of high net sandstone to gross ratios (~ 0.40). The Pocahontas compound sequence is erosively overlain by the Warren Point longitudinal fluvial facies belt.

6.2 Bottom Creek Composite Sequence (Sequences B1-B5)

The Bottom Creek composite sequence contains five to six high-frequency, unconformity-bounded sequences in the southeastern part of the study area, forming a wedge above the base of the Warren Point Sandstone. High-frequency sequences average 70 m thick, with sequence B1 the thickest and containing both the regional Warren Point Sandstone and Dark Ridge Shale members. The overlying sequences (B2-B5) contain fluvial transverse and estuarine facies associations, but are volumetrically dominated by repetitive packages of coarsening-upward deltaic facies with limited lateral continuity. Inner-shelf facies are limited to the regional Dark Ridge Shale member, in which only a single occurrence of *Phycosiphon* was recognized. Younger mudstones in the Bottom Creek compound sequence generally contain weakly developed sets of brackish trace fossils. The prevalence of thick, transgressive estuarine and progradational deltaic deposits results in an overall package of moderately low net sandstone to gross ratios (~ 0.20). In dip orientation, the Bottom Creek compound sequence is capped by the Sewanee longitudinal fluvial facies belt. Sequences B2-B5 surfaces converge updip onto the western margin toward the forebulge where they are laterally truncated and erosively overlain by

the Alvy Creek compound sequence **(Fig. 2.12)**. In the strike orientation, the B5 sequence has a lower sequence B5A, which includes a thick quartzarenite **(Fig. 2.13).**

6.3 Alvy Creek Composite Sequence (Sequences A1-A5)

The Alvy Creek composite sequence contains five high-frequency, unconformity-bounded sequences in the southeastern part of the study area above the regional disconformity at the base of the lower Sewanee Sandstone. High frequency sequences average 75 m in thickness with sequence A2 the thickest and containing both the regional upper Sewanee Sandstone and Hensley Shale members. Each of the overlying sequences (A3-A5) contain the full suite of recurring facies associations, bounded by well-developed sequence boundaries, as well as associated flooding surfaces defined by inner shelf facies that contain distinctive marine influenced ichnofabrics. The increased dominance of thick, transgressive estuarine and inner shelf mudstone facies over fluvial and deltaic sandstones results in an overall package of low net sandstone to gross ratios (~ 0.15). In both dip and strike orientations, the Alvy Creek compound sequence is capped by longitudinal fluvial facies of the Bee Rock Sandstone. Sequences A4-A5 converge updip onto the western and southern margins toward the forebulge where they are laterally truncated and erosively overlain by the Grundy compound sequence **(Figs. 2.12 and 2.13)**.

6.4 Grundy Composite Sequence (Sequences G1-G2)

The Grundy compound sequence is only partially preserved in the Pocahontas Basin, containing two high-frequency sequences above the base of the Bee Rock Sandstone member. The Grundy sequence consists of quartzarenites along the western margin that truncate older,

genetically unrelated facies of the Alvy Creek compound sequence. Sequence G2 extends broadly toward the depocenter, where the Bee Rock Sandstone is considered coeval with the sublitharenite McLure informal member and is overlain by the regional, marine-influenced Dave Branch Shale member (**Figs. 2.12 and 2.13).**

6.5 Comparison of Composite Sequences

Bundling of high-frequency sequences into composite sequences permits the evaluation of longer term accommodation trends in the Pocahontas Basin. Each composite sequence contains three or more high-frequency sequences. Composite sequences exhibit wedge geometries, with significant differential thickening from the craton toward the orogen in the southeast (**Figs. 2.12 and 2.13**). The Pocahontas and Bottom Creek composite sequences exhibit the greatest differential thickening. Decreasing trends in net sandstone to gross ratios is related to an increasing preservation of high volumes of transgressive and highstand deposits with time. This point is supported by increasing brackish and marine faunal indicators, from a barren Pocahontas composite sequence to increasing occurrences of *Teichichnus* and *Phycosiphon* in the shelf and deltaic facies of overlying composite sequences. The increased diversity in depositional settings is further supported by the palynological record, observed as an increasing diversity of spore types (**Eble, 1996; Eble et al., 2009; Eble, Personal Communication, 2010**). The appearance of the abundant cordaite pollen, *Florinites,* in the Grundy composite sequence could be ascribed to increased marine influence, as cordaites have sometimes been defined as saline-tolerant plants, similar to modern mangroves (**Eble et al., 2009**). A summary sequence stratigraphic architecture is shown in **figure 2.14**.

7. Duration of High Frequency Cycles

The average duration of sequences can be approximated by dividing the estimated duration of the study interval by the maximum number of high-frequency sequences. Sparse paleobotanical and geochronological (**Eble, 1996**) and radiometric data from an ash deposit in the Upper Banner Coal (**Lyons et al., 2006**) constrain the duration of deposition of the interval to between **317.3 Ma** (Base of Namurian C, **Menning et al., 2006**) and **316.1 ± 0.8 Ma (Fig. 2.3)**. Dividing the determined duration of the study interval (**1.2 ma ± 0.8**) by the number of sequences recognized (**15**) results in an average estimate of **80 kyr (± 50 kyr)** for the duration of each sequence. This estimate is approximate, as the duration is defined with uncertainties of the available biochronostratigraphy and assumes preservation of all high-frequency sequences. The average sequence duration suggests that base-level fluctuations approached a $\mathbf{10^5}$ yr periodicity. **Greb et al., (2008)** interpreted a similar 100 kyr duration for Middle Pennsylvanian sequences in the Central Appalachian Basin above the Banner Coal.

8. Controls on Sequence Development

The dynamic interplay between simultaneous eustasy, climatic change, and tectonic controls on relative base level in the Pocahontas Basin has led to substantial debate. A number of mechanisms have been proposed to explain the observed stratigraphic architecture of the basin. Previous workers have suggested that Pennsylvanian high-frequency cycles of the Appalachian Basin are a product of autogenic (intrinsic) factors such as delta switching and channel avulsion (**Ferm, 1970; Wizevich, 1992**), allogenic (external) factors such as eustasy (**Wanless and Shepard, 1936; Chesnut, 1994; Aitken and Flint, 1995; Greb et al., 2004;**

Korus et al., 2008), episodic tectonic flexure (**Tankard, 1986; Donaldson and Eble, 1991; Pashin, 1994**) or orbitally forced climate change (**Cecil, 1990**).

Sequence boundaries and associated flooding surfaces of basin-wide extent and continuity are herein interpreted to be a response to allogenic mechanisms. Although **Ferm and Horne (1979)** suggested autogenic controls masked any observable cyclicity in the Pocahontas Basin, the observed regional changes suggest that autogenic controls are best used to explain local heterogeneities in facies successions.

8.1 Controls on High Frequency Sequences –Eustasy

Using recent time-scales for the Early Pennsylvanian, the high frequency, base level controlled sequences in the Pocahontas Basin are interpreted to be a product of far field, glacio-eustatic fluctuations related to short eccentricity driven (~10^5 yr) Milankovitch cycles based on global observations, stratal patterns and facies trends.

It is now well established that the Carboniferous Period was a time of pronounced continental glaciation and global cooling. This is broadly inferred from evidence of high-latitude glaciogenic deposits in Gondwana (**Veevers and Powell, 1987: Isbell et al., 2003; Montanez et al., 2007; Fielding et al, 2008**), global changes in stable carbon and oxygen isotopes (**Mii et al., 1999; Grossman et al., 2008**) and well-documented, high-frequency facies cycles that have been related to periodic waxing and waning of ice sheets and associated eustatic fluctuations (**Wanless and Shepard, 1936; Heckel, 1977, 1986; Smith and Read, 200).**

High-frequency cycles in the stratigraphic record have been related to periodic variations in the Earth's orbit, (Milankovitch cycles; **Imbrie and Imbrie, 1978**) resulting in changes in solar insolation and global summer temperatures, which directly impact continental ice volumes.

Changes in the cryosphere through ice growth or decay lead to direct impacts on global sea level which in turn results in variations in sediment distribution. Changes in planetary orbital eccentricity (stretch) have two dominant periodicities of 400 kyr and 100 kyr (**Schwarzacher, 1993). Rial (1999**) demonstrated that the dominant Milankovitch orbital parameter during the Pleistocence glaciation was within the short-eccentricity band, oscillating between 120 kyr and 80 kyr.

Comparisons between previous estimates for high-frequency sequences in the Late Paleozoic and the estimate from this study reveal similar eccentricity driven periodicities. **Chesnut (1994),** estimated equivalent Breathitt Group cycles as having to 400 kyr durations, based on now obsolete timescales. This result is similar to Late Pennsylvanian cycles that were found to statistically cluster around 413 kyr in the mid-continent of North America (**Algeo and Wilkinson, 1988**), suggesting a long-eccentricity signal. In contrast, **Rasbury et al., (1998)** used radiometric dates of paleosols to estimate late Paleozoic cycles to average around 143 kyr, within the uncertainty of Pleistocene short-eccentricity cycles. **Pashin (2004) and Greb et al., (2008)** more recently inferred short-eccentricity driven cycles for Early Pennsylvanian strata in the Black Warrior Basin and Central Appalachian Basin.

Considering that calculating cycle periodicities is strongly dependent on available geochronology and preservation of sequences, additional observations of prominent facies trends are required to strengthen a glacioeustatic inference. Stratal evidence suggests basin-wide sea level changes promoted the alluvial incision of 10's of meters of relief on significant unconformities cut into highstand deltaic deposits. Incised valley incision and infill as well as progradation of unconformable, unincised fluvial bypass systems are frequent fluvial responses to changes in gradient during glacio-eustasy, dependent on both magnitude of sea level drop and

relative position along the shelf accommodation profile (**Blum and Törnqvist, 2000; Posamentier, 2001)**. Ice-sheet growth during the Pleistocene forced a eustatic drop of 120 m, which led to knickpoint migration and incision of the Mississippi River observed 370 km upstream from the shoreline at the modern Head of Passes **(Fisk, 1944; Saucier, 1981; Autin et al., 1991; Aslan and Autin, 1998)**. In addition to incision, examples from the southern Java Sea suggest that unincised fluvial systems commonly prograded across the marine shelves during Pleistocene eustatic lowstands, with rare valley incision during maximum drops in sea level (**Posamentier, 2001**). The significant lateral displacements of shelf mudstone facies over alluvial sandstones during individual transgressions within Bottom Creek and Alvy Creek sequences suggests sea-level fluctuation magnitudes of **> 20 m** of the Pocahontas Basin are similar to these Holocene examples. This is consistent with current estimates of early Pennsylvanian glacioeustasy and short-eccentricity driven eustatic change **(Rygel et al., 2008)**.

Consequently, it should be emphasized that observed facies trends track predicted magnitudes of Gondwanan ice cover and other Early Pennsylvanian eustatic records. The dominance of alluvial deposits and the scarcity of shelf facies in the Pocahontas composite sequence suggest low-magnitude relative base-level fluctuations. This glacioeustatic minima is consistent with a glacial sediment lacuna in the late Namurian (**Veevers and Powell, 1987; Isbell et al., 2003)** as well as reduced eustatically-influenced facies in the earliest Pennsylvanian archived in carbonates at Arrow Canyon, Nevada (**Bishop et al., 2010)**. The available facies record across this interval reflects a short period of reduced ice volume in the Late Paleozoic Ice Age, resulting in diminished magnitude, high-frequency (10^5 yr) glacioeustasy (**Bishop et al., 2010**). Within the Alvy Creek and Grundy composite sequences, high-frequency sequences have greater uniformity in thickness and lateral distribution of facies. Each high-frequency sequence

preserves thick inner-shelf facies with abundant marine traces, suggesting increased magnitudes of transgressions during deposition. These sequences formed during the Langsettian, a time interval of increasing Carboniferous ice volumes (**Veevers and Powell, 1987; Isbell et al., 2003; Fielding et al., 2008**) and glacioeustasy (**Ross and Ross, 1987; Rygel et al., 2008**).

Alternatively, the influence of climate change has been suggested to control high-frequency sequences. **Cecil (1990**) postulated that significant climate variations coincided with glacial-interglacial phases, controlling the development of regional high-frequency cyclothem-type sequences during the early Pennsylvanian. The main hypothesis is that fluvial incision changed the depositional landscape as increased aridity during glacial phases reduced vegetation, promoting increased rates of run off and sediment supply (**Cecil, 1990**). This presently is considered improbable, as available coal paleobotanical data (**Eble, 1996**), sandstone petrology (**Reed et al., 2005**), absence of cyclic redox controlled color changes, and recurring carbonaceous shales and base-depleted paleosols suggest climate during the early Pennsylvanian was equably humid tropical during transgressions and regressions. Additional work investigating preserved palobotanical samples from plant compressions within non-coal lithologies may give new insight into whether lowstand ecology and climate proxies suggest similar aridity as seen in Middle Pennsylvanian cycles (**Falcon-Lang et al., 2009**).

8.2 Controls on Composite Sequence Development - Tectonism

Examination of the gross wedge-shaped geometry of the Early Pennsylvanian strata of the Pocahontas Basin demonstrates that the basin was asymmetric with thickest deposits toward the adjacent orogen, suggestive of syndepositional, flexural subsidence due to tectonic loading. Flexural subsidence at the composite-sequence level is manifested by the pronounced cratonward

thinning and basinward thickening of individual wedge-shaped composite sequences along strike and dip sections (**Figs. 2.12 and 2.14, Chesnut, 1992; 1994**). High frequency sequence boundaries are also demonstrated to pinch out cratonward, toward a region of limited accommodation.

Regional changes in the rates of regional tectonic loading are suggested to have promoted significant shifts in subsidence and loci of deposition, which influenced the observed contrasts in vertical and lateral distributions of alluvial facies and resulting composite sequence architecture. Complex interactions between variations in basin subsidence and sediment supply can lead to fluctuations in the spatial domains of transverse and longitudinal fluvial systems in foreland basin systems (**Flemings and Jordan, 1990; Burbank 1992; Paola et al., 1992**). In the Pocahontas Basin, vertical stacking and lateral cratonward shifts between longitudinal fluvial facies belts (**Wizevich, 1993; Greb et al., 2004**), as well as transgressive marine shales (**Tankard, 1986; Klein and Willard, 1989)** have been suggested to be tectonically controlled or enhanced during rejuvenation of spasmodic tectonic loading. Moreover, the regional angular truncation of high-frequency sequences below composite-sequence boundaries, together with distribution and provenance trends of longitudinal and transverse facies **(Grimm and Eriksson, in prep)** indicate the influence of variable tectonic activity greatly influenced the formation of low-frequency, composite sequence boundaries..

Additionally, several characteristics of the composite sequences suggest that subsidence rates in the Pocahontas Basin were significantly spatially and temporally variable.. The Pocahontas composite sequence progressively onlaps the mid-Carboniferous unconformity within the depocenter. For example, the strike section **(Fig. 2.13)** suggests syndepositional normal motion on the Glamorgan fault during the deposition of the Pocahontas formation,

allowing preferential preservation of Late Mississippian and Early Pennsylvanian strata. These observations suggest that at the onset of orogenesis, initial subsidence was limited to the movement of semi-independent basement-cored blocks and reactivation of possibly inherited Grenvillian crustal features **(Ferm and Weisenfluh, 1989; Allen, 1993; Shumaker and Wilson, 1996).**

During deposition of the Bottom Creek composite sequence, it appears that basin faults began to lock, inducing greater subsidence and accommodation cratonward to the west. Continued differential subsidence in the depocenter led to a particularly high proportion of poorly drained alluvial plains, estuarine and deltaic deposits within the Bottom Creek composite sequence. This is attributed to an increased rate of base level rise, amplifying transgressions as well as overall accommodation of high- frequency sequences making the composite sequence more shale prone. Observations point toward a maximum rate of tectonic subsidence in the depocenter during the deposition of the middle of the Bottom Creek composite sequence, as during sequences B3 and B4 occasionally due not indicate consistently correlatable unconformities, suggesting that high frequency base level drops did not exceed rate of tectonic accommodation. As basement faults continued to lock, the entire basin began to undergo more equally distributed subsidence as indicated by the relatively tabular geometry of the regional Alvy Creek composite sequence, promoting the preservation of repeated high-frequency transgressions. Furthermore, this tectonic accommodation continued to decrease upward into the Middle Pennsylvanian **(Greb et al., 2004).**

9. Conclusions

Early Pennsylvanian strata in the Pocahontas Basin archive recurring, genetically linked facies, envisaged as stacked deposits of braided fluvial channels, broad alluvial plains, tidally influenced estuaries and small tropical delta depositional systems. Analysis of vertical stacking patterns of lithofacies on regional cross sections identified 15 unconformity-bounded depositional sequences of extremely widespread lateral extent, with an average duration of approximately 80 kyr (**± 50 kyr)**.

The observed stratigraphic architecture can be explained by the interplay of glacioeustatic and tectonic mechanisms. An interpretation for strong glacioeustatic controls on stratigraphic architecture is supported by corresponding sequence duration within the short eccentricity periodicity of the Milankovitch band and magnitude and extent of rapid facies shifts, suggesting that far-field variations in overall Gondwanan ice-sheet size and volume impacted base level changes in a low latitude, tropical basin. The progressive increase in magnitudes of transgression as indicated by ichnologic assemblages, correspond with extrabasinal, far-field trends in ice volume and eustasy.

High-frequency eustatic sequences are nested within low-frequency tectonically controlled composite sequences. Separating the contributions of any individual natural factor at a single location is impossible, but regional trends in the variations of composite sequence geometry and facies distribution highlight episodic syndepositional tectonic activity that can be defined separately from high-frequency glacioeustatic influenced sequences. These composite sequences reveal long term tectonically influenced accommodation trends overprinted by recurring high-frequency eustatic events.

Figure 2.1. Regional maps of A) the USA and B) states containing the Appalachian Basin, illustrating the distribution of Carboniferous age sedimentary rocks (shaded region); hatched area denotes the Central Appalachian Basin. C). Detailed map shows major structures within the Pocahontas Basin, including the Middlesboro Syncline, bounded by the Hunter Valley-Clinchport-St. Clair and Pine Mountain thrust faults. The Russell Fork Fault (bold) as well as minor Bradshaw, Coeburn and Glamorgan faults have measurable lateral and vertical displacement (Adapted from Cecil et. Al, 1985; Mitra, 1988; Henika, 1994; Ryder et al., 2008).

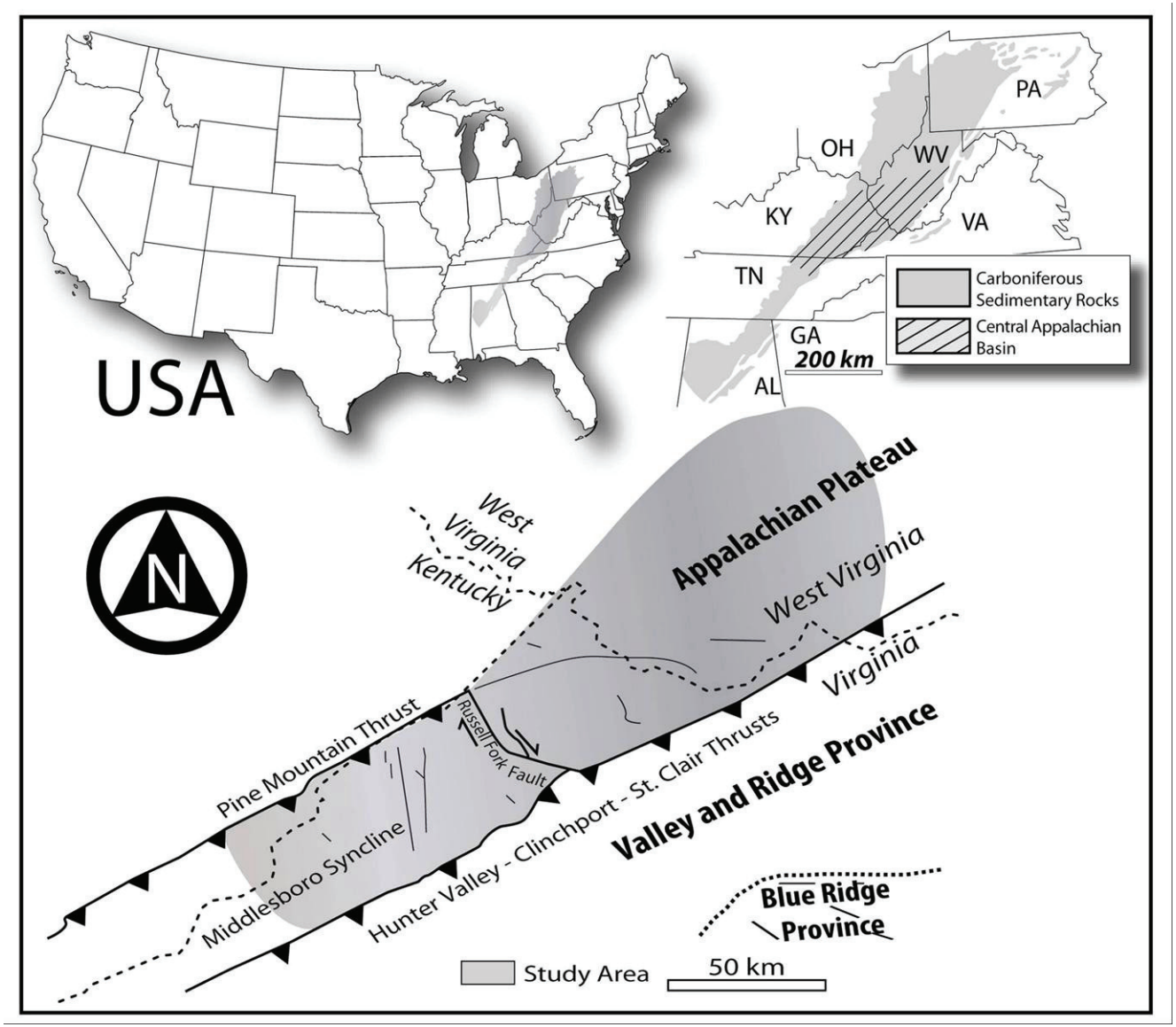
USA
PA
OH
WV
KY
VA
TN
GA
200 km
AL
Carboniferous Sedimentary Rocks
Central Appalachian Basin
N
West Virginia Kentucky
Appalachian Plateau
West Virginia
Virginia
Pine Mountain Thrust
Russell Fork Fault
Middlesboro Syncline
Hunter Valley - Clinchport - St. Clair Thrusts
Valley and Ridge Province
Blue Ridge Province
Study Area
50 km

Figure 2.2. Map of the study area showing the position of well logs, cores, cross sections and measured outcrop localities. Positions of dip cross sections A-Z and strike cross sections X-Z across southwestern Virginia are shown. Highlighted cross sections E-E' and Y-Y' are included in this paper, with supplementary cross sections in the appendix.

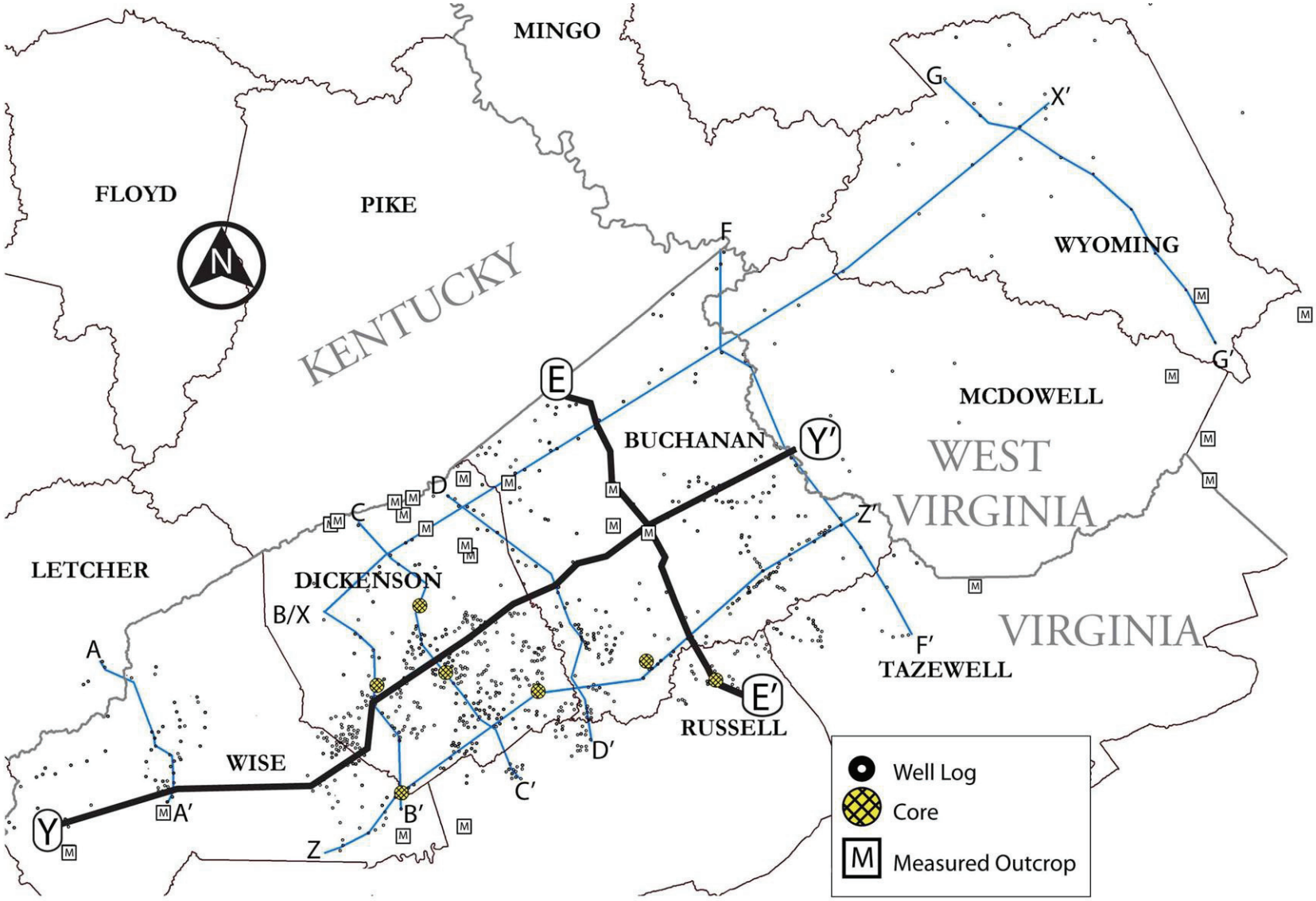
MINGO
FLOYD
PIKE
KENTUCKY
WYOMING
MCDOWELL
BUCHANAN
WEST VIRGINIA
VIRGINIA
LETCHER
DICKENSON
WISE
RUSSELL
TAZEWELL
N
G
X′
F
G′
E
Y′
D
C
Z′
B/X
A
F′
E′
D′
C′
B′
A′
Y
Z
Well Log
Core
M
Measured Outcrop

Figure 2.3. Stratigraphic chart for the study interval. Left column shows the generalized stratigraphy with age constraints for Early Pennsylvanian strata in the Pocahontas Basin. Right column shows a more detailed coal stratigraphy with type gamma ray and bulk density (RHOB) geophysical wireline log responses for the Lower Breathitt Group interval.

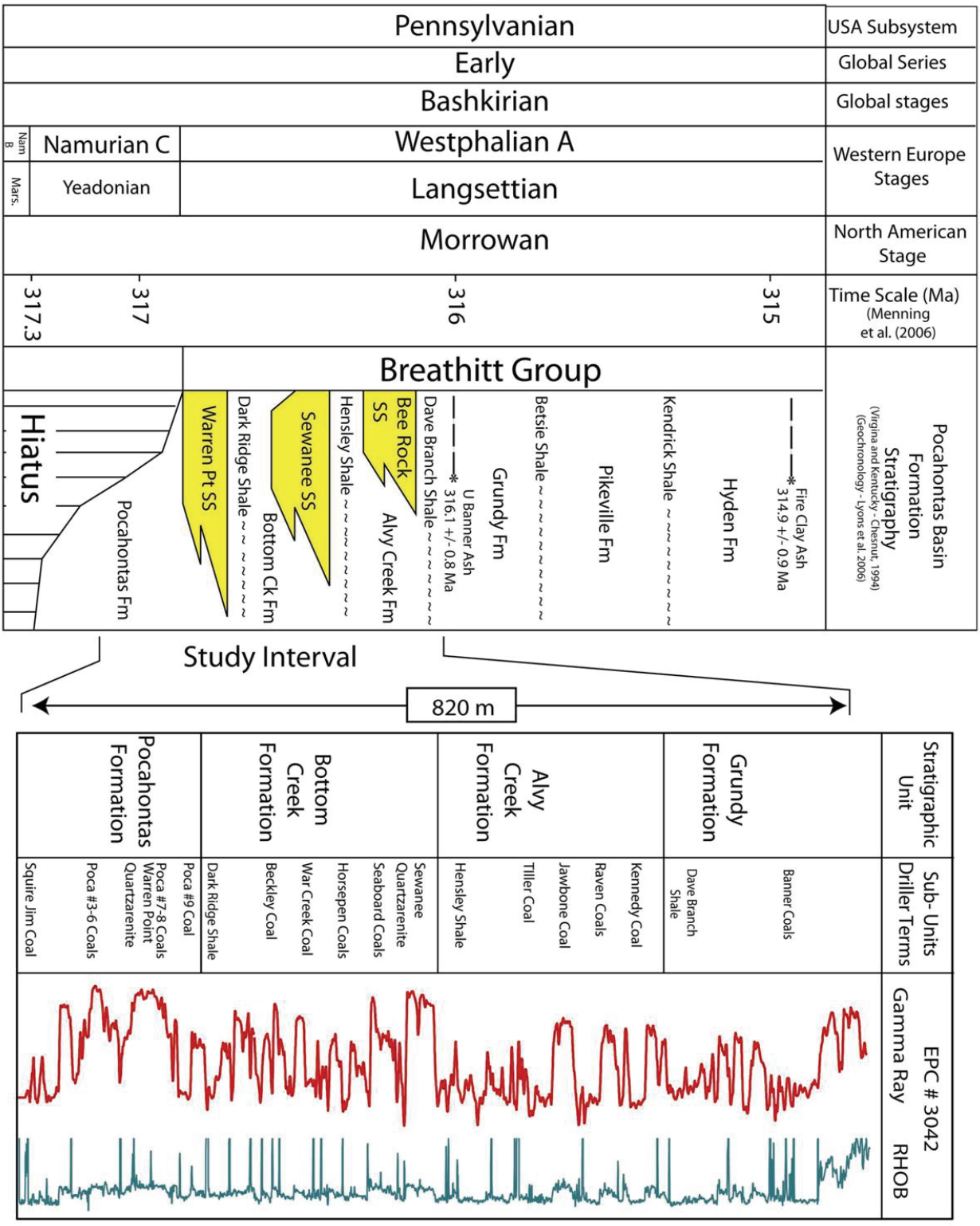
Pennsylvanian
Early
Bashkirian
Namurian C
Yeadonian
Westphalian A
Langsettian
Morrowan
USA Subsystem
Global Series
Global stages
Western Europe Stages
North American Stage
Time Scale (Ma) (Menning et al. (2006)
317.3
317
316
315
Pocahontas Basin Formation Stratigraphy
(Virgina and Kentucky - Chesnut, 1994)
(Geochronology - Lyons et al. 2006)
Breathitt Group
Fire Clay Ash 314.9 +/- 0.9 Ma
Hyden Fm
Kendrick Shale
Pikeville Fm
Betsie Shale
Grundy Fm
U Banner Ash 316.1 +/- 0.8 Ma
Dave Branch Shale
Bee Rock SS
Alvy Creek Fm
Hensley Shale
Sewanee SS
Bottom Ck Fm
Dark Ridge Shale
Warren Pt SS
Pocahontas Fm
Hiatus
Study Interval
820 m
Stratigraphic Unit
Sub- Units
Driller Terms
Grundy Formation
Banner Coals
Dave Branch Shale
Kennedy Coal
Raven Coals
Jawbone Coal
Alvy Creek Formation
Tiller Coal
Hensley Shale
Bottom Creek Formation
Sewanee Quartzarenite
Seaboard Coals
Horsepen Coals
War Creek Coal
Beckley Coal
Dark Ridge Shale
Pocahontas Formation
Poca #9 Coal
Poca #7-8 Coals
Warren Point Quartzarenite
Poca #3-6 Coals
Squire Jim Coal
EPC # 3042
Gamma Ray
RHOB

Figure 2.4. Longitudinal Fluvial Facies Association. Photographs and data are from exposures at Breaks Interstate Park and Birch Knob, Virginia. A) Channel lag quartz pebble conglomerate, hammer for scale. B) Flute casts at base of the Bee Rock Sandstone Member; current directions to the top left. C) Stacked planar crossbed sets, top set ~0.5m thick. D) Stacked planar crossbed sets, person for scale. E) Tangential crossbed set, staff is ~1.5m long. F) Compound cross bedding consisting of intrasets between inclined bounding surfaces. G) Rose diagram of paleocurrent data for the Warren Point Sandstone member. H) Rose diagram of paleocurrent data for the Bee Rock Sandstone Member.

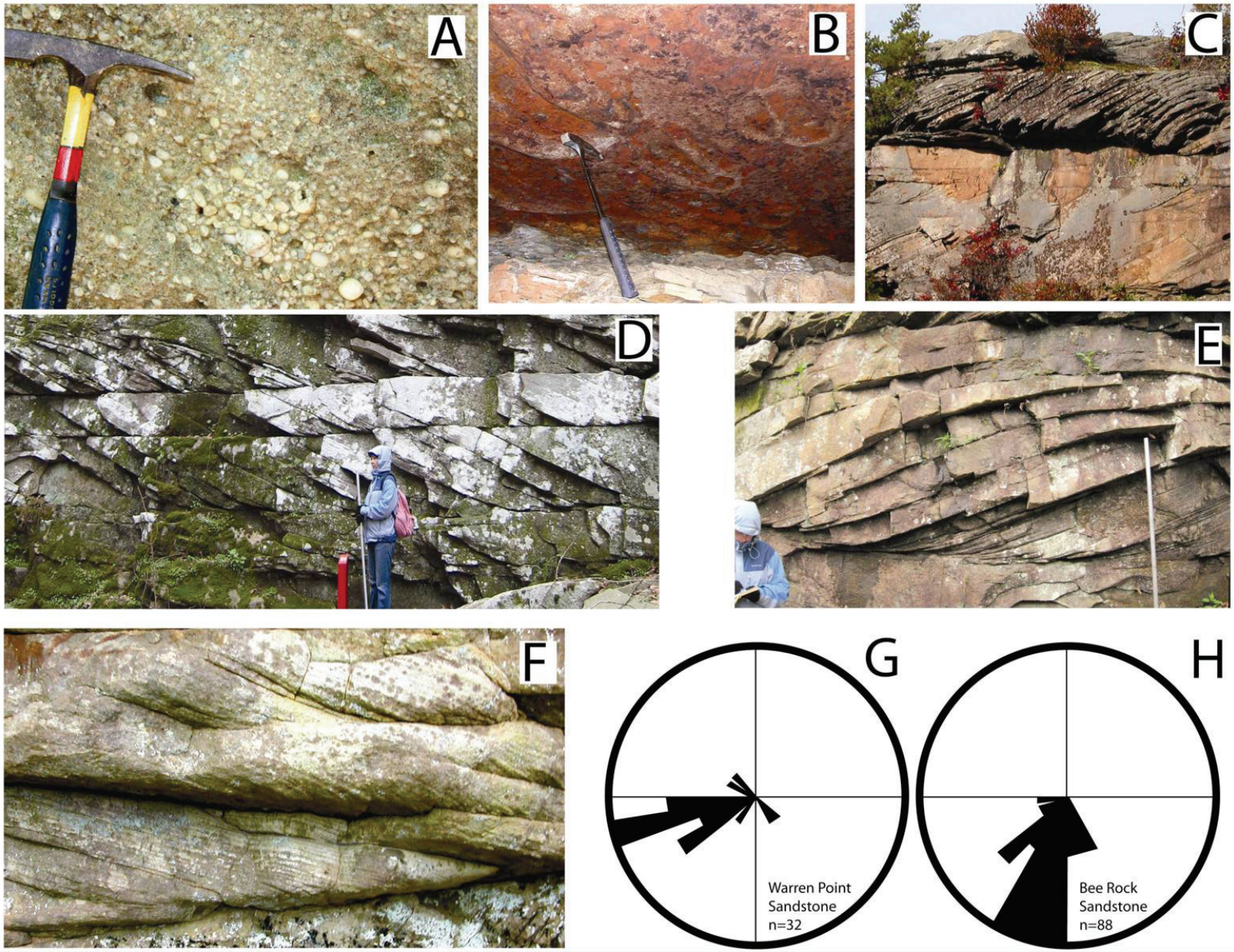
A
B
C
D
E
F
G
Warren Point
Sandstone
n=32
H
Bee Rock
Sandstone
n=88

Figure 2.5. Example of vertical succession of lithologies, sedimentary structures, facies associations and subsurface gamma ray characteristics from the Equitable Sandy Ridge Core, 1000-1500 ft.

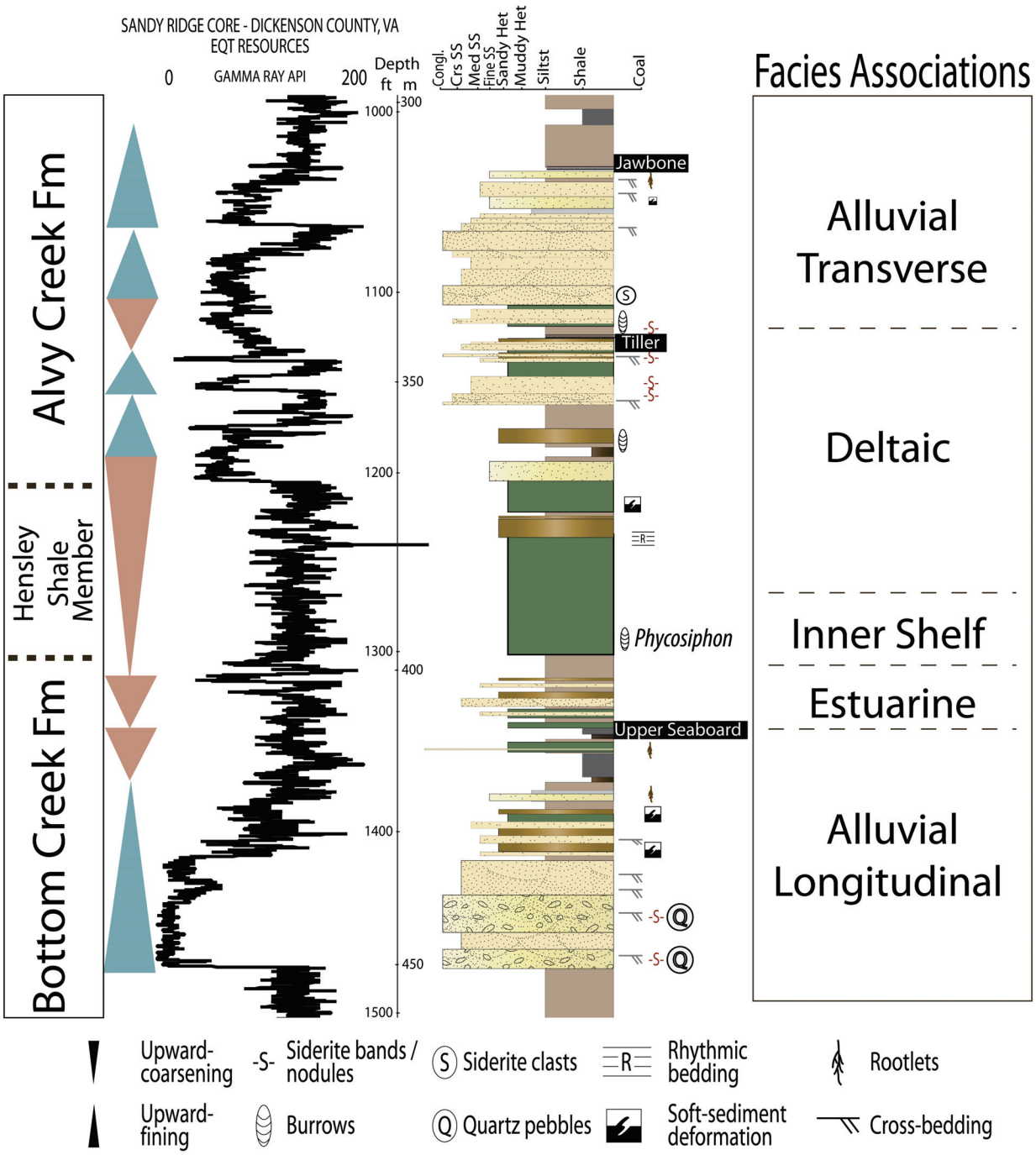
SANDY RIDGE CORE - DICKENSON COUNTY, VA
EQT RESOURCES
0
GAMMA RAY API
200
Depth
ft m
Congl.
Crs SS
Med SS
Fine SS
Sandy Het
Muddy Het
Siltst
Shale
Coal
Facies Associations
Alvy Creek Fm
Hensley Shale Member
Bottom Creek Fm
1000
300
1100
350
1200
1300
400
1400
450
1500
Jawbone
Tiller
Phycosiphon
Upper Seaboard
Alluvial Transverse
Deltaic
Inner Shelf
Estuarine
Alluvial Longitudinal
Upward-coarsening
Upward-fining
-S- Siderite bands / nodules
Burrows
S Siderite clasts
Q Quartz pebbles
R Rhythmic bedding
Soft-sediment deformation
Rootlets
Cross-bedding

Figure 2.6. Transverse Fluvial Facies Association. A) Deeply incised fluvial sandstone body along VA Route 460 near Deel, Virginia. Regional bedding nearly horizontal. B) Sharp erosional surface and localized relief below fluvial sandstone body, Grundy, Virginia. Scale bar is 1 m. C) Siderite, shale fragment and plant debris conglomerate lag. Hammer for scale, Vansant, Virginia. D) Trough cross bedding, hammer for scale, Coaldale, West Virginia. E) Rose diagram of paleocurrent data for sandstones of the Pocahontas Formation. F) Lateral accretion surfaces exposed at Highwall Park, Coaldale, West Virginia. Height of outcrop is ~8m. G) Rooted sandstone below Raven coal, Grundy, Virginia. Rooted zone is ~0.5m thick. H) Thick gleyed and rooted mudstone below tabular coal horizon, Pocahontas Formation along I-77 near Flat Top, West Virginia.

A
B
C
D
E
Pocahontas Fm
Sandstones
n=37
F
G
H

Figure 2.7. Estuarine Facies Association. A) Core photo of flaser bedding with bifurcating mudstone drapes. Scale is 1 cm. Equitable Sandy Ridge Core 2453 ft. B) Core photo of wavy bedding <containing discontinuous, mm- scale ripple cross laminae with mudstone interlaminae. Scale is 1 cm. Range Resources Nora Core. C) Outcrop photo of lenticular bedding and parallel laminations, separated by continuous mudstone partings. Scale is 1 cm, Pocahontas Formation near Matoaka, West Virginia. D & E) Core photos of laminae couplets of parallel-laminated sandstone-siltstone and thin partings of mudstone. Note apparent thick-thin trends in laminae thicknesses. Small arrows (n) indicate sediment deposited during neap intervals of tidal cycles. Scale is 1 cm. WVGS Core above the Sewanee Sandstone member and Equitable Clincho Core, 1920 ft. F) Plot of vertical trends in laminae thickness of core sample shown in Figure 7E. G) Photo of preserved *Altheopteris* fern frond. H) Core photo of local *Paleophycus* (Pa) burrows in sandy heterolithic interval. Scale is 1 cm. DOE M2 Core, 901 ft.

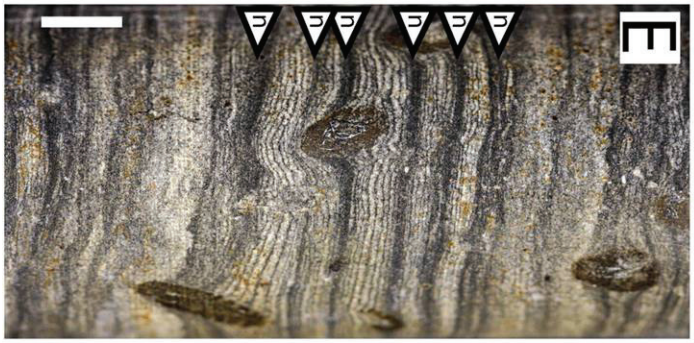
E


A


B

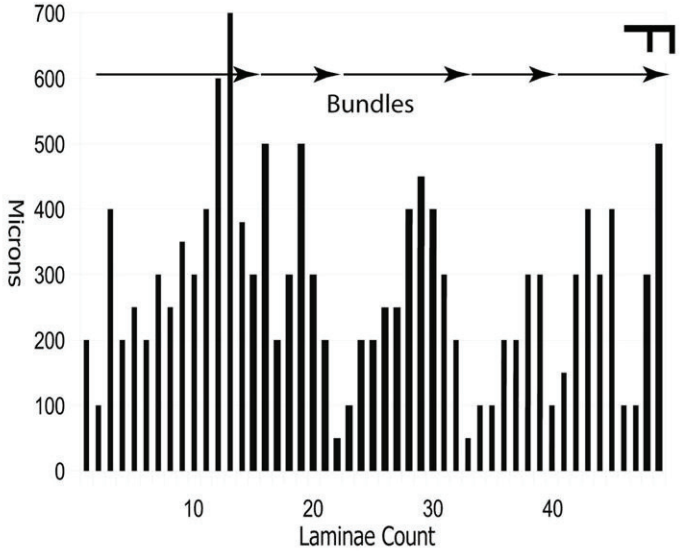
F
700
600
500
400
300
200
100
0
Microns
Bundles
10
20
30
40
Laminae Count


C


G

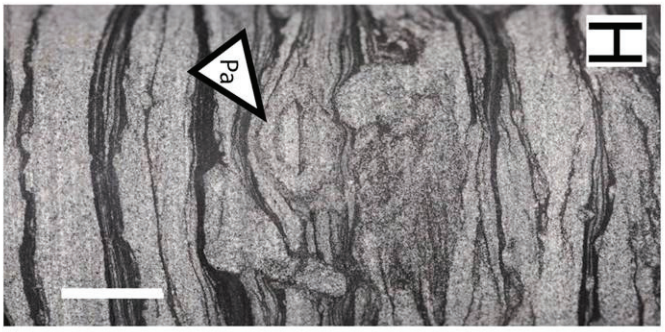
H
Pa

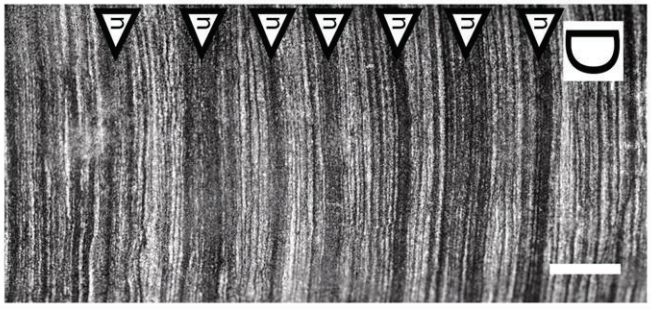
D

Figure 2.8. Inner Shelf Facies Association. A). Close-up photo of large siderite concretion in laminated, dark gray mudstone. Hammer for scale. Outcrop near Vansant, Virginia. B) Core photo of distinctive *Phycosiphon* (Ps) burrows. Scale is 1 cm. DOE M2 Core, 723 ft. C) Close-up photo of *Phycosiphon* burrows. Scale is 1 cm. DOE M2 Core, 366 ft. D) Bedding surface view of *Neonerities Missouriensis* burrows. Scale is 1 cm. Sample from Grundy, Virginia. E) Core photo of *Phycodes* (Ph) and *Paleophycus* (Pa) burrows. Scale is 1 cm. DOE M2 Core, 920 ft. F) Core photo of *Cylindrichnus* (Cy) burrow with *Phycosiphon* (Ps) traces. Scale is 1 cm. DOE M2 Core, 387 ft. G) Close-up core photo of brachiopod within mudstone facies of the Dave Branch Shale Member. Scale is 1 cm. Equitable Sandy Ridge Core, 521 ft.

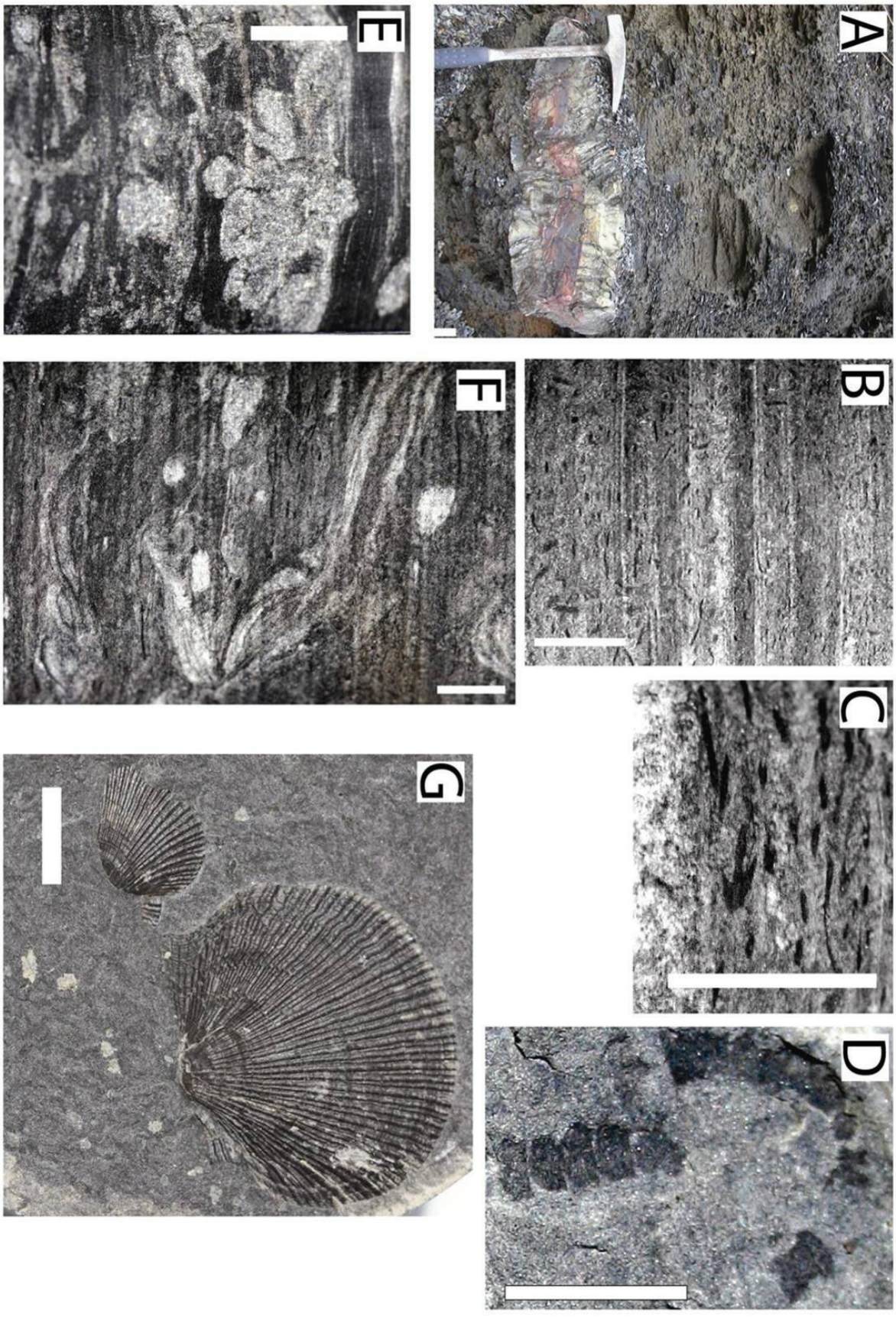
A
B
C
D
E
F
G

Figure 2.9. Deltaic Facies Association. A) Gradationally coarsening-upward succession above the Dave Branch Shale member, Breaks, Virginia. B) Core Photo of *Carbonicola sp* . body fossils from the middle of the Dave Branch shale member of the Grundy Formation. Scale is 1 cm. Equitable Sandy Ridge Core, 515 ft. C) Ball-and-pillow dewatering structures within thin sandstones of the Pocahontas Formation, Highwall Park, West Virginia. Hammer for scale. D) Core photo of soft-sediment deformation in sandstone bed. Scale is 1 cm. DOE M2 Core, 1296 ft. E) Photo of preserved detrital fronds of *Neuropteris* and *Odontopteris* fern debris. Scale is 1 cm. F) Core photo of bioturbated intervals with unidentified horizontal traces (Un), Planolites (P) and *Ophiomorpha* (Op). Scale is 1 cm. DOE M2 Core, 902 ft. G) Core photo of common *Teichichnus* (Te), *Taenidium* (Ta), and *Planolites* (P) trace associations. Scale is 1 cm. DOE M2 Core, 900 ft. H) Core photo of rare example of *Thalassinoides* (Th). Scale is 1 cm. Equitable Sandy Ridge Core, 1830 ft. I) Close-up photograph of *Lingulid* shells found within siltstones overlying the regional Dave Branch shale member near Breaks, Virginia. Scale is 1 cm. J). Core photo of sandy heterolithic facies with common *Rosselia* (Ro) traces. Scale is 1 cm. Equitable Sandy Ridge Core, 2195 ft.

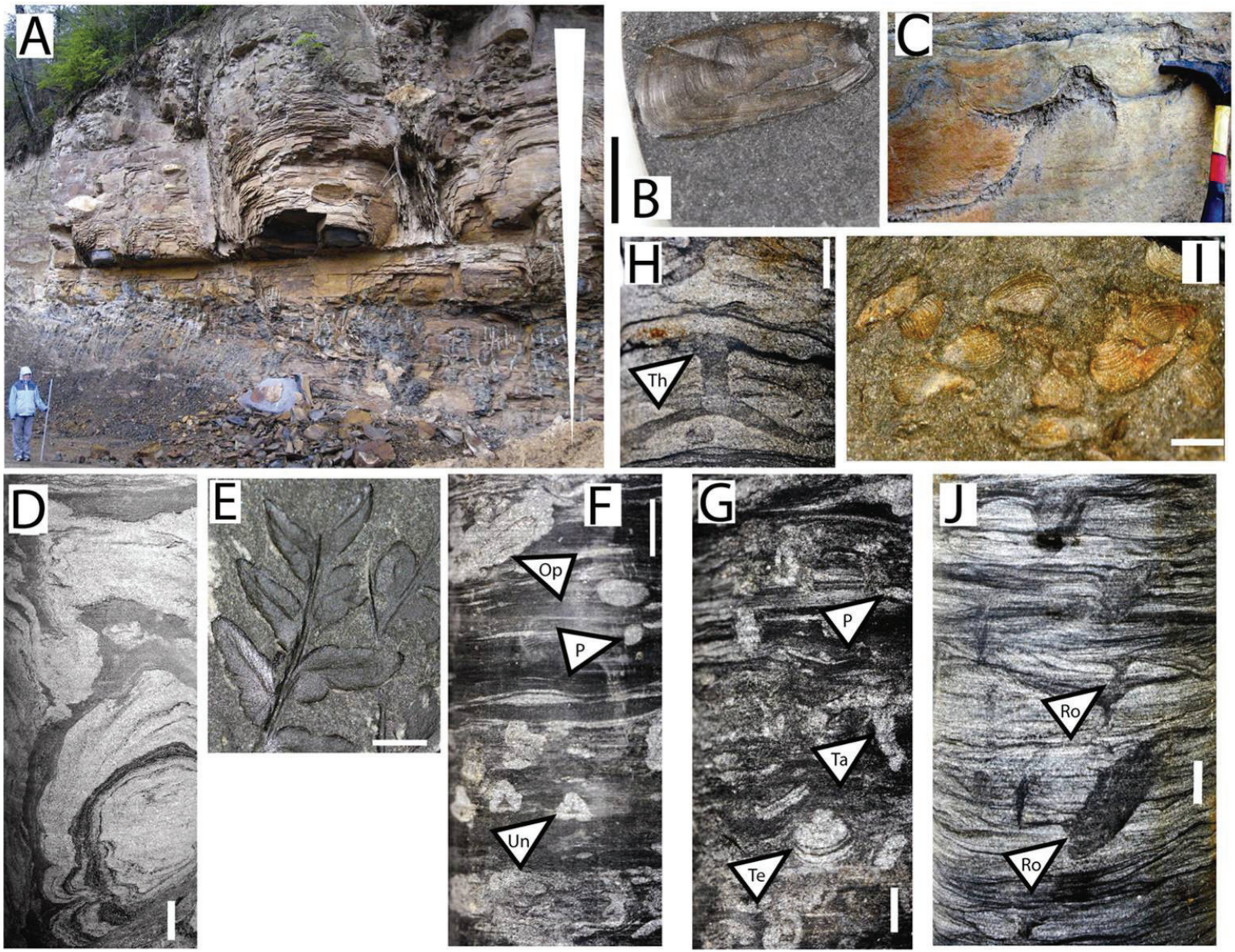
A
B
C
H
Th
I
D
E
F
Op
P
Un
G
P
Ta
Te
J
Ro
Ro

Figure 2.10. Lithologic log with gamma ray wireline log trends of the A1 and A2 sequences at the top of the Bottom Creek Formation in Equitable Sandy Ridge Core, Nora Field Virginia. The vertical facies succession is interpreted to express temporal variations in accommodation space.

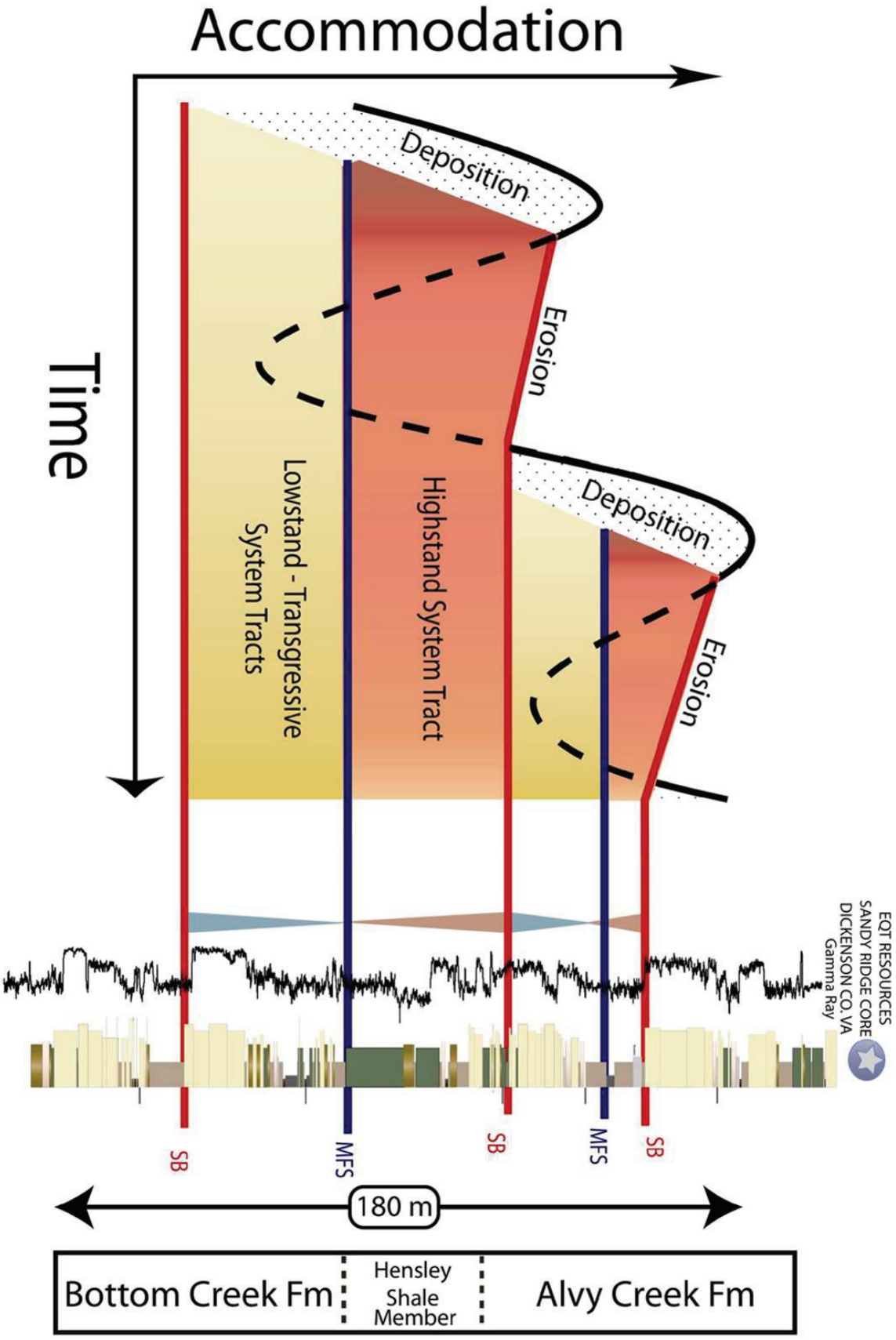
Accommodation
Time
Deposition
Erosion
Deposition
Erosion
Lowstand - Transgressive System Tracts
Highstand System Tract
EQT RESOURCES
SANDY RIDGE CORE
DICKENSON CO. VA
Gamma Ray
SB
MFS
SB
MFS
SB
180 m
Bottom Creek Fm
Hensley Shale Member
Alvy Creek Fm

Figure 2.11. Rationale for stratigraphic picks in the subsurface accompanied with facies examples at Grundy, Virginia. This succession preserves two complete depositional sequences at the top of the Alvy Creek Formation. Lithologic and field gamma ray data (γ CPS) together with inferred surfaces of subaerial erosion in outcrop provide the basis for correlation to nearby well BU-1956. SB= Sequence boundary (red line), MFS = Maximum flooding surface (blue line).

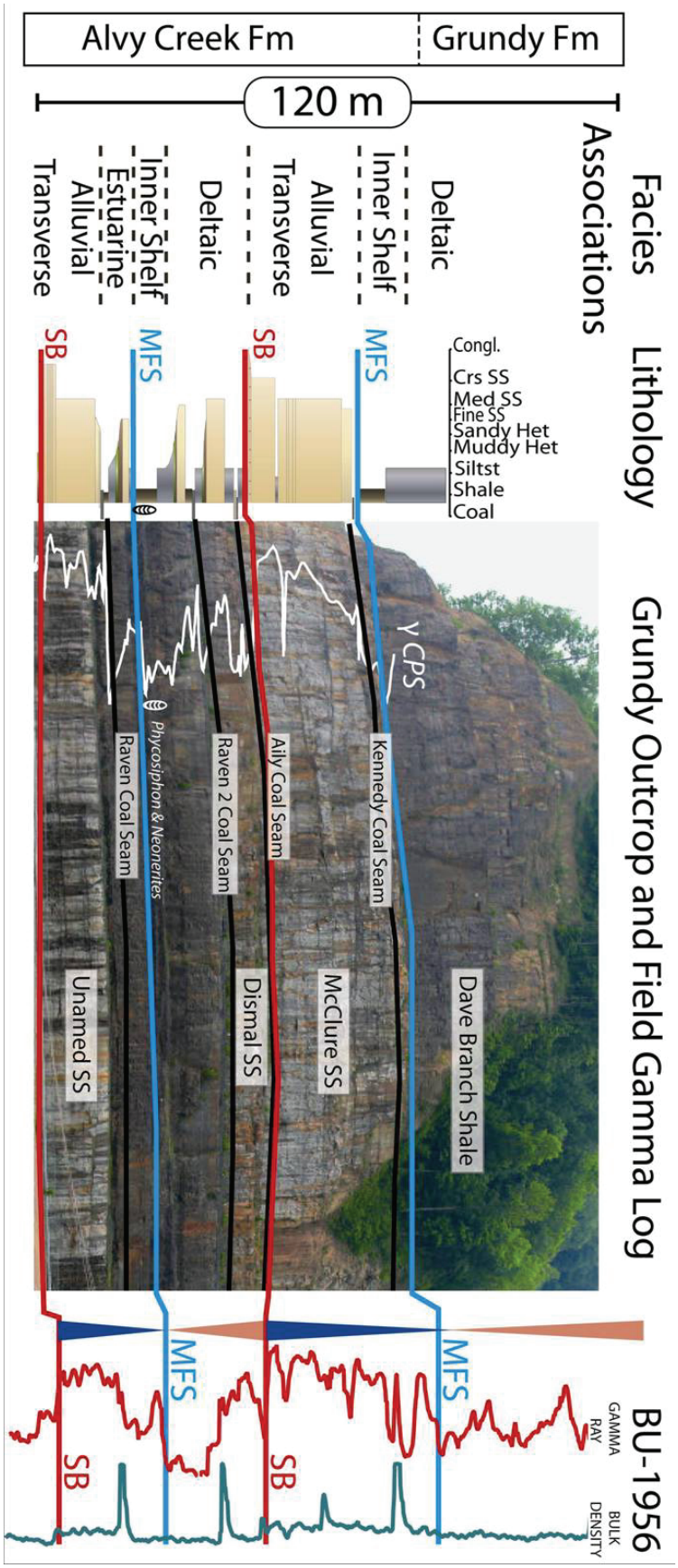
Alvy Creek Fm
Grundy Fm
120 m
Facies Associations
Lithology
Grundy Outcrop and Field Gamma Log
Deltaic
Inner Shelf
Alluvial
Transverse
Deltaic
Alluvial
Transverse
Inner Shelf
Estuarine
Alluvial
Transverse
SB
MFS
SB
MFS
Congl.
Crs SS
Med SS
Fine SS
Sandy Het
Muddy Het
Siltst
Shale
Coal
γ CPS
Kennedy Coal Seam
Ally Coal Seam
Raven 2 Coal Seam
Raven Coal Seam
Phycosiphon & Neonerites
Dave Branch Shale
McClure SS
Dismal SS
Unamed SS
BU-1956
GAMMA RAY
BULK DENSITY
MFS
SB
MFS
SB
MFS
SB

Figure 2.12. Well log correlation panel illustrating stratigraphic architecture along dip cross-section E-E'. Important lithostratigraphic members and interpreted sequence boundaries are labeled. The flooding surface at the base of the Dave Branch Shale is used as the datum surface. Paleoflow of longitudinal fluvial facies is considered oblique to the panel.

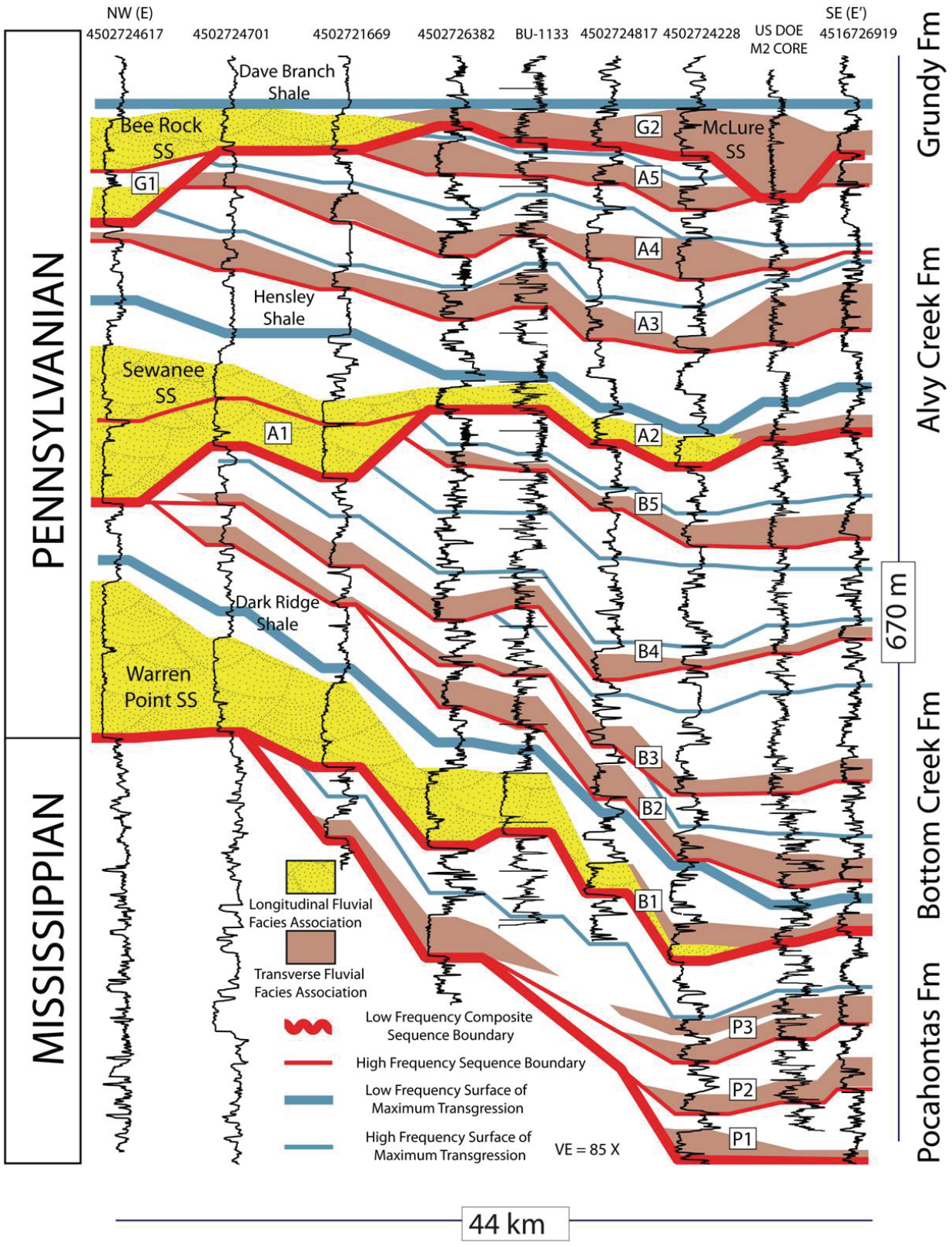
NW (E)
4502724617
4502724701
4502721669
4502726382
BU-1133
4502724817
4502724228
US DOE M2 CORE
SE (E')
4516726919
PENNSYLVANIAN
MISSISSIPPIAN
Dave Branch Shale
Bee Rock SS
G1
G2
McLure SS
A5
A4
Hensley Shale
A3
Sewanee SS
A1
A2
B5
Dark Ridge Shale
Warren Point SS
B4
B3
B2
B1
P3
P2
P1
Grundy Fm
Alvy Creek Fm
Bottom Creek Fm
Pocahontas Fm
670 m
Longitudinal Fluvial Facies Association
Transverse Fluvial Facies Association
Low Frequency Composite Sequence Boundary
High Frequency Sequence Boundary
Low Frequency Surface of Maximum Transgression
High Frequency Surface of Maximum Transgression
VE = 85 X
44 km

Figure 2.13. Well log correlation panel illustrating stratigraphic architecture along strike cross-section Y-Y'. Important lithostratigraphic members and interpreted sequence boundaries are labeled. The flooding surface at the base of the Dave Branch Shale is used as the datum surface. Paleoflow of longitudinal fluvial facies is considered parallel to oblique to the panel.

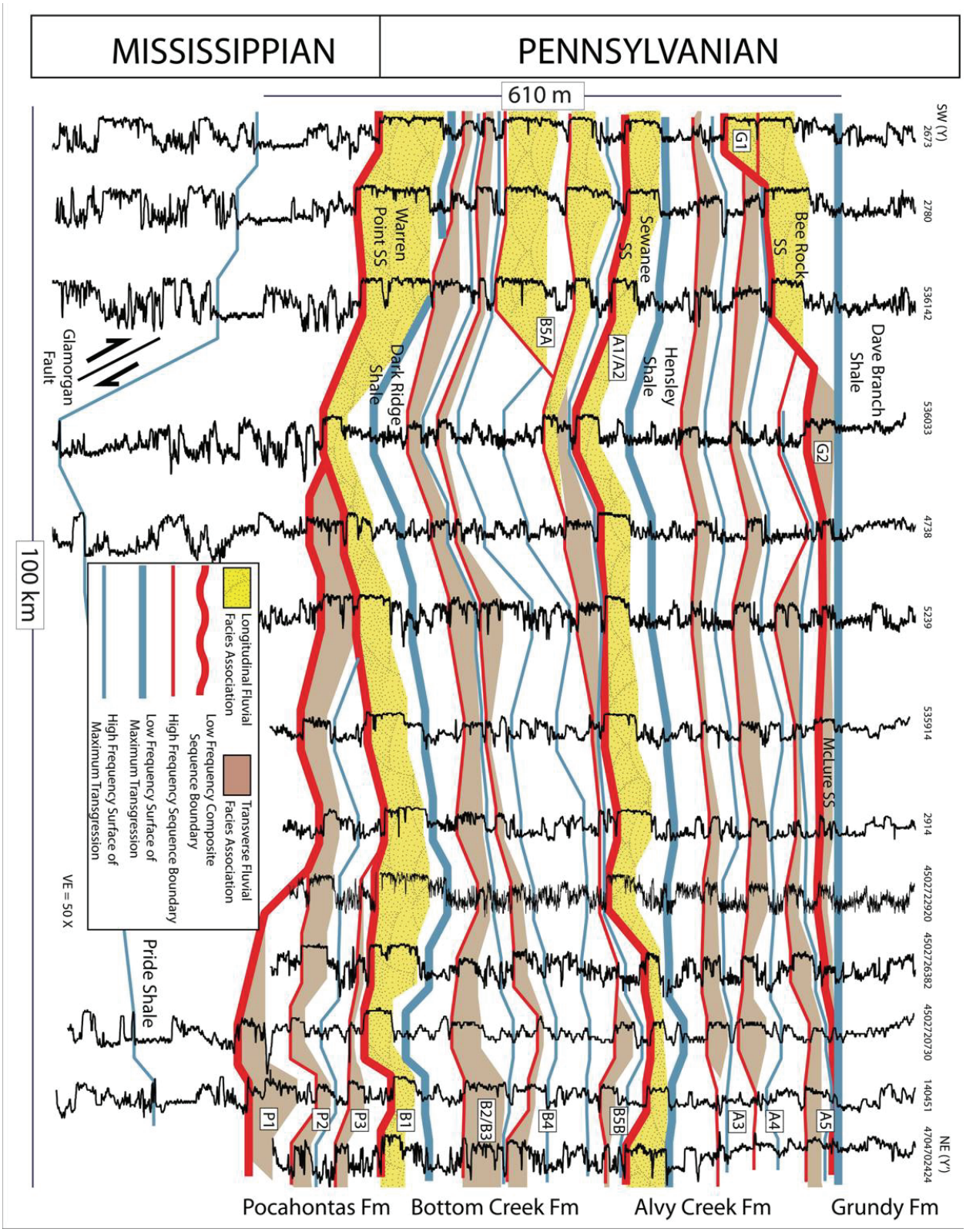
MISSISSIPPIAN
PENNSYLVANIAN
610 m
100 km
SW (Y)
2673
2780
536142
536033
4738
5239
535914
2914
4502722920
4502726382
4502720730
140451
4704702424
NE (Y')
Warren Point SS
Dark Ridge Shale
Sewanee SS
Hensley Shale
Bee Rock SS
Dave Branch Shale
McLure SS
Glamorgan Fault
G1
G2
B5A
A1/A2
P1
P2
P3
B1
B2/B3
B4
B5B
A3
A4
A5
Pride Shale
Pocahontas Fm
Bottom Creek Fm
Alvy Creek Fm
Grundy Fm
Longitudinal Fluvial Facies Association
Transverse Fluvial Facies Association
Low Frequency Composite Sequence Boundary
High Frequency Sequence Boundary
Low Frequency Surface of Maximum Transgression
High Frequency Surface of Maximum Transgression
VE = 50 X

Figure 2.14. Summary lithostratigraphic and sequence stratigraphic architecture schematic of the Early Pennsylvanian Pocahontas Basin. 15 unconformity bounded high frequency sequences are recognized within four low frequency composite sequences defined by major regional unconformities and basin-ward shifts in longitudinal fluvial facies.

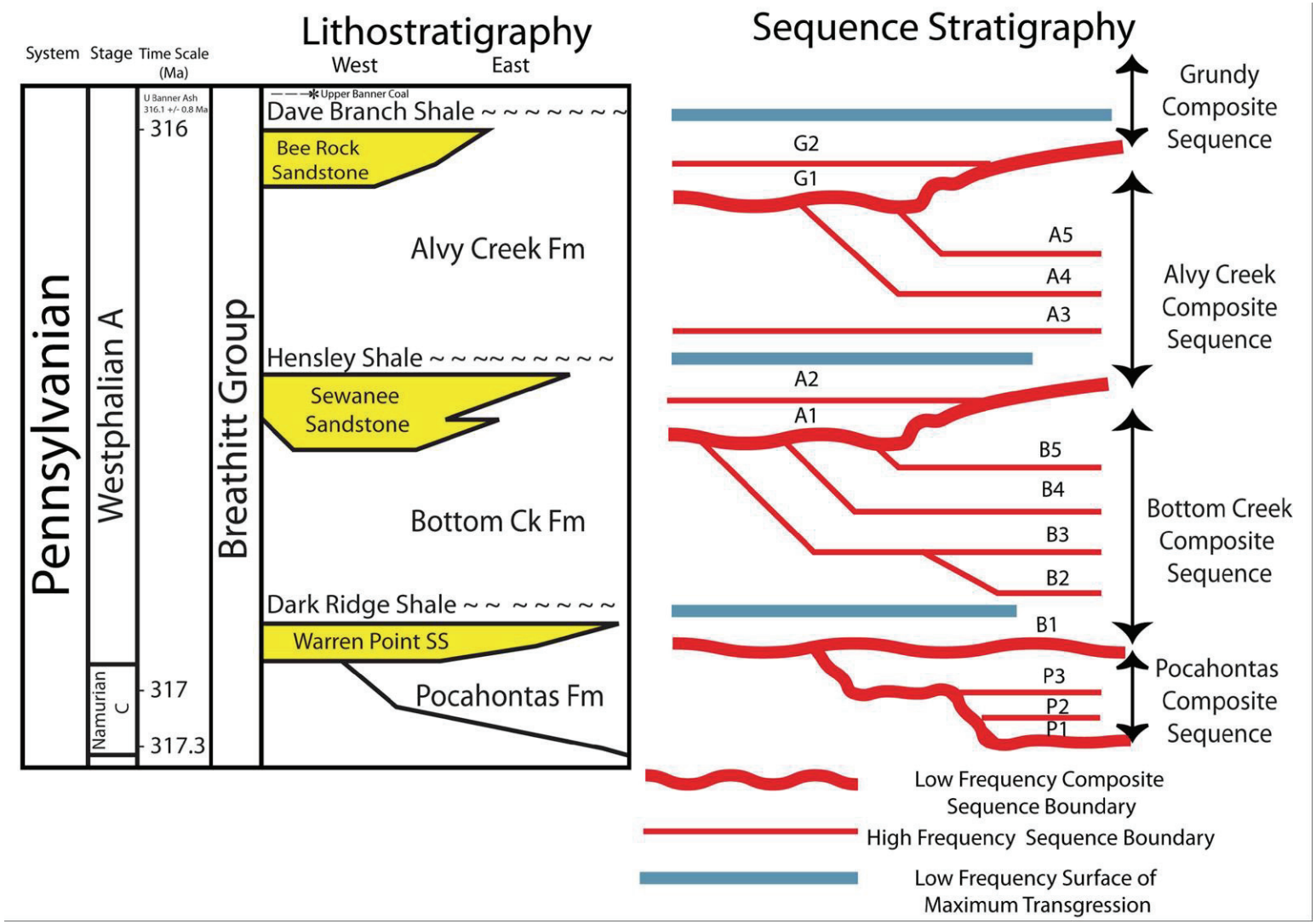
Lithostratigraphy
System
Stage
Time Scale (Ma)
West
East
Pennsylvanian
Westphalian A
Namurian C
U Banner Ash
316.1 +/- 0.8 Ma
316
317
317.3
Breathitt Group
Upper Banner Coal
Dave Branch Shale
Bee Rock Sandstone
Alvy Creek Fm
Hensley Shale
Sewanee Sandstone
Bottom Ck Fm
Dark Ridge Shale
Warren Point SS
Pocahontas Fm
Sequence Stratigraphy
Grundy Composite Sequence
G2
G1
A5
A4
A3
Alvy Creek Composite Sequence
A2
A1
B5
B4
B3
B2
Bottom Creek Composite Sequence
B1
P3
P2
P1
Pocahontas Composite Sequence
Low Frequency Composite Sequence Boundary
High Frequency Sequence Boundary
Low Frequency Surface of Maximum Transgression

Tables

Facies Code	Lithology	Sedimentary Structures	Geometry	Fossil Content	Geophysical Log Motif	Depositional Processes
Cg	Conglomerate and conglomeratic sandstone; rare rounded mudstone clasts (<20 cm), common well-rounded quartz and subrounded siderite pebbles (<5 cm) and plant fragments (< 1 m)	Poorly sorted, grain- supported in quartzose, medium-grained to granule matrix; massive to graded bedding, poorly defined cross beds	Lenticular, 0-3 m thick, average <1m, continuous laterally over 10s of m	Common plant debris	Distinctive low, blocky gamma ray signature, well- defined, sharp base; gamma ray moderate for mudclast and/or siderite pebble lithologies	Channel lag; bottomset deposits of migrating subaqueous dunes
St	Fine- to medium-grained sandstone	Tangential cross beds; foresets concave up, common reactivation surfaces, gently inclined set-bounding surfaces	Wedge to tabular shaped sets; 10-150 cm thick	None	Gamma ray values low for quartzarenites, moderately low for sublitharenites	Migration of sinuous- crested subaqueous dunes
Sp	Fine- to coarse-grained, pebbly sandstone	Planar cross beds	Tabular- and wedge-shaped sets; 0.5-3 m thick, > 100 m long		Gamma ray values low for quartzarenites, moderately low for sublitharenites	Migration of straight- crested subaqueous dunes
Sc	Fine- to coarse-grained sandstone	Compound foresets dip (< 15 degrees) in general flow direction, 10-20 cm- thick intrasets of facies St or Sp	Wedge- to tabular-shaped sets; 1-3 m thick, > 100m long		Gamma ray values low for quartzarenites	Migration of small dunes down the front of large linguoid bars
Str	Fine- to very coarse-grained sandstone	Trough cross beds; highly erosive, concave-up base, low-angle foresets	Lenticular sets 1-3 m thick, 1-5 m wide	Common plant debris	Gamma ray values low for quartzarenites, moderately low for sublitharenites	Migration of lunate subaqueous dunes
Sh	Fine- to medium-grained sandstone	Horizontally stratification	Tabular, 0.5-1 m thick	Common plant debris	Gamma ray values low for quartzarenites, moderately low for sublitharenites	Aggradation under upper-flow-regime conditions
Sr	Fine-grained sandstone	Ripple cross laminations	Tabular beds are < 1 cm thick, < 30 cm long and < 5 cm wide; form lenticular sets	Common plant debris	Gamma ray values low for quartzarenites, moderately low for sublitharenites	Downcurrent migration of ripples
Fis	Sandy heterolithic strata, very-fine to medium sand , sand content 50-90%	Flaser bedded, mm-cm thick cross laminated sandstone beds with mm thick mudstone drapes and flasers; Internal slumping	Tabular, intervals range 0.3 – 4.5m thick	Planolites common, other ichnofacies include *Teichichnus, Roselia, Paleophycus, Thalassinoides, Asterosoma, Neonerites*	Gamma ray values moderate; highly serrated, values commonly increase upward	Alternating sand ripple migration and suspension settling of fines
Fif	Muddy heterolithic	Wavy bedded, mm-cm thick	Tabular, intervals range 0.3	Common plant debris;	Gamma ray values moderate to	Suspension settling of fines

	strata very-fine to fine texture sand, sand content 10-50%	continuous laminations of rippled sandstone intercalated with mm-cm thick mudstone drapes; Lenticular bedded, mm scale laminations with discontinuous sand lenses	– 18m thick	Rare *Neonerities imbricata, Lockeia, Teichichnus, Taenidium, Gyrolithes, Ophiomorpha, Cylindrichnus, Paleophycus*	high; serrated	alternating with sand ripple migration
Fir	Rhythmic Heterolithic	Planar, vertically accreted beds of very fine-grained sandstone to siltstone capped by thin clay drapes, mm-scale laminae within cm-scale bedding couplets; rippled; rooting common	Tabular, intervals range 1.5 – 3m thick	Common plant debris and rhizoliths	Gamma ray values moderate to high; serrated	Periodic suspension settling of fines and deposition of sand laminae
Fs	Siltstone	Weak horizontal laminations	Tabular, intervals range 0.3 – 14m thick	Plant debris abundant, rare Calamites in growth position; rare *Neonerities*	Gamma ray values moderately high; values commonly increase upward	Vertical accretion of fine-grained suspended sediment plumes
Fc	Shale	Siderite nodules; basal horizons commonly carbonaceous	Tabular, intervals range 0.3 – 4m thick	Plant debris common to abundant, extremely rare bivalves, brachipods	Moderately-high to high gamma ray values, uniform motif; basal carbonaceous mudstones display a sharp, high reading	Vertical accretion of fine-grained suspended sediment plumes
Fu	Gleyed Mudstone	Massive to blocky structure; abundant root structures, redox halos and drab mottling	Tabular, intervals range 0.6 – 2m thick	Plant debris, Stigmaria and other rhizoliths	Very low spike on bulk density log (RHOB), thick coals also are characterized by a low gamma ray spike	Pedogenic alteration of suspension deposits
O	Coal	Bright to dull banding; siltstone partings common	Tabular, 0.1-2m thick, 10 m to 10's of km wide			In situ accumulation of organic matter

Table 2.1: Facies Descriptions. Lithofacies code after Miall, 1977.

Facies Association	Component Facies	Characteristics	Geometry
Fluvial – Longitudinal	Cg, St, Sp, Sc, Str, Sh, Sr, Fs, Fu, 0	25-90m thick, unimodal paleoflow, large macroforms oriented in paleoflow direction, multilateral, multistory, quartz-dominated composition	Tabular and lenticular sandstone bodies, sharp-based; channel, gravel bar and bedforms, sandy bedform, downstream accreting elements; capped by fine-grained overbank facies
Fluvial – Transverse	Cg, St, Sp, Fis, Fs, Fu, 0	6-45m thick, unimodal paleoflow, multilateral, commonly single and multistory, rooted top surfaces, complexly interbedded siltstone, immature-sublitharenite composition	Tabular and lenticular sandstone bodies, sharp/irregular-based; channel, gravel bar and bedform, sandy bedform, lateral accretion elements; capped by fine-grained overbank facies
Estuarine	Sr, Fis, Fif, Fir, Fs	10-25m thick, non–cyclic rhythmites, paired laminations, bundled foresets, burial of upright, wetland flora	Tabular bodies overlying fluvial successions, common tidally modulated deposits, grade into inner shelf & deltaic associations
Inner Shelf	Fc, Fs, Fif	10-40m thick, mudstone dominated, siderite nodules, highly marine influenced trace fossil abundances and diversity	Tabular elements of fine-grained deposits above fluvial and estuarine associations
Deltaic	Fis, Fif, Fir, Fs, Fu, Sr, Sh, O	30-160m thick, texture coarsens upward, with increasing sandstone bed thicknesses, common slump and dewatering features	Gradationally overlie estuarine and inner shelf associations with prodelta fines, delta front, mouth bar, distributary channel, and interdistributary delta plain subassociations

Table 2.2: Facies Associations. Lithofacies code after Miall, 1977; Fluvial architectural elements after Miall (1985).

References

Adkins, R.M., and Eriksson, K.A., 1998, Rhythmic sedimentation in a mid-Pennsylvanian delta front succession, Four Corners Formation (Breathitt Group), eastern Kentucky: A near complete record of daily, semi-monthly and monthly tidal periodicities: *in* Alexander, C.B., et al., eds., Tidalites: Processes and products: SEPM (Society for Sedimentary Geology) Special Publication 61, pp. 85-94.

Aitken, J.F., and Flint, S.S., 1994, High-frequency sequences and the nature of incised-valley fills in fluvial systems of the Breathitt Group (Pennsylvanian), Appalachian foreland basin, eastern Kentucky: Incised Valley Systems: Origin and Sedimentary Sequences, p. 3-368.

Aitken, J.F., and Flint, S.S., 1995, The application of high-resolution sequence stratigraphy to fluvial systems: a case study from the Upper Carboniferous Breathitt Group, eastern Kentucky, USA: Sedimentology, v. 42, p. 3-30.

Algeo, T.J., and Wilkinson, B.H., 1988, Periodicity of Mesoscale Phanerozoic Sedimentary Cycles and the Role of Milankovitch Orbital Modulation: Journal of Geology, v. 96, p. 313-322.

Allen, 1964; Allen, J.R.L., 1964, Studies in fluviatile sedimentation: six cyclothems from the Lower Old Red Sandstone, Anglo-Welsh Basin. Sedimentology, 3, 163–198.

Allen, J.L., 1993, Lithofacies relations and controls on deposition of fluvial-deltaic rocks of the upper Pocahontas Formation in southern West Virginia: Southeastern Geology, v. 33, p. 131-147.

Archer, A.W., and Greb, S.F., 1995, An Amazon-scale drainage system in the early Pennsylvanian of central North America: The Journal of Geology, v. 103, p. 611-627.

Arkle, T., Jr., 1974, Stratigraphy of the Pennsylvanian and Permian systems of the central Appalachians, in G. Briggs, ed., Carboniferous of the southeastern United States: Geological Society of America Special Paper 148, p. 5-30.

Aslan, A., and Autin, W.J., 1998, Holocene flood-plain soil formation in the southern lower Mississippi Valley: Implications for interpreting alluvial paleosols: Geological Society of America Bulletin, v. 110, p. 433-449

Autin, W.J., Burns, S.F., Miller, B.J., Saucier, R.T., and Snead, J.I., 1991, Quaternary Geology of the Lower Mississippi Valley, *in* Morrison, R.B., ed., Quaternary Nonglacial Geology; Conterminous U.S.: Boulder, Colorado, Geological Society of America, The Geology of North America, v. K-2, p. 547-581.

Baganz, B.P., 1975, Carboniferous and recent Mississippi lower delta plains [Thesis (M S) thesis], University of South Carolina, 1975.

Barrell, J. 1912. Criteria for the recognition of ancient delta deposits. Geol. Soc. America Bull 23:377–446.

Bennington, J.B., 1996, Stratigraphic and biofacies patterns in the Middle Pennsylvanian Magoffin Marine Unit in the Appalachian Basin, USA: International Journal of Coal Geology, v. 31, p. 169-193.

Best, J.L., and Bristow, C.S., 1993, Braided rivers: London, The Geological Society, vii, 419 p., [4] folded leaves of plates p.

Beuthin, J.D., 1994, A sub-Pennsylvanian paleovalley system in the central Appalachian basin and its implications for tectonic and eustatic controls on the origin of the regional Mississippian-Pennsylvanian unconformity: Tectonic and eustatic controls on sedimentary cycles: SEPM Concepts in Sedimentology and Paleontology, v. 4, p. 107–120.

Beuthin, J. D., 1997, Paleopedological evidence for a eustatic Mississippian-Pennsylvanian (mid-Carboniferous) unconformity in southern West Virginia: Southeastern Geology, v. 37, p. 25-27.

Beynon B.M. and S.G. Pemberton, Ichnological signature of a brackish water deposit: an example from the Lower Cretaceous Grand Rapids Formation, Cold Lake oil sands area, Alberta. In: S.G. Pemberton, Editor, *Applications of ichnology to petroleum exploration: a core workshop*, *Society of Economic Paleontologists and Mineralogists, Core Workshop* 17 (1992), pp. 199–221.

Bhattacharya, J., and Walker, R.G., 1991, River-Dominated and Wave-Dominated Depositional Systems of the Upper Cretaceous Dunvegan Formation, Northwestern Alberta: Bulletin of Canadian Petroleum Geology, v. 39, p. 165-191.

Bishop, J.W., Montanez, I.P., and Osleger, D.A., 2010, Dynamic Carboniferous climate change, Arrow Canyon, Nevada: Geosphere, v. 6, p. 1-34.

Blake, B.M., and Beuthin, J.D., 2008, Deciphering the mid-Carboniferous eustatic event in the Central Appalachian Foreland Basin, southern West Virginia (USA), *in* Fielding, C.R., Frank, T.D., and Isbell, J., Resolving the Late Paleozoic Ice Age in Time and Space: Geological Society of America, Special Publication 441.

Blum, M.D., and Tornqvist, T.E., 2000, Fluvial responses to climate and sea-level change: a review and look forward: Sedimentology, v. 47, p. 2-48.

Bohacs, K., and Suter, J., 1997, Sequence stratigraphic distribution of coaly rocks: Fundamental controls and paralic examples: Aapg Bulletin-American Association of Petroleum Geologists, v. 81, p. 1612-1639.

Bristow, C.S., 1987, Brahmaputra River: Channel migration and deposition, in Ethridge, F.G., Flores, R.M., and Harvey, M.D., eds., Recent Developments in Fluvial Sedimentology: SEPM Special Publication 39, p. 63-74.

Brown, L. F., and Fisher, W. L., 1977, Seismic-stratigraphic interpretation of depositional systems: examples from Brazil rift and pull-apart basins, *in* Payton, C. E., ed., Seismic Stratigraphy—Applications to Hydrocarbon Exploration: American Association of Petroleum Geologists Memoir *26, p.* 213-248

Buatois, L.A., Gingras, M.K., MacEachern, J., Mangano, M.G., Zonneveld, J.P., Pemberton, S.G., Netto, R.G., and Martin, A., 2005, Colonization of brackish-water systems through time: Evidence from the trace-fossil record: Palaios, v. 20, p. 321-347.

Buatois, L.A., Mangano, M.G., Maples, C.G., and Lanier, W.P., 1997, The paradox of nonmarine ichnofaunas in tidal rhythmites: Integrating sedimentologic and ichnologic data from the late Carboniferous of eastern Kansas, USA: Palaios, v. 12, p. 467-481.

Buatois, L.A., Mangano, M.G., Maples, C.G., and Lanier, W.P., 1998, Ichnology of an Upper Carboniferous fluvio-estuarine paleovalley: The Tonganoxie Sandstone, Buildex Quarry, Eastern Kansas, USA: Journal of Paleontology, v. 72, p. 152-180.

Burbank, D.W., 1992, Causes of Recent Himalayan Uplift Deduced from Deposited Patterns in the Ganges Basin: Nature, v. 357, p. 680-683.

Busch, R.M., and Rollins, H.B., 1984, Correlation of Carboniferous Strata Using a Hierarchy of Transgressive-Regressive Units: Geology, v. 12, p. 471-474.

Butts, C., and Virginia Geological Survey., 1927, Oil and gas possibilities at Early Grove, Scott County, Virginia: University, Va., [s.n.], 24 p. p.

Campbell, M.R., 1893, Geology of the Big Stone Gap coal field of Virginia and Kentucky: Washington,, Govt. Print. Off., 106 p. p.

Casagrande, D.J., 1987. Sulphur in peat and coal. In: Scott, A.C. (Ed.), Coal and Coal-bearing Strata: Recent Advances. Geol. Soc. Spec. Publ. 32, pp. 87–105.

Catuneanu, O., 2002, Sequence stratigraphy of clastic systems: concepts, merits, and pitfalls: Journal of African Earth Sciences, v. 35, p. 1-43.

Catuneanu, 2006 Principles of Sequence Stratigraphy, Elsevier, Amsterdam 375 pp..

Cecil, C.B., 1990, Paleoclimate Controls on Stratigraphic Repetition of Chemical and Siliciclastic Rocks: Geology, v. 18, p. 533-536.

Chesnut, D. R., JR., 1981, Marine zones of the (upper) Carboniferous of eastern Kentucky, in Cobb, J. C., Chesnut, D. R., Hester, N. C.,and Hower, J. C., eds., Coal and Coal-bearing Rocks of Eastern Kentucky, Geological Society of America Coal Geology Division field trip, November 1981: Lexington, Kentucky Geological Survey Series 11, p. 57-66

Chesnut, D. R., Jr., 1988, Stratigraphic analysis of the Carboniferous rocks of the Central Appalachian Basin: Unpublished PhD.Dissertation, University of Kentucky, Lexington, 296 p.

Chesnut, D.R., and Kentucky Geological Survey., 1992, Stratigraphic and structural framework of the Carboniferous rocks of the Central Appalachian Basin in Kentucky: Lexington, KY, Kentucky Geological Survey, 41 p., 8 folded leaves of plates p.

Chesnut, D.R., 1994, Eustatic and tectonic control of deposition of the Lower and Middle Pennsylvanian strata of the central Appalachian basin, in Dennison, J.M., and Ettensohn, F.R., eds., Tectonic and Eustatic Controls on Sedimentary Cycles: SEPM, Concepts in Sedimentology and Paleontology No. 4, p. 51-64.

Coleman, J. M., and D. B. Prior, 1982, Deltaic environments of deposition, in P. A. Scholle and D. Spearing, eds., Sandstone depositional environments: AAPG Memoir 31, p. 139-178.

Coleman, J.M., Roberts, H.H., and Stone, G.W., 1998, Mississippi River delta: an overview: Journal of Coastal Research, v. 14, p. 698-716.

Cotter, E., 1978, The evolution of fluvial style, with special reference to the central Appalachian Paleozoic, in Miall, A.D., ed., Fluvial Sedimentology: Canadian Society Petroleum Geologists Mem. 5, p. 361-383.

Cross, T. A., 1988, Controls on coal distribution in transgressive-regressive cycles, Upper Cretaceous, Western Interior, U. S. A., *in* Wilgus, C. K., Hastings, B. S., Kendall, C. G. St. C., Posamentier, H.W., Ross, C. A., and Van Wagoner, J. C., eds., Sea-level Changes: An Integrated Approach: Tulsa, Society of Economic Paleontologists and Mineralogists Special Publication 42, p. 371-380.

Dalrymple, R.W., Zaitlin, B.A., and Boyd, R., 1992, Estuarine Facies Models - Conceptual Basis and Stratigraphic Implications: Journal of Sedimentary Petrology, v. 62, p. 1130-1146.

Davis, M. W., and Ehrlich, R., 1974, Late Paleozoic crustal composition and dynamics in the southeastern United States: Geol. Soc. America Spec. Paper 148, p. 171-185.

De Raaf, J. F. M., H. G. Reading, and R. G. Walker, 1965, Cyclic sedimentation in the Lower Westphalian of North Devon, England: Sedimentology, v. 4, p. 1-52.

Diessel, C.F.K., 1992, Coal-bearing depositional systems: Berlin ; New York, Springer-Verlag, xiv, 721 p. p

Donaldson A.C and. Eble C.F, 1991. Pennsylvanian coals of central and eastern United States. In: H.J. Gluskoter, D.D. Rice and R.B. Taylor, Editors, *Economic Geology, United States. The Geology of North America, Geological Society of America* (1991), pp. 515–523.

Donaldson, A.C., Renton, J.J., and Presley, M.W., 1985, Pennsylvanian Deposystems and Paleoclimates of the Appalachians: International Journal of Coal Geology, v. 5, p. 167-193.

Dott, R. H., JR., 1964, Wacke, graywacke and matrix--what approach to immature sandstone classification?: Jour. Sed. Petrology, v. 34, p. 625-632.

Dyer, K.R., 1986, Coastal and estuarine sediment dynamics: Chichester ; New York, Wiley, xv, 342 p. p.

Eagar RMC. 1974. Shape of shell of Carbonicola in relation to burrowing. Lethaia 7: 219–238.

Eble, C., Greb, S.F., Chesnut, D.R., and Society for Organic Petrology. Meeting, 1991, Coal-bearing rocks along the western margin of the eastern Kentucky coal field: Lexington, Ky., Kentucky Geological Survey, University of Kentucky, 34 p. p.

Eble, C.F., 1996, Lower and lower Middle Pennsylvanian coal palynofloras, southwestern Virginia: International Journal of Coal Geology, v. 31, p. 67-113.

Eble et al., 2009; *Eble, Cortland F., Blake, B.M., Gillespie, WH. And Pfefferkorn, H.W., 2009. Appalachian basin Fossil Floras, in Greb, S.F. and Chesnut, D.R., Jr. (editors), Carboniferous Geology and Biostratigraphy of the Appalachian Basin .Kentucky Geological Survey Special Publication 10, Series XII, pp. 46-58.*

Elliott, T. (1974) Interdistributary bay sequences and their genesis. Sedimentology, 21, 611–622.

Englund, K.J., 1974, Sandstone distribution patterns in the Pocahontas Formation of Southwest Virginia and southern West Virginia: Special Paper Geological Society of America, no, v. 148, p. 31-45.

Englund, K. J., and DeLaney, A. O. 1966. Intertonguing relations of the Lee Formation in southwestern Virginia. U.S. Geol. Surv. Prof. Pap. 550D, p. D47–D52.

Eriksson et al., 2004; Eriksson, K.A., Campbell, I.H., Palin, J.M., Allen, C.M. & Bock, B. (2004) Evidence for Multiple Recycling in Neoproterozoic through Pennsylvanian Sedimentary Rocks of the Central Appalachian Basin. J. Geol., 112, 261–276.

Falcon-Lang, H.J., Nelson, W.J., Elrick, S., Looy, C.V., Ames, P.R., and DiMichele, W.A., 2009, Incised channel fills containing conifers indicate that seasonally dry vegetation dominated Pennsylvanian tropical lowlands: Geology, v. 37, p. 923-926

Ferm, J.C., and Horne, J.C., 1979, Carboniferous depositional environments in the Appalachian region: [Columbia, Dept. of Geology, University of South Carolina], vi, 760 p. p.

Ferm, J.C., and Weisenfluh, G.A., 1989, Evolution of Some Depositional Models in Late Carboniferous Rocks of the Appalachian Coal Fields: International Journal of Coal Geology, v. 12, p. 259-292.

Ferm, J. C., 1970, Allegheny deltaic deposits, in Morgan, J. P., ed.,. Deltaic Sedimentation Modern and Ancient: Tulsa, Society of Economic Paleontologists and Mineralogists Special Publication 15, p. 246- 255

.Fielding, C.R., 1986, Fluvial Channel and Overbank Deposits from the Westphalian of the Durham Coalfield, Ne England: Sedimentology, v. 33, p. 119-140.

Fielding, C.R., Frank, T.D., Birgenheier, L.P., Rygel, M.C., Jones, A.T., and Roberts, J., 2008, Stratigraphic imprint of the Late Palaeozoic Ice Age in eastern Australia: a record of alternating glacial and nonglacial climate regime: Journal of the Geological Society, v. 165, p. 129-140.

Fisk, H. N. and E. McFarlan, Jr., C. R. 1954. Sedimentary Framework of the Modern Mississippi Delta. *Journal of sedimentary research* Vol. 24, no. 2.

Fisk, H. N., 1944, Geological investigations of the alluvial valley of the lower Mississippi River: U.S. Army Corps of Engineers Report, Mississippi River Commission, 78 p.

Flemings, P.B., and Jordan, T.E., 1990, Stratigraphic Modeling of Foreland Basins - Interpreting Thrust Deformation and Lithosphere Rheology: Geology, v. 18, p. 430-434.

Flint, S., Aitken, J., Hampson, G. 1995. Application of sequence stratigraphy to coal-bearing coastal plain successions: implications for the UK Coal Measures. *Geological Society special publication* 82, no. 1,

Frey, R.W., and Pemberton, S.G.,1984, Trace Fossil Facies Models: *in* Walker, R.G., ed., Facies Models (2nd ed.): Geoscience Canada, Reprint Series, No. 1, p. 189–207.

Gastaldo, R.A., Stevanovic-Walls, I.M., Ware, W.N., and Greb, S.F., 2004, Community heterogeneity of early Pennsylvanian peat mires: Geology, v. 32, p. 693-696.

Gernant. 1972. The paleoenvironmental significance of Gyrolithes (Lebensspur). *Journal of paleontology* 46, no. 5 ;

Gibling, M.R., 2006, Width and thickness of fluvial channel bodies and valley fills in the geological record: A literature compilation and classification: Journal of Sedimentary Research, v. 76, p. 731-770.

Goldring, R. 2004. Climatic control of trace fossil distribution in the marine realm. *Geological Society special publication* 228, no. 1

Gradstein, F.M., Ogg, J.G., and Smith, A.G., 2004, A geologic Time Scale, Cambridge Univ. Press, 589 pp.

Graham, S.A., Dickinson, W.R., and Ingersoll, R.V., 1975, Himalayan-Bengal Model for Flysch Dispersal in Appalachian-Ouachita System: Geological Society of America Bulletin, v. 86, p. 273-286.

Greb, S.F., and Chesnut, D.R., 1992, Transgressive Channel Filling in the Breathitt Formation (Upper Carboniferous), Eastern Kentucky Coal Field, USA: Sedimentary Geology, v. 75, p. 209-221.

Greb, S.F., and Chesnut, D.R, 1996, Lower and lower middle Pennsylvanian fluvial to estuarine deposition, central Appalachian basin: Effects of eustasy, tectonics, and climate: Geological Society of America Bulletin, v. 108, p. 303-317.

Greb, S.F., Chesnut Jr, D.R., and Eble, C.F., 2004, Temporal changes in coal-bearing depositional sequences (Lower and Middle Pennsylvanian) of the central Appalachian Basin, USA: Coal-bearing strata: Sequence stratigraphy, paleoclimate, and tectonics of coal-bearing strata: American Association of Petroleum Geologists, Studies in Geology, v. 51, p. 89–120.

Greb, S.F., and Martino, R.L., 2005, Fluvial-estuarine transitions in fluvial-dominated successions; examples from the Lower Pennsylvanian of the Central Appalachian Basin: Special Publication of the International Association of Sedimentologists, v. 35, p. 425-451.

Greb, S.F., J.C. Pashin, R.M. Martino and C.F. Eble, 2008, Appalachian sedimentary cycles during the Pennsylvanian: changing influences of sea level, climate, and tectonics. In: C.F. Fielding, T.D. Frank and J.L. Isbell, Editors, *Resolving the Late Paleozoic Gondwanan Ice Age in Time and Space: Geological Society of America Special Publication Special Publication* 441 , pp. 235–248.

Hampson, G.J., Elliott, T. and Flint, S.S. 1996, Critical application of high resolution sequence stratigraphic concepts to the Rough Rock Group (Upper Carboniferous) of northern England. In: High Resolution Sequence Stratigraphy. Innovations and Applications (Eds J.A.Howell and J.F. Aitken), Geol. Soc. Spec. Publ., 104, 221 – 246

Hampson, G.J., Stollhofen, H. and Flint, S.S. 1999. A sequence stratigraphic model for the Lower Coal Measures, (Upper Carboniferous), of the Ruhr district, north west Germany. Sedimentology, v. 6, p. 1199–1231.

Han, Y.J., and Pickerill, R.K., 1994, Phycodes-Templus Sp-Nov from the Lower Devonian of Northwestern New-Brunswick, Eastern Canada: Atlantic Geology, v. 30, p. 37-46.

Heckel, P.H., 1977, Origin of Phosphatic Black Shale Facies in Pennsylvanian Cyclothems of Mid-Continent North-America: Aapg Bulletin-American Association of Petroleum Geologists, v. 61, p. 1045-1068.

Heckel, P.H., 1986, Sea-Level Curve for Pennsylvanian Eustatic Marine Transgressive-Regressive Depositional Cycles Along Midcontinent Outcrop Belt, North-America: Geology, v. 14, p. 330-334.

Heckel, P.H., Barrick, J.E., Boardman, D.R., Lambert, L.L., Watney, W.L., and Weibel, C.P., 1991, Biostratigraphic Correlation of Eustatic Cyclothems (Basic Pennsylvanian Sequence Units) from Midcontinent to Texas and Illinois: Aapg Bulletin-American Association of Petroleum Geologists, v. 75, p. 592-593.

Herz, N. & Force, E. R. 1984,. Rock suites in Grenvillian terrane of the Roseland district, Virginia, Part 1 Lithologic relations. In: Bartholomew, M. J. (ed.) The Grenville Event in the Appalachians and Related Topics. Geological Society of America, Special Papers 194, 187–199.

Hobday, D.K., and Horne, J.C., 1977, Tidally Influenced Barrier Island and Estuarine Sedimentation in Upper Carboniferous of Southern West-Virginia: Sedimentary Geology, v. 18, p. 97-122.

Houseknecht, D.W., 1980, Comparative Anatomy of a Pottsville Lithic Arenite and Quartz Arenite of the Pocahontas Basin, Southern West-Virginia - Petrogenetic, Depositional, and Stratigraphic Implications: Journal of Sedimentary Petrology, v. 50, p. 3-20.

Howard. 1975. Estuaries of the Georgia Coast, USA: Sedimentology and Biology. IX. Conclusions.. *Senckenbergiana maritima* 7 ;

Imbrie, J., 1978, Climatic Collaboration: Nature, v. 274, p. 844-844.

Isbell, J.L., Miller, M.F., Wolfe, K.L., Lenaker, P.A., 2003. Timing of late Paleozoic glaciation in Gondwana: Was glaciation responsible for the development of northern hemisphere cyclothems? In: Chan, M.A., Archer, A.W. (eds.) *Extreme Depositional Environments: Mega end Members in Geologic Time.* Geological Society of America Special Paper 340, Boulder. pp. 5–24. ;

Jervey, M.T., 1988, Quantitative geological modelling of siliciclastic rock sequences and their seismic expression, in Wilgus, C.K., Hastings, B.S., Kendall, C.G. St. C., Posamentier, H.W., Ross, C.A., and Van Wagoner, J.C., eds., Sea-level Research: An Integrated Approach: SEPM Special Publication 42, p. 47-69.

Klein, G.D., and Willard, D.A., 1989, Origin of the Pennsylvanian Coal-Bearing Cyclothems of North-America: Geology, v. 17, p. 152-155.

Korus, J.T., 2002, The lower Pennsylvanian New River Formation a nonmarine record of glacioeustasy in a foreland basin: [Blacksburg, Va. :, University Libraries, Virginia Polytechnic Institute and State University.

Korus, J.T., Kvale, E.P., Eriksson, K.A., and Joeckel, R.M., 2008, Compound paleovalley fills in the Lower Pennsylvanian New River Formation, West Virginia, USA: Sedimentary Geology, v. 208, p. 15-26.

Kranck, K., 1981, Particulate Matter Grain-Size Characteristics and Flocculation in a Partially Mixed Estuary: Sedimentology, v. 28, p. 107-114.

Kvale, E.P., Archer, A.W., and Johnson, H.R., 1989, Daily, Monthly, and Yearly Tidal Cycles within Laminated Siltstones of the Mansfield Formation (Pennsylvanian) of Indiana: Geology, v. 17, p. 365-368.

López-Gómez, J. and Arche, A., 1993. Sequence stratigraphic analysis and paleogeographic interpretation of the Buntsandstein and Muschelkalk facies (Permo–Triassic) in the SE Iberian Range, E Spain. *Palaeogeogr. Palaeoclimatol. Palaeoecol.* 103, pp. 179–201.

Lyons, P. C.; Krogh, T. E.; Kwok, Y. Y.; and Zodrow, E. L. 1997. U-Pb age of zircon crystals from the upper Banner tonstein (middle Pennsylvanian), Virginia: absolute age of the Lower Pennsylvanian-Middle Pennsylvanian boundary and depositional rates for the Middle Pennsylvanian, central Appalachian basin. *In* Podemski, M.; Dybova, J. S.; Jaworowski, K.; Jureczka, J.; and Wagner, R., eds. Proceedings of the XIII International Congress on the Carboniferous and Permian (Prace Panstwowego Instytut Geologicznego, 157). Warsaw, Prace Panstwowy Instytut Geologiczny, p. 159–166.

Lyons,P.C., T.E. Krogh, Y.Y. Kwok, D.W. Davis, W.F. Outerbridge, H.T. Evans Jr.. 2006. Radiometric ages of the Fire Clay tonstein [Pennsylvanian (Upper Carboniferous), Westphalian, Duckmantian]: A comparison of U-Pb zircon single-crystal ages and 40Ar/39Ar sanidine single-crystal plateau ages. *International journal of coal geology* 67, no. 4,

MacEachern, J.A., and Pemberton, S.G., 1994, Ichnological aspects of incised-valley fill systems from the Viking Formation of the Western Canada sedimentary basin, Alberta, Canada, *in* Dalrymple, R.W., Boyd, R., and Zaitlin, B.A., eds., Incised-Valley Systems; Origin and Sedimentary Sequences: SEPM, Special Publication 51, p. 129-157.

Mack, G.H., James, W.C. and Monger, H.C., 1993. Classification of paleosols. *Geol. Soc. Am. Bull.* 105, pp. 129–136

Mangano, M.G., Buatois, L.A., Maples, C.G., and West, R.R., 2000, A new ichnospecies of Nereites from Carboniferous tidal-flat facies of eastern Kansas, USA: Implications for the Nereites-neonereites debate: Journal of Paleontology, v. 74, p. 149-157.

Martino, R.L., 1994. Facies analysis of Middle Pennsylvanian marine units, southern West Virginia. In: Rice, C.L., Editor, 1994. *Elements of Pennsylvanian Stratigraphy, Central Appalachian BasinGeol. Soc. Am. Spec. Pap.* 294, pp. 69–86. ;

Martino, R.L., 1996, Stratigraphy and depositional environments of the Kanawha Formation (Middle Pennsylvanian), southern West Virginia, USA: International Journal of Coal Geology, v. 31, p. 217-248.

Martino, R.L., and Sanderson, D.D., 1993, Fourier and Autocorrelation Analysis of Estuarine Tidal Rhythmites, Lower Breathitt Formation (Pennsylvanian), Eastern Kentucky, USA: Journal of Sedimentary Petrology, v. 63, p. 105-119.Mangano et al., 2000

Mcbride, E.F.,. 1963. A Classification of Common Sandstones. *Journal of sedimentary research* Vol. 33, no. 3

Menning, M., Alekseev, A.S., Chuvashov, B.I., Davydov, V.I., Devuyst, F.X., Forke, H.C., Grunt, T.A., Hance, L., Heckel, P.H., Izokh, N.G., Jin, Y.G., Jones, P.J., Kotlyar, G.V., Kozur, H.W., Nemyrovska, T.I., Schneider, J.W., Wang, X.D., Weddige, K., Weyer, D., and Work, D.M., 2006, Global time scale and regional stratigraphic reference scales of Central and West Europe, East Europe, Tethys, South China, and North America as used in the Devonian-Carboniferous-Permian Correlation Chart 2003 (DCP 2003): Palaeogeography Palaeoclimatology Palaeoecology, v. 240, p. 318-372.

Miall, A.D. 1977, A review of the braided river depositional environment. Earth Science Reviews, 13, 1–62.

Miall, A.D., 1981, Alluvial sedimentary basins: tectonic setting and basin architecture, *in* Miall, A.D., ed., Sedimentation and Tectonics in Alluvial Basins: Geological Association of Canada, Special Paper 23, p. 1-33.

Miall, A.D., 1985, Architectural-element analysis: a new method of facies analysis applied to fluvial deposits: Earth-Science Reviews, v. 22, p. 261–308.

Miall, A.D., 1991, Stratigraphic Sequences and Their Chronostratigraphic Correlation: Journal of Sedimentary Petrology, v. 61, p. 497-505.

Miall, A.D, 1995, Description and Interpretation of Fluvial Deposits - a Critical Perspective: Sedimentology, v. 42, p. 379-384.

Miall, A.D., 1996, The Geology of Fluvial Deposits: New York, Springer-Verlag, 582 p.

Miall, A.D, 2006, How do we identify big rivers? And how big is big?: Sedimentary Geology, v. 186, p. 39-50.

Miall, A.D., and Jones, B.G., 2003, Fluvial architecture of the Hawkesbury Sandstone (Triassic), near Sydney, Australia: Journal of Sedimentary Research, v. 73, p. 531-545.

Milici, R.C., Kallander, W.C., Wallace, W.G., Morrissey, E.A., and Geological Survey (U.S.), 2000, Bituminous coal production in the Appalachian Basin, past, present, and future [computer file]: [Reston, Va.], The Survey,.

Miller, D.J., and Eriksson, K.A., 1997, Late Mississippian prodeltaic rhythmites in the Appalachian basin: A hierarchical record of tidal and climatic periodicities: Journal of Sedimentary Research, v. 67, p. 653-660.

Mitchum, R.M., 1977, Seismic stratigraphy and global changes of sea level, Part 1: Glossary of terms used in seismic stratigraphy: Seismic stratigraphy: Applications to hydrocarbon exploration: American Association of Petroleum Geologists Memoir, v. 26, p. 205–212.

Mitchum, R.M., and Van Wagoner, J.C., 1991, High-frequency sequences and their stacking patterns: sequence-stratigraphic evidence of high-frequency eustatic cycles: Sedimentary Geology, v. 70, p. 131-160.

Montanez, I.P., Tabor, N.J., Niemeier, D., DiMichele, W.A., Frank, T.D., Fielding, C.R., Isbell, J.L., Birgenheier, L.P., and Rygel, M.C., 2007, CO2-forced climate and vegetation instability during late Paleozoic deglaciation: Science, v. 315, p. 87-91.

Nara, M., 2002, Crowded Rosselia socialis in Pleistocene inner shelf deposits: Benthic paleoecology during rapid sea-level rise: Palaios, v. 17, p. 268-276.

Nichols, M. M., G. H. Johnson, and Peebles, P. C. 1991, Modern sediments and facies model for a microcoastal plain estuary, the James estuary, Virginia, Journal of Sedimentary. Petrology, *61*, 883–899, 1991.

Olariu, C., and Bhattacharya, J.P., 2006, Terminal distributary channels and delta front architecture of river-dominated delta systems: Journal of Sedimentary Research, v. 76, p. 212-233.

Paola, C., Heller, P.L., and Angevine, C.L., 1992, The large-scale dynamics of grain-size variation in alluvial fans, 1--Theory: Basin Research, v. 4, p. 73-90.

Pashin, J.C., 1994, Coal-Body Geometry and Synsedimentary Detachment Folding in Oak-Grove Coalbed Methane Field, Black-Warrior Basin, Alabama: AAPG Bulletin-American Association of Petroleum Geologists, v. 78, p. 960-980.

Pashin, J. C., 2004, Cyclothems of the Black Warrior Basin, Alabama, U.S.A.: Eustatic snapshots of foreland basin tectonism, in J. C. Pashin and R. A. Gastaldo, eds., Sequence stratigraphy, paleoclimate, and tectonics of coal-bearing strata: AAPG Studies in Geology 51, p. 199 –218.

Pashin, J.C., and Ettensohn, F.R., 1992, Paleoecology and Sedimentology of the Dysaerobic Bedford Fauna (Late Devonian), Ohio and Kentucky (USA): Palaeogeography Palaeoclimatology Palaeoecology, v. 91, p. 21-34.

Pemberton, S.G., and Frey, R.W., 1982, Trace Fossil Nomenclature and the Planolites-Palaeophycus Dilemma: Journal of Paleontology, v. 56, p. 843-881.

Pemberton, S.G., and Geological Association of Canada., 2001, Ichnology & sedimentology of shallow to marginal marine systems : Ben Nevis & Avalon reservoirs, Jeanne d'Arc Basin: St. John's, Nfld., Geological Association of Canada, x, 343 p. p.

Pemberton, S.G., and SEPM (Society for Sedimentary Geology), 1992, Applications of ichnology to petroleum exploration : a core workshop: Tulsa, Okla., SEPM, xii, 429 p. p.

Pemberton, S.G., Wightman, D.M., 1992. Ichnological characteristics of brackish water deposits. In: Pemberton, S.G. (Ed.), Applications of Ichnology to Petroleum Exploration. Soc. Econ. Paleontol. Mineral. Core Workshop 17, pp. 141–167.

Posamentier, H.W., 2001, Lowstand alluvial bypass systems: Incised vs. unincised: Aapg Bulletin, v. 85, p. 1771-1793.

Posamentier, H.W., and Allen, G.P., 1999, Siliciclastic sequence stratigraphy : concepts and applications: Tulsa, Okla., SEPM (Society for Sedimentary Geology), vi, 210 p. p.

Posamentier, H.W., Jervey, M.T., and Vail, P.R., 1988, Eustatic controls on clastic deposition I—conceptual framework: Sea-Level Changes: An Integrated Approach: SEPM, Special Publication, v. 42, p. 109–124.1

Quinlan, G.M., and Beaumont, C., 1984, Appalachian Thrusting, Lithospheric Flexure, and the Paleozoic Stratigraphy of the Eastern Interior of North-America: Canadian Journal of Earth Sciences, v. 21, p. 973-996.

Ranger, M.J. and S.G. Pemberton, Marine influence on the McMurray Formation in the Primrose area, Alberta. In: D.P. James and D.A. Leckie, Editors, *Sequences, Stratigraphy, Sedimentology: Surface and SubsurfaceCan. Soc. Pet. Geol. Mem.* 15 (1988), pp. 439–450. ;

Rasbury, E.T., Hanson, G.N., Meyers, W.J., Holt, W.E., Goldstein, R.H., and Saller, A.H., 1998, U-Pb dates of paleosols: Constraints on late Paleozoic cycle durations and boundary ages: Geology, v. 26, p. 403-406.

Reed, Jason Scott. 2003. *Thermal and diagenetic evolution of carboniferous sandstones, central Appalachian basin*. Blacksburg, Va: University Libraries, Virginia Polytechnic Institute and State University

Reed, J.S., Spotila, J.A., Eriksson, K.A., and Bodnar, R.J., 2005, Burial and exhumation history of Pennsylvanian strata, central Appalachian basin: an integrated study: Basin Research, v. 17, p. 259-268.

Reineck, H.E., and Wunderlich, F., 1968, Classification and origin of flaser and lenticular bedding: Sedimentology, v. 11, p. 99-104.

Retallack, Greg J. 2001. *Soils of the past: an introduction to paleopedology*. Oxford: Blackwell Science.

Rial, J.A., 1999, Pacemaking the ice ages by frequency modulation of Earth's orbital eccentricity: Science, v. 285, p. 564-568.

Rice, C.L., and Kentucky Geological Survey., 1984, Sandstone units of the Lee Formation and related strata in eastern Kentucky: Washington, U.S. G.P.O., iv, 53 p. p.

Rice, C.L., and Schwietering, J.F., 1988, Fluvial deposition in the Central Appalachians during the Early Pennsylvanian: U. S. Geological Survey Bulletin, Report: B.

Rice, C.L., and Smith, J.H., 1979, Preliminary correlation chart of coal beds and key beds of the Pennsylvanian rocks of eastern Kentucky: [Reston, Va.], U.S. Geological Survey, 1 correlation chart p.

Rich. 1933. Physiography and structure at Cumberland Gap. *Geological Society of America bulletin* 44, no. 6

Ripepi, Nino Samuel. 2009. *Carbon dioxide storage in coal seams with enhanced coalbed methane recovery geologic evaluation, capacity assessment and field validation of the Central Appalachian Basin*. Blacksburg, Va: University Libraries, Virginia Polytechnic Institute and State University. http://scholar.lib.vt.edu/theses/available/etd-08172009-121452/.

Ross, C. A., and Ross, J. R. P., 1987, Late Paleozoic sea levels and depositional sequences, in Ross, C. A., and Haman, D., eds., Timing and Depositional History of Eustatic Sequences: Constraints on Seismic Stratigraphy: Houston, Cushman Foundation for Foraminiferal Research Special Publication 24, p 137-149

Rygel, M.C., Fielding, C.R., Frank, T.D., and Birgenheier, L.P., 2008, The magnitude of late Paleozoic glacioeustatic fluctuations: a synthesis: Journal of Sedimentary Research, v. 78, p. 500-511.

Safford, J. M., 1893, The Tennessee Coal Measures: U.S. Geol. Survey, Mineral Resources for 1892, p. 477-506.

Salter, T. 1993. Fluvial scour and incision: models for their influence on the development of realistic reservoir geometries. *Geological Society special publication* 73, no. 1

Saucier, R.T., 1981, Current thinking on riverine processes and geologic history as related to human settlement in the southeast: Geoscience and Man, v. 22, p. 7-18. ;

Schumm, S.A., 1981, Evolution and response to the fluvial system, sedimentologic implications, *in* Ethridge, F.G., and Flores, R.M., eds., Recent and Ancient Nonmarine Environments: Models for Exploration: SEPM, Special Publication 31, p. 19–29.

Schumm, S.A., 1993, River Response to Baselevel Change - Implications for Sequence Stratigraphy: Journal of Geology, v. 101, p. 279-294.

Schwarzacher, W., 1993, Cyclostratigraphy and the Milankovitch theory: Amsterdam ; New York, Elsevier, xi, 225 p. p.

Scotese, C.R. & McKerrow, W.S. 1990. Revised world maps and introduction In: McKerrow, W. S. & Scotese, C. R. (eds) Palaeozoic Palaeogeography and Biogeography. Geological Society, London, Memoirs, 12, 1–21.

Sellwood, B.W. 1971: The genesis of some sideritic beds in the Yorkshire Lias. Journal of Sedimentary Petrology 41, 854–858

Shanley, K.W., and Mccabe, P.J., 1994, Perspectives on the Sequence Stratigraphy of Continental Strata: Aapg Bulletin-American Association of Petroleum Geologists, v. 78, p. 544-568.

Shumaker, R.C. and Wilson, T.H. (1996) Basement structure of the Appalachian foreland in West Virginia; its style and effect on sedimentation. In: Basement and Basins of Eastern North America (Eds B.A.Van Der Pluijm and P.A.Catacosinos), Geol. Soc. Am. Spec. Pap. 308, 139–155. Geological Society of America, Boulder, CO.

Sidi, F.H., and Allen, G.P., 2003, Tropical deltas of southeast Asia : sedimentology, stratigraphy and petroleum geology: Tulsa, Okla, SEPM (Society for Sedimentary Geology), 269 p. p.

Sloss, L.L., 1962, Stratigraphic models in exploration: American Association of Petroleum Geologists, Bulletin, v. 46, p. 1050–1057. ;

Smith Jr., L.B.. and J.F. Read, Rapid onset of late Paleozoic glaciation on Gondwana: evidence from Upper Mississippian strata of the Midcontinent, United States, *Geology* 28 (2000), pp. 279–282.

Staub, J.R., 2002, Marine flooding events and coal bed sequence architecture in southern West Virginia: International Journal of Coal Geology, v. 49, p. 123-145.

Stevenson. 1881. A geological reconnaissance of parts of Lee, Wise, Scott and Washington counties, Virginia. *Proceedings of the American Philosophical Society* 19, no. 108,

Strobl, R.S. The effects of sea-level fluctuations on prograding shorelines and estuarine valley-fill sequences in the Glauconitic Member, Medicine River Field and adjacent areas In: D.P. James and D.A. Leckie, Editors, *Sequence, Stratigraphy, Sedimentology: Surface and Sub-surface*, *Canadian Society of Petroleum Geologists, Memoir* 15 (1988), pp. 221–236. ;

Tankard, A.J., 1986, Depositional Response to Foreland Deformation in the Carboniferous of Eastern Kentucky: Aapg Bulletin-American Association of Petroleum Geologists, v. 70, p. 853-868.

Tessier, B., 1993, Upper Intertidal Rhythmites in the Mont-Saint-Michel Bay (Nw France) - Perspectives for Paleoreconstruction: Marine Geology, v. 110, p. 355-367.

Tessier, B., Archer, A.W., Lanier, W.P. and Feldman, H.R. (1995) Comparison of ancient tidal rhythmites (Carboniferous of Kansas and Indiana, USA) with modern analogues (the Bay of Mont-Saint-Michel, France). Int. Assoc. Sedimentol. Spec. Publ., 24 259–271.

United States. 1984. *Soil taxonomy: a basic system of soil classification for making and interpreting soil surveys*. New York: Wiley.

Van Heerden, I. L., and Roberts, H. H., 1988, Facies development of Atchafalaya Delta, Louisiana: a modern bayhead delta: Am. Assoc. Pet. Geol. Bull., v. 72, p. 439-453.

Van Wagoner, J.C., and American Association of Petroleum Geologists., 1990, Siliciclastic sequence stratigraphy in well logs, cores and outcrops : concepts for high-resolution correlation of time and facies: Tulsa, Oklahoma, American Association of Petroleum Geologists, 55 p., [11] folded leaves of plates p.

Van Wagoner, J.C., Posamentier, H.W., Mitchum, R.M.J., Vail, P.R., Sarg, J.F., Loutit, T.S., and Hardenbol, J., 1988, An overview of the fundamentals of sequence stratigraphy and key definitions: Sea-Level Changes: An Integrated Approach: SEPM, Special Publication, v. 42, p. 39–45.

Veevers, J.J., and Powell, C.M., 1987, Late Paleozoic Glacial Episodes in Gondwanaland Reflected in Transgressive-Regressive Depositional Sequences in Euramerica: Geological Society of America Bulletin, v. 98, p. 475-487.

Wanless, H.R., and Shepard, F.P., 1936, Sea level and climatic changes related to late Paleozoic cycles: Bulletin of the Geological Society of America, v. 47, p. 1177-1206.

Wetzel, A. and Bromley, R.G., 1994. *Phycosiphon incertum* revisited: *Anconichnus horizontalis* is its junior subjective synonym. *Journal of Paleontology* 68, pp. 1396–1402. , 1994

Wizevich, M.C., 1992, Sedimentology of Pennsylvanian Quartzose Sandstones of the Lee Formation, Central Appalachian Basin - Fluvial Interpretation Based on Lateral Profile Analysis: Sedimentary Geology, v. 78, p. 1-47.

Wizevich, M.C., 1993, Depositional Controls in a Bedload-Dominated Fluvial System - Internal Architecture of the Lee Formation, Kentucky: Sedimentary Geology, v. 85, p. 537-556.

Wright, V.P., and Marriott, S.B., 1993, The Sequence Stratigraphy of Fluvial Depositional Systems - the Role of Floodplain Sediment Storage: Sedimentary Geology, v. 86, p. 203-210.

CHAPTER 3
Orogenic Controls on the Spatial and Temporal Distribution of Longitudinal and Transverse Alluvial Facies in an Early Pennsylvanian Foreland Basin, Virginia

RYAN P. GRIMM [1], KENNETH A. ERIKSSON [1], JOYCE CARBAUGH [1]

1. *Department of Geosciences, Virginia Tech, Blacksburg, Virginia 24061, USA*

Abstract

Foreland basins provide the opportunity to review the sedimentary response to tectonic phases at convergent plate margin settings. The lower Breathitt Group of the Pocahontas Basin, a sub-basin of the Central Appalachian Basin located in Virginia, preserves an early Pennsylvanian record of sedimentation during the initial phases of foreland basin subsidence during the onset of the Alleghanian orogeny. Utilizing the relative distribution of fluvial facies and long-term stacking patterns within the context of an ancient, marginal-marine foreland basin provides independent stratigraphic evidence to disentangle a recurring, residual tectonic signature from high-frequency, periodic glacioeustatic events.

Facies analysis supports a two end-member depositional system of coexisting transverse and longitudinal alluvial systems infilling the Pocahontas Basin foredeep during eustatic lowstands. Petrology and detrital zircon geochronology indicates that sediment was derived from low-grade metamorphic Grenvillian-Avalonian terranes and recycling of older Paleozoic sedimentary rocks uplifted as part of the Alleghanian orogen towards the southeast and, in part, from the Archean Superior Province to the north. Immature sediments, including lithic sandstone bodies, were deposited within a southeast-northwest oriented transverse drainage system. Quartzarenites were deposited within a strike-parallel northeast-southwest oriented axial drainage, forming elongate belts along the western periphery of the basin. These mature quartzarenites are braided fluvial in origin which originated from a northerly cratonic source area.

Integrating subsurface datasets with sandstone provenance observations indicates significant, repeated paleogeographic shifts in alluvial facies distribution. Distinct composite

sequence wedges are bounded by successive shifts in alluvial facies and define three tectonic accommodation cycles. Each tectonic accommodation cycle is represented by a phase of accelerated tectonic advance and subsidence, followed by mass redistribution and slowed regional subsidence. During episodes of thrust load advance, the medial-distal Pocahontas foredeep was starved of orogen sourced sediment supply. The decreased sediment delivery from the orogen allowed longitudinal fluvial systems to comb toward the orogen and deposit sediment of cratonic heritage. Continued loading enhanced high frequency transgressions and preserved thick, regional, marine-influenced mudstones. Rates of subsidence slowed and orogenic sediment supplies returned to be redistributed by cratonward prograding transverse fluvial systems. Longitudinal drainages were subsequently diverted to distal foredeep and forebulge positions.

These cycles are inferred to have controlled the short-term (~ 0.5 Ma) variability in basin accommodation and hinterland sediment supply during the long-term cratonward progression of the Alleghanian orogenic wedge. The proposed tectonic accommodation cycles provide an explanation for the observed low-frequency composite sequences and most likely record transient deformation events during the Alleghanian Orogeny.

Keywords

Appalachian Basin, Foreland Basin, Detrital Zircon, Alluvial Facies, Pennsylvanian, Alleghanian Orogeny

1. Introduction

Alluvial facies distributions and resultant stratal patterns in alluvial/shallow marine foreland basins have been demonstrated to be controlled by a combination of tectonic phases and glacioeustatic sea level fluctuations (**Miall, 1981; Posamentier and Allen, 1993; Wright and Marriott, 1993; Shanley and McCabe, 1994; Mackey and Bridge, 1995).** Fundamental criteria for the recognition of tectonic controls in foreland basins include rapid changes in the relative distribution of longitudinal and transverse alluvial facies belts (**Burbank, 1992; Paola et al., 1992),** enhanced transgressions (**Tankard, 1986; Blair and Bilodeau, 1988),** intraformational unconformities and abrupt changes in siliciclastic provenance (**Miall and Arush, 2001**). In the Early Pennsylvanian Pocahontas Basin, a subbasin of the Central Appalachian Basin located in Virginia, the relative distribution of lowstand fluvial facies and long-term stacking patterns within the context of an ancient, marginal-marine foreland basin may provide independent stratigraphic evidence to disentangle a recurring, residual tectonic signature from high- frequency, periodic glacioeustatic events.

Foreland basins form along active collisional margins during plate convergence between the advancing orogenic wedge and the craton (**Beaumont, 1981**). Topographic loading by orogenic thickening and stacked thrust-sheets as well as subsurface loads on the margin of the craton deflect the elastic lithosphere due to isostatic compensation (**Turcotte and Schubert, 1982; Flemings and Jordan, 1990).** Crustal flexure results in cratonward upwarping to form a forebulge (**Flemings and Jordan, 1990),** while concurrent backward rotational subsidence toward the load forms accommodation for the accumulation of sediment eroded from the orogenic belt (**DeCelles and Giles, 1996).** Stratal thinning toward the forebulge, hinterland

thickening and thinning of deposits toward and onto the orogenic wedge form a doubly tapered prism (**DeCelles and Giles, 1996**).

Accommodation within these convergent settings preserves important sedimentary records of long term, large-scale river systems (**Miall, 1981; Tandon and Sinha, 2007).** As the orogen rises, mountain-fed transverse alluvial systems drain toward longitudinal alluvial systems flowing axially along the structural grain of the orogen (**Potter, 1978)**. Sediment in transverse systems is mostly sourced from the fold-thrust belt, whereas longitudinal systems gather discharge from both transverse alluvial systems and extrabasinal drainages sourced from the craton and flowing toward the subsiding foreland region **(Miall, 1981**). Modern foreland basin examples of transverse and longitudinal drainages infilling active foredeeps include the Po Basin (**Ori, 1993**), Ganga Basin (**Sinha and Friend, 1994; Gupta, 1997**), Euphrates-Tigris Basin (**Baltzer and Purser, 1990**) and the Amazonian Basin (**Rasanen et al., 1992)**.

Variability in hinterland tectonic activity can develop alternating episodes of increased loading and quiescence, directly impacting rates of basin-floor subsidence as well as available sediment supply and delivery routes from the orogen to the foredeep (**Garcia-Castellanos, 2002)**. These episodic variations in sediment supply and differential foredeep accommodation promote rapid shifts in drainage patterns and relative spatial positions of transverse and longitudinal systems (**Burbank, 1992; Garcia-Castellanos, 2002)**. In foredeep successions with strong contrasts in scale, fluvial style and catchment source areas between longitudinal and transverse systems, the possibility exists to utilize the produced distribution of alluvial facies to interpret the role of tectonic events on foreland basin architecture.

This paper presents an integrated study of sandstone petrography, provenance analysis, subsurface facies mapping and stratal stacking patterns to: 1) define the spatial and temporal

distribution of longitudinal and transverse alluvial facies in the project area to constrain paleogeography; 2) highlight stratigraphic indications of low-frequency orogenic activity; and 3) reconstruct the tectono-sedimentary evolution of the Early Pennsylvanian Pocahontas Basin.

2. Geologic Background

2.1 Tectonic Setting

The Appalachian Basin extends approximately 1800 km from Alabama to New York, ranges 100- 500 km in width and is partitioned into a series of sub-basins, including the Pocahontas Basin in southern West Virginia and southwest Virginia (**Fig. 3.1)**. The Pocahontas Basin is delineated by major bounding structures: the Appalachian Valley and Ridge to the east in southwestern Virginia, the Cincinnati Arch marks the western limit of the basin in eastern Kentucky and eastern Tennessee and a structural hingeline accompanied by series of fault systems separate the Pocahontas Basin from the more northerly Dunkard Basin of south central West Virginia (**Fig. 3.1).**

Early Pennsylvanian sedimentation in the Pocahontas Basin was concurrent with the Alleghanian orogeny. Plate reconstructions indicate that Laurentia (N. Am) was situated in tropical equatorial latitudes (**Scotese, 2003**), undergoing oblique convergence with Gondwana (Africa) and zipper-like closure of the Iapetus Ocean during the assembly of Pangaea, as evident from the collisional suture along the margins of Laurentia and Gondwana (**Van der Voo, 1983; Hatcher, 1989, 2002**).

Early Pennsylvanian flexure is suggested to be related to the Lackawanna Tectophase**,** a period of regional layer-parallel shortening that was a precursor event to the Main Tectophase of Permian collision **(Geiser and Engelder, 1983).** Paleostress analyses indicate that early

Alleghanian jointing is preserved close to the study area in the Greenbrier Limestone of southwestern West Virginia (**Dean et al., 1988).** Several studies suggest that the initial phase of the Alleghanian orogeny was highly oblique and transpressive, citing translation along dextral strike-slip faults and dextral shear along the Brevard fault (**Vauchez, 1987; Gates et al., 1988; Valentino and Gates, 2001).** Penecontemporaneously, Gondwana began to rotate clockwise around the New York promontory and initiated collision with southeastern Laurentia (**Hatcher, 2002**), leading to accretion of peri-Gondwanan terranes, including the Suwannee Terrane (**Horton et al., 1989)** and the emplacement of granitoid plutons with associated deformation of the Piedmont dated ~ 327-295 Ma (**Secor et al., 1986**). Deformation continued and advanced into a main phase of collision in the Permian (**Secor et al., 1986),** leading to large-scale overthrusting of Grenvillian Basement and development of the Blue Ridge megathrust in eastern Virginia and the Carolinas (**Hatcher, 1972, 2002).** Final orogenic-phase, thin-skinned deformation led to overthrusting of Pennsylvanian rocks along the Pine Mountain Fault, to define the geographic western limit of Alleghanian deformation **(Mitra, 1988) (Figs. 3.1 and 3.2).**

2.2 Stratigraphic Setting

In the Central Appalachian Foreland Basin, the craton responded to the initial phase of compressional loading (Lackawanna Tectophase) by forming a broad, ~1300 km-long, 500 km-wide and relatively shallow foredeep depozone (**Ettensohn, 2004**), controlled by an exceedingly rigid crust (~10^{24} Nm) after successive orogens and long term crustal cooling (**Turcotte and Schubert, 1982; Watts,1992**). This flexural downwarping generated the greatest accommodation in the foredeep adjacent to the thrust front, forming a southeasterly thickening

clastic wedge of Early Pennsylvanian sedimentary rocks, with the thickest package preserved in southwestern Virginia.

Early Pennsylvanian sedimentary rocks of the Lee Formation and Breathitt Group unconformably overlie the late Mississippian Bluestone Formation and attain a maximum thickness of approximately 900m (2950 ft) along the southeast margin of the Pocahontas Basin in Virginia and West Virginia (**Englund et al., 1979; Englund and Thomas, 1990; Korus, 2002; Blake and Beuthin, 2008**). The four coal-bearing lithostratigraphic units of the Breathitt Group investigated include the Pocahontas, Bottom Creek, Alvy Creek and Grundy Formations, which are juxtaposed against and intercalated with the Warren Point, Sewanee and Bee Rock quartzarenite lenses of the Lee Formation along the western margin of the study area (**Rice and Schwietering, 1988; Chesnut, 1994).** These lithostratigraphic units are further subdivided by regionally thick, marine-influenced shale members, the Dark Ridge, Hensley and Dave Branch shales, as summarized in the chart of lithostratigraphic relationships in **Fig. 3.3 (Chesnut, 1994)**.

The current paleogeographic model depicts the interaction of longitudinal and transverse fluvial systems draining contrasting terranes. During eustatic lowstands, transverse fluvial systems draining the Alleghanian fold and thrust belt flowed westerly, eventually merging into large, bedload-dominated longitudinal braided river system draining an Amazon- scale cratonic watershed (**Rice and Schwietering, 1988; Greb and Chesnut, 1996; Korus et al., 2008).** The axial drainage dispersed sediment down a paleoslope to the southwest, toward open-marine settings in the Black Warrior Basin and Ouachita Foredeep (**Shlee, 1963; Graham et. al., 1975; Archer and Greb, 1995; Churnet, 1996).** During subsequent sea level rise, these fluvial systems were transgressed forming broad estuaries (**Greb and Chesnut, 1996; Greb and Martino, 2005; Bodek, 2006; Korus et al,. 2008)**. Following drowning, small, tropical, fluvial-

dominated deltas prograded across the basin, infilling available accommodation space **(Korus et al., 2008).**

Transverse fluvial facies of sublithic sandstones and intercalated mudstones are preserved in the coal-bearing, immature siliciclastic strata of the Breathitt Group. Lithic sandstones accumulated as channeled sandstone-mudstone bodies 1-10 km wide and up to 30 m thick that filled broad alluvial valleys transverse to the thrust front (**Korus, 2002).** These immature sandstones have been interpreted to be derived from mountain fed alluvial systems draining low grade metamorphic terranes uplifted to the southeast during the Alleghanian orogen **(Davis and Ehrlich, 1974**; **Houseknecht, 1980; Reed et al., 2005).**

Longitudinal fluvial facies of quartz pebble bearing, texturally and mineralogically mature quartzarenites with rare intercalated siltstones are preserved in strike-parallel elongate belts 17-100 km wide and up to 200 m thick along the western periphery of the basin, situated between the lithic-rich Breathitt Group and the elevated Cincinnati Arch (**Rice, 1984; Chesnut, 1988)**. This mature sandstone belt is interpreted as the product of a long lived, southwesterly flowing longitudinal braided river system that was fed by an extensive cratonic drainage network **(Houseknecht, 1980; Rice, 1984; Rice and Schwietering, 1988; Archer and Greb, 1995; Greb and Chesnut, 1996; Eriksson et al., 2004).**

3. Methods

In this study, facies and facies associations were described at **23** outcrop-measured sections in large roadcuts, abandoned mine workings and several natural ravines and in **7** continuous cores donated to Virginia Tech from coal exploration operations (**Fig. 3.2**). Facies were described based on color, lithology, bounding contacts, sedimentary structures,

fossil/ichnofabric content and stratal geometries (**Table 3.1)**. Paleocurrent data were measured at several field locations, primarily where three-dimensional access to tabular and trough cross-bedded sandstones was available. Collected paleocurrent data was plotted as rose diagrams for each sandstone unit. Gamma ray scintillometer data were collected from outcrops as well as core descriptions were used to calibrate geophysical well logs and allow facies variability and key sequence surfaces to be traced into the subsurface.

In the subsurface, a dataset of **> 1,200** gamma ray wireline logs from natural gas development wells were compiled to develop a series of cross sections and isopach maps through the study interval (**Fig. 3.2**). The constructed cross sections are NW-SE dip-oriented and SW-NE strike-oriented. These wire-line sections incorporated core logs and were tied at shared well points. Gamma ray and bulk density curves provided proxies for lithologies. Trends in texture and distinctive lithological contacts were interpreted from gamma ray log motifs and bulk density curves define coal horizons, which have dramatically lower densities than surrounding siliciclastic lithologies. Correlations were accomplished using pattern matching of distinctive stratigraphic surfaces and marker beds such as regional coals and thick shale submembers. Following correlation, three isopach maps and three net sandstone maps were constructed to establish a temporal-spatial distribution of thickness trends for each formation of the Breathitt Group and sandstone member of the Lee Formation. Footages of gamma ray API values <35 were tabulated for each formation to map quartzarenite sandstone members.

In addition to facies mapping, petrologic and detrital zircon geochronology data were collected to establish provenance heritage of alluvial facies. Petrologic data for Early Pennsylvanian sandstone members were compiled from thin sections of **57** samples collected from **3** cores acquired across southwestern Virginia, providing unweathered samples to

accurately evaluate labile framework grain contents (**Fig. 3.3).** Framework grains were identified based on optical petrographic microscope properties using a Nikon polarizing light microscope and a Leitz mechanical stage. Two-hundred points were counted on all thin sections using point counting procedures of Glagolev-Chayes method **(Galehouse, 1971).** K-Ferricyanide stain was applied to determine potassium feldspar abundance. Previous petrographic datasets were assembled from published work on Pennsylvanian sandstones by **Siever (1957), Houseknecht (1978, PhD), Wizevich (1991, PhD) and Reed (2005, PhD)** to supplement our dataset with petrographic data from an additional **213** samples**.** This aggregate of petrologic data was plotted on QFL and QmFLt ternary diagrams of **Dickenson et al., (1983)** to graphically determine dominant petrographic modes.

The detrital zircon dataset was assembled from published sources (**Eriksson et al., 2004; Becker et al., 2005**) and previously unpublished zircon data. Zircon ages from U-Pb SHRIMP ion microprobe data are derived from the weighted means of ^{207} Pb / ^{206} Pb and ^{206} Pb / ^{238} U ratios.

Ages older than 800 Ma are calculated from ^{207} Pb / ^{206} Pb ratios, younger ages based on ^{206} Pb / ^{238} U Ratios. These results were sorted for grains <10% discordant and plotted in histograms for comparison.

4. Facies Associations

Observed facies are organized into two end-member fluvial facies associations in **Table 3.1.** The facies associations represent the depositional products of fluvial-longitudinal and fluvial-transverse settings, each defined by physical, compositional and geometric characteristics.

4.1 Longitudinal Fluvial Facies Association

The longitudinal fluvial facies association is dominated by 10-50 m thick, regional multistory quartzarenite sandstone bodies of the Warren Point, Sewannee and Bee Rock members (**Fig. 3.2**). Lithofacies range from massive quartz pebble conglomerate to fine-grained sandstone. These white to light gray sandstones are commonly coarser grained toward the base, with channel lags of 1-5 cm diameter quartz pebbles, 0.2-1m long logs and oriented plant fragments observed along scoured basal contacts at outcrops and in core (**Fig. 3.4A**). Sandstones are commonly cross-bedded with planar (**Fig. 3.4B**), tangential (**Fig. 3.4C**) and trough crossbed forms and make up long (15-100 m), traceable tabular to wedge-shaped bedsets, 0.5-1.5 m thick. Rarely, tabular crossbed sets are truncated by reactivation surfaces, which form the base for compound cross bedding (**Fig. 3.4D**). Foreset measurements of cross-bedded units correspond with the orientation of flute structures and log casts, demonstrating unimodal paleocurrents to the west-southwest and south-southwest for the Warren Point and Bee Rock Sandstone members, respectively (**Fig. 3.4E and 3.4F**). Sandstone intervals are mantled by heavily rooted siltstones. Characteristics of the longitudinal fluvial association are summarized in **Table 3.1.**

A braided fluvial origin for this facies association is supported by the presence of thick conglomerate lags, variety of cross strata, channel scour-and-fill structures, development of downstream accreting elements and compound channel macroforms, unidirectional paleocurrents for bedforms and macroforms, closely spaced erosion surfaces, fining-upward sequences, floodplain paleosols, and the absence of marine body fossils (**Grimm et al., submitted**). Initially, these mature quartzarenites were reported as barrier bar deposits (**Hobday and Horne,**

1977; Ferm and Horne, 1979) but were later demonstrated to be multi-cycle, braided fluvial deposits based on detailed sedimentology and architectural element analysis (**Wizevich, 1992).**

4.2 Transverse Fluvial Facies Association

The transverse fluvial facies association is dominated by 5-25 m thick, regional, single to amalgamated multistory litharenite sandstone bodies intercalated within the coal-bearing intervals of the Pocahontas, Bottom Creek and Alvy Creek Formations (**Fig. 3.2**). Lithofacies range from massive siderite-pebble, shale-fragment and plant-debris conglomerate lags **(Figs. 3.5A and 3.5B**) fining upward to rooted, silty-sandstones and coals (**Fig. 3.5C)**. In outcrop and core, medium gray sandstone bodies overlie sharp erosional surfaces that exhibit 2-10 m of localized relief in outcrop (**Fig. 3.5D)** and are also commonly observable in core (**Fig. 3.5E).** Sedimentary structures are predominantly trough cross beds **(Fig. 3.5F)** with minor planar crossbeds, horizontal parting laminations and climbing ripples at the top of sandstone bodies. Cosets range from 0.1-2 m thick. Paleocurrent modes are dominantly to the northwest (**Fig. 3.5G**). At several large outcrop exposures, lateral accretion sets are observed near the top of several major sublitharenite sandstone bodies. Such accretion surfaces can be traced laterally for 10's of meters and are oblique to west-southwesterly paleoflow. Characteristics of the transverse fluvial association are summarized in **Table 3.1.**

The fluvial transverse facies association is interpreted as the deposit of braided fluvial channels and overbank and floodplain settings (**Grimm et al., submitted**). A non-marine setting is substantiated by an abundance of terrestrial sedimentological evidence, such as regional and local coals with associated rooting, pedogenetic modification of exposed substrates, as well as plant-debris lags found within basal bedload lags. In addition, a freshwater setting is supported

by the rarity of bioturbation or marine body fossils. Conglomerate compositions of siderite pebbles and angular shale-fragments in basal lags have similar properties to subjacent shales, indicative of an intrabasinal provenance. Furthermore, scour-and-fill structures, trough cross-bedding and lateral accretion elements suggest a bed-load dominated fluvial system with greater variation in channel sinuosity than longitudinal drainage settings.

5. Stratal Patterns and Architectural Elements

5.1 Subsurface Results

In the subsurface, quartzarenites provide a very distinctive low (0-35 API units), blocky gamma ray signature, with a well-defined, sharp base and with gamma ray values gently increasing at the top of sandstone bodies as a result of an increase in siltstone content as exhibited at the top of the Warren Point Sandstone Member (**Fig. 3.6A**). Similar to the longitudinal fluvial facies association, the transverse fluvial facies association exhibits a blocky gamma ray signature that is capped by a sharp, bell shaped increase in gamma ray values related to an increase in clay content, with examples from the Pocahontas Formation **(Fig. 3.6B)**. Sublitharenite is differentiated from quartzarenite by slightly higher gamma ray values (35-50 API units) due to an overall increased lithic content**.** Although rare, basal siderite and mudstone-clast conglomerates can be determined from increased gamma ray values at the base of major sublitharenite sandbodies.

In outcrop and core, the sharp, erosional bases beneath fluvial facies association deposits of cross-bedded sandstone and conglomerate are interpreted as sequence boundaries (*sensu* **Van Wagoner et al., 1988)**. These disconformable surfaces are commonly incised 5 – 10 m into underlying deltaic and inner shelf facies associations and can be traced regionally (10's of km) in

the subsurface. Sequence boundaries are indicated on wire line logs by sudden gamma ray decreases to the left with blocky, low gamma ray signatures, confirmed by core where sharp-based sandstones or a sudden coarsening of facies of braided fluvial gravel bar deposits overlie mudstones. These sequence interpretations utilize an updated sequence stratigraphic framework based on detailed interpretations of core and cross sections developed by **Bodek (2006)** and a companion study **Grimm et al., (submitted).**

In addition to sequence boundaries, maximum flooding surfaces (MFS) were identified from wireline log interpretations and verified with core and outcrop facies observations. On gamma ray logs, the MFS is directly related to a high spike in gamma ray values as a result of increased uranium concentrations within a condensed shale. Furthermore, MFS are defined on gamma ray logs at the inflection from increasing gamma ray values (fining-upward) to decreasing (coarsening-upward) successions

Based on the interpretation of depositional facies stacking patterns and sequence stratigraphic surfaces of >**1200** closely spaced (2-5 km) well logs and **7** cores distributed across the Pocahontas Basin, at least **13** regionally extensive unconformity-bounded depositional sequences can be identified in the lower Breathitt Group (**Fig. 3.7)**. Initial correlations were based on the bottom three regional marine zones proposed by **Chesnut (1994)**, the Dark Ridge, Hensley and Dave Branch Shale members, as well as identifiable coal seams. Cross section D-D' is stratigraphically balanced on the Hensley Shale Member datum, the first major flooding surface within the Alvy Creek Formation and is closely associated with the Upper Seaboard coal bed.

The unconformity-bounded sequences are nested within lower-frequency, composite sequences **(sensu Mitchum and Van Wagoner, 1991)**, divided by major discontinuities. The

bounding surfaces for composite sequences are defined by significant depth of incision, truncation of older sequences and changes in clast composition over wide aerial extent. Major low-frequency discontinuities are located at the Mississippian-Pennsylvanian unconformity and at the base of the widespread, sheet-like, fluvial, longitudinal quartzarenite bodies of the uppermost tongues of the Warren Point, Sewanee and Bee Rock Sandstone members (**Fig. 3.7**). The major discontinuities form the composite sequence boundaries of the Pocahontas, Bottom Creek and Alvy Creek composite sequences. These bounding surfaces regionally truncate underlying strata, including several eastward-dipping sequences, and to diverge away from the western forebulge toward the eastern orogenic front (**Fig. 3.7**).

Capping each quartzarenite member is a regionally distinct, mappable shale, preserving intervals of especially thick (~30m) mudstone. These units contain marine influenced shelf facies with diagnostic *Teichichnus* and *Phycosiphon* ichnofabrics and rare marine fossils suggestive of normal salinity. The base of each shale member is mapped as a low-frequency surface of maximum transgression.

5.2 Stratal Architecture Interpretation

High-frequency sequences are characterized by alternating alluvial and shallow-marine deposits, interpreted as a result of glacioeustasy. During relative sea-level rise, both longitudinal and transverse alluvial systems were transgressed forming estuaries (**Greb and Chesnut, 1996; Greb and Martino, 2005; Bodek, 2006; Korus et al,. 2008)** and inner shelf settings**.** Following drowning, small, tropical, fluvial-dominated deltas prograded across the basin, infilling available accommodation space during highstand and relative sea level fall **(Korus et al., 2008).** Based on available age constraints, the frequency of regional high-frequency sequences is **~10^5 yr**s and

likely reflects Milankovitch glacioeustatic controls **(Chesnut, 1994; Bodek, 2006; Grimm et al, submitted).**

Composite sequences are characterized by wedge geometries, suggestive of asymmetric basin subsidence. Individual composite sequences thin toward the western forebulge and internal high-frequency sequence boundaries timelines diverge toward the thrust, indicating greater proximal accommodation. Major unconformities below composite sequences reflect basin-wide erosion during episodic basin readjustment, as evidenced by lateral truncation of underlying high-frequency sequences beneath quartzarenite bodies. Quartzarenites are also demonstrated to merge laterally with transverse fluvial associations (**Fig. 3.7**), as indicated by slightly higher lithic contents on wireline logs and constrained where available by cores. Low-frequency surfaces of maximum transgression are interpreted to correspond to a point in time where the rate of accommodation space creation was regionally at a maximum. The juxtaposition of these regional shale members immediately above regional quartzarenite members suggests a similar genetic origin, possibly linked to rapid variance in subsidence rates.

6. Isopach Mapping

6.1 Isopach Map Results

Isopach maps of the total thickness of composite sequences and thicknesses of each composite sequence, and isolith maps of net quartzose sandstone (<35 API) for each composite sequence were generated from a data base of >1200 wells (**Figs. 3.8, 3.9A-3.9F**). The total isopach map thickens from 1200-2200 ft (375-670 m) monotonically toward the east **(Fig. 3.8)**. Similarly, observations show that composite sequences have generally prismatic geometries thinning from east to west (**Figs. 3.9A, 3.9B, 3.9C).** The Pocahontas composite sequence

thickens from 200-800 ft (61-244 m), average 516 ft (157 m) (**Fig. 3.9A),** Bottom Creek composite sequence ranges from 300-1100 ft (91-335 m), average 760 ft (232 m) (**Fig. 3.9B),** and the Alvy Creek composite sequence expands from 400-800 ft (122-244 m), averaging 611 ft (186 m) in thickness (**Fig. 3.9C).**

General spatial trends of stratal thicknesses of quartzarenite members display an opposite trend. Each quartzarenite member thickens generally toward the distal (western) margin (**Figs. 3.9D, 3.9E, 3.9F).** The Warren Point Sandstone member ranges from 0-400 ft (0-122 m), thickest in northern Dickenson County (**Fig. 3.9D).** The Sewanee Sandstone member thickens from 0-450 ft (0-137 m), thickest in northwestern Buchanan County (**Fig. 3.9E).** The Bee Rock Sandstone member ranges from 0-275 ft (0-84 m) and thickens markedly into western Wise County (**Fig. 3.9F).** The progressive westward migration of each quartzarenite from isopach maps compares favorably with facies trends seen in cross section **(Fig. 3.7).**

6.2 Isopach Map Interpretations

The wedge-shaped thickness variations reflect typical asymmetric isopach patterns of foreland basins. Marked thickening from the distal basin boundary toward the orogen for each composite sequence provides evidence for syndepositional subsidence within an asymmetric depocenter. Furthermore, isopach maps of each composite sequence exhibit highly variable patterns in accommodation generated by flexural subsidence. The greatest net accommodation (average 760 ft, 211 m) and variance in accommodation between distal and proximal locations in the basin (Δ800 ft, 244 m) is evident for the Bottom Creek composite sequence. The least net accommodation is evident for the Pocahontas composite sequence (average 516 ft, 157 m), with

the most regional equally distributed subsidence evident for the Alvy Creek composite sequence (Δ400 ft, 122 m).

7. Sandstone Petrology

7.1 Petrographic Results

The petrographic means and standard deviation domains determined for the framework grain compositions of longitudinal and transverse fluvial sandstones are presented on QFL and QmFLt diagrams in **Figs. 3.10A and 3.10B**. Such ternary diagrams allow for rapid statistical comparison of framework compositional modes within large populations of sample data, as well as to differentiate between distinct tectonic settings (**Dickenson and Suczek, 1979).**

Two dominant petrofacies are recognized from graphical ternary plots. Longitudinal fluvial sandstones of the Lee Formation are classified as quartzarenites to sublitharenites (**sensu Dott, 1964**), with mean **QFL%=92%/1%/7%** and mean **QmFLt%= 83%/1%/16% (n=71).** Lithic grain types observed are dominantly polycrystalline quartz, muscovite mica, labile metamorphic rock fragments and rare accessory minerals such as rutile and zircon. An example photomicrograph of a Lee Formation quartzarenite is shown in **Fig. 3.10C.**

Transverse fluvial sandstones of the Breathitt Group sandstone members are classified as litharenites with mean **QFL% = 78%/ 4%/18%** and mean **QmFLt %= 70%/ 4%/ 26% (n =157)**. Lithic grain types are dominantly metamorphic rock fragments, including quartz-sericite schist and quartz-chlorite schist, detrital mica and polycrystalline quartz. Subordinate sedimentary rock fragments are primarily siltstone, chert, and siderite. An example photomicrograph of a Breathitt group litharenite is shown in **Fig. 3.10D.**

7.2 Petrographic Interpretation

A compositional contrast between longitudinal and transverse sandstone petrofacies is apparent, suggesting significant differences in provenance histories. Applying the QFL descriptions to the tectonic provenance domains of **Dickenson and Suczek (1979)** suggests provenance differences may be the result of paleogeography and catchment bedrock types. The longitudinal alluvial system that deposited the Lee Sandstones is interpreted to have supplied sediments from both the cratonic interior and recycled orogen settings, while the QFL values of Breathitt Group transverse alluvial system plot solely within the recycled orogen domain (**Fig. 3.10B)**.

The framework petrology of the quartzarenites suggests derivation from a mature source, fed with sediment from tropical plains of the Laurentian cratonic interior, as well as material supplied from eroding orogenic highlands. Tropical, humid climates provide settings for intense chemical weathering of labile sand grains and the generation of first cycle quartzarenites (**Suttner, 1981; Franzinelli and Potter, 1983; Johnsson et al., 1988).** Given the low-latitude paleogeography of the Pocahontas Basin during the Early Pennsylvanian, it may be appropriate to consider the ancient craton of Laurentia as analogous to the modern Guayana Shield of Venezuela, a quartz-rich cratonic source area for the Orinoco River (**Johnsson et al., 1988)**.

The predominance of metamorphic rock fragments and detrital mica and the lack of extrabasinal sedimentary rock fragments indicate the dominance of sediment supplied from a low-grade metamorphic source area. Previous petrographic work on the Breathitt Group has interpreted these schistose grains to have been derived from exposed Grenvillian basement, exhumed during the growth of the orogenic belt to the east of the study area **(Davis and Ehrlich, 1974; Houseknecht, 1980; Reed et al., 2005)**. Conglomerate samples contain rare, bluish tint

quartz pebbles, providing further petrographic support for a Grenvillian provenance (**Herz and Force, 1984)**.

8. Detrital Zircon Geochronology

8.1 Detrital Zircon Geochronology Results

Detrital zircon separates for comparative age histogram analysis are from the Lower Pennsylvanian Pocahontas, Warren Point, lower and upper Raleigh (Sewanee equivalent of West Virginia, thus defined herein), and Bottom Creek Formations (P1-1, P1-2, P1-3, P1-4, P1-5; **Fig. 3.11**) and provide distinctive crystallization ages from a variety of Laurentian crustal provinces and peri-Gondwanan terranes.

Zircons from the Warren Point and Sewanee quartzarenite bodies (P1-2, P1-4) display a wide spread in ages with broad Grenvillian peaks (0.9-1.25 Ga) and subordinate Proterozoic clusters corresponding with Granite-Rhyolite (1.3-1.5 Ga), Yavapai-Mazatal (1.6-1.8 Ga**)** and Penokean (1.8-1.9 Ga) provenances as well as significant (>10%) Superior (2.7-2.8 Ga**)** and older Archean contributions (**Fig. 3.11; Eriksson et al., 2004; Bekker et al., 2005).**

Litharenite bodies (Pocahontas, Bottom Creek and lower Raleigh) are dominated by zircons of Grenvillian and Granite-Rhyolite provenance but lack Archean zircons (**Fig. 3.11; Eriksson et al., 2004; Bekker et al., 2005).** Notable contributions from Taconic (0.44-0.5 Ga) and Pan-African (0.5-0.7 Ga) provenances are represented within the Bottom Creek **(P1-5, Fig. 3.11).**

8.2 Sandstone Provenance Interpretation

Detrital zircon ages of alluvial sandstones combined with petrography confirm separate fluvial systems of distinctly different provenance, reinforcing previous models of longitudinal and transverse delivery systems and evaluations of facies distribution. Two distinct zircon age populations emerge through comparison of the presence or absence of ages in detrital zircon data. Ages of detrital zircons in litharenites of the transverse system are restricted to Grenvillian ages, suggesting evidence for recycling of older Neoproterozoic and Paleozoic sedimentary successions uplifted in fold-thrust belts as well as the possibility of direct delivery of metamorphic sediments from proximal sources exhumed in the Blue Ridge Province (**Aleinikoff et al., 2000; Eriksson et al., 2004; Thomas et al, 2004; Becker et al., 2005**). The cluster of young Taconic ages in the Bottom Creek suggests continued unroofing of Taconic plutonic and metasedimentary rocks of the Piedmont province and/or recycling of Acadian clastic wedge sedimentary rocks.

Quartzarenites of the longitudinal alluvial system are dominated by an admixture of Grenvillian and Archean age detrital zircons with subordinate Yavapai-Mazatzal ages. Grenvillian age zircons were incorporated into the longitudinal fluvial deposits via dispersal of sediment from transverse fluvial systems draining orogenic hinterlands. Previous geochronological studies of older Paleozoic sandstones in the Appalachian basin determined that Archean zircons are limited to the Early Pennsylvanian sandstones **(Eriksson et al., 2004),** indicative of a first cycle origin unique to Alleghanian paleogeography. Late Archean detrital zircon ages are equivalent to the crustal age of the Superior Province, part of the Canadian Shield (**Hoffman, 1989; Stott, 1997**). The presence of Archean zircons in the Pocahontas Basin indicates a fluvial system with considerably distant headwaters and provides a linkage with Early Pennsylvanian sandstones in the northern Appalachian Basin of Pennsylvania. Similarly mature,

quartz-pebble-bearing quartzarenites of the Olean–Sharon–Sharp Mountain-Pottsville System have been interpreted as derived from cratonic sources (**Robinson and Prave, 1995).** Alleghanian flexural upwarping along the southern margin of the Canadian Shield has been proposed to have produced a south-facing paleoslope, dispersing sediments down the axis of the actively deepening foreland basin (**Robinson and Prave, 1995).** Although **Thomas et al., (2004)** postulated the potential for a recycled origin of Archean zircons from Early Paleozoic passive margin and synrift deposits observed in New England, the absence of Archean detrital zircons in passive margin deposits of similar age in the Central Appalachian Basin, by **Eriksson et al., (2004**), suggest primacy of first cycle, cratonically derived zircons within Early Pennsylvanian longitudinal system sandstones. Yavapai-Mazatal age zircons are common components of Appalachian Mississippian and Devonian Sandstones (**Park et al., 2010, Thomas et al., 2004, Eriksson et al., 2004)** as well as Pennsylvanian quartzarenites (**Fig. 3.11)** but are notably absent from interfingering Pennsylvanian litharenites, suggesting a first cycle origin from cratonic sources into longitudinal fluvial systems compared to limited recycling of previous clastic wedges into transverse fluvial systems.

9. Discussion

9.1 Foreland Basin Sedimentation and Tectonics

Variations in sediment supply and accommodation form distinct facies successions linked to tectonic controls within foreland basin settings, herein referred to as tectonic accommodation cycles. At the onset of each tectonic accommodation cycle, tectonic loading of the rigid, elastic crust by an advancing of the orogenic wedge resulted in geologically instantaneous subsidence of

the basin floor, with greatest rates of subsidence in proximal foredeep settings due to asymmetric flexure (**Beaumont et al., 1988; Heller et al., 1988; Flemings and Jordan, 1990**).

Loading can be inferred from dramatic changes in transverse sediment influx. Modelling of foreland basin subsidence and surface process response suggests the rate of proximal accommodation during loading increases faster than hinterland sediment supply, inducing rapid retrogradation of transverse systems as alluvial fans systems withdraw toward the orogen (**Flemings and Jordan, 1990; Heller et al., 1988; Paola et al., 1992; Clevis et al., 2004).**

In addition to interrupting sediment supply by increasing proximal accommodation, rising in-sequence thrusts during orogenic advance can trap eroded sediment within thrust-bounded intermontane basins of the wedgetop depozone, adjacent to the orogen **(Blair and Bilodeau, 1988; Heller et al., 1988; Tucker and Slingerland, 1996; DeCelles and Giles, 1996; Houston et al., 2000).** Temporary sediment ponding and diversion by thrust structures leads to episodic decreases in sediment flux directed into the foredeep from transverse systems. Comparable geomorphic diversions have been observed along thrust fronts in the transverse systems of the Mesopotamian, Ganga, and Ebro foreland basins (**James and Wynd, 1965; Gupta, 1997; Barrier et al., 2010)** and have been recognized as possible mechanisms to regulate orogenic sources of sediment supply in the Ganges-Brahmaputra system (**Burbank, 1992; Goodbred and Kuehl, 2000).**

9.2 Tectono-Sedimentary History of the Pocahontas Basin

The distribution of alluvial facies based on subsurface analysis combined with sandstone provenance data supports a two end-member alluvial depositional system within the Pocahontas Basin, during eustatic lowstands. Observations support a paleogeography of transverse rivers

originating in the growing Alleghanian highlands and a coexisting and significantly more powerful longitudinal fluvial system flowing axially to the southwest along the distal margin of the foredeep (**Fig. 3.12)**.

Within the medial foredeep depozone preserved in the study area, longitudinal and transverse fluvial systems competed for the available accommodation space. Abrupt lateral shifts between these contrasting fluvial systems produced sharp changes in the distribution of lowstand alluvial facies that can be used in combination with variations in high frequency stacking patterns to track changes in long-term foreland basin accommodation.

On the basis of observed alluvial facies distributions, composite stratal architecture and our current understanding of foreland basin tectonic process-sedimentary response relationships, three distinct tectonic accommodation cycles are proposed for the Early Pennsylvanian stratigraphy of the Pocahontas Basin (**Fig. 3.13)**. Each tectonic cycle is theorized to be impacted by variations in accommodation and sediment supply, inferred to be linked to long-term fluctuations in rates of orogenic advance onto the foreland.

The described changes in hinterland-basin connectivity on transverse sediment supply have been recognized to directly alter the distribution of alluvial facies within the foredeep depozone of the Pocahontas Basin. Decreased orogenic sediment supply limited the cratonward extent extent of lithic sandstone deposition, leaving medial and proximal foredeep accommodation underfilled. The availability of this accommodation space and the perpetually high cratonic sediment supply of longitudinal fluvial system drove the rapid lateral migration of longitudinal systems from the distal edge of the foredeep into medial-proximal foredeep depozones, truncating tilted, underlying strata **(Fig. 3.7 and 3.12)**. With this perspective, the episodic occurrence of the upper member of each quartzarenite represents the initial depositional

response to cratonward movement of the thrust system at tectonic events marked **T_1, T_2** and **T_3 (Fig. 3.13).**

During initiation of thrust events **T_1, T_2** and **T_3**, the punctuated propagation of thrust-sheets may have periodically developed thrust front structural topography, such as foreland folds, blind and emergent thrusts that may have strongly influenced transverse drainages. Regional thrusts of passive margin carbonates within the Pulaski Thrust Sheet are postulated to have been active as early as the Late Mississippian (**Bartholomew and Whitaker, 2010**), representing the frontal portion of the Blue Ridge Crystalline Sheet **(Lowry, 1971)**. This main frontal thrust may have formed temporary buttresses that diverted lithic sediments during a single advance of the thrust sheet, only to be rapidly overcome or incised to supply lithic sandstones that later prograded across the basin. Similarly, transverse diversions by structural ponding of sediment supply have been cited for episodic underfilling of the Middle Pennsylvanian foredeep of the Alleghany Formation of Maryland and West Virginia (**Wise et al., 1991**).

Accelerating subsidence can lead to regionally underfilled accommodation in foredeep settings, represented by widespread flooding and fine-grained sedimentation (**Blair and Bilodeau, 1988; Flemings and Jordan, 1989; Plint, Hart, Donaldson, 1993; Marr et al., 2000; Clevis et al., 2004).** In the Pocahontas Basin, thick, regional, marine-influenced shales immediately overlie extensive quartzarenite members, suggesting a continuum of increased rates of subsidence **(Fig. 3.13).** As a result, episodes of rejuvenated subsidence rates enhanced high-frequency, ~100 kyr eccentricity eustatic transgressions and provided a prolonged period to preserve a greater thickness of shelf and deltaic mudstone facies. Moreover, similar marine zones in the Middle Pennsylvanian of the Central Appalachian Basin have been interpreted to be the

result of enhanced transgressions by basin overdeepening (**Tankard, 1986; Klein and Kupperman, 1992; Chesnut, 1994; Ettensohn, 2008**).

The conclusion of each tectonic accommodation cycle is represented by high-frequency sequences dominated by lithic-rich transverse fluvial deposits. Present foreland basin models suggest that as rates of orogenic advance and differential basin subsidence slow, prograding proximal wedgetop deposits rejuvenate orogen-sourced sediment supply to transverse fluvial systems of the medial-distal foredeep (**Paola et al., 1992; Burbank, 1992; Garcia-Castellanos, 2002).** Within the Pocahontas Basin, as transverse sediment flux increased, longitudinal fluvial systems were rapidly diverted cratonward to the distal margin of the basin by dynamic transverse drainages unloading lithic sediment from the orogen into the overfilled foredeep during eustatic lowstands (**Fig. 3.13)**. The perennially humid tropical climate provided a setting of intense chemical and physical weathering, which maintained high sediment flux from the orogen into the basin and redistributed the topographic load, providing slowed, more regionally equable subsidence.

Utilizing the observed tectonic cycles allows the development of first order estimates of relative subsidence rates and accommodation history of the basin. Relative subsidence curves are derived from observed tectonic accommodation curves, scaled to each composite sequence in **Fig. 3.13**. A relative accommodation curve is generated by the combination of the basin subsidence curve and the assumed oscillatory, high-frequency eustatic sequences curve. The derived relative accommodation curve provides an additional reference for the regional review of sequence boundaries and flooding surfaces formed during concurrent phases of tectonic and eustatic driven accommodation.

9.3 Tectono-Sedimentary Trends

Long term depocenter trends can be deduced by developing paleogeographic maps of the eastern limit of quartzarenite facies during events **T_1, T_2** and **T_3** (**Figs. 3.14A-3.14C**). Lowstand fluvial facies distributions were derived from the position of the **50 ft (15 m)** isolines of quartzarenite member isopach maps in **Figs. 3.9D-F.** Corresponding cross-sectional basin architectures are displayed for each event in **Figs. 3.14D-3.14F,** derived from numerous dip sections balanced on low-frequency maximum flooding surfaces immediately following each event.

The resulting series of maps and basin architectures record the progressive migration of alluvial depozones to the west and orogen-ward tilting of underlying strata in response to episodic propagation of the orogenic wedge and cratonward advance of a conjectural thrust front. During **T_1,** increased tectonic loading resulted in tilting of the earlier Pocahontas Composite Sequence followed by widespread deposition of the Warren Point Sandstone Member, which is absent from the most eastern portions of the study area (**Figs. 3.14A and 3.14D)**. This was followed by deposition of the Dark Ridge Shale Member and the lithic-dominated Bottom Creek Composite Sequence. During **T_2** , increased tectonic loading resulted in continued tilting of the earlier Pocahontas and Bottom Creek Composite Sequences followed by widespread deposition of the Sewanee Sandstone Member, restricted from central and eastern Buchanan County where equivalent thick litharenites of the Upper Raleigh member dominated (**Figs. 3.14B and 3.14E)**. Continued subsidence preserved the regional Hensley Shale Member and lithic-dominated Alvy Creek Composite Sequence. At the onset of **T_3** , increased tectonic loading resulted in continued tilting of the earlier Pocahontas, Bottom Creek and Alvy Creek Composite Sequences (**Fig. 3.14F).** Map data suggests that transverse fluvial systems dominated the study area during **T_3**,

with longitudinal fluvial deposition of the Bee Rock Sandstone Member restricted to the extreme western limit of the study area, where it is observed to onlap toward the forebulge in eastern Kentucky **(Fig. 3.14C, Chesnut, 1994).** The observed progressive migration and onlap of the craton are common in pro-foreland basin settings, where the rate of onlap is considered equivalent to the rate of plate convergence (**Naylor and Sinclair, 2008).**

9.4 Implications for the Alleghanian Orogeny

Although continental convergence and crustal shortening during the Alleghanian Orogeny is considered nearly constant, diachronous internal adjustments within the orogenic wedge may explain the observed tectonic accommodation cycles. Complex interactions to maintain a critical taper of Coulomb wedge, such as out-of-sequence, back-thrusting phases, as well as variations in fluid availability may have provided a mechanism for unsteady topographic loading of the lithosphere and incremental fault slip (**DeCelles and Mitra, 1995; Butler, 2004; Hoth et al., 2007**).

The observed basin architecture is inferred to record transient deformational events, as tectonic cycles are estimated to recur at intervals of 0.3-0.6 Ma, based on estimates of high-frequency eustatic cycles nested within (**Grimm et al., submitted**). This is on the same order of magnitude as the recurrence intervals of sporadic orogenic deformation during frontal accretion cycles (**Hoth et al., 2007)** as well as tectonically influenced depositional cycles interpreted from other foreland basin facies successions in the geologic record **(Burbank and Reynolds, 1984; Catuneanu and Miall, 1997; Catuneanu and Elango, 2001; Ballato et al., 2008; Varban and Plint, 2008; Yang and Miall, 2008).**

10. Conclusions

Facies analysis supports a two end member depositional system of coexisting transverse and longitudinal alluvial systems infilling the Pocahontas Basin foredeep during eustatic lowstands in the Early Pennsylvanian. Sandstone provenance observations from petrologic and detrital zircons, integrated with subsurface wireline log correlations and net sandstone maps indicate significant, repeated paleogeographic shifts in alluvial facies distribution. Successive shifts of interfingering longitudinal and transverse alluvial facies are combined with wedge-shaped composite sequence geometries to define three distinct tectonic accommodation cycles.

Each tectonic accommodation cycle is represented by a phase of accelerated tectonic advance and subsidence, followed by mass redistribution and slowed regional subsidence. During episodes of thrust load advance, the medial-distal Pocahontas foredeep was starved of orogen-sourced sediment supply. The decreased sediment delivery from the orogen allowed longitudinal fluvial systems to comb toward the orogen and deposit sediment of cratonic heritage. Continued loading enhanced high frequency transgressions and preserved thick, regional, marine-influenced mudstones. Rates of subsidence slowed and orogenic sediment supplies returned to be redistributed by cratonward prograding transverse fluvial systems. Longitudinal drainages were subsequently diverted to distal foredeep and forebulge positions.

In summary, these cycles are inferred to have controlled the short-term (~ 0.5 Ma) variability in basin accommodation and hinterland sediment supply during the long-term cratonward progression of the Alleghanian orogenic wedge. The proposed tectonic accommodation cycles provide an explanation for the observed low-frequency composite sequences and most likely record transient deformation events during the Alleghanian Orogeny.

Figure 3.1. Regional map illustrating the distribution of Carboniferous sedimentary rocks in the Appalachian Basin (shaded region); hatched area denotes the Pocahontas Basin, dots denote distribution of detrital zircon dataset. Detailed map shows major structures within the Pocahontas Basin, including the Middlesboro Syncline, bounded by the Hunter Valley-Clinchport-St. Clair and Pine Mountain thrust faults. The Russell Fork Fault (bold) as well as minor Bradshaw, Coeburn and Glamorgan faults have measurable lateral and vertical displacement (Adapted from Cecil et. al, 1985; Mitra, 1988; Henika, 1994; Ryder et al., 2008).

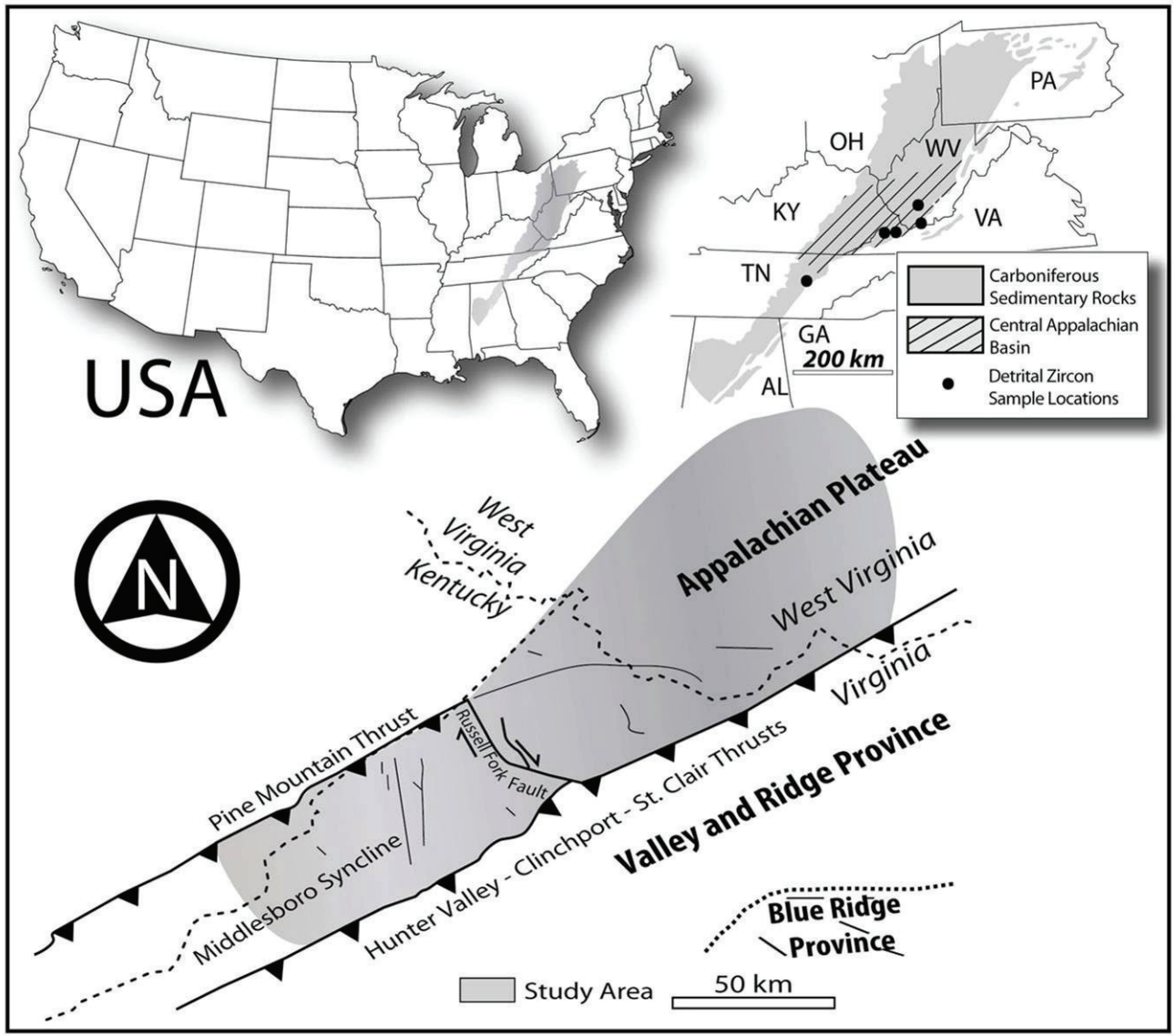
USA
PA
OH
WV
KY
VA
TN
GA
200 km
AL
Carboniferous Sedimentary Rocks
Central Appalachian Basin
Detrital Zircon Sample Locations
N
West Virginia
Kentucky
Appalachian Plateau
West Virginia
Virginia
Pine Mountain Thrust
Russell Fork Fault
Middlesboro Syncline
Hunter Valley - Clinchport - St. Clair Thrusts
Valley and Ridge Province
Blue Ridge Province
Study Area
50 km

Figure 3.2. Map of the study area showing the position of well logs, cores, cross sections and measured outcrop localities. Positions of dip cross sections A-Z and strike cross sections X-Z across southwestern Virginia are shown. Highlighted cross section D-D' is included in this paper.

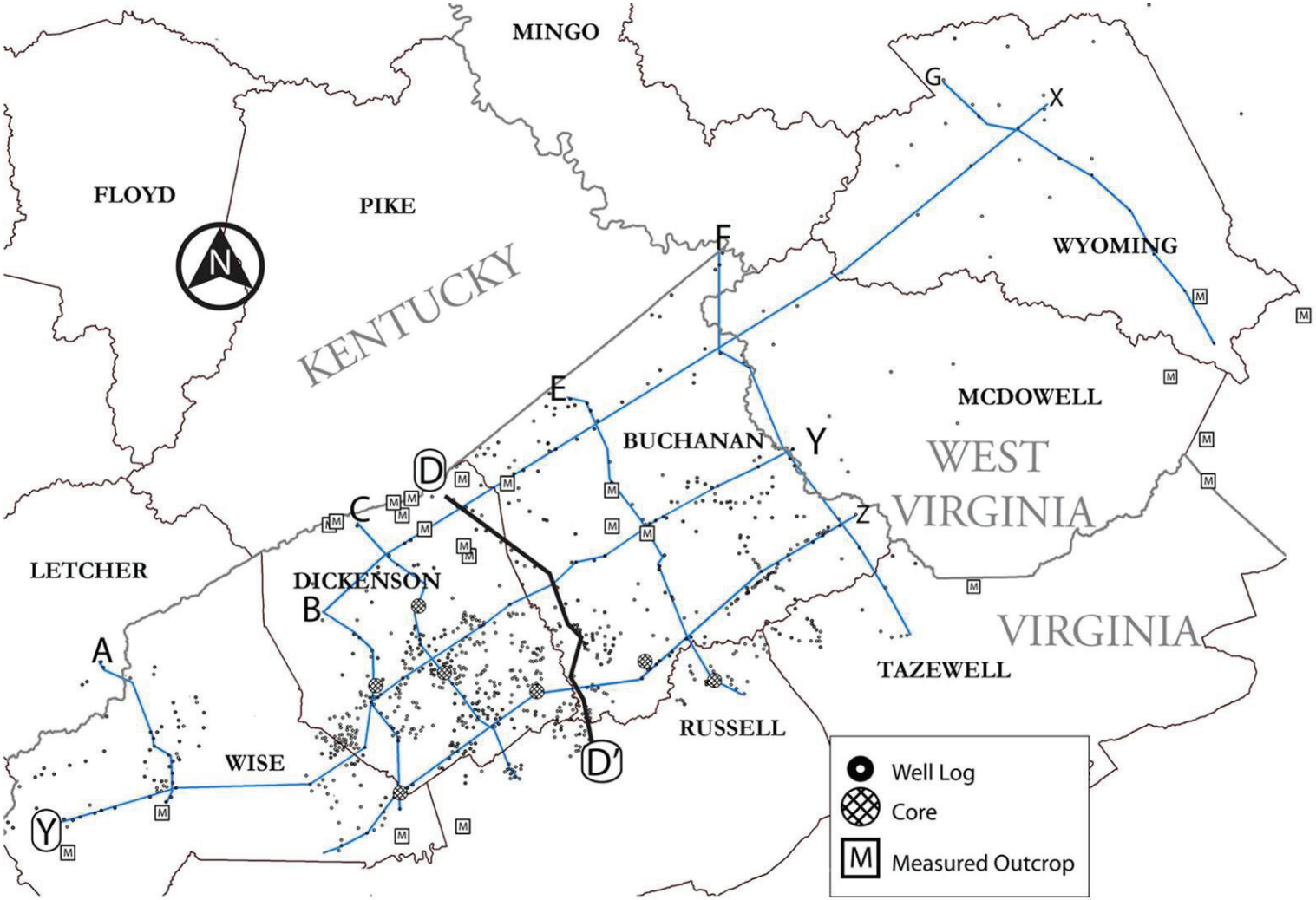
MINGO
FLOYD
PIKE
KENTUCKY
WYOMING
MCDOWELL
BUCHANAN
WEST
VIRGINIA
VIRGINIA
LETCHER
DICKENSON
WISE
RUSSELL
TAZEWELL
A
B
C
D
D'
E
F
G
X
Y
Z
Well Log
Core
Measured Outcrop

Figure 3.3. Stratigraphic chart for the study interval. Left column shows a generalized stratigraphic column with age constraints for Early Pennsylvanian strata in the Pocahontas Basin. Right column shows a more detailed coal stratigraphy with type gamma ray and bulk density (RHOB) geophysical wireline log responses for the Lower Breathitt Group interval.

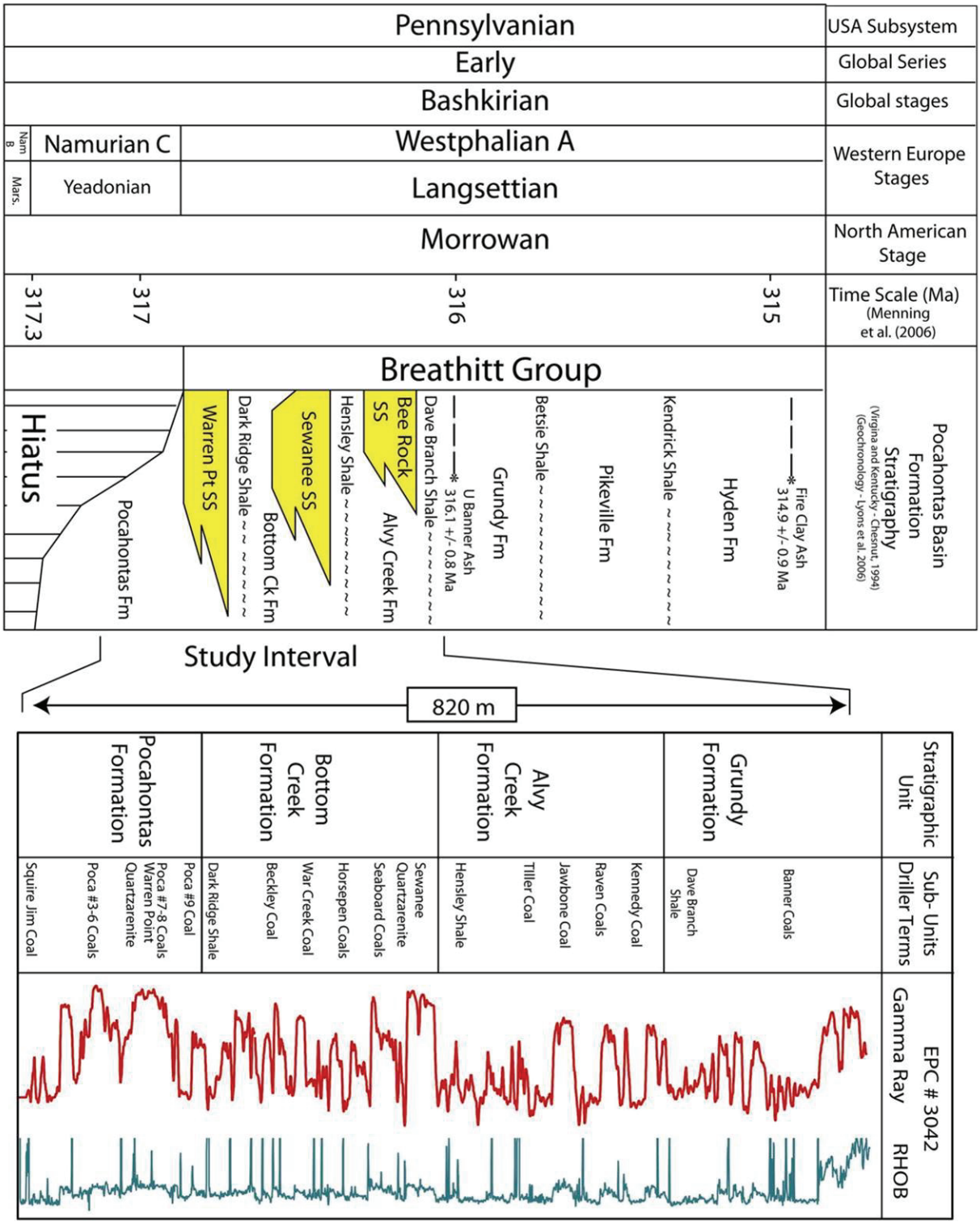
Pennsylvanian
Early
Bashkirian
Namurian C
Yeadonian
Westphalian A
Langsettian
Morrowan
USA Subsystem
Global Series
Global stages
Western Europe Stages
North American Stage
Time Scale (Ma) (Menning et al. (2006)
317.3
317
316
315
Pocahontas Basin Formation Stratigraphy (Virginia and Kentucky - Chesnut, 1994) (Geochronology - Lyons et al. 2006)
Breathitt Group
Fire Clay Ash 314.9 +/- 0.9 Ma
Hyden Fm
Kendrick Shale
Pikeville Fm
Betsie Shale
Grundy Fm
U Banner Ash 316.1 +/- 0.8 Ma
Dave Branch Shale
Alvy Creek Fm
Bee Rock SS
Hensley Shale
Sewanee SS
Bottom Ck Fm
Dark Ridge Shale
Warren Pt SS
Pocahontas Fm
Hiatus
Study Interval
820 m
Stratigraphic Unit
Sub- Units Driller Terms
EPC # 3042
Gamma Ray
RHOB
Grundy Formation
Banner Coals
Dave Branch Shale
Alvy Creek Formation
Kennedy Coal
Raven Coals
Jawbone Coal
Tiller Coal
Hensley Shale
Bottom Creek Formation
Sewanee Quartzarenite
Seaboard Coals
Horsepen Coals
War Creek Coal
Beckley Coal
Dark Ridge Shale
Pocahontas Formation
Poca #9 Coal
Poca #7-8 Coals
Warren Point Quartzarenite
Poca #3-6 Coals
Squire Jim Coal

Figure 3.4. Longitudinal Fluvial Facies Association. Photographs and data are from exposures at Breaks Interstate Park and Birch Knob, Virginia. A) Quartz pebble-bearing quartzarenite, Warren Point Sandstone Member, hammer for scale. B) Stacked planar crossbed sets, staff is 1.2m long. C) Tangential crossbed set, scale is 0.5m. D) Compound cross-bedding consisting of intrasets between inclined bounding surfaces, scale is 0.3m. E) Rose diagram of paleocurrent data for the Warren Point Sandstone member. F) Rose diagram of paleocurrent data for the Bee Rock Sandstone Member.

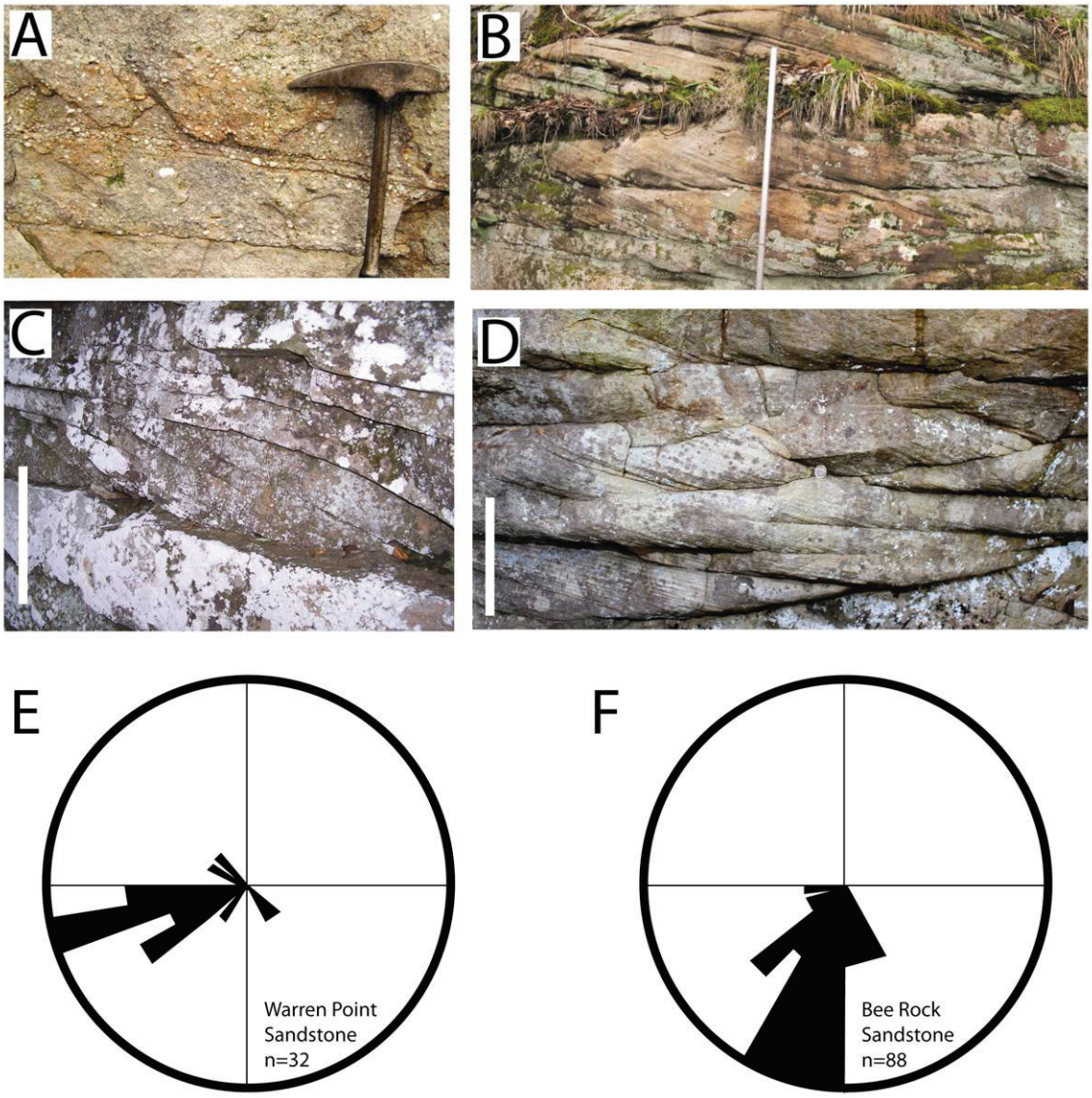
A
B
C
D
E
Warren Point
Sandstone
n=32
F
Bee Rock
Sandstone
n=88

Figure 3.5. Transverse Fluvial Facies Association. A) Siderite conglomerate lag. Pen for scale, Pocahontas, West Virginia. B) Mudstone conglomerate lag. EQT #1 Sandy Ridge Core, 1927 ft. Scale bar is 1 cm. C) Thick gleyed and rooted mudstone below tabular coal horizon, Pocahontas Formation along I-77 near Flat Top, West Virginia. D) Deeply incised fluvial sandstone body along VA Route 460 near Deel, Virginia. E)Erosive surface in core beneath major litharenite sandstone. DoE M2 Core, 2070 ft. F) Trough cross bedding, hammer for scale, Grundy, Virginia. G) Rose diagram of paleocurrent data for sandstones of the Pocahontas Formation.

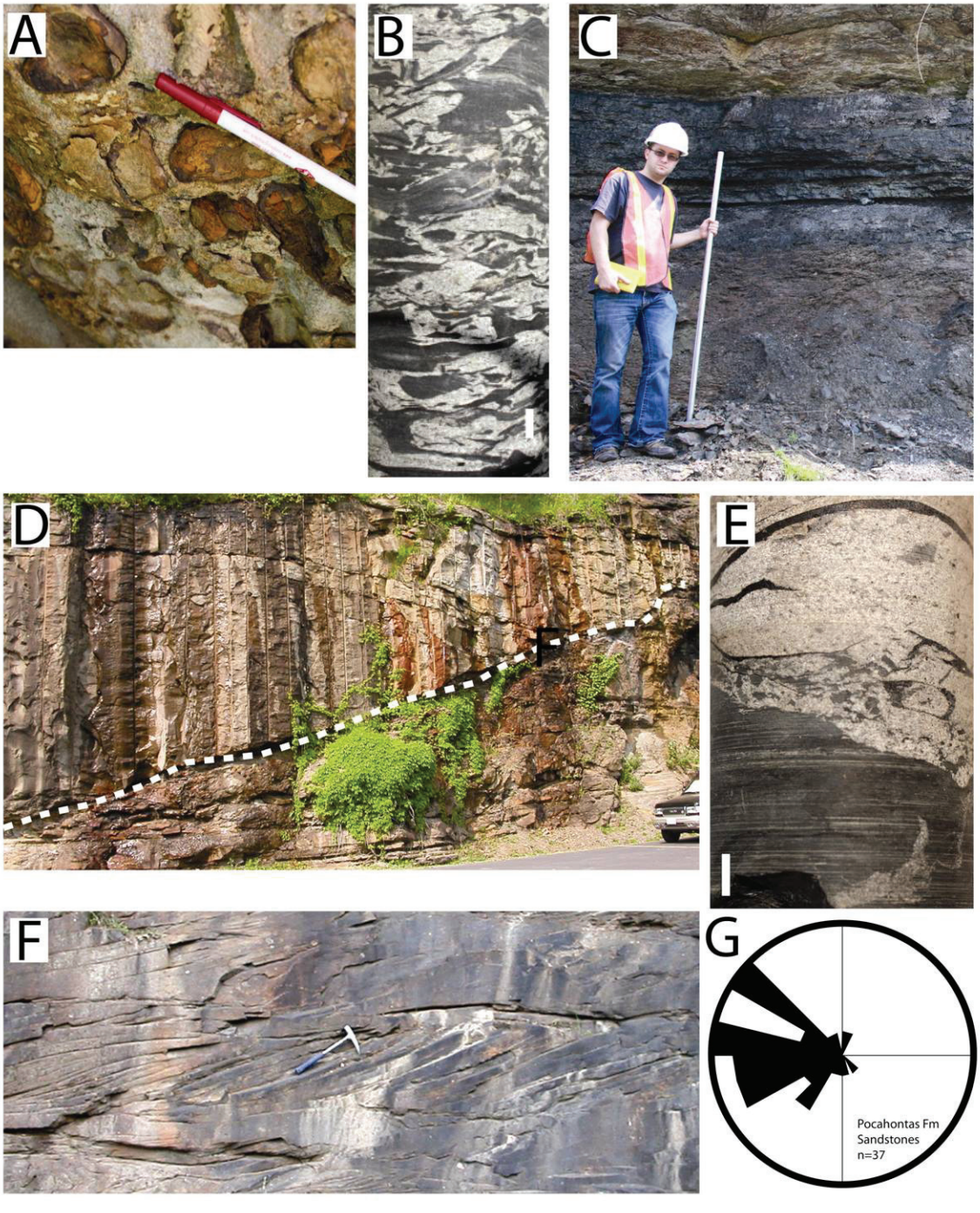
A
B
C
D
E
F
G
Pocahontas Fm
Sandstones
n=37

Figure 3.6. Example vertical successions of lithologies, sedimentary structures, facies associations and subsurface gamma ray characteristics described through the Warren Point and Pocahontas Formations from the Equitable Sandy Ridge Core (A) and (B) US Dept. of Energy CO_2 –ECBM monitoring well #2.

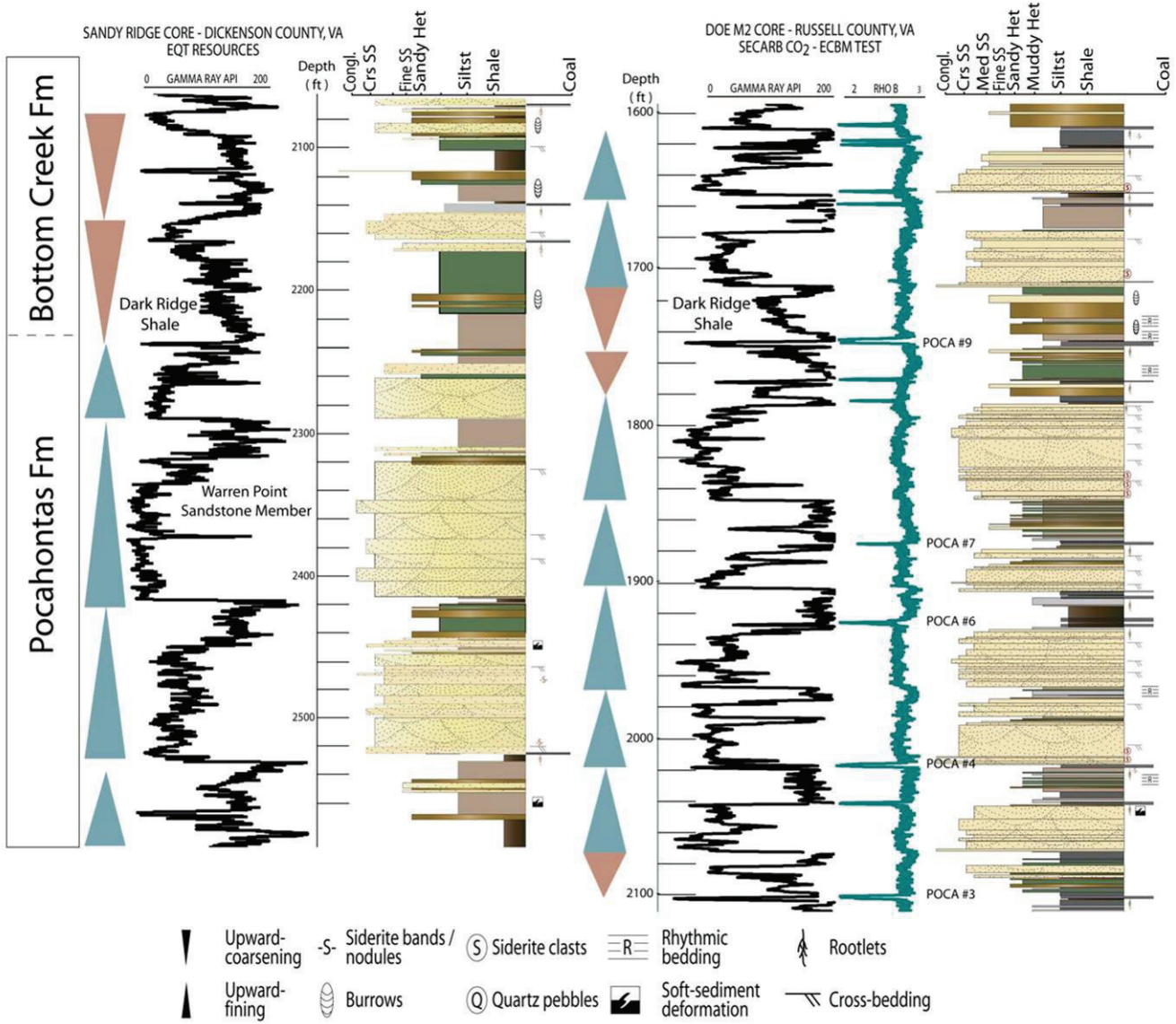
SANDY RIDGE CORE - DICKENSON COUNTY, VA
EQT RESOURCES
0 GAMMA RAY API 200
Depth (ft)
Congl.
Crs SS
Fine SS
Sandy Het
Siltst
Shale
Coal
2100
2200
2300
2400
2500
Bottom Creek Fm
Pocahontas Fm
Dark Ridge Shale
Warren Point Sandstone Member
DOE M2 CORE - RUSSELL COUNTY, VA
SECARB CO2 - ECBM TEST
0 GAMMA RAY API 200
2 RHOB 3
Depth (ft)
1600
1700
1800
1900
2000
2100
Dark Ridge Shale
POCA #9
POCA #7
POCA #6
POCA #4
POCA #3
Congl.
Crs SS
Med SS
Fine SS
Sandy Het
Muddy Het
Siltst
Shale
Coal
Upward-coarsening
Upward-fining
-S- Siderite bands / nodules
Burrows
S Siderite clasts
Q Quartz pebbles
R Rhythmic bedding
Soft-sediment deformation
Rootlets
Cross-bedding

Figure 3.7. Well log correlation panel**,** illustrating the stratigraphic architecture along dip cross-section **D-D'**. Important lithostratigraphic members and interpreted sequence boundaries are labeled. The flooding surface at the base of the Dave Branch Shale is used as the datum surface. Paleoflow of longitudinal fluvial facies is considered oblique to the panel.

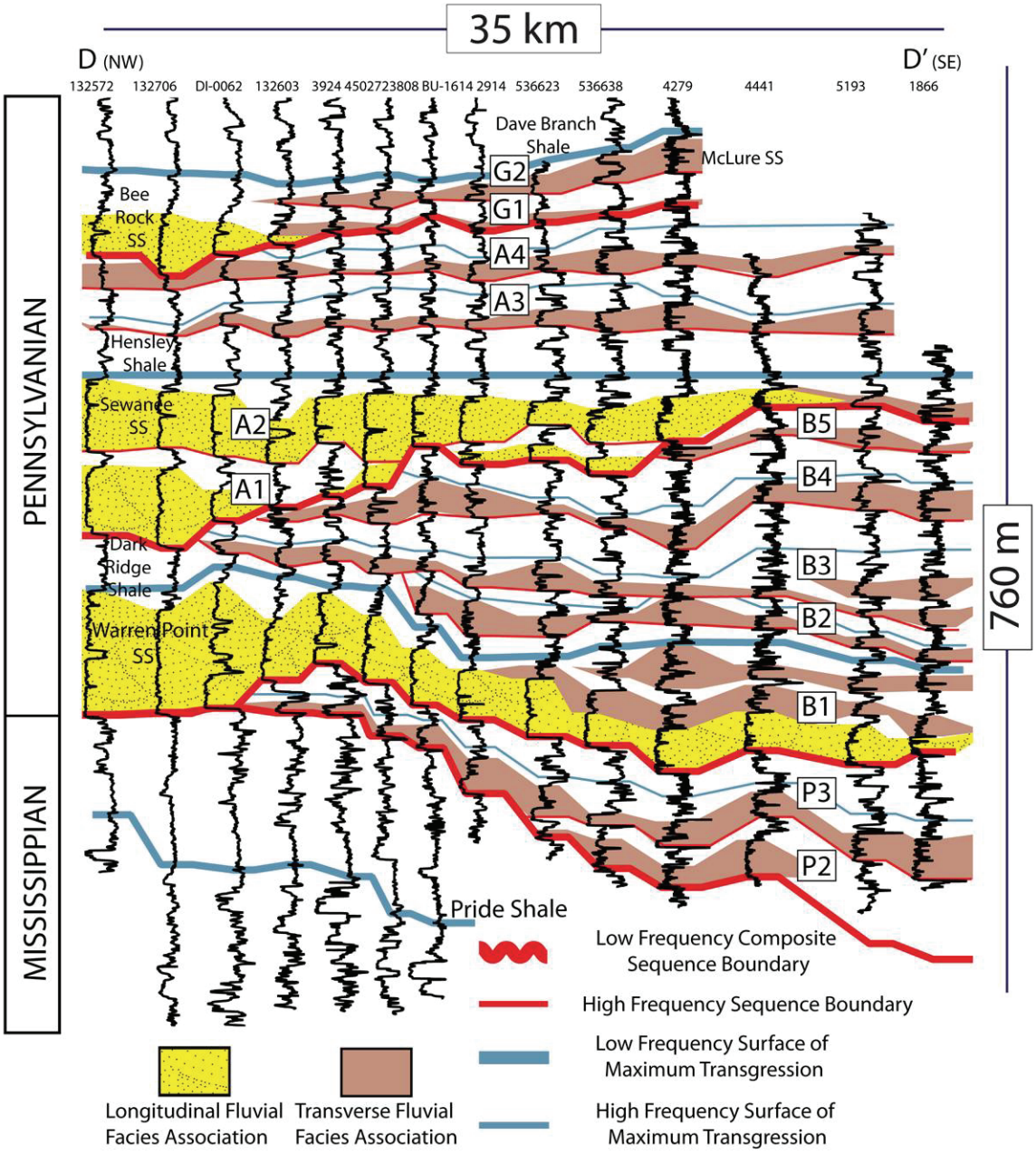
35 km
D (NW)
D′ (SE)
132572 132706 DI-0062 132603 3924 4502723808 BU-1614 2914 536623 536638 4279 4441 5193 1866
PENNSYLVANIAN
MISSISSIPPIAN
760 m
Dave Branch Shale
McLure SS
Bee Rock SS
Hensley Shale
Sewanee SS
Dark Ridge Shale
Warren Point SS
Pride Shale
G2
G1
A4
A3
A2
A1
B5
B4
B3
B2
B1
P3
P2
Low Frequency Composite Sequence Boundary
High Frequency Sequence Boundary
Low Frequency Surface of Maximum Transgression
High Frequency Surface of Maximum Transgression
Longitudinal Fluvial Facies Association
Transverse Fluvial Facies Association

Figure 3.8. Isopach map of the total combined thickness of Pocahontas, Bottom Creek and Alvy Creek composite sequences.

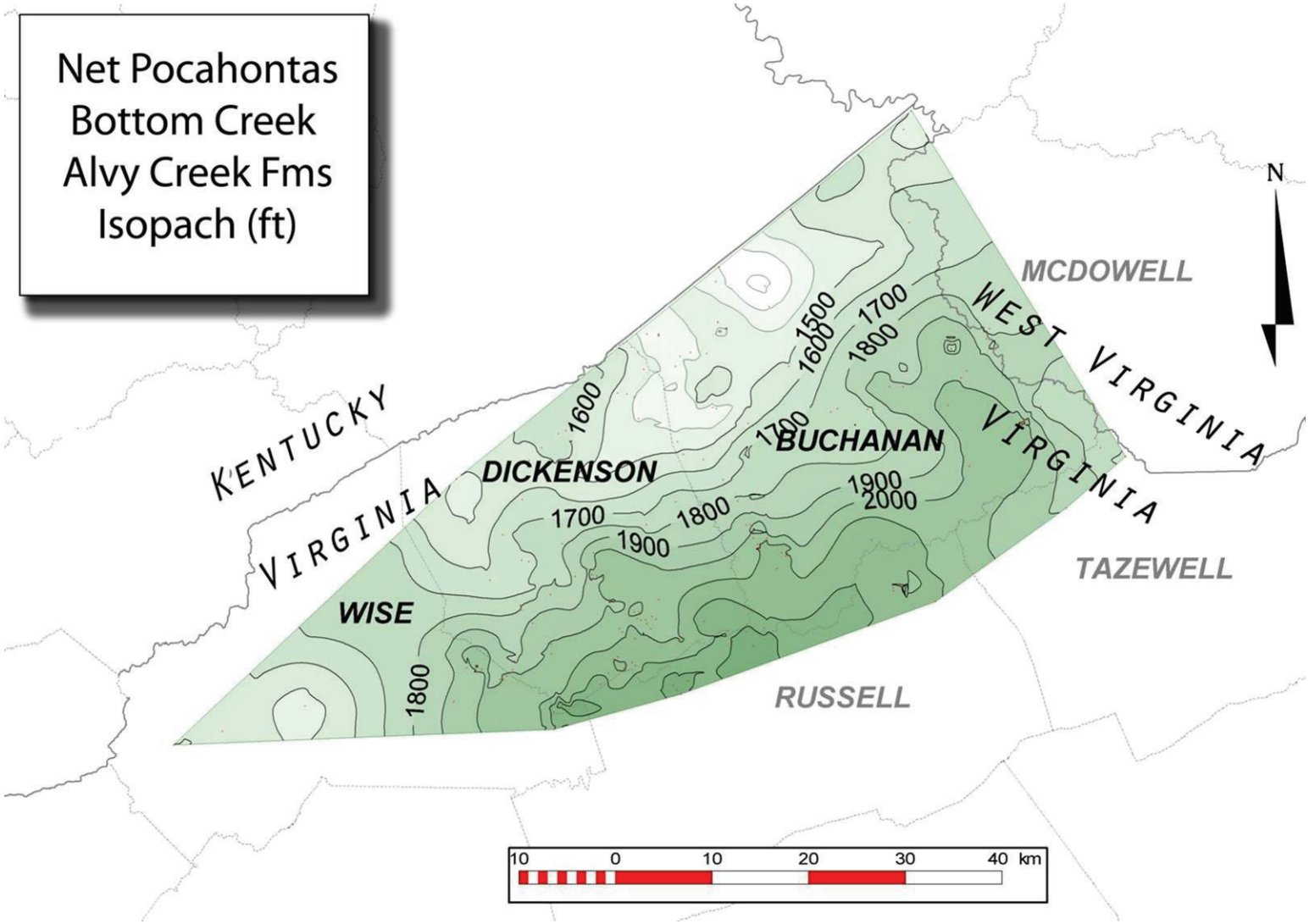
Net Pocahontas
Bottom Creek
Alvy Creek Fms
Isopach (ft)
N
KENTUCKY
VIRGINIA
WEST VIRGINIA
VIRGINIA
MCDOWELL
TAZEWELL
RUSSELL
DICKENSON
BUCHANAN
WISE
1500
1600
1700
1800
1900
2000
10 0 10 20 30 40 km

Figure 3.9. Isopach maps (A-C) of Pocahontas, Bottom Creek and Alvy Creek composite sequences and net sandstone maps (<35 API) of the Warren Point, Sewanee and Bee Rock quartzarenite Members (D-F).

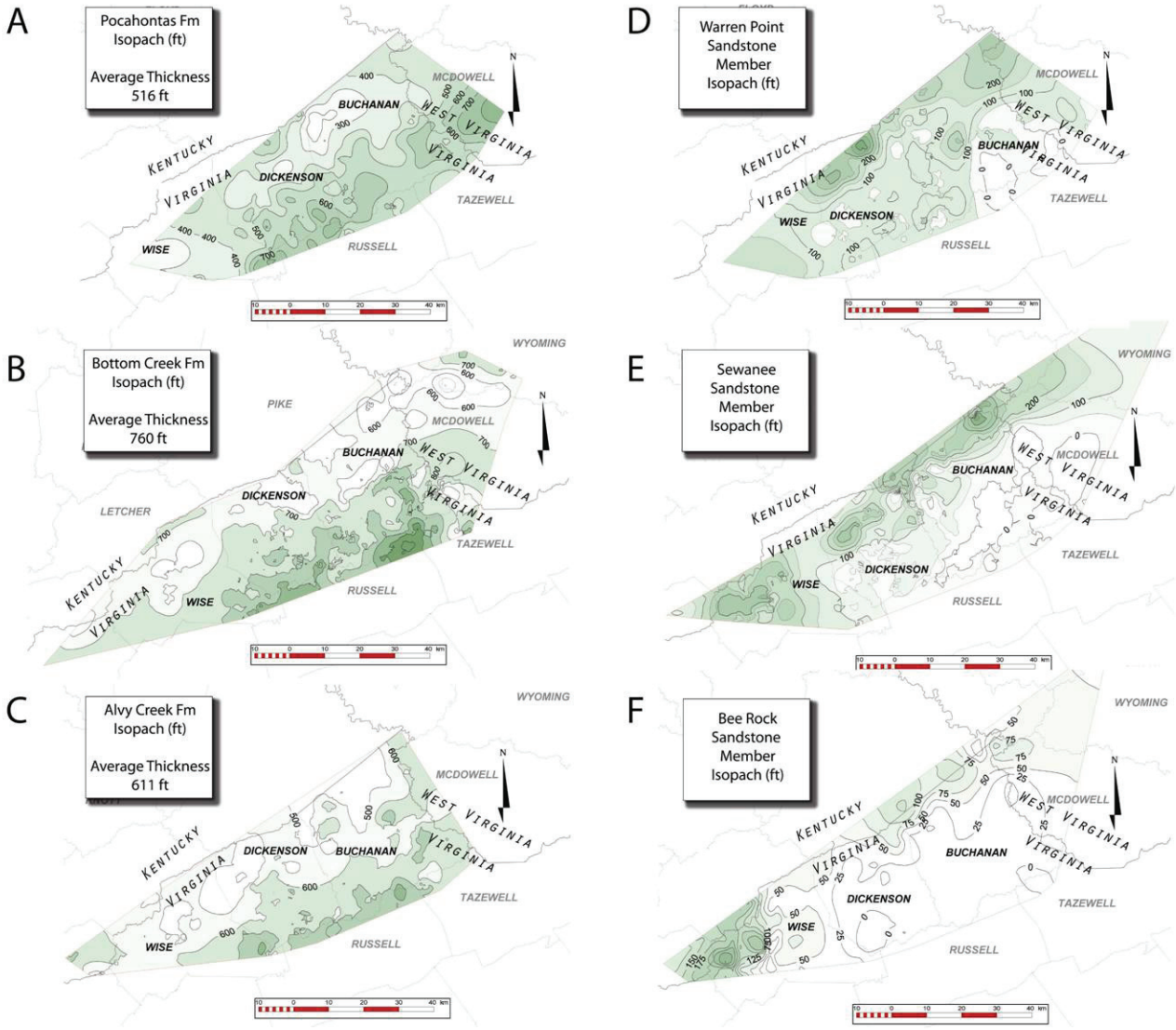
A
Pocahontas Fm
Isopach (ft)
Average Thickness
516 ft
B
Bottom Creek Fm
Isopach (ft)
Average Thickness
760 ft
C
Alvy Creek Fm
Isopach (ft)
Average Thickness
611 ft
D
Warren Point
Sandstone
Member
Isopach (ft)
E
Sewanee
Sandstone
Member
Isopach (ft)
F
Bee Rock
Sandstone
Member
Isopach (ft)
KENTUCKY
VIRGINIA
WEST VIRGINIA
VIRGINIA
WYOMING
PIKE
LETCHER
MCDOWELL
BUCHANAN
DICKENSON
WISE
RUSSELL
TAZEWELL
N

Figure 3.10. A) QFL and **B)** QmFLt Ternary diagrams illustrating the summary data for the Pennsylvanian sandstones of the Pocahontas Basin. Petrographic data from Siever (1957), Houseknecht (1978), Wizevich (1991), Reed (2005) and this study. *Q*, total quartz; *F*, feldspar; *L*, lithics; *Qm*, monocrystalline quartz; *Lt*, lithics plus polycrystalline quartz including chert. Hexagons represent one standard deviation to the mean QFL and QmFLt, respectively. **C)** Photomicrographs of Lee Type sandstones, and **D)** Breathitt Group sandstones. Monocrystalline quartz (Q), polycrystalline quartz (Qp) metamorphic rock fragments (MRF) and detrital mica (m). Scale bar is 0.5 mm.

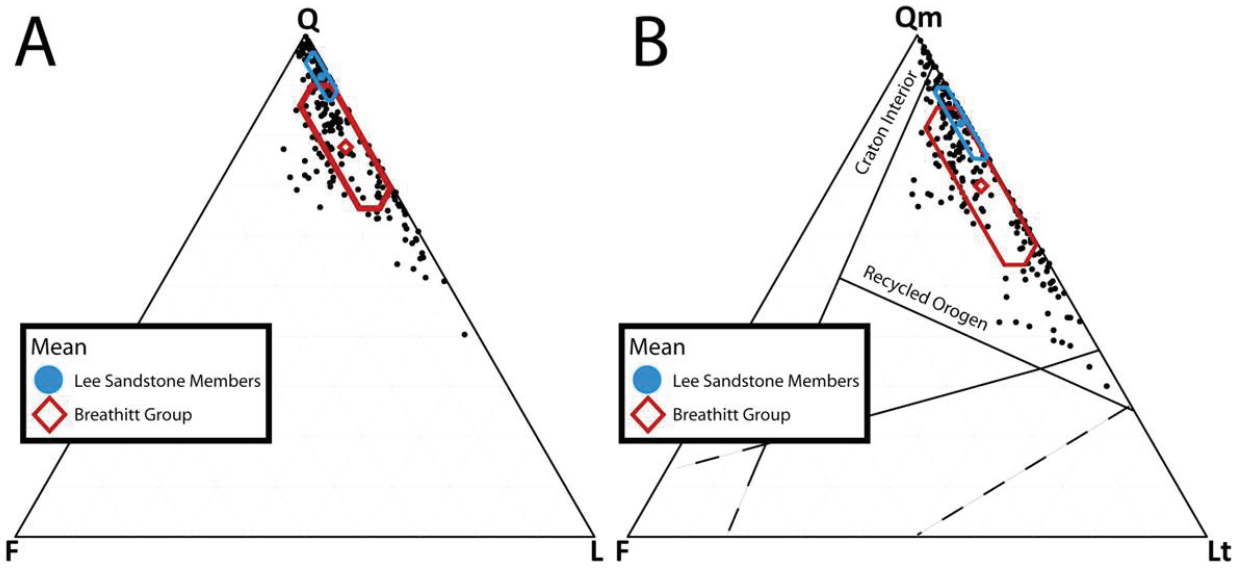

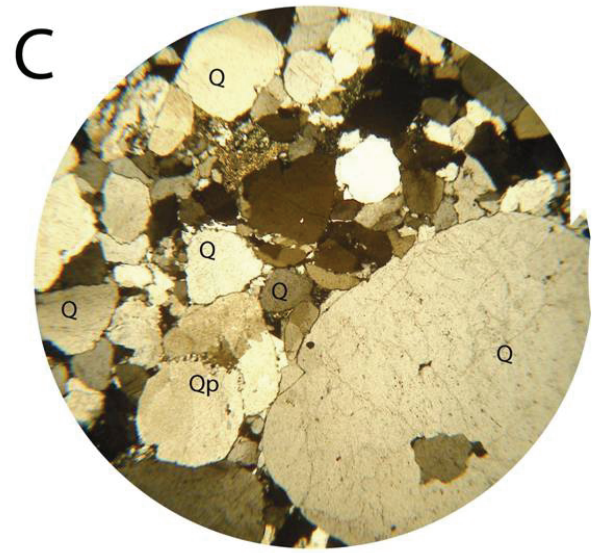

Lee Type Sandstone

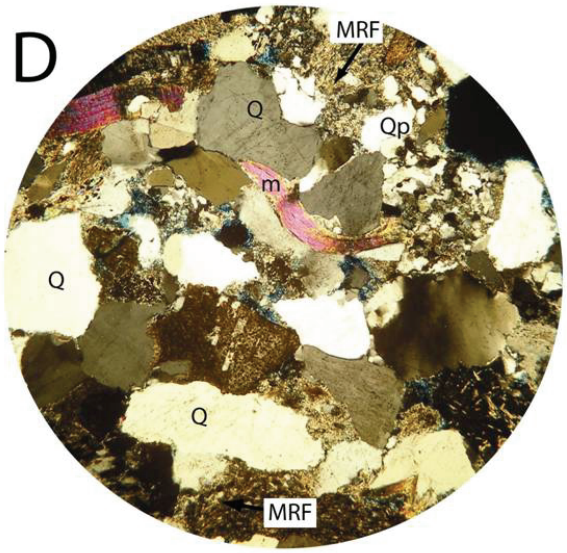

Breathitt Type Sandstone

Figure 3.11. Histograms of U-Pb ages for detrital zircon plots of Pennsylvanian sandstones of the Central Appalachian Basin from Virginia and southern West Virginia. Histograms are arranged stratigraphically, with youngest samples at the top. PZ: Paleozoic Crust; PA: Pan-African-Braziliano Province; GRN: Grenville Basement; GR: Granite-Rhyolite Province; Y-M: Yavapai-Mazatal Province; PN: Penokean Province; TM: Trans-Amazonian Province; SUP: Superior Province. Bin sizes are 50 million years. Data from: **Eriksson et al., (2004); Becker et al., (2005); and this study.**

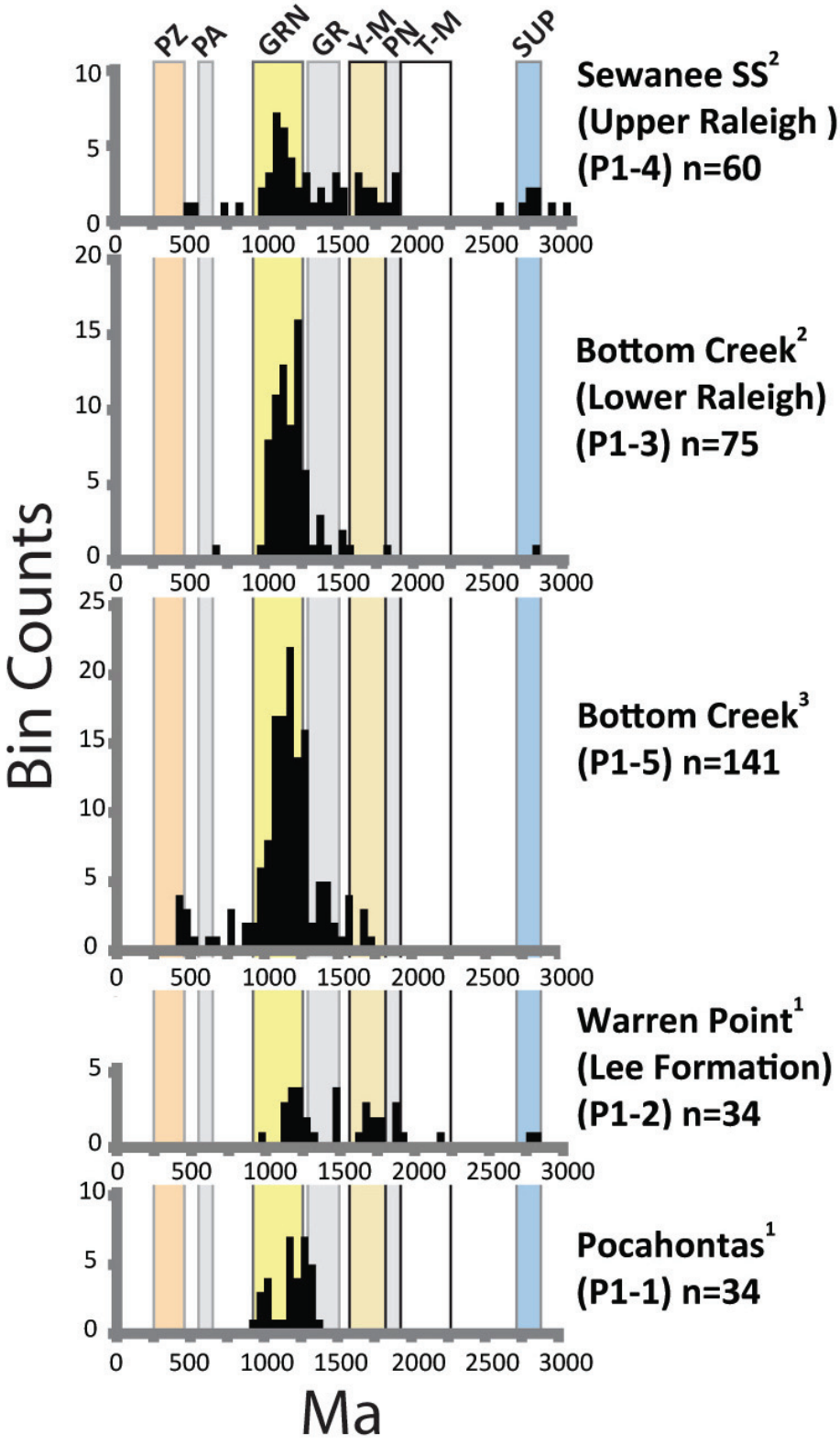
PZ
PA
GRN
GR
Y-M
PN
T-M
SUP
Sewanee SS[2]
(Upper Raleigh)
(P1-4) n=60
Bottom Creek[2]
(Lower Raleigh)
(P1-3) n=75
Bottom Creek[3]
(P1-5) n=141
Warren Point[1]
(Lee Formation)
(P1-2) n=34
Pocahontas[1]
(P1-1) n=34
Bin Counts
Ma
0
500
1000
1500
2000
2500
3000

Figure 3.12. Generalized block model cartoon of longitudinal and transverse fluvial systems tectonic domains within the Pocahontas foredeep study area.

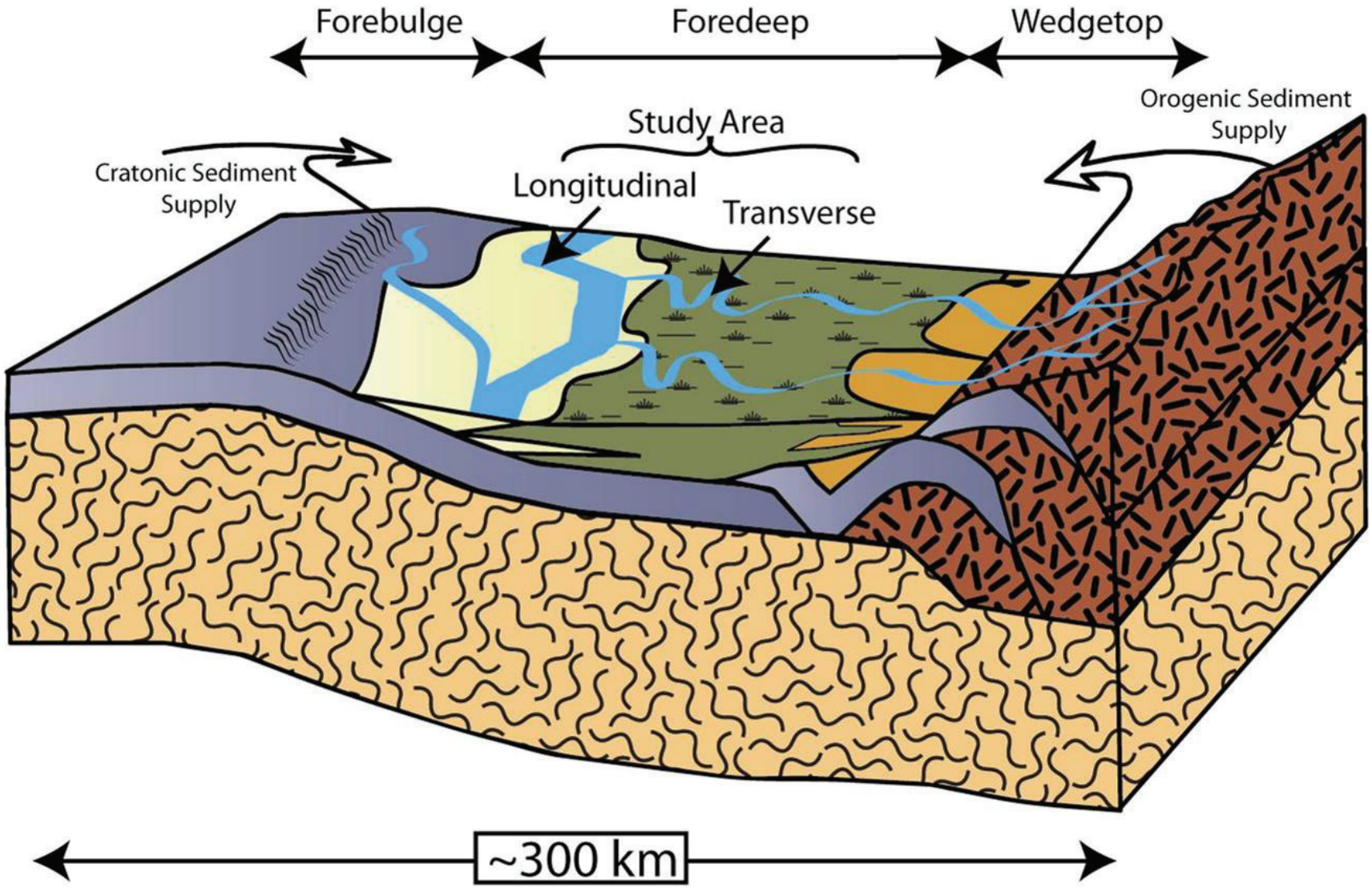
Forebulge
Foredeep
Wedgetop
Orogenic Sediment Supply
Study Area
Cratonic Sediment Supply
Longitudinal
Transverse
~300 km

Figure 3.13. A) Schematic diagram of interpreted spatial-temporal facies distribution along a theoretical W-E dip transect, defining tectonic events T_1, T_2 and T_3. **B)** Chart of sediment supply and relative subsidence trends delineate tectonic accommodation cycles of thrust advance and load redistribution. Tectonic accommodation cycles are compared with the concurrent high-frequency sequences curve and combined to form a relative accommodation curve.

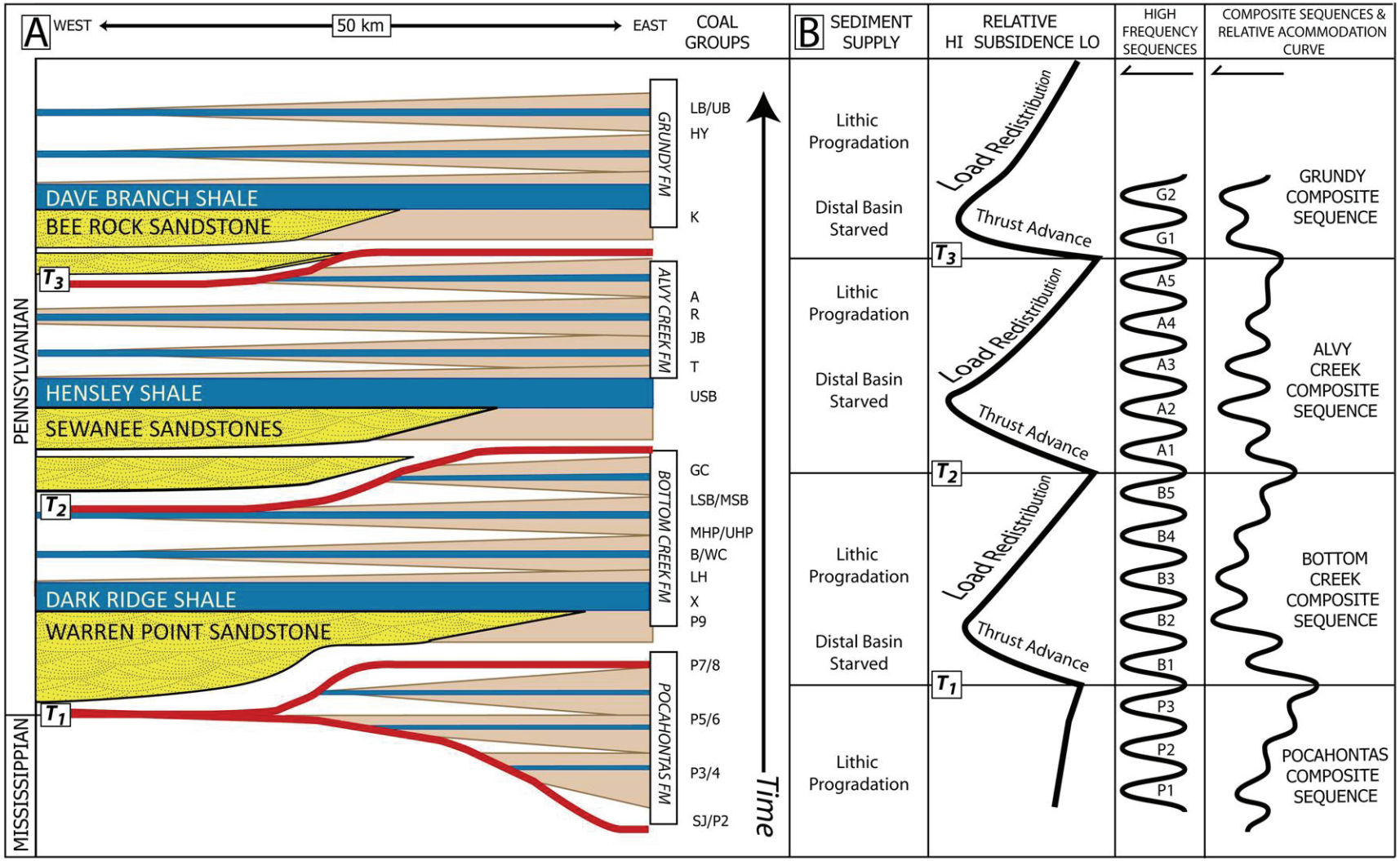
A
WEST
50 km
EAST
COAL GROUPS
PENNSYLVANIAN
MISSISSIPPIAN
DAVE BRANCH SHALE
BEE ROCK SANDSTONE
HENSLEY SHALE
SEWANEE SANDSTONES
DARK RIDGE SHALE
WARREN POINT SANDSTONE
T3
T2
T1
GRUNDY FM
ALVY CREEK FM
BOTTOM CREEK FM
POCAHONTAS FM
LB/UB
HY
K
A
R
JB
T
USB
GC
LSB/MSB
MHP/UHP
B/WC
LH
X
P9
P7/8
P5/6
P3/4
SJ/P2
Time
B
SEDIMENT SUPPLY
RELATIVE HI SUBSIDENCE LO
HIGH FREQUENCY SEQUENCES
COMPOSITE SEQUENCES & RELATIVE ACOMMODATION CURVE
Lithic Progradation
Distal Basin Starved
Load Redistribution
Thrust Advance
G2
G1
A5
A4
A3
A2
A1
B5
B4
B3
B2
B1
P3
P2
P1
GRUNDY COMPOSITE SEQUENCE
ALVY CREEK COMPOSITE SEQUENCE
BOTTOM CREEK COMPOSITE SEQUENCE
POCAHONTAS COMPOSITE SEQUENCE

Figure 3.14. Series of paleogeographic maps tracking trends in the eastern limit of quartzarenite facies during tectonic events **T_1 (A), T_2 (B),** and **T_3 (C**). Lowstand fluvial facies distributions were derived from the position of the **50 ft (15 m)** isolines of quartzarenite member isopach maps. Corresponding cross-sectional basin architectures are displayed for each event in **D, E & F,** derived from numerous dip sections balanced on low-frequency maximum flood surfaces.

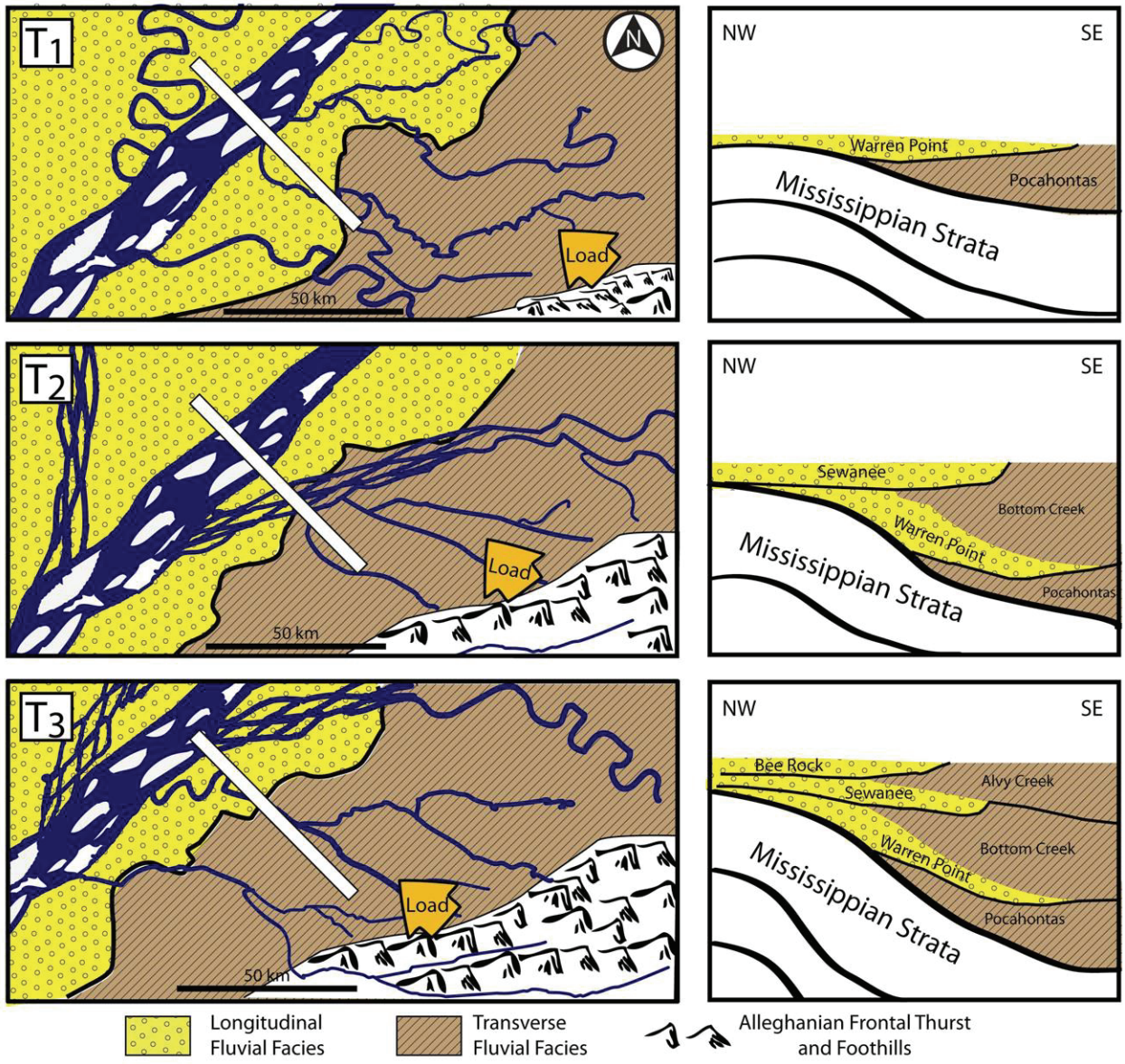
T1
N
Load
50 km
NW
SE
Warren Point
Pocahontas
Mississippian Strata
T2
Load
50 km
NW
SE
Sewanee
Bottom Creek
Warren Point
Pocahontas
Mississippian Strata
T3
Load
50 km
NW
SE
Bee Rock
Alvy Creek
Sewanee
Bottom Creek
Warren Point
Pocahontas
Mississippian Strata
Longitudinal Fluvial Facies
Transverse Fluvial Facies
Alleghanian Frontal Thurst and Foothills

TABLES

Facies Association	Component Facies	Characteristics	Geometry – Architectural Elements
Longitudinal Fluvial System	Quartz pebble bearing conglomerates, large (~1m) trough, tangential, planar and compound crossbedded sandstones, rooted siltstones, coals	25-90m thick, unimodal S-SW paleoflow, large macroforms oriented in paleoflow direction, multilateral, multistory, quartz-dominated composition	Tabular and lenticular sandstone bodies, sharp-based; channel, gravel bar and bedforms, sandy bedform, downstream accreting elements; capped by fine-grained overbank facies
Transverse Fluvial System	Siderite and mudstone conglomerates, Trough and planar crossbedded sandstones, trough and planar crossbedded sandstones, rooted siltstones, coals	6-45m thick, unimodal W paleoflow, multilateral, commonly single and multistory, rooted top surfaces, complexly interbedded siltstone, immature-litharenite composition	Tabular and lenticular sandstone bodies, sharp/irregular-based; channel, gravel bar and bedform, sandy bedform, lateral accretion elements; capped by fine-grained overbank facies

Table 3.1. Facies Associations. Fluvial facies observed are organized into two fluvial facies associations, interpreted to represent longitudinal and transverse fluvial depositional settings. Fluvial architectural elements after **Miall (1985)**.

REFERENCES

Aleinikoff, J.N., Burton, W.C., Lyttle, P.T., Nelson, A.E., and Southworth, C.S., 2000, U-Pb geochronology of zircon and monazite from Mesoproterozoic granitic gneisses of the northern Blue Ridge, Virginia and Maryland, USA: Precambrian Research, v. 99, p. 113-146.

Archer, A.W., and Greb, S.F., 1995, An Amazon-scale drainage system in the early Pennsylvanian of central North America: The Journal of Geology, v. 103, p. 611-627.

Ballato, P., Nowaczyk, N.R., Landgraf, A., Strecker, M.R., Friedrich, A., and Tabatabaei, S.H., 2008, Tectonic control on sedimentary facies pattern and sediment accumulation rates in the Miocene foreland basin of the southern Alborz mountains, northern Iran: Tectonics, v. 27.

Baltzer, F., and Purser, B.H., 1990, Modern Alluvial-Fan and Deltaic Sedimentation in a Foreland Tectonic Setting - the Lower Mesopotamian Plain and the Arabian Gulf: Sedimentary Geology, v. 67, p. 175-197.

Barrier, L., Proust, J.N., Nalpas, T., Robin, C., and Guillocheau, F., 2010, Control of Alluvial Sedimentation at Foreland-Basin Active Margins: A Case Study from the Northeastern Ebro Basin (Southeastern Pyrenees, Spain): Journal of Sedimentary Research, v. 80, p. 728-749.

Bartholomew, M.J. and Whitaker, A.E., 2010, The Alleghanian deformational sequence at the foreland junction of the Central and Southern Appalachians *in* From Rodinia to Pangea: The Lithotectonic Record of the Appalachian Region, ed.R.P. Tollo.,Geological Society of America Memoir 206.

Beaumont, 1981, Foreland Basins, Geophys. J. R. Astron. Soc., v. 65, p.291-329

Beaumont, C., Quinlan, G., and Hamilton, J., 1988, Orogeny and Stratigraphy - Numerical-Models of the Paleozoic in the Eastern Interior of North-America: Tectonics, v. 7, p. 389-416.

Becker, T.P., Thomas, W.A., Samson, S.D., and Gehrels, G.E., 2005, Detrital zircon evidence of Laurentian crustal dominance in the lower Pennsylvanian deposits of the Alleghenian clastic wedge in eastern North America: Sedimentary Geology, v. 182, p. 59–86.

Blair, T.C., and Bilodeau, W.L., 1988, Development of Tectonic Cyclotherms in Rift, Pull-Apart, and Foreland Basins - Sedimentary Response to Episodic Tectonism: Geology, v. 16, p. 517-520.

Blake, B.M., and Beuthin, J.D., 2008, Deciphering the mid-Carboniferous eustatic event in the central Appalachian foreland basin, southern West Virginia, USA: Resolving the Late Paleozoic Ice Age in Time and Space, v. 441, p. 249-260

Bodek, R.J., 2006, Sequence stratigraphic architecture of early Pennsylvanian, coal-bearing strata of the Cumberland Block a case study from Dickenson County, Virginia: [Blacksburg, Va. :, University Libraries, Virginia Polytechnic Institute and State University.

Burbank, D.W., 1992, Causes of Recent Himalayan Uplift Deduced from Deposited Patterns in the Ganges Basin: Nature, v. 357, p. 680-683.

Burbank, D.W., and Reynolds, R.G.H., 1984, Sequential Late Cenozoic Structural Disruption of the Northern Himalayan Foredeep: Nature, v. 311, p. 114-118.

Butler, R.W.H., 2004, The nature of 'roof thrusts' in the Moine Thrust Belt, NW Scotland: implications for the structural evolution of thrust belts: Journal of the Geological Society, v. 161, p. 849-859.
Catuneanu, O., and Elango, H.N., 2001, Tectonic control on fluvial styles: the Balfour Formation of the Karoo Basin, South Africa: Sedimentary Geology, v. 140, p. 291-313.
Catuneanu, O., Sweet, A.R., and Miall, A.D., 1997, Reciprocal architecture of Bearpaw T-R sequences, uppermost Cretaceous, Western Canada Sedimentary Basin: Bulletin of Canadian Petroleum Geology, v. 45, p. 75-94.
Cecil, C.B., Stanton, R.W., Neuzil, S.G., Dulong, F.T., Ruppert, L.F., and Pierce, B.S., 1985, Paleoclimate Controls on Late Paleozoic Sedimentation and Peat Formation in the Central Appalachian Basin (USA): International Journal of Coal Geology, v. 5, p. 195-230.
Chesnut, D. R., Jr., 1988, Stratigraphic analysis of the Carboniferous rocks of the Central Appalachian Basin: Unpublished PhD.Dissertation, University of Kentucky, Lexington, 296 p
Chesnut, D.R., Jr., 1994, Eustatic and tectonic control of deposition of the Lower and Middle Pennsylvanian strata of the Central Appalachian Basin: Concepts in Sedimentology and Paleontology, v. 4, p. 51-64.
Churnet, H.G., 1996, Depositional environments of Lower Pennsylvanian coal-bearing siliciclastics of southeastern Tennessee, northwestern Georgia, and northeastern Alabama, USA: International Journal of Coal Geology, v. 31, p. 21-54.
Clevis, Q., De Boer, P.L., and Nijman, W., 2004, Differentiating the effect of episodic tectonism and eustatic sea-level fluctuations in foreland basins filled by alluvial fans and axial deltaic systems: insights from a three-dimensional stratigraphic forward model: Sedimentology, v. 51, p. 809-835.
Davis, M.W. and Ehrlich R. 1974, Late Paleozoic crustal composition and dynamics in the southeastern United States: in Briggs, Garrett (ed.), Carboniferous of the southeastern United States, Geol. Soc. America Special Paper 148, p. 171-185.
Dean, S.L., Kulander, B.R., and Skinner, J.M., 1988, Structural Chronology of the Alleghanian orogeny in southeastern West Virginia: Geological Society of America Bulletin, v. 100, p. 299-310.
DeCelles, P.G., and Giles, K.A., 1996, Foreland basin systems: Basin Research, v. 8, p. 105-123.
Decelles, P.G., Lawton, T.F., and Mitra, G., 1995, Thrust Timing, Growth of Structural Culminations, and Synorogenic Sedimentation in the Type Sevier Orogenic Belt, Western United-States: Geology, v. 23, p. 699-702.
Dickinson, W. R., Beard, L. S., Brakenridge, G. R., Erjavec, J. L., Ferguson, R. C., Inman, K. F., Knepp, R. A., Lindberg, F. A., and Ryberg, P. T., 1983, Provenance of North American Phanerozoic sandstones in relation to tectonic setting: Geol. Soc. America Bull., v. 94, p. 222-235.
Dickinson, W.R. and Suczek, C. A., 1979, Plate tectonics and sandstone compositions: Am. Assoc. Petroleum Geologists Bull., v. 63, p. 2164-2182.
Dott, R. H., Jr., 1964, Wacke, graywacke and matrix--what approach to immature sandstone classification? : Jour. Sed. Petrology, v. 34, p. 625-632.
Englund, K.J., and Thomas, R.E., 1990, Late Paleozoic depositional trends in the central Appalachian Basin: U. S. Geological Survey Bulletin, Report: B.

Englund, K.J., Arndt, H.H., and Henry, T.W., 1979, Proposed Pennsylvanian system stratotype, Virginia and West Virginia: [Falls Church, Va., American Geological Institute], vi, 136 p. p.

Eriksson, K.A., Campbell, I.H., Palin, J.M., Allen, C.M., and Bock, B., 2004, Evidence for multiple recycling in neoproterozoic through Pennsylvanian sedimentary rocks of the central Appalachian basin: Journal of Geology, v. 112, p. 261-276.

Ettensohn, F.R., 2004, Modeling the nature and development of major Paleozoic clastic wedges in the Appalachian Basin, USA: Journal of Geodynamics, v. 37, p. 657-681.

Ettensohn, F.R., 2008, The Appalachian foreland basin in eastern United states: *in* Hsu K.J., ed., Sedimentary Basins of the World, Volume 5, The Sedimentary Basins of the United States and Canada: The Netherlands, A.D. Miall, Elsevier, p. 105–179.

Ferm, J.C., and Horne, J.C., 1979, Carboniferous depositional environments in the Appalachian region: [Columbia, Dept. of Geology, University of South Carolina], vi, 760 p. p.

Flemings, P.B., and Jordan, T.E., 1990, Stratigraphic Modeling of Foreland Basins - Interpreting Thrust Deformation and Lithosphere Rheology: Geology, v. 18, p. 430-434.

Franzinelli, E., and Potter, P.E., 1983, Petrology, Chemistry, and Texture of Modern River Sands, Amazon River System: Journal of Geology, v. 91, p. 23-39.

Galehouse, J.S., 1971, Point counting, *in* Carver, R.E., ed., Procedures in Sedimentary Petrology: New York, Wiley-Interscience, p. 385-407.

Garcia-Castellanos, D., 2002, Interplay between lithospheric flexure and river transport in foreland basins: Basin Research, v. 14, p. 89-104.

Gates, A.E., Speer, J.A. and Pratt, T.L., 1988. The Alleghanian southern Appalachian Piedmont: a transpressional model. Tectonophysics 7, pp. 1307–1324

Geiser, P., and Engelder, T., 1983, The Distribution of Layer Parallel Shortening Fabrics in the Appalachian Foreland of New-York and Pennsylvania - Evidence for 2 Non-Coaxial Phases of the Alleghanian Orogeny: Geological Society of America Memoirs, v. 158, p. 161-175.

Goodbred, S.L., and Kuehl, S.A., 2000, The significance of large sediment supply, active tectonism, and eustasy on margin sequence development: Late Quaternary stratigraphy and evolution of the Ganges-Brahmaputra delta: Sedimentary Geology, v. 133, p. 227-248.

Graham, S.A., Dickinson, W.R., and Ingersoll, R.V., 1975, Himalayan-Bengal Model for Flysch Dispersal in Appalachian-Ouachita System: Geological Society of America Bulletin, v. 86, p. 273-286.

Greb, S.F., and Chesnut, D.R., 1996, Lower and lower middle Pennsylvanian fluvial to estuarine deposition, central Appalachian basin: Effects of eustasy, tectonics, and climate: Geological Society of America Bulletin, v. 108, p. 303-317.

Gupta, S., 1997, Himalayan drainage patterns and the origin of fluvial megafans in the Ganges foreland basin. Geology, v. 25; no. 1; p. 11–14.

Hatcher, R.D. Jr., 1972, Developmental model for the southern Appalachians, *in*. Hatcher, R.D., Thomas, W.A., Viele, G.W., and Geological Society of America., 1989, The Appalachian-Ouachita orogen in the United States: Boulder, Colo., Geological Society of America Bulletin **v.**83, pp. 2735–2760.

Hatcher, R.D., Jr., 2002, Alleghanian (Appalachian) orogeny, a product of zipper tectonics: Rotational, transpressive continent–continent collision and closing of ancient oceans along irregular margins, *in* Martínez Catalán, J.R., Hatcher, R.D., Jr., Arenas, R., and

Díaz García, F., eds., Variscan-Appalachian dynamics: The building of the Late Paleozoic basement: Boulder, Colorado, Geological Society of America Special Paper 364, p. 199–208.
Heller, P.L., Angevine, C.L., Winslow, N.S., and Paola, C., 1988, 2-Phase Stratigraphic Model of Foreland-Basin Sequences: Geology, v. 16, p. 501-504.
Henika, W. S., 1994, Internal structure of the coal bearing portion of the Cumberland Overthrust Block in Southwestern Virginia and adjoining areas, in Geology and Mineral Resources of the Southwestern Virginia Coalfield, Virginia Division of Mineral Resources Publication 131, p.100-120.
Herz, N. & Force, E. R. 1984,. Rock suites in Grenvillian terrane of the Roseland district, Virginia, Part 1 Lithologic relations. In: Bartholomew, M. J. (ed.) The Grenville Event in the Appalachians and Related Topics. Geological Society of America, Special Papers 194, 187–199.
Hobday, D.K., and Horne, J.C., 1977, Tidally Influenced Barrier Island and Estuarine Sedimentation in Upper Carboniferous of Southern West-Virginia: Sedimentary Geology, v. 18, p. 97-122.
Hoffman, P.F., 1989, Precambrian geology and tectonic history of North America, *in* Bally A.W., Palmer A.R., eds., The Geology of North America: An Overview: Boulder, Colorado, Geological Society of America, Geology of North America, v. A, p. 447–512.
Horton, J.W. Jr., Drake, A.A. Jr., and Rankin, D.W. 1989, Tectonostratigraphic terranes and their Paleozoic boundaries in the central and southern Appalachians. *In*: R.D. Dallmeyer, Editor, Terranes in the Circum-Atlantic Paleozoic orogens. GSA, pp. 213–246 Spl. Paper 230.
Hoth, S., Hoffmann-Rothe, A., and Kukowski, N., 2007, Frontal accretion: An internal clock for bivergent wedge deformation and surface uplift: Journal of Geophysical Research-Solid Earth, v. 112.
Houseknecht, D. W., 1978, Petrology and stratigraphy of some Pottsville quartzites and graywackes of West Virginia [unpub. Ph.D. thesis]: University Park, Penn. State Univ., 197 p.
Houseknecht, D.W., 1980, Comparative Anatomy of a Pottsville Lithic Arenite and Quartz Arenite of the Pocahontas Basin, Southern West-Virginia - Petrogenetic, Depositional, and Stratigraphic Implications: Journal of Sedimentary Petrology, v. 50, p. 3-20.
Houston, W.S., Huntoon, J.E., and Kamola, D.L., 2000, Modeling of Cretaceous foreland-basin parasequences, Utah, with implications for timing of Sevier thrusting: Geology, v. 28, p. 267-270.
James, G.A. and Wynd, J.G., 1965. Stratigraphic nomenclature of Iranian Oil Consortium Agreement area, Am. Assoc. Pet. Geol. Bull. 49, pp. 2182–2245.
Johnsson, M.J., Stallard, R.F., and Meade, R.H., 1988, 1st-Cycle Quartz Arenites in the Orinoco River Basin, Venezuela and Colombia: Journal of Geology, v. 96, p. 263-2771.
Klein, G.D., and Kupperman, J.B., 1992, Pennsylvanian Cyclothems - Methods of Distinguishing Tectonically Induced Changes in Sea-Level from Climatically Induced Changes: Geological Society of America Bulletin, v. 104, p. 166-175.
Korus, J.T., 2002, The lower Pennsylvanian New River Formation a nonmarine record of glacioeustasy in a foreland basin: [Blacksburg, Va. :, University Libraries, Virginia Polytechnic Institute and State University.

Korus, J.T., Kvale, E.P., Eriksson, K.A., and Joeckel, R.M., 2008, Compound paleovalley fills in the Lower Pennsylvanian New River Formation, West Virginia, USA: Sedimentary Geology, v. 208, p. 15-26.
Lowry, W. D., 1971, Appalachian Overthrust belt, Montgomery County, southwestern Virginia, in Guidebook to Appalachian tectonics and sulfide mineralization of southwestern Virginia: Virginia Polytechnic Institute and State University, Department of Geological Sciences Guidebook 5, p. 143-165.
Mackey, S.D., and Bridge, J.S., 1995, 3-Dimensional Model of Alluvial Stratigraphy - Theory and Application: Journal of Sedimentary Research Section B-Stratigraphy and Global Studies, v. 65, p. 7-31.
Marr, J.G., Swenson, J.B., Paola, C., Voller, V.R., 2000. A two-diffusion model of fluvial stratigraphy in closed depositional basins. Basin Res. 12, 381– 398.
Miall, A.D., 1981, Sedimentation and tectonics in alluvial basins: Waterloo, Ontario, Geological Association of Canada, vi, 272 p. p.
Miall, A.D., 1985, Architectural-element analysis: a new method of facies analysis applied to fluvial deposits, *Earth Sci. Rev.* 22, pp. 261–308.
Miall, A.D., and Arush, M., 2001, Cryptic sequence boundaries in braided fluvial successions: Sedimentology, v. 48, p. 971-985.
Mitchum, R.M.. Jr., and Van Wagoner, J.C. 1991, High-frequency sequences and their stacking patterns; sequence-stratigraphic evidence of high-frequency eustatic cycles, *in* Biddle K.T., Schlager W.eds., The record of sea-level fluctuations: Sedimentary Geology, v. 70, p. 131–160.
Mitra, G., 1988, 3-Dimensional Geometry and Kinematic Evolution of the Pine Mountain Thrust System, Southern Appalachians: Geological Society of America Bulletin, v. 100, p. 72-95.
Naylor and Sinclair, 2008 Naylor, M., and Sinclair, H.D., 2008, Pro- vs. retro-foreland basins: Basin Research, v. 20, p. 285-303.
Nieuwland, D.A., Leutscher, J.H., and Gast, J., 2000, Wedge equilibrium in fold-and-thrust belts: prediction of out-of-sequence thrusting based on sandbox experiments and natural examples: Geologie En Mijnbouw-Netherlands Journal of Geosciences, v. 79, p. 81-91.
Ori, G.G., 1993, Continental Depositional Systems of the Quaternary of the Po Plain (Northern Italy): Sedimentary Geology, v. 83, p. 1-14.
Paola, C., Heller, P. L. and Angevine, C. L., 1992, The large-scale dynamics of grain-size variation in alluvial basins, 1: Theory, Basin Res., 4, 73–90.
Park, H., Barbeau, D.L. Jr., Rickenbaker, A., Bachmann-Krug, D., Gehrels, G., 2010, Application of Foreland Basin Detrital-Zircon Geochronology to the Reconstruction of the Southern and Central Appalachian Orogen: Journal of Geology, vol. 118, no. 1, pp. 23-44.
Plint, A.G., Hart, B.S. and Donaldson, W.S., 1993, Lithospheric flexure as a control on stratal geometry and facies distribution in Upper Cretaceous rocks of the Alberta foreland basin, Basin Research 5, pp. 69–77.
Posamentier, H.W., and Allen, G.P., 1993, Siliciclastic Sequence Stratigraphic Patterns in Foreland Ramp-Type Basins: Geology, v. 21, p. 455-458.
Potter, P.E., 1978, Significance and Origin of Big Rivers: Journal of Geology, v. 86, p. 13-33.

Rasanen, M., Neller, R., Salo, J., and Jungner, H., 1992, Recent and Ancient Fluvial Deposition Systems in the Amazonian Foreland Basin, Peru: Geological Magazine, v. 129, p. 293-306.
Reed, J.S., 2003, Thermal and Diagenetic Evolution of Carboniferous Sandstones, Central Appalachian Basin: unpublished Ph.D. dissertation, Virginia Polytechnic Institute and State University, Blacksburg, Virginia, 115 p.
Reed, J.S., Eriksson, K.A., and Kowalewski, M., 2005, Climatic, depositional and burial controls on diagenesis of Appalachian Carboniferous sandstones: qualitative and quantitative methods: Sedimentary Geology, v. 176, p. 225-246.
Rice, C.L., 1984, Sandstone units of the Lee Formation and related strata in eastern Kentucky: Washington, U.S. G.P.O., iv, 53 p. p.
Rice, C.L., and Schwietering, J.F., 1988, Fluvial deposition in the Central Appalachians during the Early Pennsylvanian: U. S. Geological Survey Bulletin, Report: B.
Robinson, R.A.J., and Prave, A.R., 1995, Cratonal Contributions to a Classic Molasse - the Carboniferous Pottsville Formation of Eastern Pennsylvania Revisited: Geology, v. 23, p. 369-372.
Ryder, R.T., and Geological Survey (U.S.), 2008, Geologic cross section E-E' through the Appalachian Basin from the Findlay Arch, Wood County, Ohio, to the Valley and Ridge Province, Pendleton County, West Virginia, Scientific investigations map 2985: Reston, Va.
Schlee, J., 1963, Early Pennsylvanian currents in the southern Appalachian Mountains: Geological Society of America Bulletin, v. 74, p. 1439–1452.
Scotese, C., 2004, A continental drift flipbook: Journal of Geology, v. 112p. 729-741.
Secor, D.T., Snoke, A.W., and Dallmeyer, R.D., 1986, Character of the Alleghanian Orogeny in the Southern Appalachians .3. Regional Tectonic Relations: Geological Society of America Bulletin, v. 97, p. 1345-1353.
Shanley, K.W., and Mccabe, P.J., 1994, Perspectives on the Sequence Stratigraphy of Continental Strata: AAPG Bulletin-American Association of Petroleum Geologists, v. 78, p. 544-568.
Siever, R., 1957, Pennsylvanian sandstones of the Eastern-Interior coal basin; Jour. Sed. Petrology, v. 27, p. 227-250.
Sinha, R., and Friend, P.F., 1994, River Systems and Their Sediment Flux, Indo-Gangetic Plains, Northern Bihar, India: Sedimentology, v. 41, p. 825-845.
Stott, G.M., 1997. The Superior Province, Canada. In: de Wit, M. and Ashwal, L.D., Editors, 1997. Greenstone Belts, Clarendon Press, Oxford, pp. 480–507.
Suttner, L.J., Basu, A., Mack, G.H., 1981. Climate and origin of quartz arenites. Journal of Sedimentary Petrology v.51, 4, 1235–1246.
Tandon, S.K. and Sinha, R., 2007, Geology of large river systems. *In:* A. Gupta (Ed.), Large Rivers: Geomorphology and Management. John Wiley and Sons, UK., 689p.
Tankard, A.J., 1986, Depositional Response to Foreland Deformation in the Carboniferous of Eastern Kentucky: Aapg Bulletin-American Association of Petroleum Geologists, v. 70, p. 853-868.
Thomas, W.A., Becker, T.P., Samson, S.D., and Hamilton, M.A., 2004, Detrital zircon evidence of a recycled orogenic foreland provenance for Alleghanian clastic-wedge sandstones: Journal of Geology, v. 112, p. 23-37.

Tucker, G.E., and Slingerland, R., 1996, Predicting sediment flux from fold and thrust belts: Basin Research, v. 8, p. 329-349.
Turcotte, D.L., and Schubert, G., 1982, Geodynamics : applications of continuum physics to geological problems: New York, Wiley, 450 p. p.
Valentino, D.W., and Gates, A.E., 2001, Asynchronous extensional collapse of a transpressional orogen: the Alleghanian central Appalachian Piedmont, USA: Journal of Geodynamics, v. 31, p. 145-167.
Van der Voo, R., 1983, A plate tectonics model for the Paleozoic assembly of Pangea based on paleomagnetic data, *in* Hatcher, R.D. Jr., Williams, H., and Zietz, I., eds., Contributions to the tectonics and geophysics of mountain chains: Geological Society of America Memoir 158, p. 19-24.
Van Wagoner, J.C., Posamentier, H.W., Mitchum, R.M.J., Vail, P.R., Sarg, J.F., Loutit, T.S., and Hardenbol, J., 1988, An overview of the fundamentals of sequence stratigraphy and key definitions: Sea-Level Changes: An Integrated Approach: SEPM, Special Publication, v. 42, p. 39–45.
Varban, B.L., and Plint, A.G., 2008, Sequence stacking patterns in the Western Canada foredeep: influence of tectonics, sediment loading and eustasy on deposition of the Upper Cretaceous Kaskapau and Cardium Formations: Sedimentology, v. 55, p. 395-421.
Vauchez, A., 1987, Brevard Fault Zone, Southern Appalachians - a Medium-Angle, Dextral, Alleghanian Shear Zone: Geology, v. 15, p. 669-672.
Watts, A. B., 1992, The effective elastic thickness of the lithosphere and the evolution of foreland basins: Basin Research, v. 4, p. 169-178.
Wise, D.U., Belt, E.S., and Lyons, P.C., 1991, Clastic Diversion by Fold Salients and Blind Thrust Ridges in Coal-Swamp Development: Geology, v. 19, p. 514-517.
Wizevich, M. C. 1991. Sedimentology and regional implications of fluvial quartzose sandstones of the Lee Formation, central Appalachian basin. Ph.D. dissertation, Virginia Polytechnic Institute and State University, Blacksburg.
Wizevich, M.C., 1992, Sedimentology of Pennsylvanian Quartzose Sandstones of the Lee Formation, Central Appalachian Basin - Fluvial Interpretation Based on Lateral Profile Analysis: Sedimentary Geology, v. 78, p. 1-47.
Wright, V.P., and Marriott, S.B., 1993, The Sequence Stratigraphy of Fluvial Depositional Systems - the Role of Floodplain Sediment Storage: Sedimentary Geology, v. 86, p. 203-210.
Yang, Y.T., and Miall, A.D., 2008, Marine transgressions in the mid-Cretaceous of the Cordilleran foreland basin re-interpreted as orogenic unloading deposits: Bulletin of Canadian Petroleum Geology, v. 56, p. 179-198.

CHAPTER 4
Seal Evaluation of Early Pennsylvanian coal-bearing strata, Virginia: The Potential for Safe Carbon Dioxide Storage with Enhanced Coal Bed Methane Recovery

RYAN P. GRIMM [1], KENNETH A. ERIKSSON [1], NINO RIPEPI [2], CORTLAND EBLE [3], STEPHEN F. GREB [3]

1. Department of Geosciences, Virginia Tech, Blacksburg, Virginia 24061, USA
2. Virginia Center for Coal and Energy Research, Virginia Tech, Blacksburg, VA 24061, USA
3. Kentucky Geological Survey, University of Kentucky, Lexington, KY 40506, USA

Abstract

The geological storage of carbon dioxide in Appalachian basin coal seams is one possible sink for sequestration of this greenhouse gas, with the added benefit of potential enhanced-coalbed methane recovery. The Pocahontas Basin (part of the central Appalachian Basin) of southwestern Virginia is a major coal bed methane (CBM) field. Production is mostly from coal beds in the Lower Pennsylvanian Pocahontas and New River formations. As part of the Southeast Regional Carbon Sequestration Partnership's Phase 2 research program, a CO_2-injection demonstration well was drilled into Lower Pennsylvanian coal bed-methane producing strata in southwest Virginia. Samples of siliciclastic lithologies above coal beds in this Oakwood Field well, and from several other cores in the Nora Field were taken to determine the seal competency of overlying strata at local and regional scales.

Strata above CBM-producing coal beds in the Pocahontas and New River formations consist of dark-gray shales; silty gray shales; heterolithic siltstones, sandstones, and shales; lithic sandstones, and quartzose sandstones. Standard measurements of porosity, permeability and petrography were used to evaluate potential leakage hazards and any possible secondary storage potential for typical lithologies. Both lithic- and quartz-rich sandstones exhibit only minor porosity, with generally low permeabilities (< 0.042 md). Interconnected porosity and permeability is strongly impacted by diverse cementation types and compaction. Sandstones sampled are considered tight, with limited matrix permeability risks for leakage.

One of the most promising confining intervals above the major coal bed-methane producing interval is the Hensley Shale Member. Analyses of 1500 geophysical logs in southwest Virginia indicates this unit is thick (> 50 ft, 15 m), laterally continuous (>3000 km^2), and a homogenous, low-porosity shale, which coarsens upward into siltstone and sandstone, or is

truncated by sandstone. Calculations from two mercury injection capillary porosimetry tests of the shale indicate a displacement entry pressure of 207 psia (1427 kPa) would generate an estimated seal capacity of 1365 ft (416 m) of CO_2 before buoyant leakage. Scanning electron microscopy indicates a microfabric of narrow pore throats between quartz grains floating in a clay matrix. Modeled median pore throat size between micro-fabric matrix grains for the shale is estimated at 0.26 μm. These characteristics indicate that the shale, where unfractured, would be a good confining interval for deeper CO_2 storage with ECBM.

Estimated maximum seal capacities are far greater than ECBM reservoir thicknesses in the Nora Field, with no danger of capillary failure in the sealing interval based on core data. An evaluation of local structural integrity and abandoned wellbores will be critical to define secondary leakage risks to ECBM injection site conditions, as small zones of brittle fracture and improperly plugged wells may pose leakage risks. Another major consideration in this, and other CBM fields, will be the influence of treatment-induced fractures. If hydraulic fractures have propagated out of a coal bed, then heights and orientations of fractures may need to be geomechanically evaluated prior to injection to ensure injected CO_2 remains within the coal target. Injection wells should be selected where only coal zones below the Hensley Shale were hydraulically fractured, and wells in which the Hensley Shale is below the level of surface fracture influence (more than 180 m deep) This selection process will help to ensure the integrity of the sealing lithologies and adequate confinement for CO_2-ECBM .

KEYWORDS: seal characterization, carbon sequestration, enhanced coal bed methane, Appalachian Basin, carbon dioxide

1. Introduction

A potential method for reducing the amount of anthropogenic carbon dioxide (CO_2) released to the atmosphere is carbon capture and storage (e.g., Pacala and Socolow, 2004). Carbon storage research in geological reservoirs has expanded in importance for industrial, academic, and government carbon management studies (Reichle et al., 1999; Benson and Cole, 2008; USDOE - NETL, 2008a). In the Appalachian region of the United States, research into potential geological storage reservoirs is especially important because much of this region relies on coal-fired electricity generation and has high per capita CO_2 emissions (USDOE NatCarb Atlas, 2008). The central Appalachian basin has several types of potential geologic storage options, including the use of deep, unmineable coal seams. This technique may allow for simultaneous carbon storage with the added economic benefit of CO_2 enhanced recovery of coal bed methane (ECBM). Conventional methods of coal bed methane (CBM) production leave economic volumes of methane adsorbed in the coal reservoir after depressurization and production. With ECBM, gaseous carbon dioxide would be injected into coal seams to fill available cleat and pore space to displace remaining methane to production wells, comparable to secondary recovery techniques in mature oil fields (Wong and Gunter, 1999; Mavor et al., 2002; Koeperna and Riestenberg, 2009). Once CO_2 broke through to the production well, injection would stop. In some cases, gas separators would be used on production wells to split off any CO_2 that was produced with the methane for re-injection and pressure management elsewhere in the field.

In Appalachia, CBM is produced primarily from Lower (Early) Pennsylvanian coal seams of the Pocahontas and Lee Formations in the Pocahontas Basin of southwestern Virginia, and southern West Virginia (**Figure 4.1**). Recent investigations by the U.S. Department of

Energy's Southeast Regional Carbon Sequestration Partnership (SECARB) suggest that these coal-bearing sedimentary rocks have potential for use of CO2 with ECBM production (USDOE-NETL, 2008a). SECARB estimates 1.3 billion tons of technically feasible CO_2 storage capacity in coal beds of the Pocahontas Basin, with enhanced recovery potentially increasing CBM reserves by an additional 2.5 TCF (Ripepi, 2009). In 2009, a test well was drilled in southwest Virginia, as part of SECARB's Phase II research program to inject small amounts CO_2 into coal beds of the Pocahontas and Lee Formations and determine the potential of this technology in the Pocahontas Basin ***(*Nino, 2009*).*** Aside from technical details about the actual coal reservoirs, evaluations were also needed for seal capacity, structural integrity, and secondary trapping effectiveness of the overlying strata to ensure injected CO_2 would remain in the coal reservoirs and not leak to the potable water table or surface.

The objectives of this study are to evaluate the petrophysical and geochemical properties of units above the CBM-producing coal beds in the Pocahontas basin to better predict potential pathways and behaviors of injected CO_2 in a future ECBM system. The results are critical to developing a regional leakage risk screening model suitable for ECBM site and target selection in central Appalachia.

2. GEOLOGIC SETTING

2.1 Structural Setting

The Appalachian Basin is a northeast-southwest trending Paleozoic foreland basin, formed as a collective result of repeated collisional tectonism during the Taconic, Acadian, and Alleghanian orogenies (Quinlan and Beaumont, 1984; Tankard, 1986; Thomas, 1995).

Accommodation for as much as 2.8 km of early Pennsylvanian through early Permian terrestrial and marginal marine siliciclastic rocks was provided by thrust-load induced subsidence of the Laurentian Craton during the Alleghanian orogeny (Rice and Schwietering, 1988; Ettensohn, 2004). Pennsylvanian-age sedimentary units are preserved in three depocenters in the greater Appalachian Basin, the northern Appalachian (Dunkard) Basin, the central Appalachian basin (including the Pocahontas Basin) and the southern Appalachian basin (including the Black Warrior Basin) (**Figure 4.1**; Arkle, 1974; Greb et al., 2008, 2009).

The Pocahontas Basin is a narrow, structurally-defined northeast-southwest trending basin, spanning nearly 40,000 km^2 of Tennessee, Kentucky, Virginia, and West Virginia, in which the early Pennsylvanian Pocahontas Formation is preserved (**Figure 4.1**). The Virginia portion of the Pocahontas Basin is exposed on the Pine Mountain Thrust Sheet, and areas to the northeast along strike of the thrust sheet. The western limit of the thrust sheet is the Pine Mountain Thrust Fault, in Kentucky, which is the western limit of surficial Alleghanian deformation. The eastern limit of the block is the Hunter Valley ─ St. Clair Fault Zone and older folded Paleozoic rocks (**Figure 4.1**). The Pine Mountain Thrust Sheet is limited to the northeast by the Bishop-Bradshaw lineament/Cambria Fault (Henika, 1994). These faults have been mapped at the surface and in the subsurface as thin-skin faults offsetting Carboniferous and Devonian strata and are parallel to the primary vergence direction of other Valley and Ridge structures (Henika, 1994). Portions of the study area are transected by several north-south-oriented, strike-slip faults, including the Russell Fork Fault (**Figure 4.1**). A variety of thin-skinned folds of compressional origin have been identified in the Pocahontas Basin (Henika, 1994). These subtle but significant structural features have been determined to influence gas and water production in the CBM system (Conrad, personal communication) and may create zones

that both aid carbon storage efforts (e.g. increase coal permeability, structural closure) or increase leakage risks (e.g. shallow faults or joints in seal units). Several structural closures in the Nora Field of southwest Virginia are producing gas fields (from deeper Mississippian and Devonian non-coal reservoirs) or gas fields under development and would be large enough for future CO_2 storage when the gas in the fields is depleted.

2.2 Stratigraphy

Early Pennsylvanian sedimentary rocks of the Lee, Pocahontas, and New River Formations unconformably overlying the late Mississippian Bluestone Formation and attain a maximum thickness of approximately 2950 ft (900 m) along the southeast margin of the Pocahontas Basin in Virginia and West Virginia (Englund et al., 1979; Englund and Thomas, 1990; Chesnut, 1994; Korus, 2002; Blake and Beuthin, 2008). Quartzarenites dominate the Lee Formation and coal-bearing, immature, siliciclastic strata dominate the Pocahontas and New River Formations (Rice, 1985; Englund et al., 1986; Rice and Schwietering, 1988).

Chesnut (1992) developed a stratigraphic nomenclature for the central Appalachian basin based on marine flooding surfaces, and widespread quartzose sandstones. Although not formally adopted in Virginia, it is used herein to further subdivide the Early Pennsylvanian interval and define the potential future for CO_2-ECBM within specific zones for evaluation.

Several widespread marine-influenced, shale horizons subdivide the Breathitt Group into eight third-order sequences (Chesnut, 1992; 1994); The Early Pennsylvanian part of the group contains at least four sequences, in ascending order, the Pocahontas, Bottom Creek, Alvy Creek and Grundy Formations (**Figure 4.2**). The base of the Bottom Creek, Alvy Creek, and Grundy Formations are marine-influenced shale the Dark Ridge, Hensley and Dave Branch Shale

members respectively (**Figure 4.2**; Chesnut, 1992, 1994; Bodek, 2006). These members consist of dark gray shale, which coarsens upwards into heterolithic strata, and sandstone, or is truncated by a sandstone. Shales in these members are potential confining units for seal evaluation in the ECBM system.

2.3 Southwest Virginia CBM

The majority of coal bed methane production in the Pocahontas Basin is clustered in the Oakwood and Nora fields of Virginia **(Figure 4.1).** Exploration for CBM began in 1988 with Equitable Resources development of the Nora Field in Dickenson County, Virginia followed by CONSOL Energy developing the Oakwood Field in Buchanan County, Virginia. From 1988 through 1999, over 5400 CBM wells have been drilled and brought on-line as producing gas wells in southwest Virginia **(VDMME, 2009).**

Coal zones in the Pocahontas, Bottom Creek and Alvy Creek Formations are completed at depths as shallow as 375 ft (115 m), but most CBM production ranges from 1000 ft (300 m) to more than 2000 ft (610 m) due to low water contents in shallower zones (**Nolde and Spears, 1998; Zuber, 1998)**. Coal bed methane wells typically target six to fifteen seams, penetrating a minimum of 15-40 ft (4.5-12m) of net coal. The most significant producing seams in the Pocahontas Basin are the Pocahontas No. 1 through 9, Lower Horsepen, Beckley, War Creek, Middle and Upper Horsepen, Middle and Upper Seaboard, Greasy Creek and Jawbone horizons (**Figure 4.2)**.

In the Pocahontas Basin, successful well completion practices are commonly vertical, limited entry cased-hole completions followed with multi-stage foam stimulations (**Zuber, 1998**). Cased-hole completions maintain wellbore integrity by installing a well casing

completely through the target coal bearing formation. The casing is then perforated with directional charges in the production horizon to link the well to the gas-bearing coal reservoirs. CBM wells are then almost universally stimulated using nitrogen gas-based foam and water-sand hydraulic fracture techniques to increase the natural permeability of the coal seam surrounding the well while avoiding chemical damage to the coal formation (**Loomis, 1997**). Wells in the Nora Field are drilled on 24 ha (60 acre) per well spacing, with completions in seven to ten individual CBM intervals (**Zuber, 1998**). In the Oakwood Field, multi-seam wells are completed ahead of underground coal mining and in deep, currently unmineable coal seams (**Nino, 2009**). The Oakwood Field produces CBM through fracture stimulating 15 to 25 coal seams with four- to six-stage fracture treatments (**Rodvelt et al., 2009**). Where thicker coal seams are present, multilateral horizontal wells have been implemented to increase productivity, predominantly in the Loup Creek Field of Wyoming County, West Virginia (**Nino, 2009**).

Adsorbed gas contents range 282 – 688 cubic feet (8.0 – 19.5 m^3) of gas per short ton of coal **(Diamond et al., 1986; Conrad, 2006**). Estimates for the average gas in place for an individual CBM well in the Nora Field is approximately 675 MMcf / well (19,100 m^3 / well), (**Zuber, 1998**). With a vertical well recovery factor of 30-60%, production volumes of 200 to 400 MMcf / well (5600 to 11,300 m^3/well) are anticipated (**Zuber, 1998).** Proven CBM reserves in Virginia account for nearly 12% of the national CBM reserves, currently near 1.8 trillion cubic feet (Tcf) (**USDOE-EIA, 2009)**. The original CBM in-place resource in the Pocahontas Basin has been estimated at 7.1 Tcf (**Kelefant and Boyer, 1988; Nolde and Spears, 1998; Lyons, 1998**), with 3.6 Tcf deemed technically recoverable (**Milici et al, 2003**). Annual CBM production for 2009 was a record 113 billion cubic feet (bcf), with more than half of the state total produced from the Oakwood Field alone **(VDMME, 2009).**

3. Seal Evaluation

Seals and trap integrity are a critical component in the evaluation and development of a CO_2 enhanced coal bed methane recovery project. In an ECBM sequestration system, the first CO_2 trapping mechanism would be the coal itself, through adsorption of CO_2 onto internal surfaces of the coal matrix (A, **Figure 4.3**). Several field and lab studies have demonstrated that the coal matrix has a stronger affinity for CO_2 than for CH_4, at a ratio of 2:1 or greater (Gale and Freund, 2001; Gluskoter et al., 2002; Mastalerz et al., 2004; Nelson et. al., 2005; Ripepi, 2009). Additional trapping mechanisms also need to be investigated in case the coal swells or CO_2 leaks from the coal into surrounding strata. These traps include the structural and capillary trapping of free gas and solubility trapping through the slow dissolution of CO_2 into reservoir micro pore waters in coal cleats and overlying strata (B, **Figure 4.3**), hydrodynamic trapping, and potentially, slow, long term mineral trapping as CO_2 reacts with rock units bounding the coal seams (C, **Figure 4.3**; Nelson et. al., 2005). These mechanisms might occur in the laterally variable lithofacies immediately above each coal bed reservoir, and/or in more regional, low-permeability shales, which occur at the base of the Early Pennsylvanian formations.

CO_2 can potentially leak through traps or through surrounding strata in several different ways. Poorly sealed injection well casings, abandoned well bores (D, **Figure 4.3**), transmissive fractures and faults in the cap rock(s) that penetrate the injection zone may serve as conduits for the relatively rapid vertical movement of CO_2 out of the reservoir (E, **Figure 4.3**: Nelson et. al., 2005). Slow escape pathways include transport of diffuse CO_2 out of the coal reservoir by hydrodynamic flow of formation water out of the geologic sink (F, **Figure 4.3**), and slow

buoyant flow of CO_2 through permeable overburden where seal thins or facies change (G, **Figure 4.3**).

In order to prevent vertical movement from the coal reservoir, an effective seal or confining unit needs to be identified prior to CO_2 injection. Seals are commonly laterally continuous, thick (> 30 ft, 9 m), low-permeability, sedimentary horizons with homogenous mineralogy and fine grain size, small pore throats, and are unfaulted or fractured in the injection area of review (Sneider et al., 1997; Christopher and Iliffe, 2006). Low-permeability units above the primary seal will function as secondary seals, reinforcing the effectiveness of trapping CO_2 in the ECBM sequestration system. Seal effectiveness is evaluated by integrating subsurface and structure maps for seal extent and continuity with petrophysical core data to determine seal capacity.

Candidate ECBM production coal seams require a sufficient overburden with a greater seal capacity and structural integrity than for many conventional CBM wells in order to sustain CO_2 injection rates with negligible leakage of CO_2 from the reservoir (Pashin et al., 2001). Additionally, injection of CO_2 must avoid damage of the seal by pressure-induced geomechanical deformation or by geochemical interactions. The best scenario includes both a competent overlying seal supplemented with a bottom seal underlying the storage formation, as this provides maximum CO_2 drive through the coal reservoir and ensures subsurface storage.

4 Methods

A variety of stratigraphic, structural and petrophysical techniques are used for identifying and evaluating potential seals above hydrocarbon reservoirs (Berg, 1975; Schowalter, 1979; Downey, 1984; Jennings, 1987; Vavra et al., 1992; Krushin, 1997; and Sneider et al., 1997), which can also be applied to CO_2 reservoirs or ECBM with CO_2. To provide accurate input parameters for leakage risk models, we chose to measure the porosity, permeability and other properties of a limited number of shale and sandstone samples from the ECBM interval of Virginia. For ECBM seal evaluation in the Pocahontas Basin, seal effectiveness, solution trapping availability, and potential CO_2-rock-water reactions were investigated in strata above the main CBM-producing coal beds of the Pocahontas Basin. Variations in seal thickness, structure, petrophysical seal capacity and rock mineralogy of characteristic units above CBM-producing coals in the Pocahontas Basin were also examined.

4.1 Identification of potential seals

Geologic seals in the Pocahontas Basin are determined using a number of geophysical and petrophysical tools to integrate stratigraphic and structural mapping of lithofacies with laboratory analyses of core samples. This study integrates publicly available geophysical data from approximately 4,500 wells with five borehole cores drilled in the Pocahontas Basin for coal bed methane exploration and conventional gas development (**Figure 4.4**). Geophysical log data were collected primarily from the Virginia Division of Gas and Oil and cores were donated by industry partners.

4.2 Subsurface Mapping

The extensive natural gas development in the study area provides for a dense framework of tightly-spaced borehole data for subsurface correlation of key stratigraphic horizons. Development of cross sections correlating gamma ray and bulk density values of specific sedimentary units from geophysical logs serve as a basis for regional analysis (lithology, depth, thickness, lateral extent) of the caprocks above the major CBM-producing coal beds and more regionally extensive potential sealing units, as well as defining large-scale structures, horizon depth-structure, and major unit thickness maps.

4.3 Core Analyses

Since 2004, Virginia Tech has acquired and retrieved nearly 12,000 ft (3600 m) of core from the CBM fields of southwestern Virginia. Twenty-four samples of typical facies within the CBM-producing part of the stratigraphic section were analyzed. Mercury injection capillary pressure, porosity and permeability tests, standard petrographic analyses, and electron microprobe analyses of selected samples were undertaken to better understand the pore network character and geochemistry of potential immediate seals (lithofacies above CBM-producing coal beds) and potential regional seals (marine shales) in the subsurface ECBM system.

4.3.1 Core Analyses - Standard Plug Permeability and Porosity

Twelve core samples were selected to determine porosity, grain density and permeability data representative of multiple lithofacies commonly found above CBM-producing coal beds in the subsurface mapping and cross sections. Vertically oriented sample plugs were drilled from each of the submitted samples. Plugs were dried in a humidity-controlled oven at 180° F (82° C) and an estimated net lithostatic stress of 800 psi (5515 kPa) was applied for porosity and permeability determinations at reservoir conditions. Porosity tests define the volume of available open space to the total volume of the rock by measuring helium invasion using Boyles' Law double-cell methods. From these data, grain density, the ratio of the weight of a sample to its grain volume can be measured. Permeability measurements flow air along the long axis of the plug to determine the ability of fluid movement through connected pores.

4.3.2 Petrographic Analysis

A suite of petrographic assessments were performed on core samples from the typical strata above the CBM-producing coal horizons to assess relationships between shale pore structure and sandstone mineralogy on subsurface fluid-flow properties. Twenty polished thin sections were prepared for petrographic analyses by scanning electron microscope (SEM) and optical microscopy techniques.

4.3.3 Rock Chemistry

Electron Microprobe element mapping and total organic carbon (TOC) measurements were made of selected shales to develop baseline conditions for possible CO_2 – rock interactions. Inorganic element maps of two samples were developed with the X-ray energy dispersion techniques on the electron microprobe at Virginia Tech Department of Geosciences. Total organic carbon contents of 15 samples were measured by mass loss before and after furnace combustion at 400° C (752° F) and corrected for inorganic carbon loss using a UIC Coulometer at the Kentucky Geological Survey.

4.3.4 Mercury Injection Capillary Pressure

The seal capacity of a caprock can be measured by determining its capillary entry pressure ***(Vavra et al., 1992; Krushin, 1997; and Sneider et al., 1997)***. The capillary entry pressure is the buoyancy pressure value at which a fluid will enter and leak into a seal. This entry pressure is controlled by the distribution of the largest, interconnected, continuous pore throats and is measured using mercury injection capillary pressure curves.

The maximum column height of a buoyant fluid is calculated using:

[1] $$H_{max} = \frac{P_{ds} - P_{dr}}{0.433(\rho_w - \rho_{hc})}$$ (Vavra et al., 1992)

where H_{max} = maximum hydrocarbon (or fluid) column in feet, P_{ds} and P_{dr} = displacement pressures of seal and reservoir, P_{ds} is determined from the MICP test, P_{dr} is assumed to be negligible in a dewatered, hydro-fractured coal system. $0.433(\rho_w-\rho_{hc})$ = buoyancy derived pressure between brine and gas, g/cm^3 and 0.433 is the gravitational constant. Two samples of the Hensley Shale, a regional mudstone unit considered a likely regional seal, were sent to

Weatherford-Omni Labs for mercury injection tests to determine entry and displacement pressures for maximum CO_2 gas column calculations.

5 Results

5.1 Subsurface Mapping Results

In the suite of 4500 wells, 17 key stratigraphic surfaces (coal horizons, marine flooding surfaces, unconformities) were picked using core-calibrated gamma ray and density borehole data. Multiple cross sections were constructed to correlate these surfaces across the basin (**Figure 4.5**). The Hensley Shale Member is used as a chronostratigraphic datum for stratigraphic analysis. The Hensley Shale Member was selected as an interval of interest because of its regional extent, thickness and stratigraphic position between the majority of methane-producing coal beds. A structure map on the base of the Hensley Shale (**Figure 4.6**) illustrates the general synclinal structure of the basin and the position of faults which truncate this potential regional seal. The structure shows a gently NW-dipping eastern backlimb and a western forelimb that rises abruptly at the Pine Mountain Thrust Fault. The regional thickness of the Hensley Shale ranges from 100-250 feet (30-76 m) and is thickest in parts of Dickenson and Wise Counties (**Figure 4.7**). The shale is overlain by 800-1200 ft (244-366 m) of Pennsylvanian strata, which is thickest in Wise County along the Virginia-Kentucky border (**Figure 4.8**).

5.2 Petrophysics Results

5.2.1 Porosity/Permeability

Table 4.1 shows the results of porosity and permeability lab test of core samples. This data set illustrates maximum and minimum porosity and permeability values for siliciclastic

lithologies within the Breathitt Group ECBM injection interval. Maximum permeability and porosity values are 0.0420 mD and 5.0%. Minimum permeability and porosity values are 0.0014 mD and 0.1%. Modal pore throat apertures were derived from porosity and permeability data using methods from Pittman (1992) to define a suite of micro to nano-type pore geometries with port sizes < 0.15 μm. The general trends porosity and permeability facies relationships indicate a clustering of fine-grained lithofacies with porosity values less than 0.5% and permeability values less than 0.005 mD, whereas sandstone facies have a broader range of porosity and permeability values (**Figure 4.9**), as would be expected.

5.2.2 Mercury Injection Capillary Porosimetry Results

A high-pressure mercury injection capillary porosimetry (MICP) test was conducted on a Hensley Shale sample from a depth of 1367 feet (416 m) in the Equitable 539898 core (**Figure 4.10).** Results from the MICP test on the Hensley Shale depict the relationship between Hg saturation and injection pressure (**Figure 4.11**). The pressure at 10% saturation and the shape of the curve allow for the determination and calculation of displacement pressure and pore-throat-size distribution, respectively. **Figure 4.12** displays the pore-throat-size distributions calculated from the Hg saturation/pressure chart. Pore throat radii range from < 0.0018 μm to 0.525 μm, with a median radius width of 0.260 μm, classifying its pore geometry as within the nano- to micro-port size types (Pittman, 1992).

The MICP displacement pressure results are used to quantitatively determine the seal capacity of the Hensley Shale. Using the inputs in **Table 4.2**, at a gas saturation of 10% of this seal, the Hensley Shale was determined to have a gas-water displacement pressure of 207 psi and

an estimated capacity to hold a buoyant CO_2 gas-column height of 1365 ft (416 m) or a 603 ft (184 m) column of CH_4 before pore displacement of capillary waters and seal failure.

5.3 Petrographic Results

Optical petrography determined the dominant mineralogies and porosity types for the sandstone and siltstone samples in the ECBM interval. Quartzarenite porosities are commonly formed from intragranular dissolution of framework grains. Common diagenetic cements include early, pore-lining, fine crystalline siderite followed by pore-filling, coarse, quartz overgrowths (**Figure 4.13**). Sublitharenites are rich in micaceous, metamorphic rock fragments and feldspars (**Figure 4.14, 4.15A**). The interconnected porosity is impacted by diverse cement types (e.g., quartz overgrowths, kaolinite, calcite) and compaction. Common secondary intragranular porosity is a result of the dissolution of K-feldspar framework grains (**Figure 4.15 B**). Primary intergranular pore networks are plugged by alteration and replacement of feldspars/lithic grains to kaolinite (**Figure 4.15C**). Deformation of ductile micaceous lithic grains records pervasive mechanical compaction in sublitharenites (**Figure 4.15D**) and reduced pore volume and sandstone permeability.

5.4 Scanning Electron Microscope (SEM) Results

SEM analyses of two core samples show that the Hensley Shale is a silty, claystone containing abundant, very fine silt-sized (maximum grain diameter <78μm) detrital grains of quartz (Q),feldspars (K), micas (M) and carbonaceous detritus (org), which is widely disseminated in a firmly-packed clay matrix (**Figure 4.16A, B**). Framboidal pyrite (pyr) and iron oxides are scattered throughout the silty shale as small, bright spots on the SEM. Limited

porosity development in this tightly packed microfabric may be associated with clay draping around compaction-resistant, silt-sized grains.

5.5 Geochemistry Results

Microprobe elemental mapping provides qualitative data on the principal elemental components of the Hensley Shale. Back-scatter electron data show that the major ions in the Hensley Shale are Si, Al, O, K, Mg, Fe, and Ti (**Figure 4.17A**). Microprobe wave-length-dispersive X-ray element maps of a Hensley Shale sample from drill hole EQT No.1 identify quartz silt grains (SiO_2), iron oxides (Fe-Ox) and detrital organic fragments (org), floating in a fine-grained, silicate phase of potassium and aluminum, likely illite as the dominant components (**Figure 4.17B**). An EDS map spectrum (**Figure 4.18**) confirms the presence of these minerals. Total organic contents (TOC) of selected organic-rich bands in 10 shales range from 2% to as high as 37% TOC (**Table 4.3**).

6. Discussion

6.1 Fluid-flow Properties

Several confined-sequestration systems for potential CO_2-ECBM development in the Pocahontas Basin can be defined based on geological mapping, petrological and petrophysical analyses, and seal-capacity assessments. Of these, the ~1000-3000 ft (~300-900 m) deep coal beds of Pocahontas and Bottom Creek Formation with the Hensley Shale as a principal top seal are perceived to have a very low risk for matrix leakage during CO_2 injection and storage.

The Dark Ridge and Hensley Shales are regionally continuous shales, extending beyond the areal limits of optimal ECBM reservoirs based on regional mapping and cross sections (**Figures 4.5-4.7**). Of the two shales, the Hensley is more widespread updip to the northeast (Greb et al., 2004; Bodek, 2006). The Dark Ridge Shale was not sampled for petrophysical tests in this investigation, but has similar lithology to the Hensley Shale Member.

MICP entry pressures of 15 bars for the Hensley Shale ranks the interval within the capillary barrier effectiveness of similar prodeltaic shales (Benson and Cole, 2008). Weir et al (1996) suggested that effective seals should be more than 30 ft (9 m) thick and have permeabilities <0.1 mD. The Hensley Shale is more than 100 ft (30 m) thick and has permeabilities, < 0.04 mD, so it should be an effective seal for limiting leakage risks of any CO_2 injected into underlying coal beds where it is unfractured or unfaulted. With a CO_2 seal capacity of 1365 ft (416 m) and a calculated CH_4 sealing capacity of 603 ft (184 m), the Hensley Shale would be classified as a B Type seal by Snieder (1991).

In the case of leakage through the Hensley Shale, the Alvy Creek and Grundy Formations could act as secondary seals, providing an additional 500-2500 ft (152-762 m) of multiple, stacked, low-permeability siliciclastic units above the Hensley top seal, increasing the effective thickness of the overlying confining unit (**Figure 4.8**).

Petrophysical and geochemical results of shales and sandstone samples within the Pocahontas and Bottom Creek Formations show they have low permeability so should be equally significant intra-formational seals. The sandstones sampled have very low relative permeabilities. Regionally, some quartzarenites are called “salt sands” because they contain significant brine, and therefore may have higher permeabilities than are indicated from results in

this study. These thick quartzarenites are increasingly common updip in the basin, northwest of the main CBM fields.

Organic-rich shales in the ECBM interval also have low permeabilities and may have an additional ability to adsorb any free CO_2 that may migrate from CBM reservoirs where they are thick and unfractured. The presence of organic matter should enhance the role of a roof-shale horizon as an effective secondary sink and local seal, because it should allow adsorption of CO_2. Moreover, the Pocahontas and Lee Formation coal beds are reservoirs for more than 3.58 TCF of natural gas in the basin (Milici et al., 2003), which demonstrates that the various capping lithofacies are effective seals for buoyant methane, and would likely be effective caprocks for injected CO_2.

Results from petrography, SEM, and microprobe analyses further highlight the limited potential for CO_2-rock-fluid chemical interactions in the facies sampled. Silicate minerals dominate all lithofacies and likely would have very low reactivities with increased CO_2 concentrations. Research on gaseous CO_2 – sulfide reactions suggests the breakdown of pyrite in coals and organic shales would be limited (Alymore and Lincoln, 2001). Dissolution and mineral trapping would be restricted to brief reactions between feldspars and iron-rich cements along the permeated edges of any lithologic unit encountering the injected CO_2-fluid front during its phase transition from liquid to gas. This occurs in the deepest injection intervals, where the injected CO_2 plume reaches its critical point as a liquid that then expands away from the injection well and vaporizes as it enters a lower pressure regime in the reservoir (Jack Pashin, personal communication). In a CO_2-rich fluid, feldspars may breakdown to dawsonite, trapping some of the CO_2 in the mineral structure (Pawar et al., 2006). This may cause a further decrease in the sandstone permeability, as pore throats become plugged with liberated fines. Kharaka et al.

(2006) demonstrated that the CO_2 interactions with iron oxides and siderite may mobilize Fe and Mn into reservoir fluids. Any mobilized Fe and other metals could cause potential toxicity and pipeline-scaling, so waters produced from ECBM sites in the Pocahontas basin would have to be tested and carefully managed.

6.2 Existing Pathways through Caprock and Overburden

Possible failures in the integrity of ECBM seals in the Pocahontas Basin include vertical migration of CO_2 out of the ECBM reservoirs through excessive injection fluid pressures, non-sealing faults/fractures, and existing boreholes (**Figure 4.3**). In order to obtain CO_2 injection permits for ECBM, chosen sites will need to show distribution of mapped faults and structure, have some knowledge of fracture intensity, and test the geomechanical limits (breakdown pressures) of the coal-hosting rocks and major seals (confining intervals) to demonstrate that injected CO_2 will remain in the injection reservoir(s). ECBM CO_2 injections will increase pore pressures locally around injection sites, and injection pressures will not be allowed to exceed the capillary entry pressure or hydraulic fracture pressure of the seals, or pressures that could lead to reactivation of preexisting faults.

The depth to naturally-occurring surface-connected fractures in the basin is generally considered to be 600 ft (183 m) for coal mining and shallower depths are not optimal for CBM operators (Rice and Finn, 1996; Markowski, 1998). Hence, greater depths are needed for use of CO_2 for ECBM in the basin. Most producing wells are 1800-2800 ft (549-853 m) deep, so are beneath the level of surface fractures.Additionally it will be important for the main sealing shales above the defined confined intervals (Pocahontas Formation, and Bottom Creek Formation) to be

at depths greater than 600 ft (183 m), especially where injection intervals extend across multiple coal beds.

Known faults in the region are shown in **Figure 4.1**. As these cut all seals, future ECBM with CO_2 would likely have to be away from these faults unless it could be demonstrated that the faults were sealing at the depths of injection, and the depths of the sealing interval.

Most of the producing CBM wells in the basin use hydro-fracturing treatment to enhance gas recovery. Man-made fractures will be zones of potential leakage or bypass for injected CO_2 if the fractures have propagated out of the coal beds into the surrounding rock units. Fracture height and orientation will need to be investigated locally at injection sites to optimize design for CO_2 floods and to model likely migration pathways. Primary seals will need to be above the level of hydro-fracturing prior to any CO_2 injection. This is especially important as operators have occasionally stimulated seams above these regional seals, such as the Jawbone Coal seam, increasing the local risk for leakage.

Although the maximum seal capacity estimated for the Hensley Shale is greater than the thickness of the net ECBM coal reservoirs, this capacity is static and the temporary high pressures that could be generated during injection would need to be carefully monitored to avoid damaging seal integrity. As there is no established injection pressure limit for the Pocahontas Basin, injection designs must carefully "history-match" formational break-down pressures experienced during hydraulic fracture treatments at surrounding wells. Breakdown pressures for the Pennsylvanian interval at the Russell County ECBM injection well ranged from 0.92-1.22 psi/ft. Applying this breakdown pressure range to the measured depth range of the regional Hensley Shale (800-1200 ft) suggests injection shut-in pressures will likely not be allowed to exceed ~ 750-1400 psia (5200-9600 kPa) above the base of this confining unit.

The seal capacity calculation assumes that CO_2 is in a gaseous phase with a shale–CO_2 contact angle of 0°. For those areas where coals are more than 2,000 ft (610 m) deep or at pressures in access of 1073 psi (7400 kPa), CO_2 may be injected as a super-critical liquid in the reservoir, and the contact angle with the lithologic seal may be non-zero and its capacity estimate may be reduced by 20-30%.

Additional leakage risk from existing gas wells is possible considering the dense spacing of wells in some areas. Old wells provide the most rapid potential escape path for injected CO_2 (**Figure 4.3**). More than 9,000 wells (Pennsylvanian CBM and deeper Mississippian and Devonian natural gas and oil) have been completed in the study area, and these penetrate the ECBM seals (Virginia Department of Mines Minerals and Energy, 2010). Corrosion of vintage casing cements with CO_2-enriched fluids has been demonstrated to be a leakage risk in the geological storage of carbon dioxide (IEA GHG, 2005). Other seal-penetration risks include unregulated (unmapped) exploration boreholes from coal mining, CBM core-sampling efforts, pre-regulation gas wells, and mine workings. The southwest Virginia CBM field is an active coal mining field, with active mining occurring at depths of 2200-2500 ft (671-762 m). Any future injection of CO_2 for ECBM would likely have to be away from areas of active or potential future coals that could be mined. Mine map locations, known well locations, and known completion techniques for existing wells, should be compiled into an inventory of potential leakage hazards in the area of a predicted CO_2-ECBM plume.

7 Conclusions

CO_2-ECBM provides a potential market-based method to produce revenue from coal bed methane while simultaneously reducing atmospheric greenhouse gases. An understanding of

confining seal characteristics is fundamental to determining the feasibility, design, and containment risks of CO_2-ECBM in the southwest Virginia CBM field. The geological characteristics of the lower Pennsylvanian strata surrounding CBM-producing coal beds have been effective for naturally-trapping coal bed methane, and preliminary analyses in this investigation indicate they should be favorable for confining CO_2 with ECBM.

Based on this study, it is recommended that CO_2-ECBM storage and recovery should be in the stratigraphic interval below the Hensley Shale where this confinement horizon is greater than 600 ft (183 m) below the surface and is above the level of hydrofracturing in treated CBM wells, in order to provide adequate protection against leakage into underground sources of drinking water and the atmosphere. Sites should also be away from faults and active mining areas, and should be in areas where past borehole and well locations are known, and well casing histories are well understood. Careful site selection with these parameters will allow the ECBM injection zone to be hydrologically isolated by several thick, overlying, extensive shale-seal barriers and low-matrix permeability sandstone baffles to restrict the vertical migration of CO_2, CH_4, and mobilized brine metals.

This ongoing research is performed under the direction of the Virginia Center for Coal Energy Research, as part of the Southeast Regional Carbon Sequestration Partnership Phase II: Task 10 Characterization of Potential Sites for a Large-Volume Carbon Sequestration Test in Coal Seams with Enhanced Coal Bed Methane Recovery in Central Appalachia. This project is funded by the U.S. Department of Energy through the National Energy Technology Laboratory, Subgrant No. DE-PS26-05NT42255 as supplied by the Southern States Energy Board for Regional Carbon Sequestration Partnerships - Phase II. Support also was provided by the

Department of Geosciences, Virginia Tech. Cross sections and maps were prepared using Geographix Software by Landmark. Geochemical, petrophysical and petrographic analyses were conducted by Kentucky Geological Survey, Weatherford Labs and Virginia Tech Department of Geosciences Microprobe Lab.

Figure 4.1. Regional map illustrating the distribution of Carboniferous sedimentary rocks in the Appalachian Basin (shaded region); hatched area denotes the Pocahontas Basin. Detailed map shows major structures within the Pocahontas Basin, including the Middlesboro Syncline structure of the principal study area, bounded by the Hunter Valley – Clinchport – St. Clair and Pine Mountain thrust faults. The Russell Fork Fault (bold) as well as minor Bradshaw, Coeburn and Glamorgan faults have measurable lateral and vertical displacement features (Adapted from Cecil et. al, 1985; Mitra, 1988; Henika, 1994; Ryder et al., 2008).

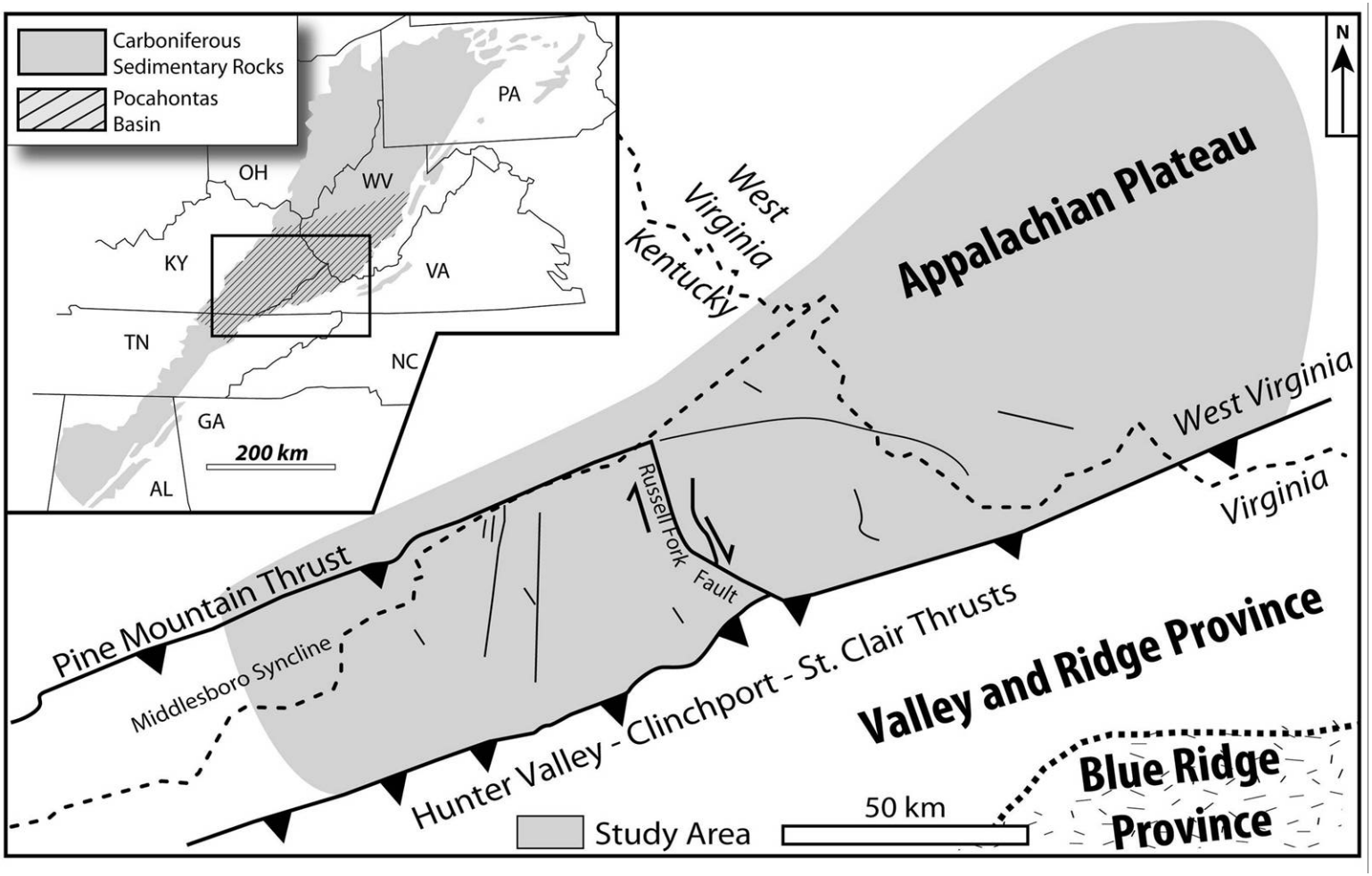
Carboniferous Sedimentary Rocks
Pocahontas Basin
PA
OH
WV
KY
VA
TN
NC
GA
AL
200 km
N
West Virginia
Kentucky
Appalachian Plateau
West Virginia
Virginia
Russell Fork Fault
Pine Mountain Thrust
Middlesboro Syncline
Hunter Valley - Clinchport - St. Clair Thrusts
Valley and Ridge Province
Blue Ridge Province
Study Area
50 km

Figure 4.2. Stratigraphic column and type logs illustrating the stratigraphic order, hydrology and typical gamma ray and bulk density (RHOB) geophysical well log responses to the lithologies of major and minor stratigraphic units of the Pennsylvanian interval of the Pocahontas Basin. Coal bed methane reservoirs for CO2 enhanced production are in the Pocahontas, Bottom Creek and Alvy Creek Formations. Well number 3042 is from Dickenson County, Virginia and gamma ray and RHOB log values increase to the right.

Stratigraphic Column and Type Logs of the Early Pennsylvanian Pocahontas Basin

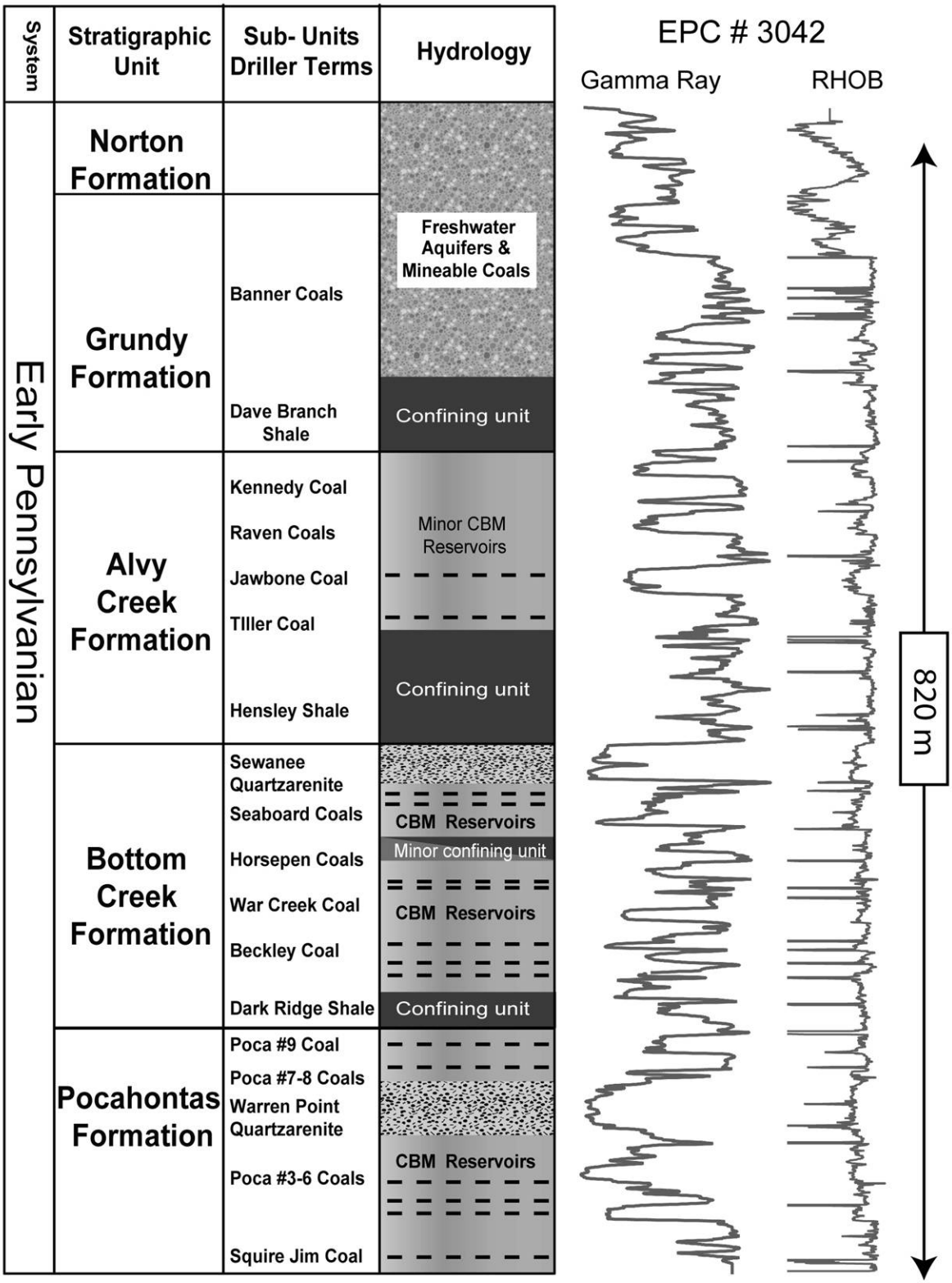

Figure 4.3. Enhanced Coal Bed Methane Sequestration System - Potential sinks for CO2 in the subsurface ECBM system include: (A) coal maceral adsorption, (B) solution trapping, and (C) mineralization. Leakage risks include (D) abandoned boreholes, (E) transmissive faults or fractures, (F) hydrodynamic surface migration and (G) injection or buoyancy pressures that exceed seal capillary pressures.

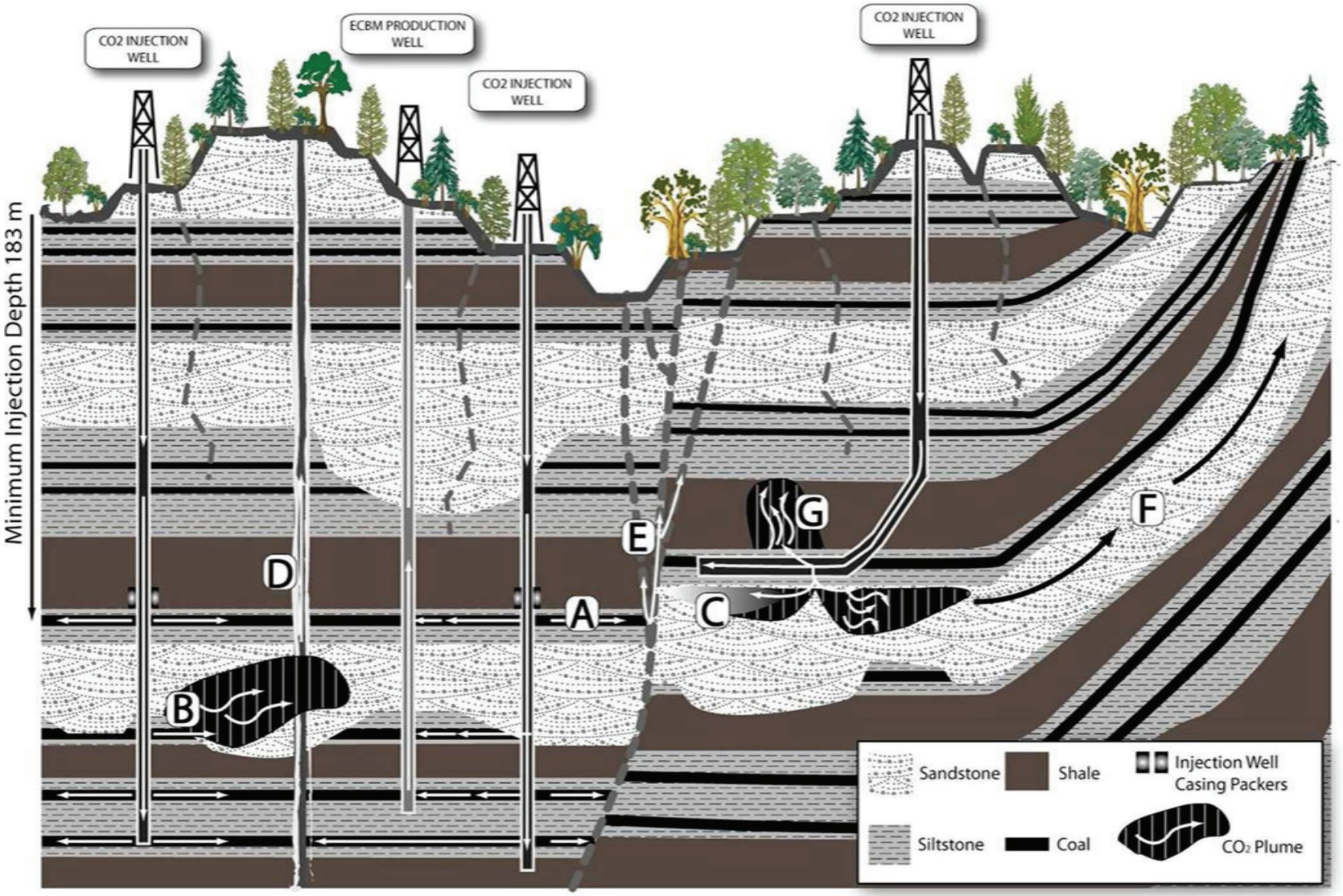
CO2 INJECTION WELL
ECBM PRODUCTION WELL
CO2 INJECTION WELL
CO2 INJECTION WELL
Minimum Injection Depth 183 m
A
B
C
D
E
F
G
Sandstone
Shale
Injection Well Casing Packers
Siltstone
Coal
CO2 Plume

Figure 4.4. Map showing the location of well logs and cores used in this study. The dashed line indicates the location of cross section A-A' of Figure 5

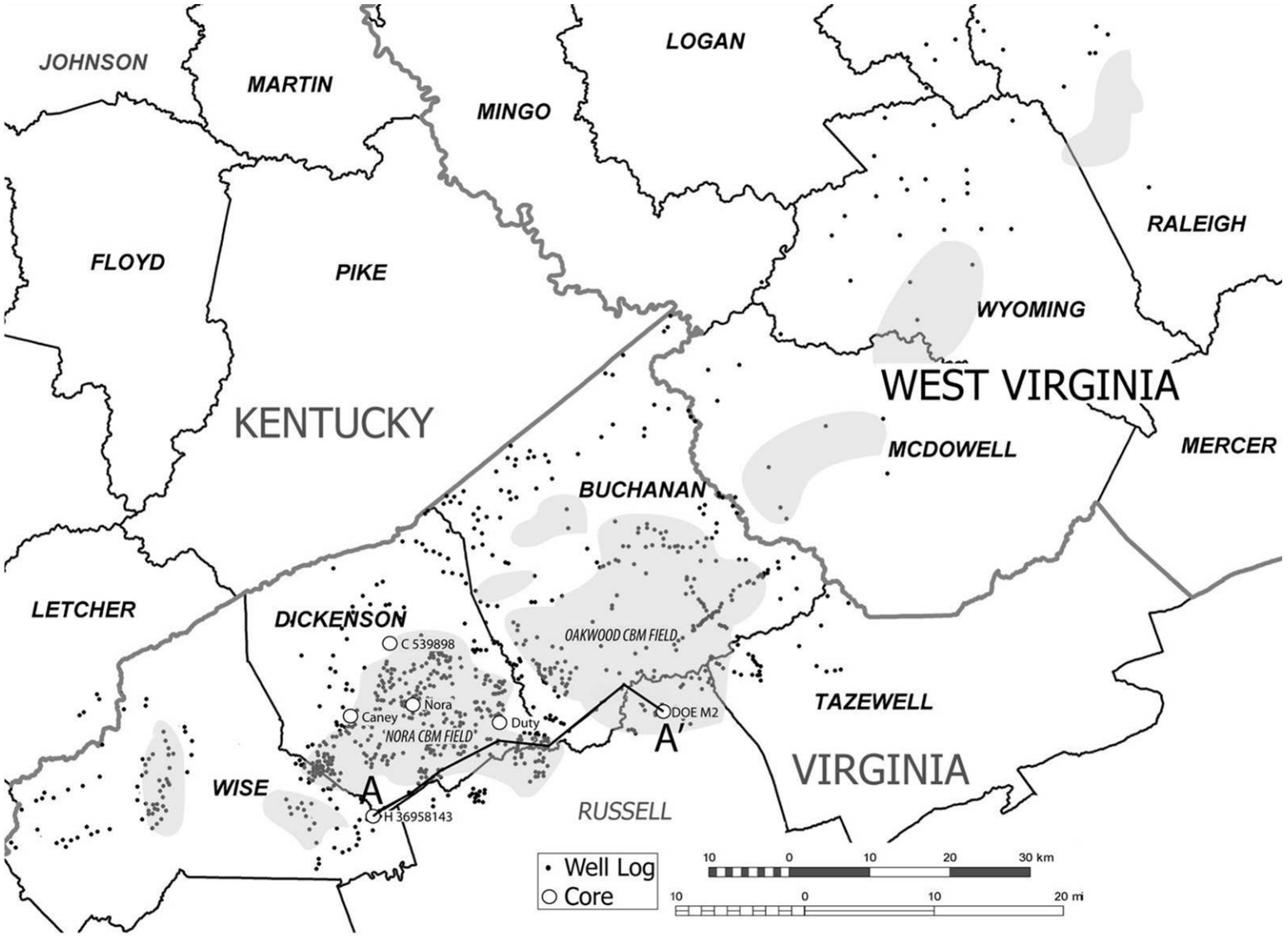
JOHNSON
MARTIN
MINGO
LOGAN
RALEIGH
FLOYD
PIKE
WYOMING
WEST VIRGINIA
KENTUCKY
MCDOWELL
MERCER
BUCHANAN
LETCHER
DICKENSON
OAKWOOD CBM FIELD
C 539898
Nora
Caney
Duty
DOE M2
TAZEWELL
'NORA CBM FIELD'
A'
A
WISE
VIRGINIA
RUSSELL
H 36958143
Well Log
Core
10 0 10 20 30 km
10 0 10 20 mi

Figure 4.5. Subsurface Cross Section A-A' from EQT Core 36958143 to DOE Core BD–114-M2. Gamma ray well log curve values increase to the right. Subsurface correlations of units between wells are based on gamma ray values, with darker tones representing increased gamma ray values of clay rich units and lighter tones for sand rich units. Major sandbodies are stippled. Cross section is stratigraphically balanced on the base of the Hensley Shale. Depth location of the samples in this study are shown as small circles. Location of cross section is shown on Figure 4.

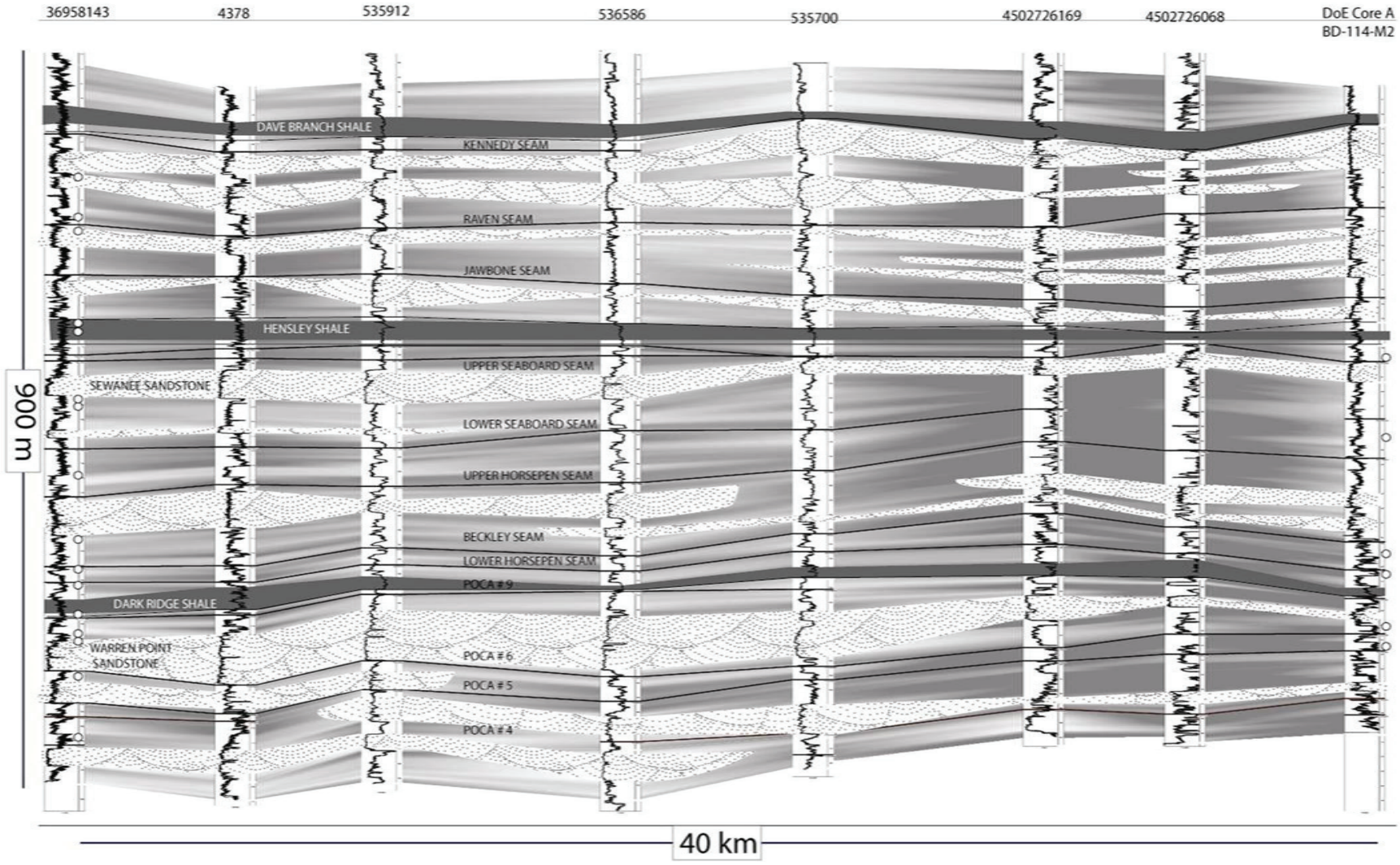
36958143
4378
535912
536586
535700
4502726169
4502726068
DoE Core A
BD-114-M2
DAVE BRANCH SHALE
KENNEDY SEAM
RAVEN SEAM
JAWBONE SEAM
HENSLEY SHALE
UPPER SEABOARD SEAM
SEWANEE SANDSTONE
LOWER SEABOARD SEAM
UPPER HORSEPEN SEAM
BECKLEY SEAM
LOWER HORSEPEN SEAM
POCA # 9
DARK RIDGE SHALE
WARREN POINT SANDSTONE
POCA # 6
POCA # 5
POCA # 4
900 m
40 km

Figure 4.6. Regional structure contour map of the base of the Hensley Shale interval. Elevations are in feet above sea level

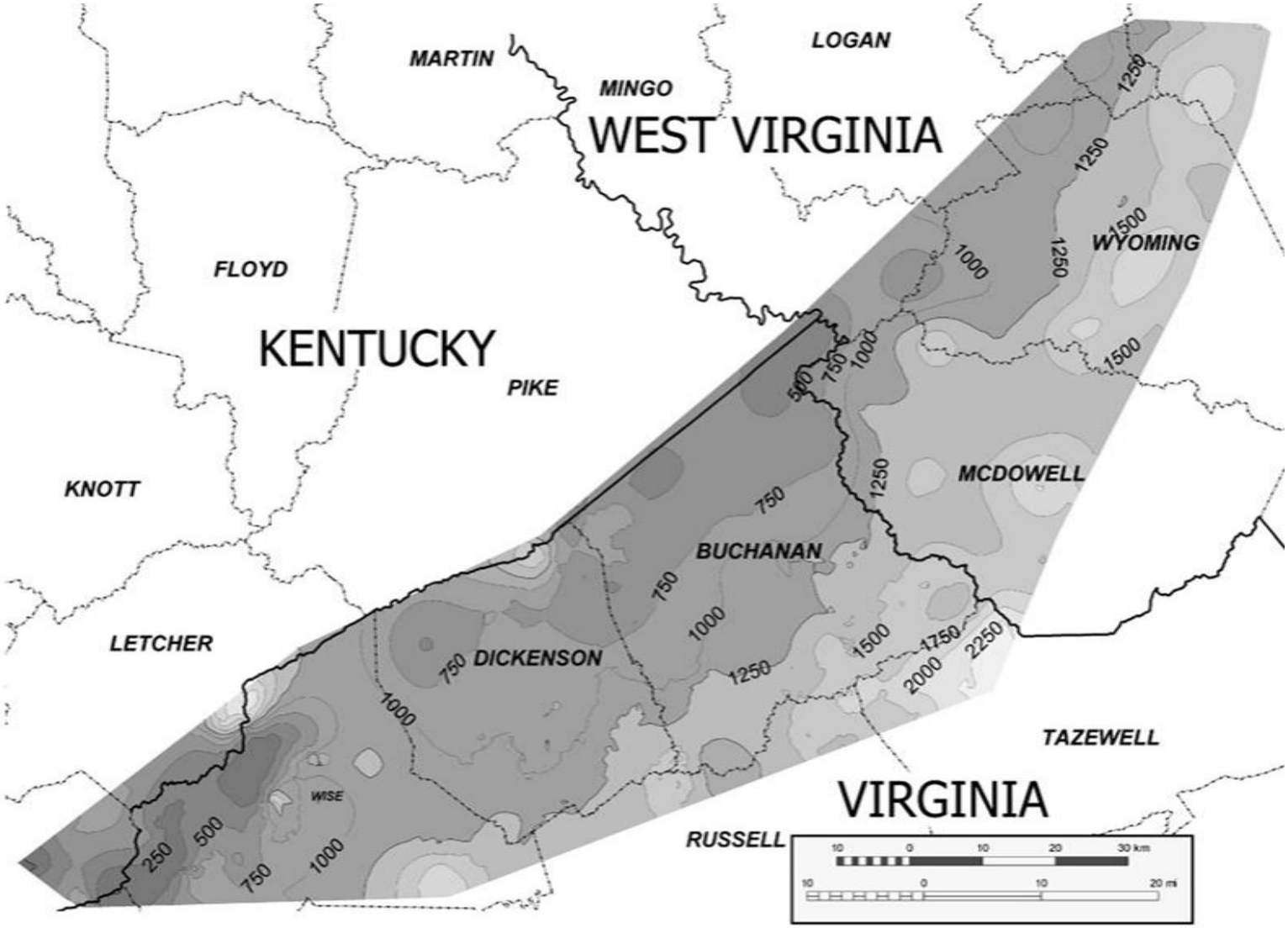
MARTIN
MINGO
LOGAN
WEST VIRGINIA
FLOYD
KENTUCKY
PIKE
WYOMING
KNOTT
MCDOWELL
BUCHANAN
LETCHER
DICKENSON
TAZEWELL
WISE
VIRGINIA
RUSSELL
250
500
750
1000
1250
1500
1750
2000
2250
10 0 10 20 30 km
10 0 10 20 mi

Figure 4.7. Regional Isopach Map of the thickness of the Hensley Shale ECBM Seal Interval. Thicknesses are in feet.

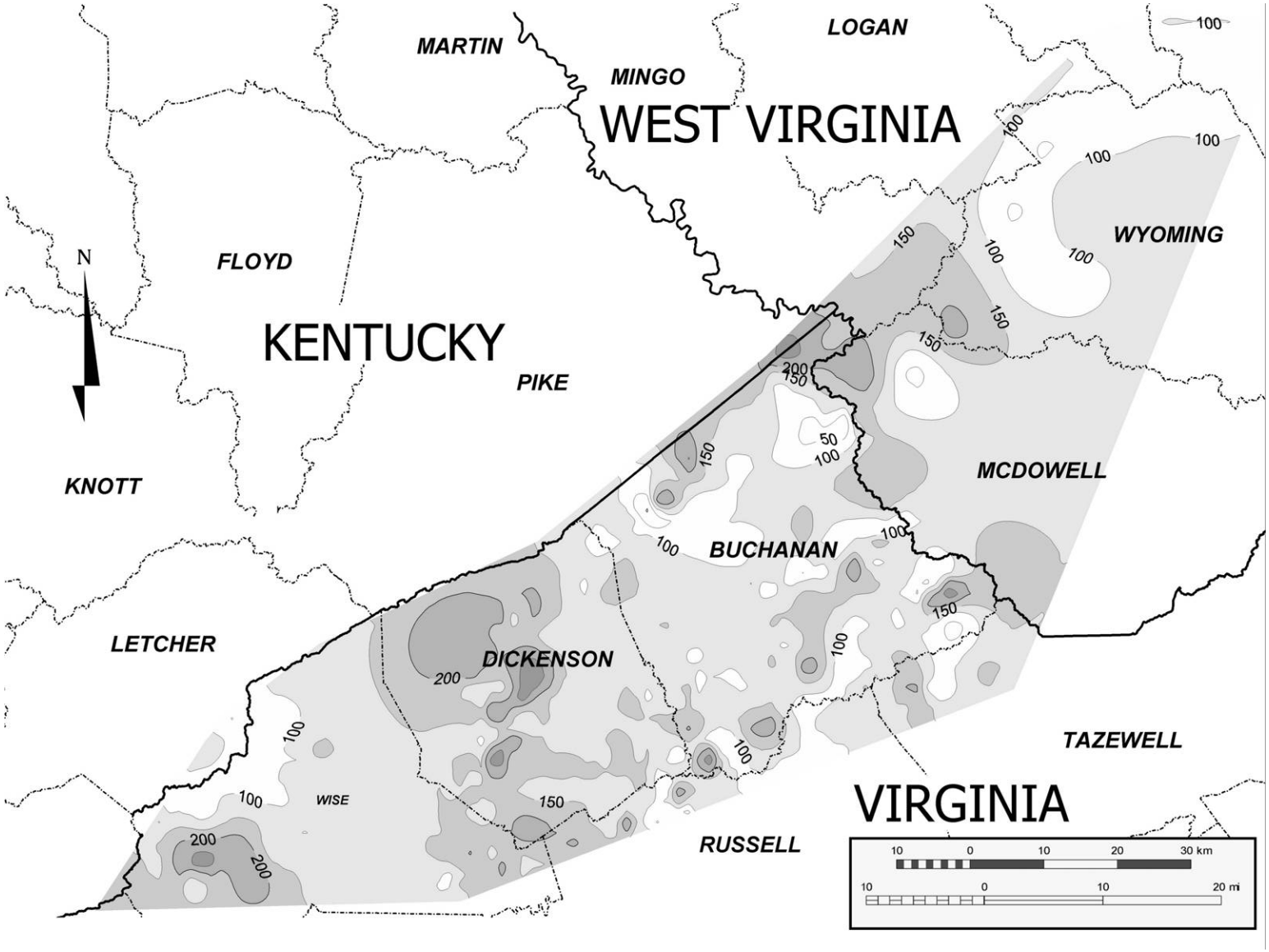
MARTIN
LOGAN
MINGO
WEST VIRGINIA
WYOMING
N
FLOYD
KENTUCKY
PIKE
KNOTT
MCDOWELL
BUCHANAN
LETCHER
DICKENSON
TAZEWELL
WISE
RUSSELL
VIRGINIA
100
150
200
50
10 0 10 20 30 km
10 0 10 20 mi

Figure 4.8. Regional thickness contour map of overburden above the Hensley Shale Member. Measured depth elevations are in feet.

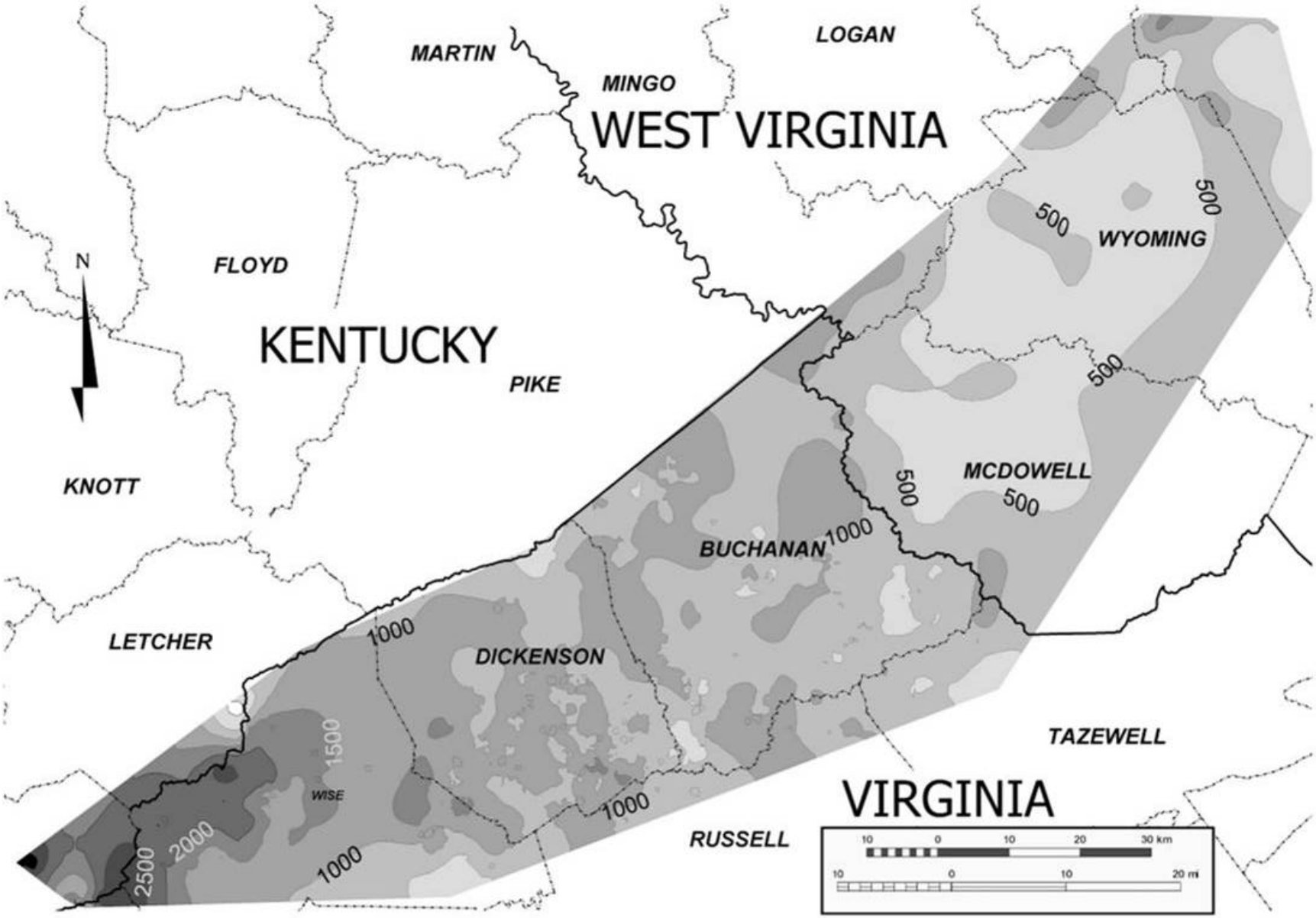
MARTIN
MINGO
LOGAN
WEST VIRGINIA
N
FLOYD
KENTUCKY
PIKE
KNOTT
LETCHER
WISE
DICKENSON
BUCHANAN
MCDOWELL
WYOMING
TAZEWELL
RUSSELL
VIRGINIA
500
1000
1500
2000
2500
10 0 10 20 30 km
10 0 10 20 mi

Figure 4.9. Cross Plot of Siliclastic Facies Relationships to Porosity & Permeability. Solid gray boxes are permeability to air values, lower case k boxes are Klinkenberg permeabilities for the same sample.

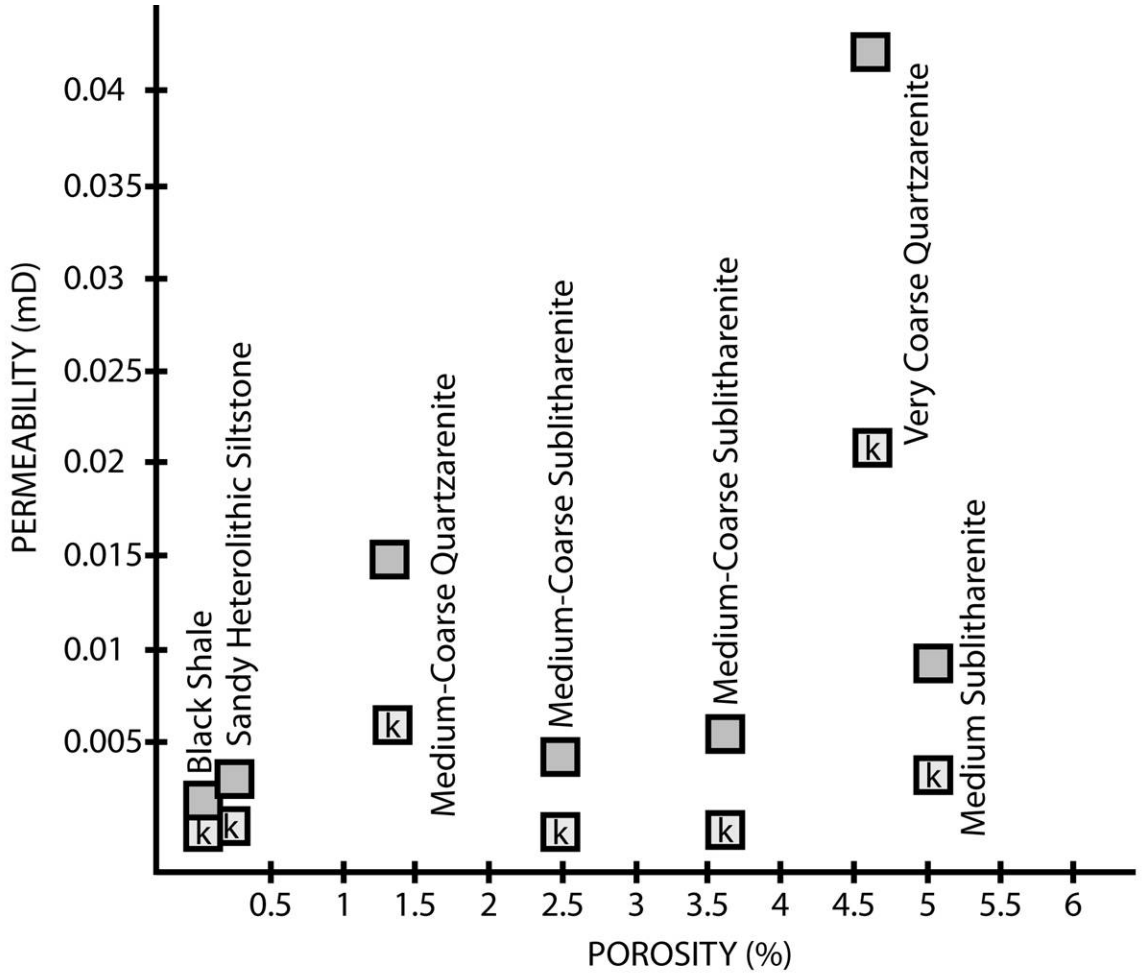
PERMEABILITY (mD)
0.04
0.035
0.03
0.025
0.02
0.015
0.01
0.005
Black Shale
Sandy Heterolithic Siltstone
Medium-Coarse Quartzarenite
Medium-Coarse Sublitharenite
Medium-Coarse Sublitharenite
Very Coarse Quartzarenite
Medium Sublitharenite
k
0.5
1
1.5
2
2.5
3
3.5
4
4.5
5
5.5
6
POROSITY (%)

Figure 4.10. Mercury Injection Capillary Porosimetry Core sample and Results Table.

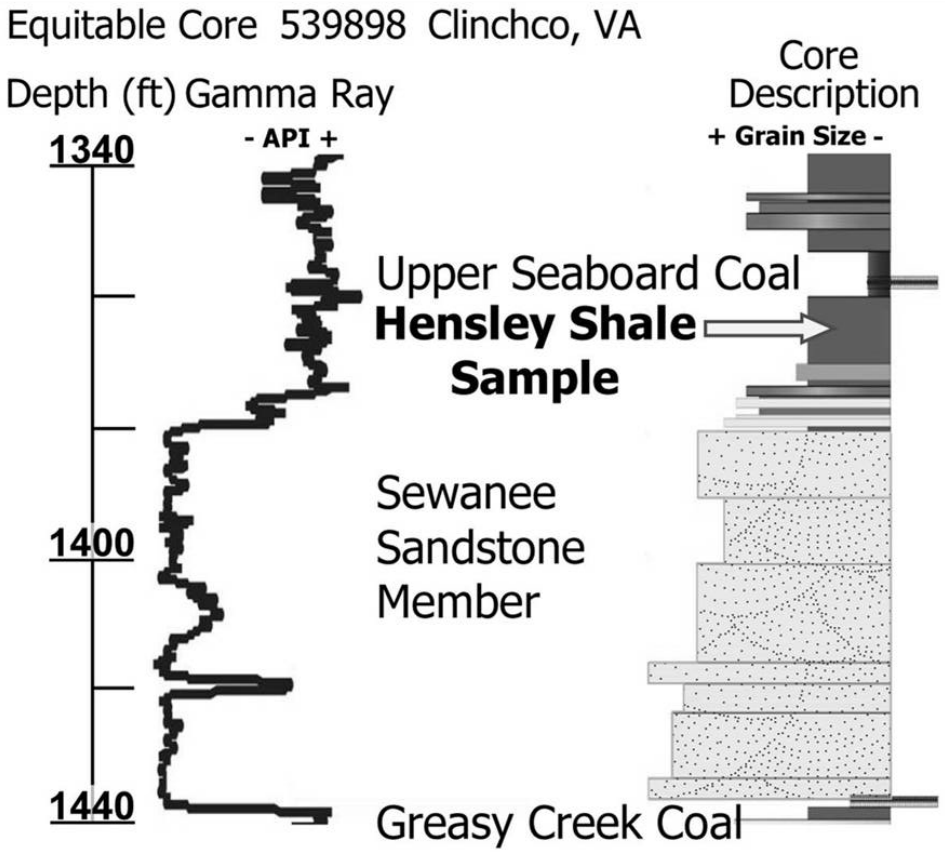

Depth (ft)	**1367**
Lithology	**Silty-Shale**
Permeability to Air (md)	**0.037**
Porosity (fraction)	**0.035**
Median Pore Throat Radius (μm)	**0.26**
Displacement Entry Pressure (psia)	**207**

Figure 4.11. Mercury Injection Capillary Pressure (MICP) Graph displays the results from the MICP test on the Hensley Shale and the relationship between Hg saturation and injection pressure. Sample from EQT Core #539898, 1367ft.

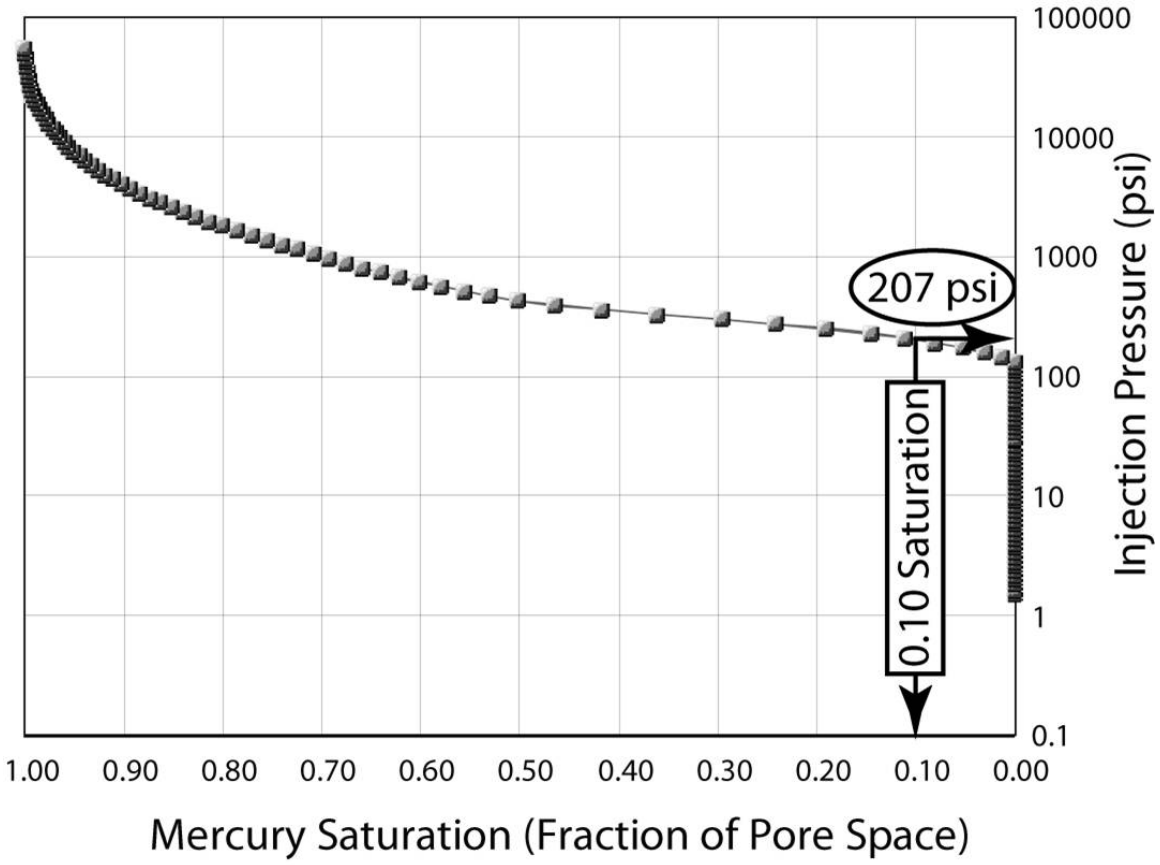
100000
10000
1000
100
10
1
0.1
Injection Pressure (psi)
207 psi
0.10 Saturation
1.00
0.90
0.80
0.70
0.60
0.50
0.40
0.30
0.20
0.10
0.00
Mercury Saturation (Fraction of Pore Space)

Figure 4.12. Pore Throat Radius Size Distribution. Radius widths range from < 0.0018 μm to 0.525 μm. The median radius width is 0.260 μm. EQT Core #539898, 1367ft.

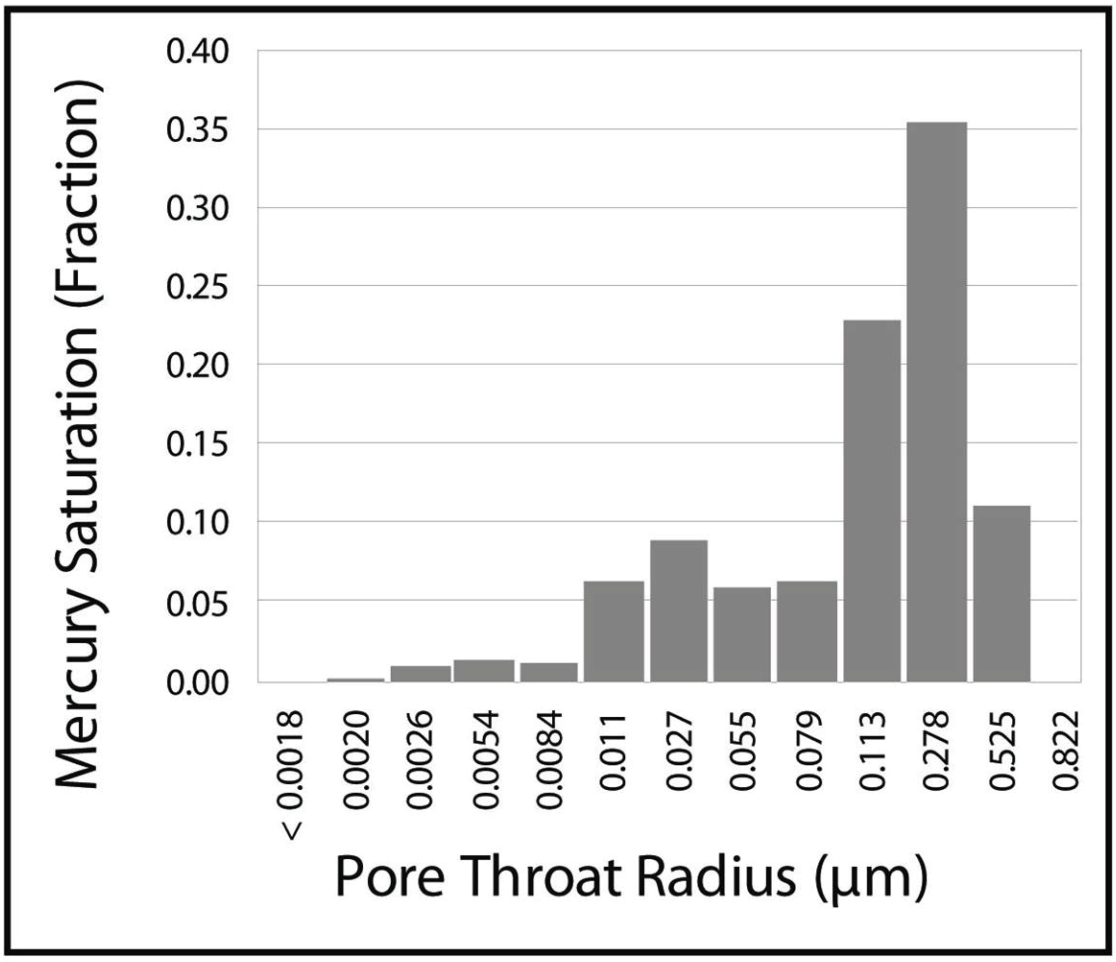
Mercury Saturation (Fraction)
0.40
0.35
0.30
0.25
0.20
0.15
0.10
0.05
0.00
< 0.0018
0.0020
0.0026
0.0054
0.0084
0.011
0.027
0.055
0.079
0.113
0.278
0.525
0.822
Pore Throat Radius (µm)

Figure 4.13. A. EQT#36958143 Borehole Gamma Ray Log Signature and Core Description for depth interval 1740-1970 ft. B. Photomicrograph of the quartzarenite sampled at 1963 ft. Quartz grains (Q) are rimmed with euhedral siderite (sid) and isolated pockets of secondary porosity (Φ). Field of view is 1mm.

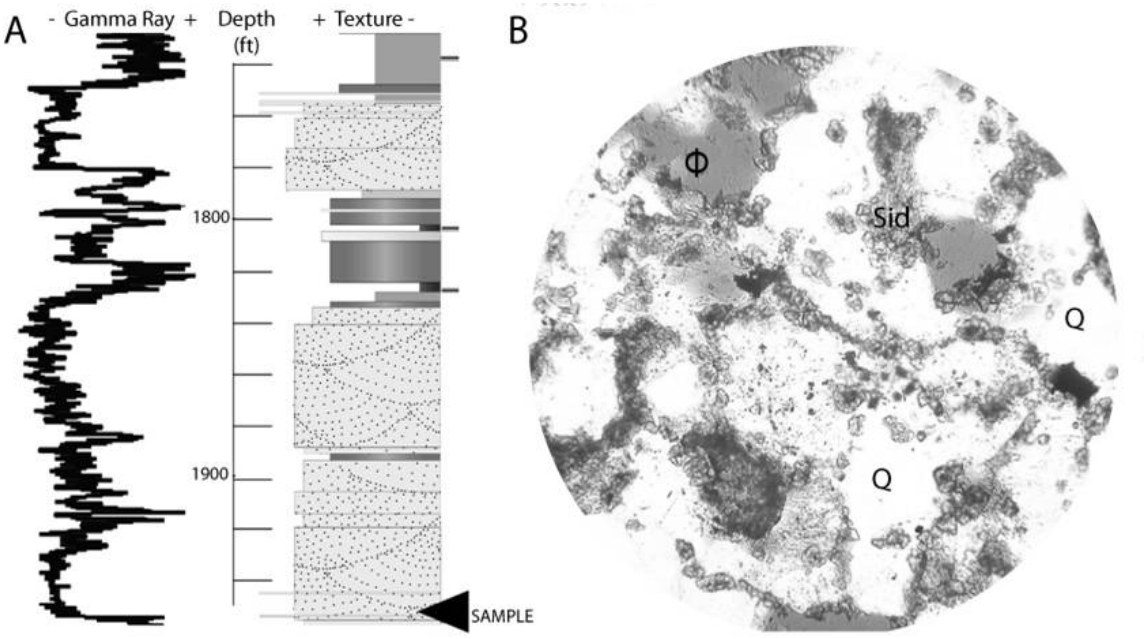
A
- Gamma Ray +
Depth
(ft)
+ Texture -
1800
1900
SAMPLE
B
Φ
Sid
Q
Q

Figure 4.14. A. EQT#36958143 Corehole Gamma Ray Log Signature and Core Description for depth interval 2140-2420 ft. B. Polarized photomicrograph of a sublitharenite sampled at 2279 ft. Mineral assemblages in sublitharenites include a tightly packed fabric of monocrystalline (Qm) and polycrystalline quartz grains (Qp) with common metamorphic rock fragments (MRF) and feldspars (K). Field of view is 1mm.

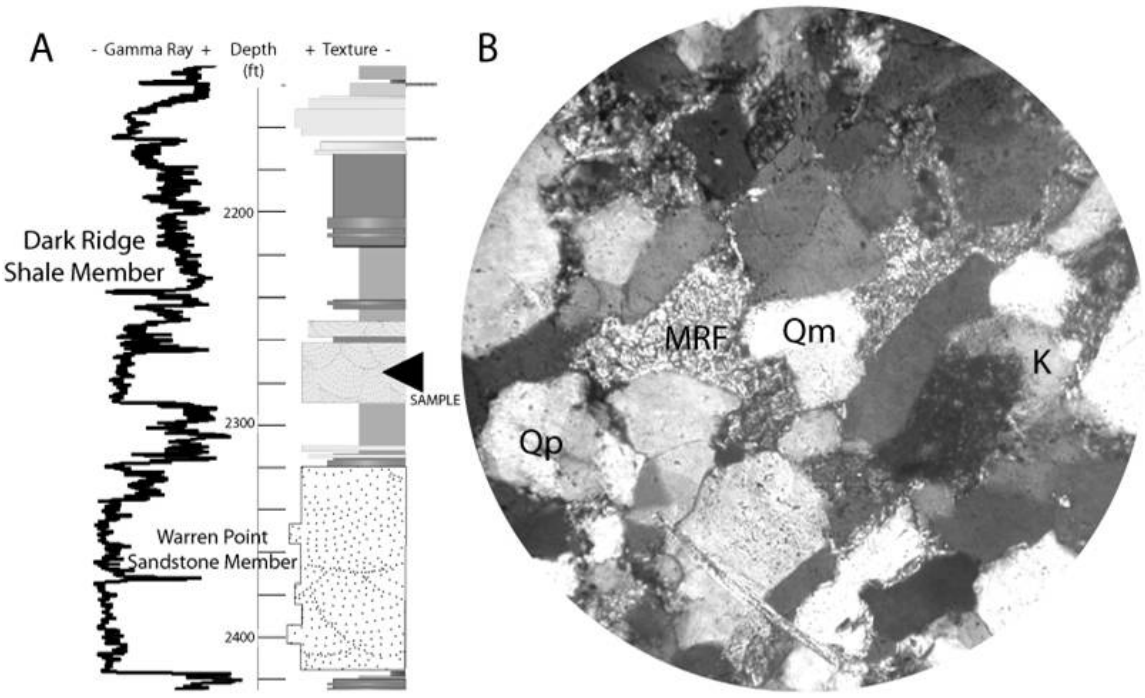
A
- Gamma Ray +
Depth (ft)
+ Texture -
2200
2300
2400
Dark Ridge Shale Member
Warren Point Sandstone Member
SAMPLE
B
MRF
Qm
K
Qp

Figure 4.15. Photomicrographs of prominent petrologic features found within Breathitt Group sandstones: A. Sublitharenite sample from core EQT #539898, 1367ft, 1517 ft with tightly packed quartz, feldspar and metamorphic rock fragments. Crossed nicols, field of view is 2 mm. B. Secondary, intragranular porosity development in sublitharenite (dark voids) after dissolution of K-feldspar. Field of view is 1 mm. C. Kaolinite replacement of unstable framework grain and microporosity development in sublitharenite from core EQT #36958143, 2726 ft. Field of view is 0.45 mm. D. Sublitharenite from core EQT #36958143, 2503 ft, displays common primary porosity destruction by compaction of ductile micaceous schist fragments. Field of view is 1 mm.

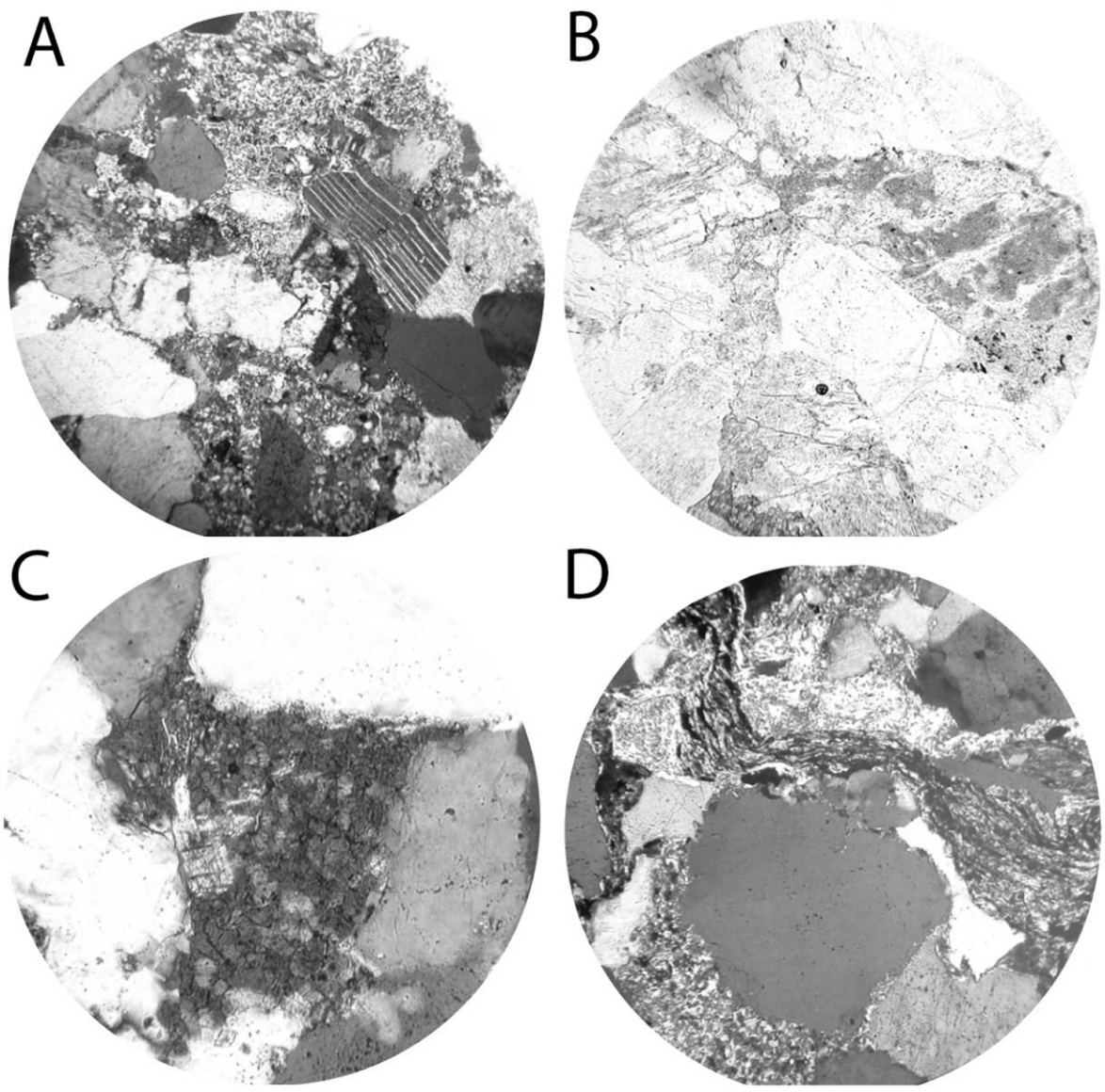
A
B
C
D

Figure 4.16. Hensley Shale Scanning Electron Microfabric Images. Sample A is from Equitable Core #36958143, 1000 ft, and B is from Equitable Core #539898, 1367ft. Dull gray fragments are quartz silt grains (Q), light gray fragments are feldspars (K), bright fragments are micas (M) with small pyrite framboids throughout (pyr). Black fragments are detrital organic fragments (org).

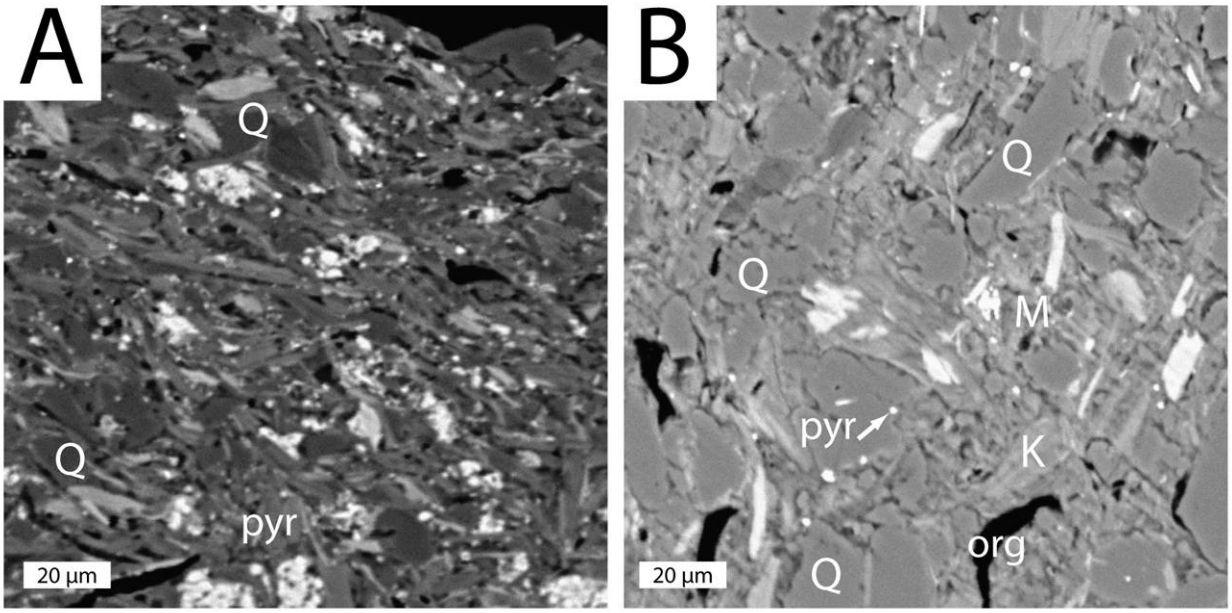
A
Q
Q
pyr
20 µm
B
Q
Q
M
pyr
K
org
Q
20 µm

Figure 4.17. A: Backscatter Electron image of the Hensley Shale, Core #36958143, 1000 ft. Dull gray fragments are quartz silt grains (Q), bright fragments are iron oxides (Fe-O) with black fragments of detrital organic fragments (org). B: Microprobe Wavelength-dispersive X-ray Element Map defines the distribution of dominant elements, O, Si, Al, Fe and Ti and resultant mineralogies.

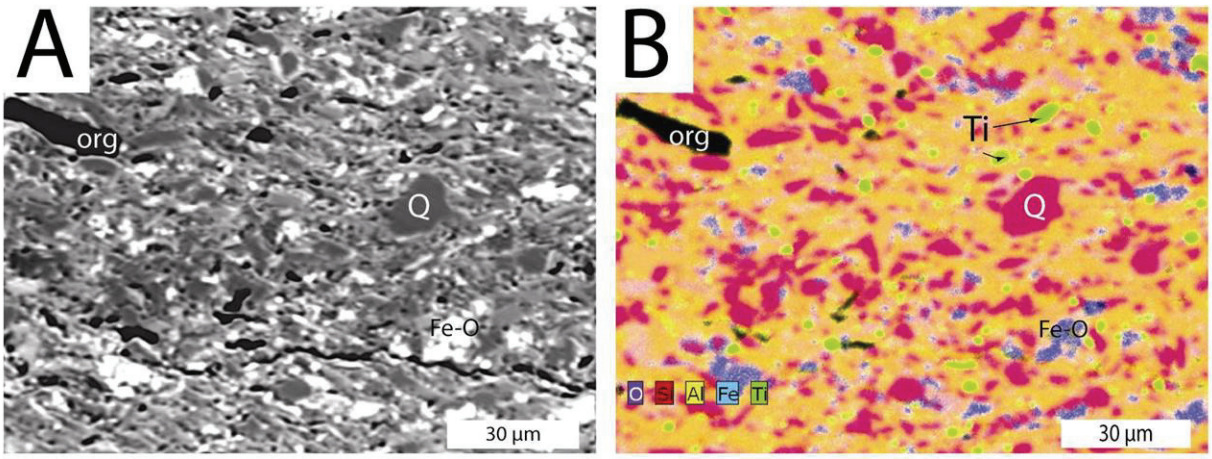
A
org
Q
Fe-O
30 µm
B
org
Ti
Q
Fe-O
O Si Al Fe Ti
30 µm

Figure 4.18. Microprobe EDS Map Spectrum – Hensley Shale sample from drill hole EQT#36958143 1000ft. Dominate elements in the energy-dispersive X-ray pattern are Si, Al, O, K, Mg, Fe and Ti, indicative of quartz, illite, iron oxides and rutile.

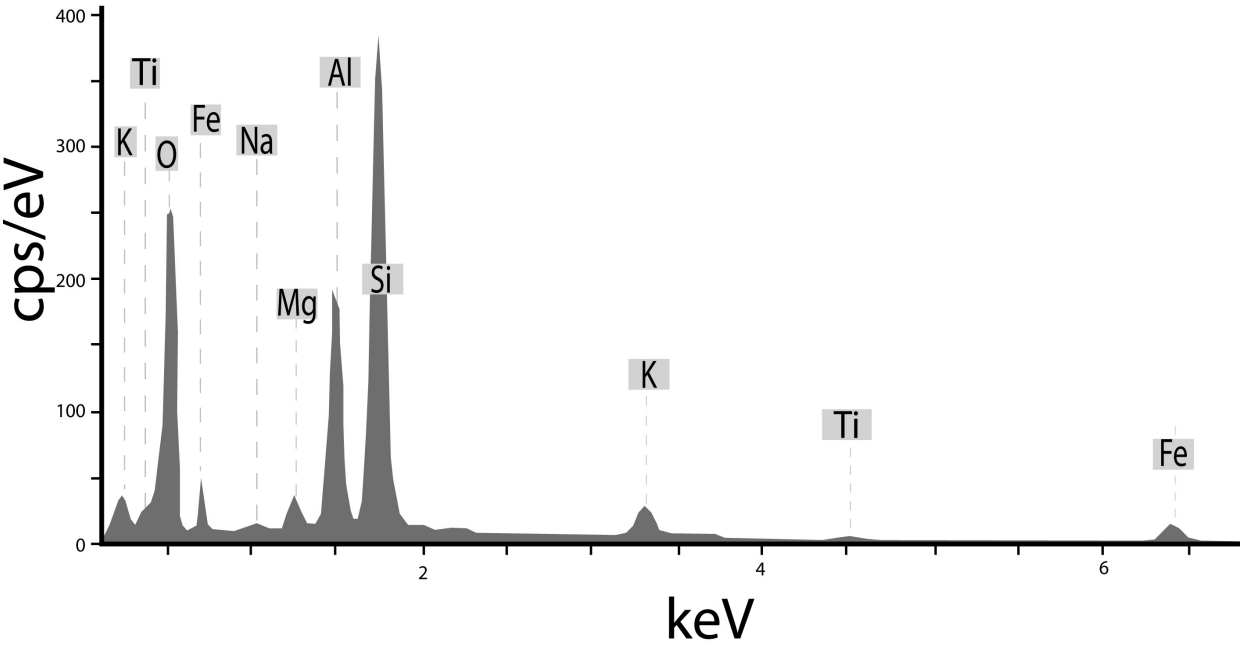
400
300
200
100
0
cps/eV
Ti
K
O
Fe
Na
Mg
Al
Si
K
Ti
Fe
2
4
6
keV

Sample ID	Permeability (millidarcys)		Porosity (%)		Grain Density (g/cc)	Lithofacies	Modal Pore Aperture (um)
	to Air	Klinkenberg	Ambient	NCS			
C1205	0.0014	0.0003	0.1	0.1	2.84	Sandy Heterolithic Siltstone	0.04
C1352	-	-	0.9	-	2.53	Dark Gray Siltstone	-
C1415	0.0150	0.0059	1.3	1.3	2.64	Med- Coarse Quartzarenite	0.1
H0900	0.0046	0.0013	2.5	2.4	2.69	Medium-Coarse Sublitharenite	0.05
H1215	0.0018	0.0004	0.1	0.1	2.71	Black Shale	0.05
H1232	0.0017	0.0003	0.1	0.1	2.72	Sandy Heterolithic Siltstone	0.05
H1484	0.0420	0.0210	4.6	4.6	2.65	Coarse Quartzarenite	0.15
H1504	-	-	1.5	-	2.69	Dark Gray Siltstone	-
H1963	0.0092	0.0032	5	5	2.71	Medium Sublitharenite	0.07
H2279	0.0064	0.0020	3.6	3.6	2.67	Medium-Coarse Sublitharenite	0.06

Table 4.1. Porosity and Permeability lab test results for siliciclastic lithologies surrounding Enhanced Coal Bed Methane target seams. Confining pressure is 800 psi. Cores samples are from near Clincho and Herald, Virginia. Depth denoted in the sample ID is in feet below surface. Permeability values for all facies are in millidarcies.

Seal Displacement Pressure (psia)	207
Reservoir Displacement Pressure (psia)	0
Density of Reservoir Water (g cm $^{-3}$)	1.05
Reservoir Injection Density of CO_2 (g cm $^{-3}$) @1800 psi, 65 deg F	0.70

Table 4.2. Input Parameters for Seal Capacity Estimation

Sample	% TOC
DOEM2 1195	7.05
DOEM2 1675	37.80
DOEM2 1875	3.68
DOEM2 1922	2.74
EQT#36958143 0857	3.44
EQT#36958143 1743	2.58
EQT#36958143 1810	4.06
EQT#36958143 2057	4.20
EQT#36958143 2115	2.16
EQT#36958143 2427	11.70

Table 4.3. Total Organic Contents of selected shales in ECBM injection intervals of the Breathitt Group from Drill Hole DOEM2 and EQT#36958143. Depths are second value in sample number.

REFERENCES

Alymore, M.G., Lincoln, F.J., 2001. , Mechanochemical milling-induced reactions between gases and sulfide minerals: II. Reactions of CO2 with arsenopyrite, pyrrhotite and pyrite, Journal of Alloys and Compounds, v.314, Issues 1-2, pp. 103-113

Archer, A.W., and Greb, S.F., 1995, An Amazon-scale drainage system in the early Pennsylvanian of central North America: The Journal of Geology, v. 103, p. 611-627.

Arkle, T., 1974, Stratigraphy of the Pennsylvanian and Permian systems of the central Appalachians, in G. Briggs, ed., Carboniferous of the southeastern United States: Geological Society of America Special Paper 148, p. 5-30.

Benson, S.M., and Cole, D.R., 2008, CO2 Sequestration in Deep Sedimentary Formations: Elements, v. 4, p. 325-331.

Berg, R. R., 1975, Capillary pressures in stratigraphic traps: AAPG Bulletin, v. 59, p. 939-956.

Blake, B.M., and Beuthin, J.D., 2008, Deciphering the mid-Carboniferous eustatic event in the central Appalachian foreland basin, southern West Virginia, USA: Resolving the Late Paleozoic Ice Age in Time and Space, v. 441, p. 249-260.

Blakey, R., 2005, North American Paleogeography, Late Pennsylvanian (300 Ma.) Paleogeography and Geologic Evolution of North America, http://jan.ucc.nau.edu/~rcb7/namPP300.jpg, accessed April, 2010.

Bodek, R.J., 2006, Sequence stratigraphic architecture of early Pennsylvanian, coal-bearing strata of the Cumberland Block a case study from Dickenson County, Virginia: Blacksburg, Va., University Libraries, Virginia Polytechnic Institute and State University.

Cecil, C.B., Stanton, R.W., Neuzil, S.G., Dulong, F.T., Ruppert, L.F., and Pierce, B.S., 1985, Paleoclimate Controls on Late Paleozoic Sedimentation and Peat Formation in the Central Appalachian Basin (USA): International Journal of Coal Geology, v. 5, p. 195-230.

Chesnut, D.R., Jr., 1992, Stratigraphic and structural framework of the Carboniferous rocks of the central Appalachian Basin in Kentucky: Kentucky Geological Survey, ser. 11, Bulletin 3, 42 p

Chesnut, D.R., Jr., 1994, Eustatic and tectonic control of deposition of the Lower and Middle Pennsylvanian strata of the Central Appalachian Basin: Concepts in Sedimentology and Paleontology, v. 4, p. 51-64.

Christopher, C.A. and Iliffe, J. 2006, Reservoir Seals: How they work and how to choose a good one. Proceedings, CO2SC Symposium, Lawerence Berkeley National Laboratory, Berkeley, California, March 20-22, 2006.

Cook P. 2006, Site Characterization for CO2 Geological Storage. International Symposium on Site Characterization for CO2 Geological Storage - CO2SC., 20-22 March 2006., Berkeley, CA, USA.

Conrad, J.M., Miller, M.J., Phillips, J., Ripepi, N. 2006, Characterization of Central Appalachian Basin CBM Development: Potential for Carbon Sequestration and Enhanced CBM Recovery," 2*006 International Coal bed Methane Symposium*, Preprint 0625, Tuscaloosa, AL

Diamond, W. P., LaScola, J. C., and Hyman, D. M., 1986, Results of direct-method determination of the gas content of U.S. coal beds: U.S. Department of Interior, Bureau of Mines, Information Circular 9067, 95 p.

Downey, M. W., 1984, Evaluating seals for hydrocarbon accumulations: AAPG Bulletin, v. 68, p.1752-1763.

Englund, K.J., Arndt, H.H., and Henry, T.W., 1979, Proposed Pennsylvanian system stratotype, Virginia and West Virginia: [Falls Church, Va., American Geological Institute], vi, 136 p. p.

Englund, K.J., and Thomas, R.E., 1990, Late Paleozoic depositional trends in the central Appalachian Basin: U. S. Geological Survey Bulletin, Report: B.

Englund, K.J., Windolph, J.F., Jr., and Thomas, R.E., 1986, Origin of thick, low-sulphur coal in the Lower Pennsylvanian Pocahontas Formation, Virginia and West Virginia: Special Paper Geological Society of America, v. 210, p. 49-61.

Ettensohn, F.R., 2004, Modeling the nature and development of major Paleozoic clastic wedges in the Appalachian Basin, USA: Journal of Geodynamics, v. 37, p. 657-681.

Gale, J., and Freund, P., 2001, Coal-bed methane enhancement with CO2 sequestration worldwide potential: Environmental Geosciences, v. 8, p. 210.

Gluskoter, H., Stanton, R.W., Flores, R.M., and Warwick, P.D., 2002, Adsorption of carbon dioxide and methane in low-rank coals and the potential for sequestration of carbon dioxide: Environmental Geosciences, v. 9, no. 3, p. 160-161.

Greb, S.F., Eble, C.F., Hower, J.C., and Andrews, W.M., 2002, Multiple-bench architecture and interpretations of original mire phases - Examples from the Middle Pennsylvanian of the Central Appalachian Basin, USA: International Journal of Coal Geology, v. 49, p. 147-175.

Greb, S.F., Chesnut Jr, D.R., and Eble, C.F., 2004, Temporal changes in coal-bearing depositional sequences (Lower and Middle Pennsylvanian) of the central Appalachian Basin, USA: Coal-bearing strata: Sequence stratigraphy, paleoclimate, and tectonics of coal-bearing strata: American Association of Petroleum Geologists, Studies in Geology, v. 51, p. 89–120.

Henika, W. S., 1994, Internal structure of the coal bearing portion of the Cumberland Overthrust Block in Southwestern Virginia and adjoining areas, in Geology and Mineral Resources of the Southwestern Virginia Coalfield, Virginia Division of Mineral Resources Publication 131, p.100-120.

Hovorka, S.D. 1999. Optimal geological environments for carbon dioxide disposal in saline aquifers in the United States. Bureau of Economic Geology Report for DOE, 55 p.

IEA GHG (International Energy Agency Greenhouse Gas R&D Programme), 2005, Report on Wellbore Integrity Workshop, Houston: http://www.co2captureandstorage.info/docs/wbifinalreport.pdf (accessed May 2010).

Jennings, J. J., 1987, Capillary pressure techniques: application to exploration and development geology,:AAPG Bulletin, v. 71, p.1196-1209.

Kelafant, J.R., Boyer, C.M., 1988, A geologic assessment of natural gas from coal seams in the central Appalachian basin. Topical Report (January 1988–November 1988) prepared under Contract No. 5084-214-1066. Gas Research Institute, Chicago, IL, 66 pp.

Kharaka, Y.K., Cole, D.R., Hovorka, S.D., Gunter, W.D., Knauss, K.G., Freifeld, B.M., 2006, Gas-water-rock interactions in Frio Formation following CO_2 injection: Implications for the storage of greenhouse gases in sedimentary basins: Geology, v. 34, p. 577 -580.

Koperna G.J. and Riestenberg, D.E., 2009, Carbon Dioxide Enhanced Coal bed Methane and Storage: Is There Promise? Advanced Resources International, SPE International Conference on CO2 Capture, Storage and Utilization. 2-4 November 2009., San Diego California, USA.

Korus, J.T., 2002, The lower Pennsylvanian New River Formation a nonmarine record of glacioeustasy in a foreland basin: Blacksburg, Va., University Libraries, Virginia Polytechnic Institute and State University.

Krushin, J. T., 1997, Seal capacity of non-smectite shale, in R. C. Surdam, ed., Seals, traps, and the petroleum system: AAPG Memoir 67, p. 31-67.

Loomis, I., 1997, Experiments concerning the Commercial Extraction of Methane from Coal bed Reservoirs, Ph.D. Dissertation, Virginia Polytechinic Institute and State University, Blacksburg, VA

Lyons, P.C. 1998. The central and northern Appalachian Basin—a frontier region for coal bed methane development. International Journal of Coal Geology, v. 38 p. 61–87

Markowski, A. K., 1998, Coal bed methane resource potential and current prospects in Pennsylvania: International Journal of Coal Geology, v. 38, p. 137-159.

Martino, R.L. 1996, Stratigraphy and depositional environments of the Kanawha Formation (Middle Pennsylvanian), southern West Virginia, U.S.A. International Journal of Coal Geology, v. 31, p. 217-248.

Mastalerz, M., Gluskoter, H., and Rupp, J., 2004, Carbon dioxide and methane sorption in high volatile bituminous coals from Indiana, USA: International Journal of Coal Geology, v. 60, p. 43-55.

Mavor M. J., Gunter, W.D., Robinson, J.R., Law, D.H.S., Gale, J., 2002, Testing for CO2 Sequestration and Enhanced Methane Production from Coal, IEA Greenhouse Gas R&D Programme Source Society of Petroleum Engineers Gas Technology Symposium, 30 April-2 May 2002, Calgary, Alberta, Canada.

Milici, R.C., Ryder, R.T., Swezey, C.S., Charpentier, R.R., Cook, T.A., Crovelli, R.A., Klett, T.R., Pollastro, R.M., and Schenk, C.J., 2003, Assessment of Undiscovered Oil and Gas Resources of the Appalachian Basin Province, 2002**:** U.S. Geological Survey Fact Sheet FS-009-03, 4 p.

Nelson, C.R. Steadman E.N. and Harju, J.A., 2005, Geologic CO_2 sequestration potential of the Wyodak-Anderson coal zone in the Powder River Basin, Plains CO2 Reduction (PCOR) Partnership Topical Report for U.S. Department of Energy; Energy and Environmental Research Center: University of North Dakota.

Nolde, J.E., Spears, D. 1998. A preliminary assessment of in place coal bed methane resources in the Virginia portion of the central Appalachian Basin, International Journal of Coal Geology, v. 38 p.115–136

Pacala, S., and Socolow, R., 2004, Stabilization wedges: Solving the climate problem for the next 50 years with current technologies: Science, v. 305, p. 968-972.

Pashin., J.C., Groshong Jr., R.H., Carroll, R.E., 2001, Enhanced Coal bed Methane Recovery Through Sequestration of. Carbon Dioxide: Potential for a Market-Based Environmental. Solution in the Black Warrior Basin of Alabama.

Pawar, R.J., Warpinski, N.R., Lorenz, J.C., Benson, R.D., Grigg, R.B., Stubbs, B.A., Stauffer, P.H., Krumhansl, J.L., Cooper, S.P., Svec, R.K., 2006, Overview of a CO2 sequestration field test in the West Pearl Queen reservoir, New Mexico. Environmental Geosciences. v. 13, p. 163–180

Pittman, E.D. 1992, Relationship of Porosity and Permeability to Various Parameters Derived from Mercury Injection-Capillary Pressure Curves for Sandstone. Bull. American Association of Petroleum Geologists, 76, 191-198.

Quinlan, G.M., and Beaumont, C., 1984, Appalachian Thrusting, Lithospheric Flexure, and the Paleozoic Stratigraphy of the Eastern Interior of North-America: Canadian Journal of Earth Sciences, v. 21, p. 973-996.

Reichle, D., Houghton, J., Kane, B., Ekmann, J., Benson, S., Clarke, J., Dahlman, R., Hendrey, G., Herzog, H., and Hunter-Cevera, J., 1999, Carbon Sequestration, State of the Science: US Department of Energy, Office of Science, Office of Fossil Energy, Washington 1999.

Rice, C.L., and Schwietering, J.F., 1988, Fluvial deposition in the Central Appalachians during the Early Pennsylvanian: U. S. Geological Survey Bulletin, Report: B.

Rice, C.L., 1985, Terrestrial Vs Marine Depositional Model - a New Assessment of Subsurface Lower Pennsylvanian Rocks of Southwestern Virginia: Geology, v. 13, p. 786-789.

Rice, C.L., and Schwietering, J.F., 1988, Fluvial deposition in the Central Appalachians during the Early Pennsylvanian: U. S. Geological Survey Bulletin, Report: B

Rice, D.D., Finn, T.M., 1996, Geologic framework and description of coal bed gas plays: Appalachian basin province. In: Gautier, D.L., Dolton, G.L., Takahaski, K.I., Varnes, K.L. (Eds.), 1995 National Assessment of United States Oil and Gas Resources — Results, Methodology, and Supporting Data, U.S. Geological Survey Digital Data Series DDS-30, CD-ROM, Denver, CO, 134 pp.

Ripepi, N.S., 2009, Carbon dioxide storage in coal seams with enhanced coal bed methane recovery geologic evaluation, capacity assessment and field validation of the Central Appalachian Basin: Blacksburg, Va.:, University Libraries, Virginia Polytechnic Institute and State University.

Rodvelt , G.D., Moyers, W.L., Malamisura, P.R., Hagy, C.W., Greer, S. 2009, Recompletions in a Virginia Coal bed-Methane Field Yield Additional Gas, SPE Eastern Regional Meeting, 23-25 September 2009, Charleston, West Virginia, USA

Showalter, T. T., 1979, Mechanics of secondary hydrocarbon migration and entrapment: AAPG Bulletin, v. 63, p. 723-760.

Sneider, R.M., J.S. Sneider, G.W. Bolger, and J.W. Neasham, 1997, Comparison of seal capacity determinations: conventional cores vs. cuttings, in R.C. Surdam, ed., Seals, traps, and the petroleum system: AAPG Memoir 67, p. 1–12.

Sneider,R.M.,1991, Evaluation of reservoirs and seals– Amer. Assoc Petroleum Geol .Education Dept. Short Course Notes. Midland, TX. 347pp

United States Department of Energy - Energy Information Administration 2009, *Coal bed Methane Proved Reserves*, , accessed August 15, 2010: http://www.eia.gov/dnav/ng/ng_enr_coalbed_s1_a.htm

United States Department of Energy - National Energy Technology Laboratory, 2008a, Carbon Sequestration Atlas of the United States and Canada - Atlas II. http://www.netl.doe.gov/technologies/carbon_seq/refshelf/atlas/index.html, (accessed May 17, 2010).

United States Department of Energy - National Energy Technology Laboratory, 2008b, Phase II CO_2 Sequestration in Coal Seams Factsheet - Central Appalachian Coal Seam Project <http://www.netl.doe.gov/publications/proceedings/08/rcsp/factsheets/5-SECARB_Central%20Appalachian_Coal.pdf >Accessed August 15, 2010.

Vavra, C. L., J. G. Kaldi, and R. M. Sneider, 1992, Geological applications of capillary pressure: a review: AAPG Bulletin, v. 76, p.840-850.

Virginia Department of Mines Minerals and Energy, Division of Gas and Oil, http://www.dmme.virginia.gov/dgoinquiry/, accessed May 17, 2010).

Virginia Department of Mines, Minerals and Energy, 2009. Gas and Oil Production Statistics. http://www.dmme.virginia.gov/DGO/Production/gasoilproductionstats.shtml , accessed August 13, 2010.

Weir, G. J., White, S. P., and Kissling, W. M., 1996, Reservoir storage and containment of greenhouse gases, Transport in Porous Media, v. 23, p. 37−60

Wong, S., Gunter, B., 1999. Testing CO2-Enhanced Coal bed Methane Recovery. Greenhouse Issues, v. 45.

Zuber, M.D. 1998. Production characteristics and reservoir analysis of coal bed methane reservoirs. International Journal of Coal Geology, v. 38, p.27–45

APPENDIX - SUPPLEMENTARY CROSS SECTIONS

Cross-section A-A’

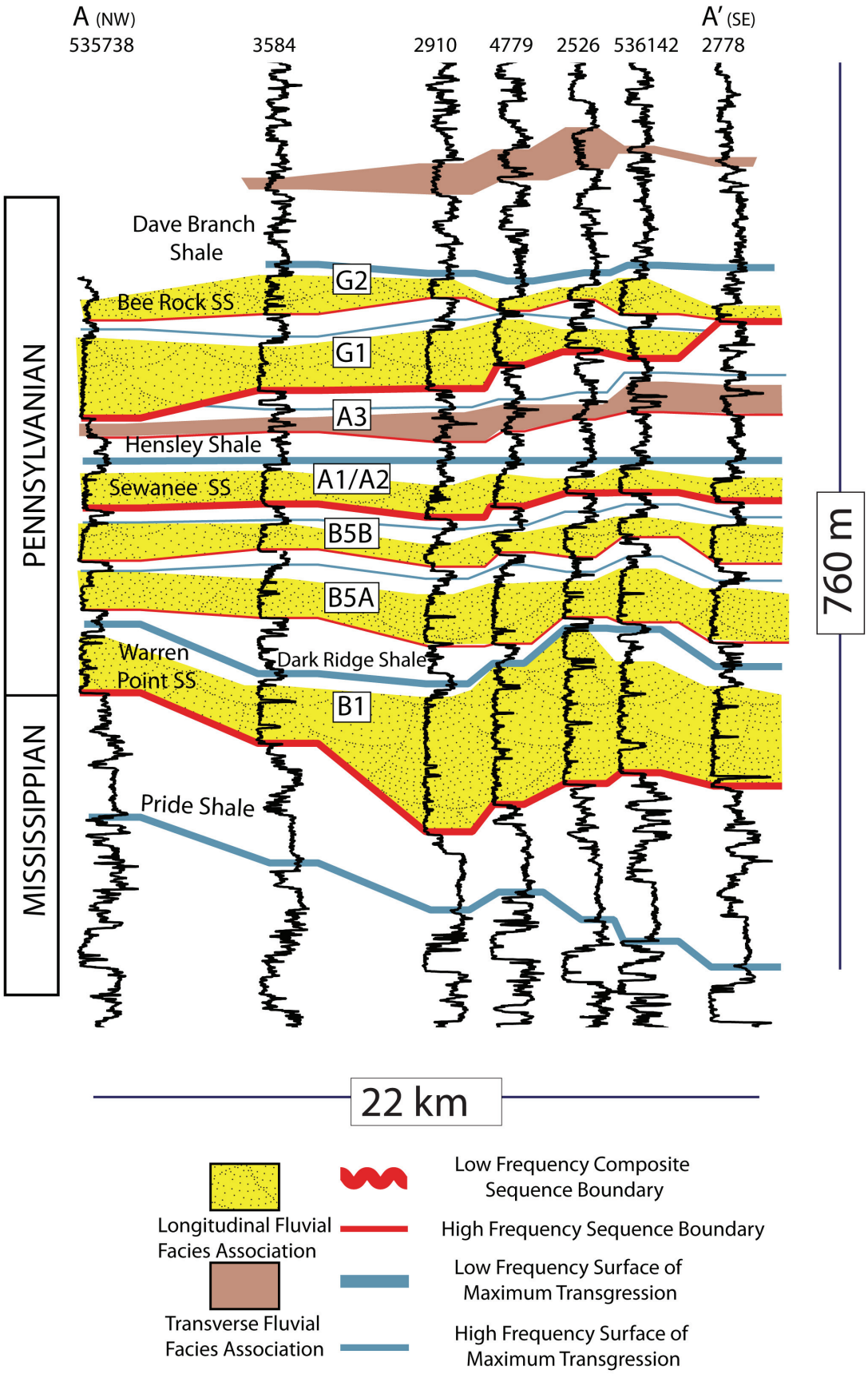

Cross-section B-B’

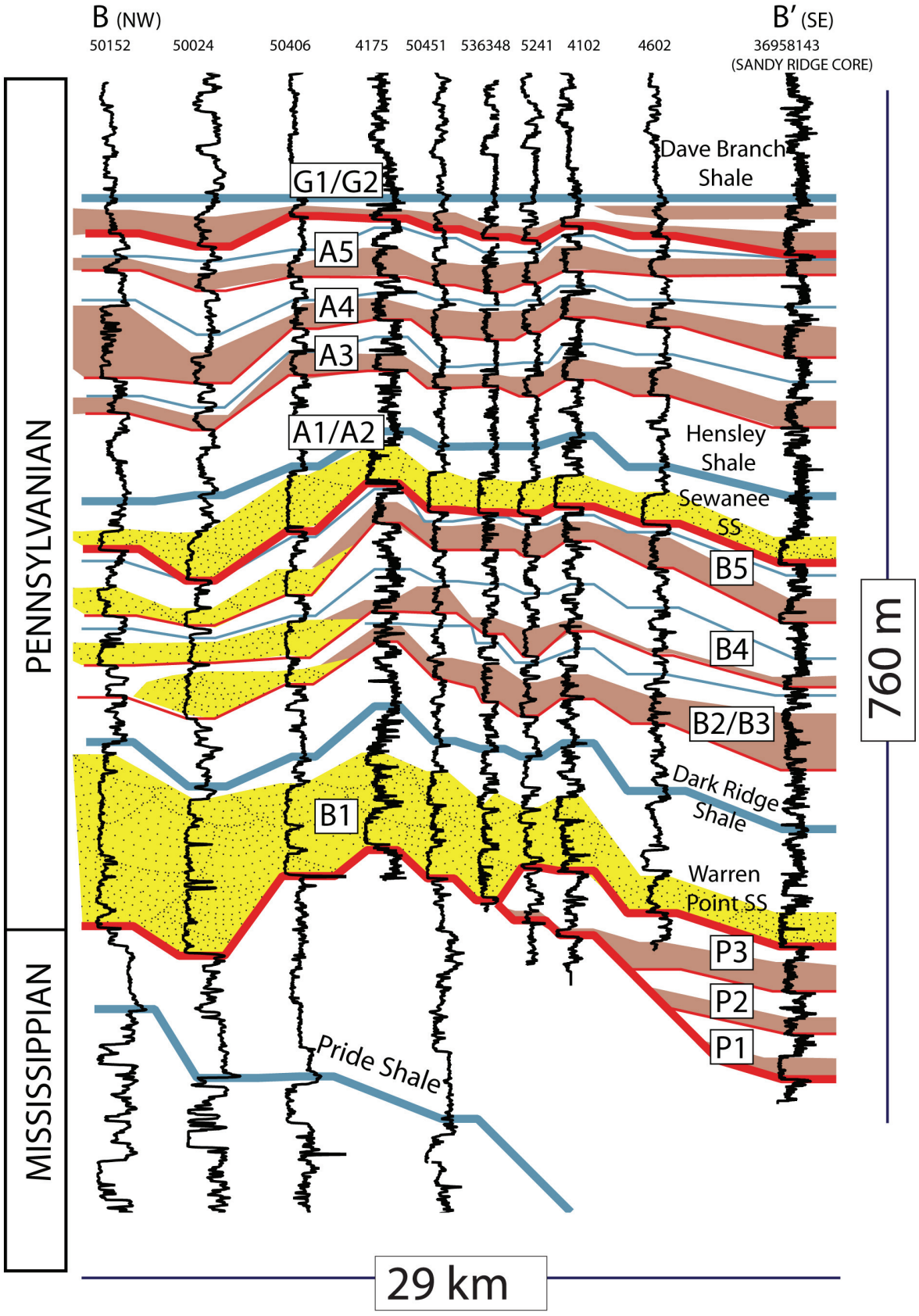

Cross-section C-C’

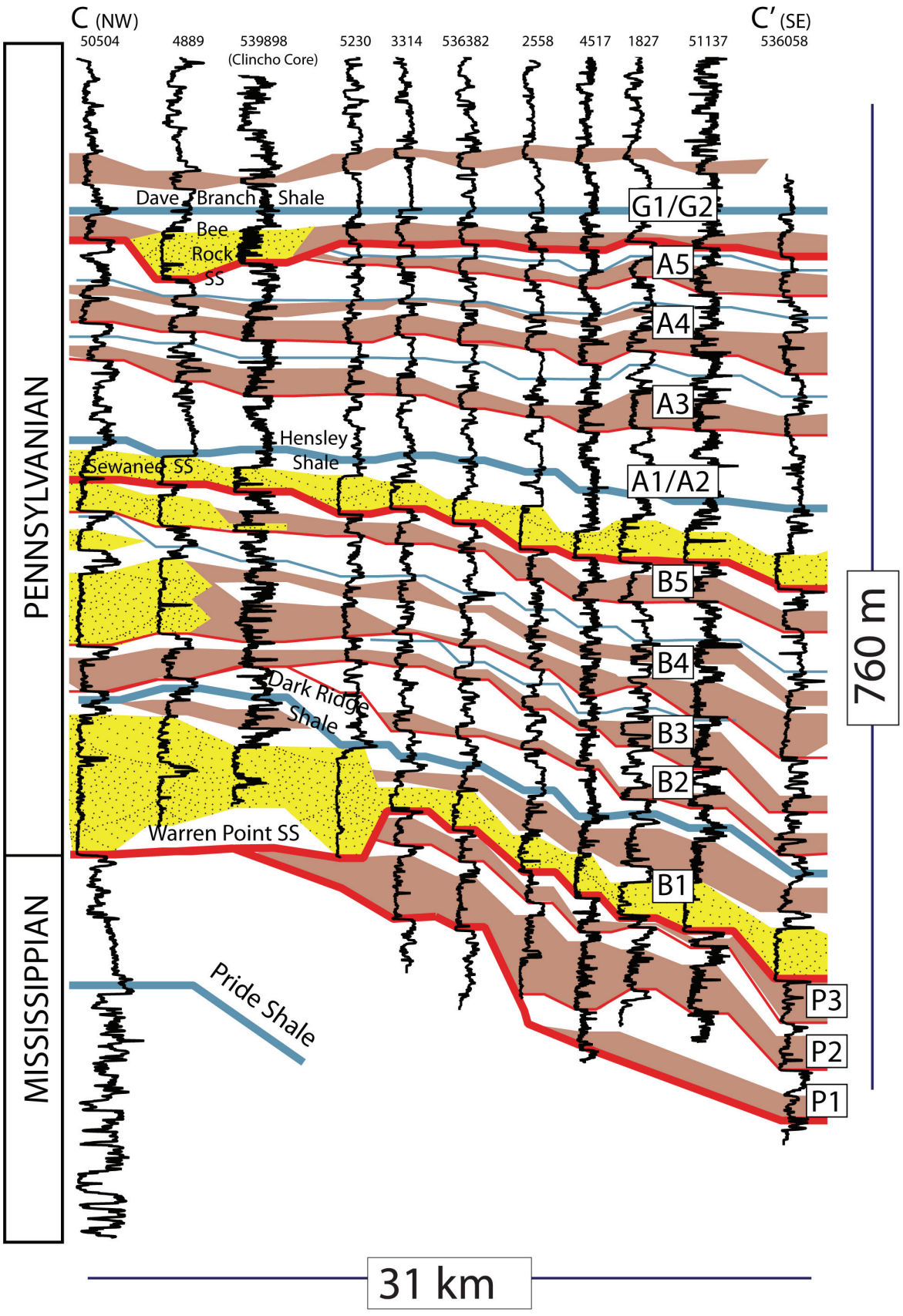

Cross-section D-D’

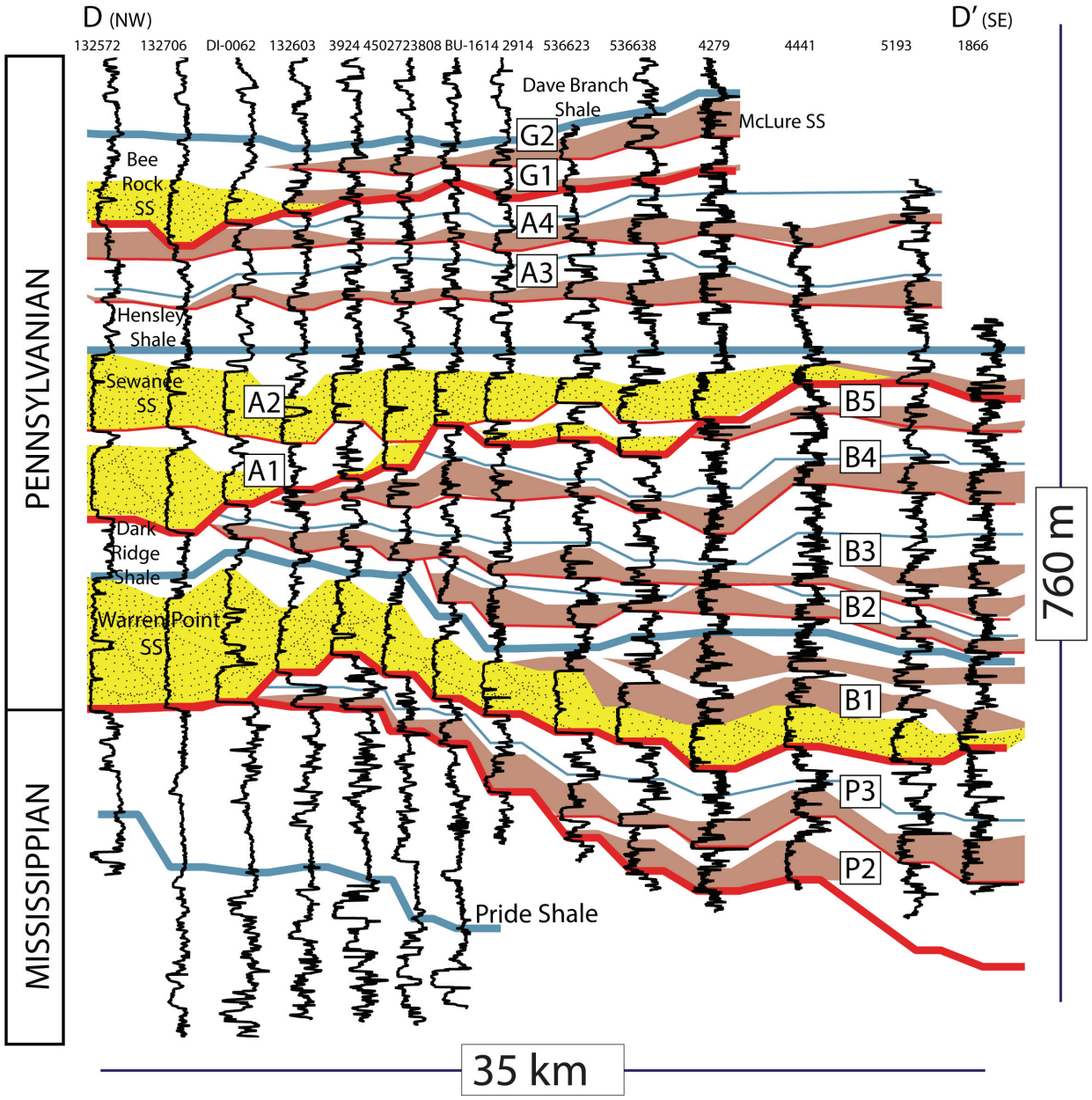

Cross-section F-F’

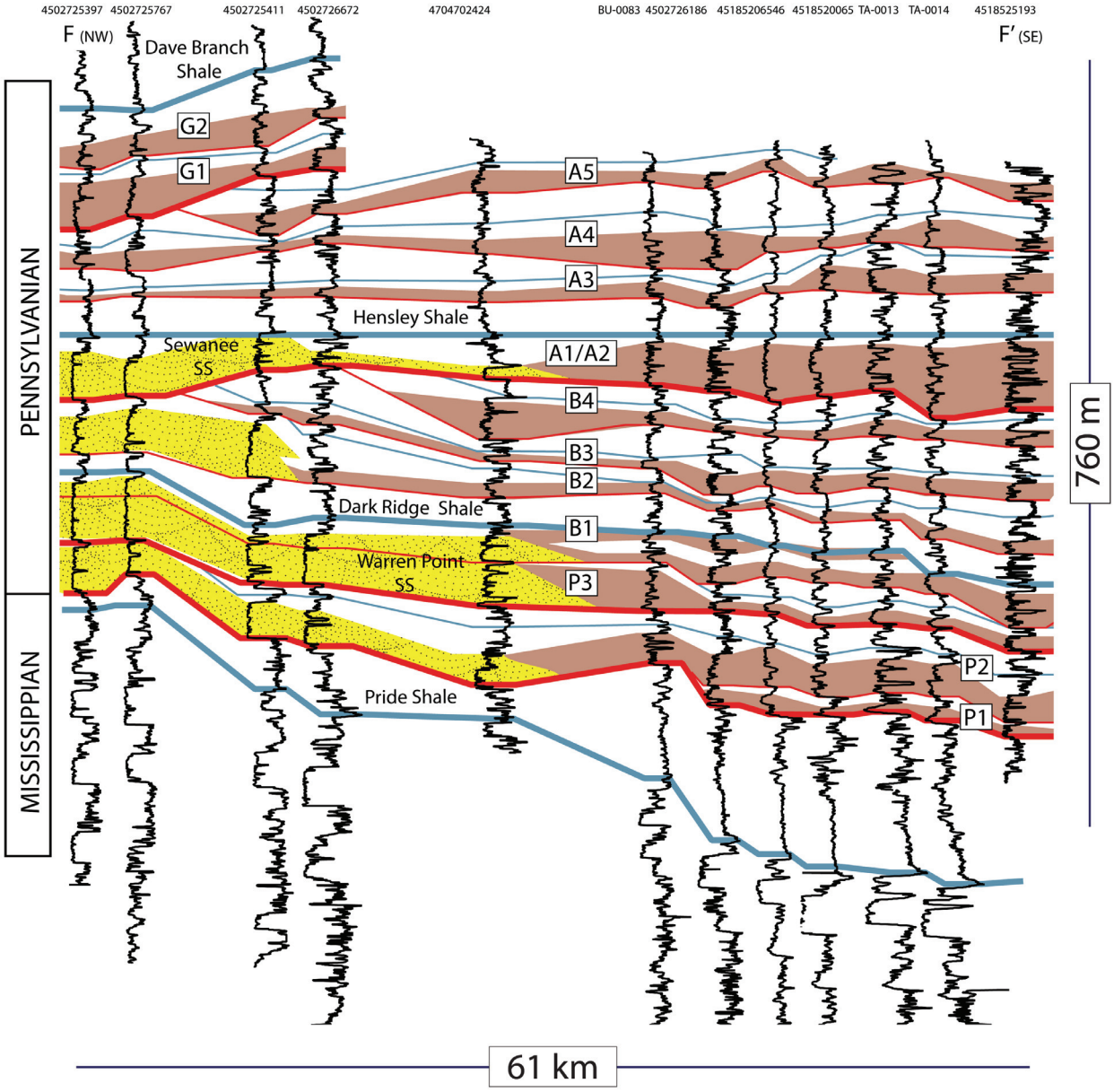

Cross-section G-G’

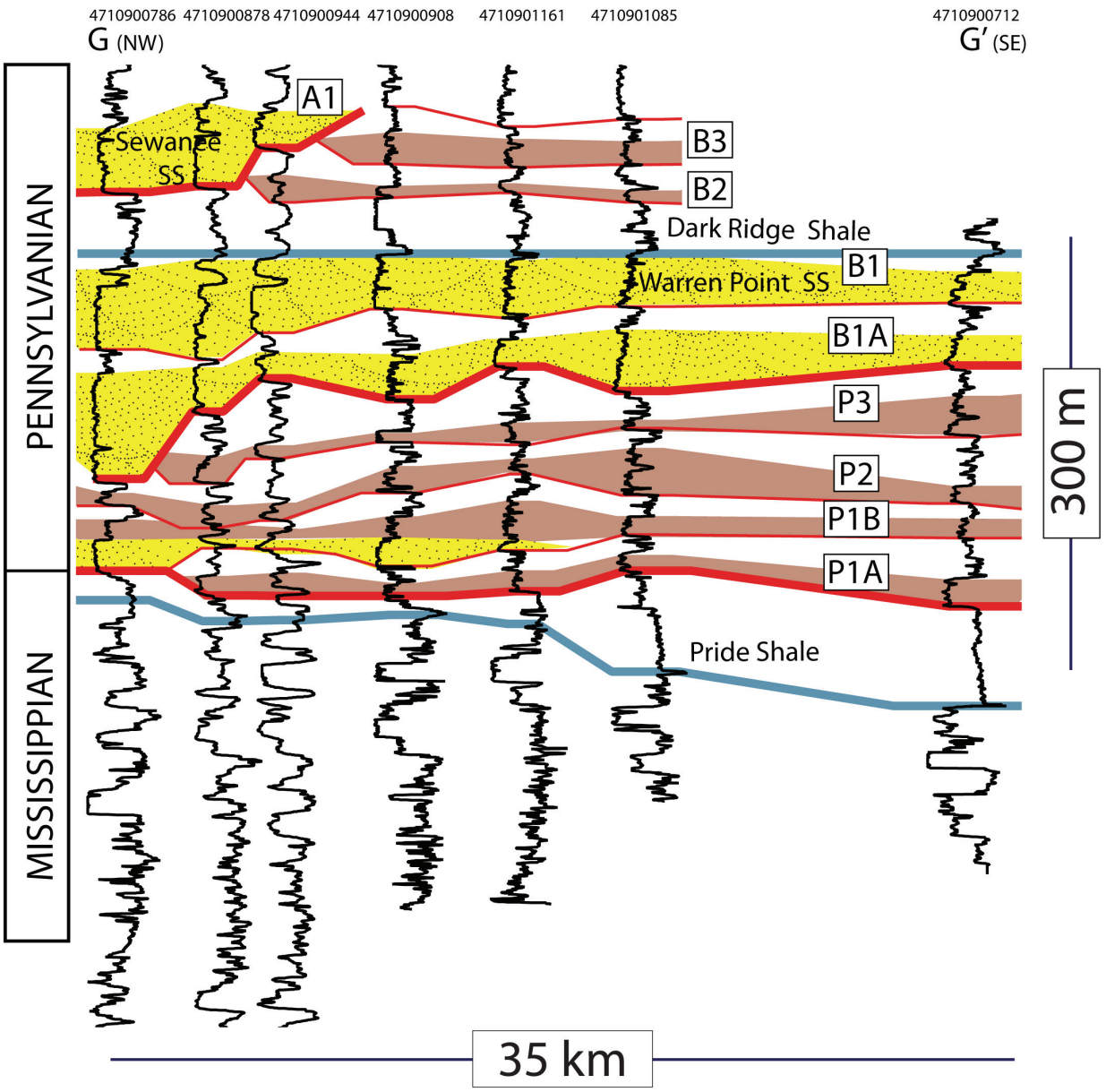

Cross-section X-X’

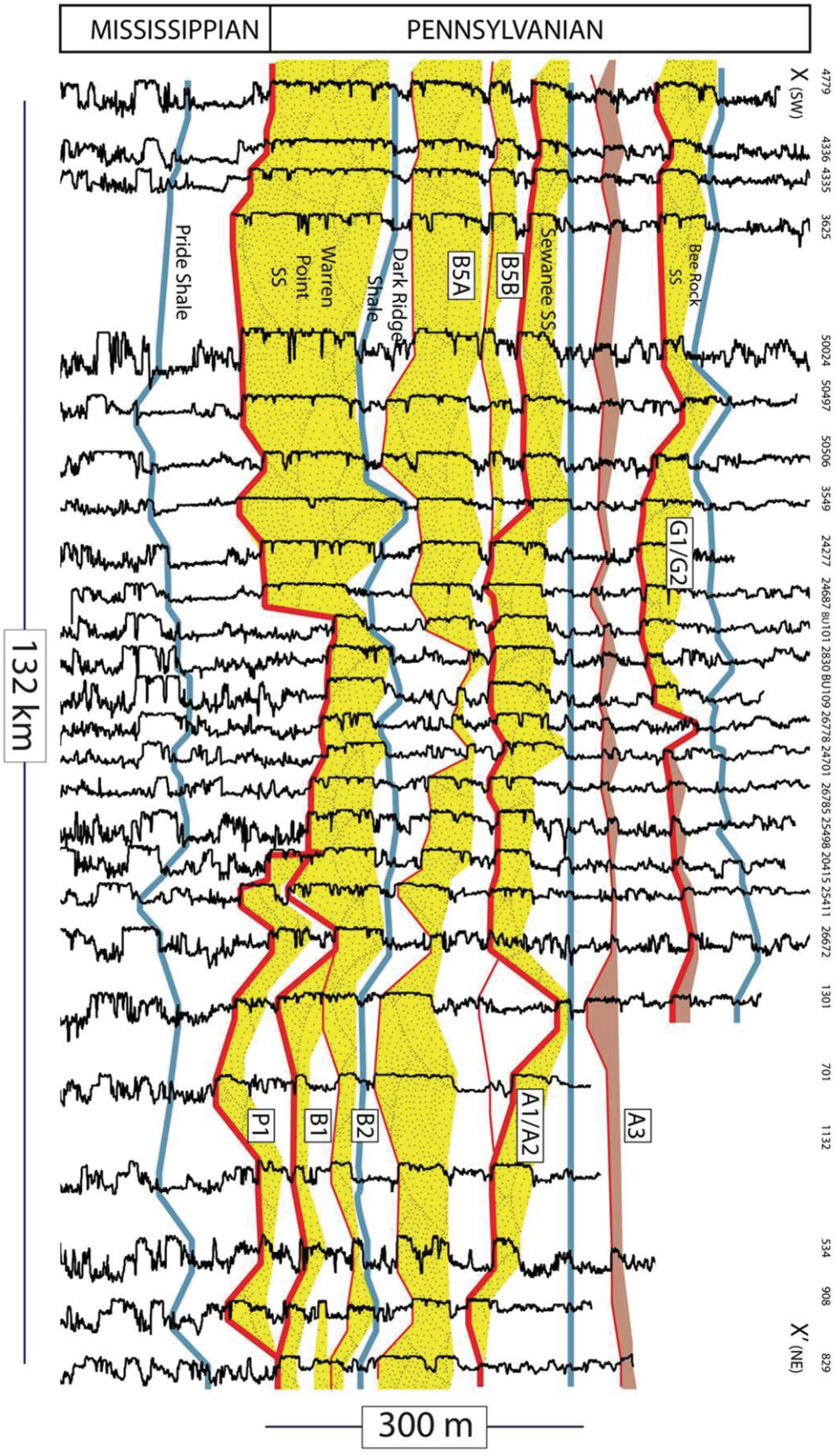

Cross-section Z-Z’

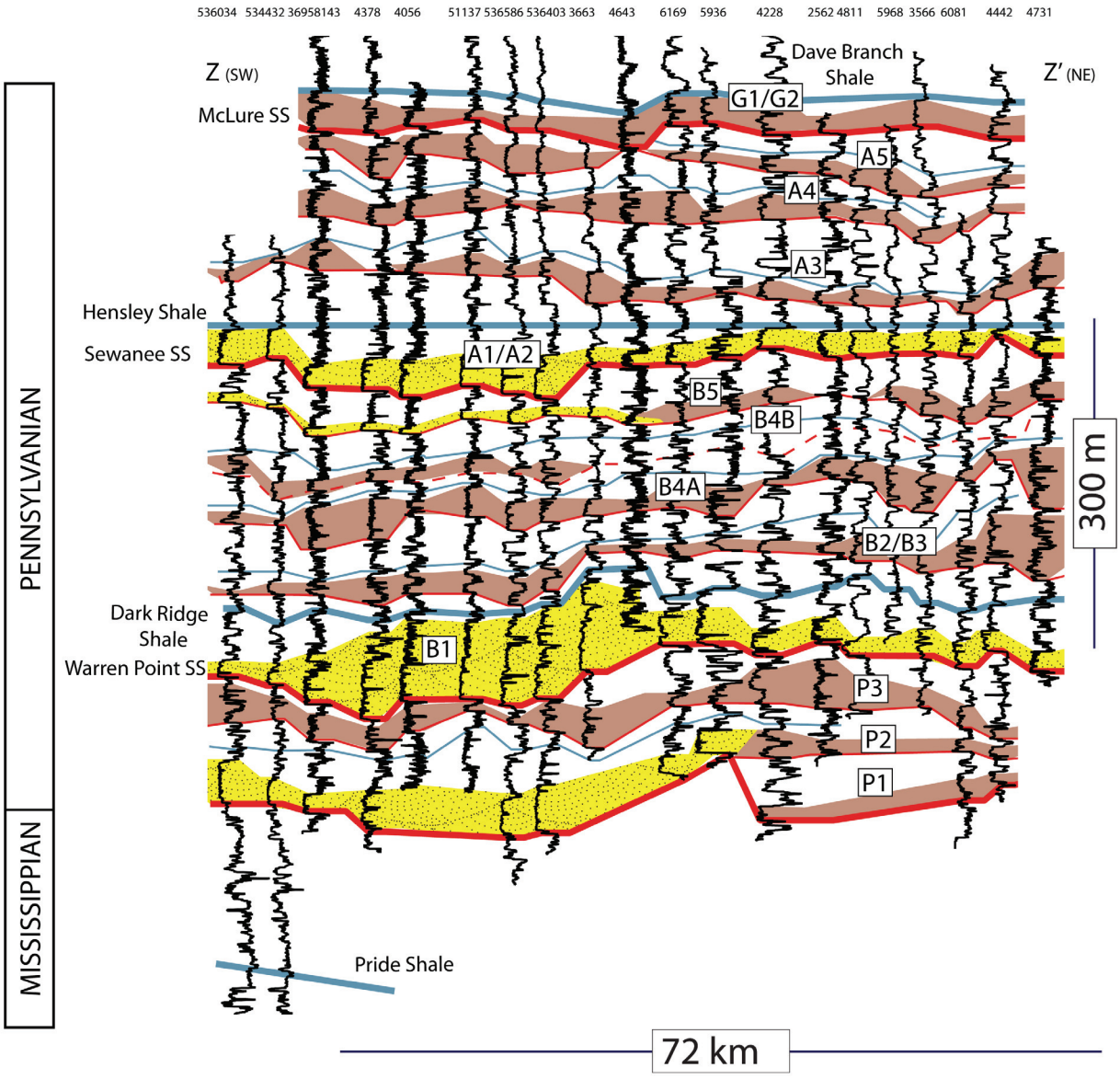

APPENDIX - PETROGRAPHIC DATASET

Listed as percentages; Qm = Monocrystalline Quartz, Qp = Polycrystalline quartz, F= Feldspar, L=Lithic

Breathitt Group
Sandstones

	Qm	Qp	F	L
Reed, 2003	83.48	2.90	3.77	9.86
	87.24	3.86	4.75	4.15
	89.34	5.74	2.46	2.46
	90.50	5.31	3.07	1.12
	90.88	3.91	1.30	3.91
	70.55	5.52	3.68	20.25
	78.65	4.68	3.22	13.45
	79.62	4.27	5.21	10.90
	75.95	4.69	7.92	11.44
	77.18	6.01	2.40	14.41
	75.15	7.99	3.25	13.61
	69.54	6.15	9.23	15.08
	67.55	7.08	7.96	17.40
	64.84	8.06	9.03	18.06
	68.09	8.26	5.70	17.95
	66.39	8.12	8.68	16.81
	70.75	5.67	4.18	19.40
	66.67	8.26	12.54	12.54
	71.09	6.19	15.04	7.67
	65.90	5.78	9.25	19.08
	62.42	5.76	9.09	22.73
	68.26	3.93	7.87	19.94
	64.90	2.65	6.19	26.25
	65.38	3.85	6.21	24.56
	90.31	2.85	0.28	6.55
	80.82	1.71	1.37	16.10
	80.56	4.39	0.31	14.73
	80.97	2.11	1.21	15.71
	78.27	2.08	3.57	16.07
	78.65	0.58	8.19	12.57
	80.54	4.49	8.98	5.99
	81.40	2.74	7.32	8.54
	79.61	6.91	4.61	8.88
	76.69	7.77	4.39	11.15
	79.35	6.52	6.88	7.25
	76.71	4.82	4.82	13.65
	73.49	9.06	3.02	14.43
	75.16	5.81	5.16	13.87
	70.93	6.71	6.71	15.65
	78.15	5.93	3.33	12.59
	67.56	2.98	10.42	19.05
	68.11	3.41	13.62	14.86

65.42	3.74	16.82	14.02
Qm	**Qp**	**F**	**L**
68.27	3.40	16.71	11.61
68.38	3.70	13.96	13.96
93.73	3.48	1.74	1.05
88.89	4.32	0.62	6.17
90.96	6.63	0.90	1.51
96.50	1.75	0.00	1.75
94.56	1.81	2.11	1.51
95.40	1.72	0.29	2.59
90.63	5.31	2.81	1.25
97.63	0.89	0.00	1.48
94.64	3.15	0.32	1.89
96.59	3.13	0.00	0.28
92.16	4.39	2.82	0.63
93.71	2.20	1.57	2.52
97.16	0.63	0.32	1.89
86.44	4.73	2.84	5.99
95.86	0.30	0.00	3.85
78.55	7.85	2.11	11.48
83.82	3.88	1.94	10.36
83.71	5.43	1.28	9.58
98.92	0.00	0.00	1.08
94.07	4.15	1.19	0.59
83.51	11.11	0.36	5.02
87.70	1.26	0.63	10.41
83.91	7.89	3.47	4.73
96.52	0.63	0.63	2.22
68.09	13.30	3.19	15.43
62.95	11.75	0.60	24.70
83.63	1.19	0.00	15.18
88.33	5.00	0.67	6.00
94.59	1.99	0.28	3.13
72.84	11.04	2.69	13.43
72.75	4.49	7.02	15.73
76.47	3.53	7.65	12.35
76.07	5.90	5.57	12.46
72.78	3.85	3.85	19.53
61.86	2.40	6.91	28.83
73.67	4.67	7.00	14.67
74.42	2.91	6.69	15.99
67.46	3.88	6.27	22.39
69.74	3.75	7.78	18.73
70.72	11.51	4.93	12.83
78.26	11.80	3.11	6.83
85.59	12.01	1.80	0.60
76.01	21.97	0.58	1.45
78.30	4.40	2.52	14.78

	71.59	3.41	7.95	17.05
	Qm	**Qp**	**F**	**L**
	74.40	3.01	7.23	15.36
	73.91	2.48	9.32	14.29
	76.11	3.54	8.85	11.50
	71.47	2.82	6.50	19.21
	74.40	2.98	9.52	13.10
	78.24	3.82	8.82	9.12
	80.26	1.94	4.21	13.59
	76.33	4.44	6.21	13.02
	81.58	3.95	4.93	9.54
	76.85	4.15	4.75	14.24
	77.88	4.72	3.83	13.57
Carbaugh, 2011	41.18	22.22	5.88	30.72
	44.51	20.23	5.20	30.06
	47.80	22.01	10.69	19.50
	51.27	24.68	5.70	18.35
	51.50	22.75	8.98	16.77
	41.94	29.03	9.68	19.35
	42.77	30.06	11.56	15.61
	43.02	22.67	14.53	19.77
	43.68	18.39	1.72	36.21
	54.88	19.51	1.22	24.39
	43.70	14.81	2.22	39.26
	38.07	15.34	4.55	42.05
	38.76	24.72	5.62	30.90
	33.89	17.78	3.33	45.00
	53.76	19.65	0.58	26.01
Houseknecht, 1978	73.00	10.95	0.36	15.69
	67.02	18.09	0.00	14.89
	62.99	14.95	0.00	22.06
	61.31	13.51	0.00	25.18
	68.60	4.69	0.00	26.71
	64.57	4.06	0.00	31.36
	56.97	3.90	0.00	39.13
	56.21	13.45	1.72	28.63
	58.73	8.97	2.15	30.15
	50.54	10.88	1.75	36.84
	52.94	12.46	5.20	29.40
	30.03	10.28	2.28	57.41
	52.27	15.33	3.14	29.26
	54.52	9.02	3.61	32.85
	60.58	9.31	2.51	27.60
	49.22	6.25	2.34	42.19
	48.58	16.42	0.36	34.64
	71.24	5.01	0.92	22.83

	61.40	5.81	0.83	31.95
	Qm	**Qp**	**F**	**L**
	56.44	9.48	0.75	33.33
	57.40	10.56	3.52	28.52
	42.94	8.01	0.47	48.58
	50.34	8.85	3.06	37.75
	39.13	15.22	6.88	38.77
	53.34	14.39	3.51	28.77
	61.79	8.93	1.79	27.49
	56.68	11.28	1.76	30.28
	60.49	7.35	0.69	31.47
	62.45	10.18	2.45	24.92
	62.68	9.16	1.41	26.76
	47.83	7.84	1.73	42.60
	50.18	14.84	3.18	31.80
	57.54	10.95	3.08	28.43
	49.44	7.11	1.49	41.95
	63.14	1.11	0.55	35.20
	52.92	6.22	1.17	39.69
	50.95	8.43	1.15	39.47
	59.32	6.97	0.77	32.94
	64.19	1.76	0.43	33.62
	58.66	20.14	1.06	20.13
	55.17	21.00	0.72	23.12
Statistics				
Mean	69.86	7.85	4.10	18.20
Standard Deviation	15.67	4.60	3.76	8.29

Lee Formation

	Qm	Qp	F	L
Siever, 1957	64	33.98	1.52	0.51
	75.6	22.11	1.60	0.69
	66.5	29.86	0.00	3.64
	68.5	25.80	0.52	5.18

Wizevich, 1991	84.33	5.23	2.36	8.08
	75.33	8.85	4.71	11.11
	84.67	4.86	3.38	7.09
	77.67	3.94	3.34	15.05
	84.33	6.27	1.34	8.05
	77.33	5.22	4.03	13.42
	80.67	4.61	3.68	11.04
	86.67	2.93	4.36	6.04
	85.67	4.66	3.33	6.33
	82.33	2.34	2	13.33
	86.00	2.67	2	9.33
	87.00	2.60	2.35	8.05
	86.33	4.95	1.34	7.38
	90.00	2.93	1.68	5.39
	89.33	2.67	3.33	4.67

Qm	Qp	F	L
89.67	3.66	1	5.67
84.33	1.91	3.36	10.4
82.33	3.82	4.05	9.8
86.67	3.00	2.33	8
91.33	3.67	0.67	4.33
89.67	2.28	1.01	7.05
88.00	2.97	1.67	7.36
84.67	5.30	1.67	8.36
84.33	3.34	3.33	9
75.67	12.96	4.35	7.02
85.67	6.95	1.68	5.7
87.67	6.33	0.67	5.33
81.67	6.00	3	9.33
83.67	5.63	3.68	7.02
85.33	6.31	2.01	6.35
93.67	2.00	0	4.33
92.00	2.33	0	5.67
93.67	1.00	0.33	5
89.33	2.98	1	6.69
88.00	7.30	0	4.7

Houseknecht, 1978	75.30	15.54	0.00	9.16
	90.04	8.90	0.00	1.07
	90.11	6.01	0.00	3.88
	76.03	19.86	0.00	4.11
	85.98	9.59	0.34	4.09
	90.21	7.22	0.00	2.57
	54.45	43.78	0.00	1.77
	79.44	13.93	0.00	6.63
	84.43	10.38	0.00	5.19
	77.99	13.36	0.00	8.65
	75.01	18.66	0.00	6.34
	84.64	13.11	0.00	2.25
	79.10	13.93	0.00	6.96
	76.95	14.54	0.35	8.16
	80.43	8.18	1.07	10.32
	65.40	3.07	0.38	31.15
	79.72	8.70	0.36	11.23
	86.34	8.87	0.00	4.79
	86.15	7.11	0.00	6.74
	78.19	13.09	0.00	8.72
	83.22	11.43	0.00	5.35
	82.27	9.43	0.00	8.30
	85.38	7.70	0.00	6.92
	81.53	12.32	0.00	6.15
	77.82	12.73	0.00	9.45
	80.22	9.53	0.00	10.25
	Qm	**Qp**	**F**	**L**
	85.23	10.33	0.00	4.44
	86.13	8.76	0.00	5.11
	86.63	10.20	0.00	3.17
	82.48	13.14	0.00	4.38
	81.23	13.00	0.00	5.77
	82.79	10.66	0.00	6.55
Statistics				
Mean	82.54	9.20	1.20	7.06
Standard Deviation	7.09	7.70	1.45	4.10